SPM Simulator Guidebook

Produced by
Advanced Algorithm & Systems Co., Ltd.
Tohoku University, WPI-AIMR

December 9, 2014

Version 1.6

Supervising Editor:
Masaru Tsukada

Authors:
Masaru Tsukada[†] (Chapters 1 and 2)
Hiroo Azuma[‡] (Chapters 3, 4, 5, 6 and 7)
Mamoru Shimizu[‡] (Chapters 8, 9 and 10)
Toru Ogata[‡] (Chapter 11)
Hiroshi Shinotsuka[‡] (Chapter 12)

[†]Tohoku University
[‡] Advanced Algorithm & Systems Co., Ltd.

Contents

Chapter 1 Introduction

1.1 Purpose and circumstance of the development of SPM Simulator

The scanning probe microscope (SPM) is the powerful experimental technique to observe the super fine structures and to measure the physical properties in fine scale of materials in nature or artificial materials: e.g. inorganic crystal surfaces, fine structures of semiconductors, organic molecules, self-organizing films, protein molecules and bio-nano structures like DNAs. The top of the probe tip of the SPM sensitively detects quite weak forces and charge transfers which act in the atomic scale from a sample. Then the microscopic information is transmitted to the mesoscopic or macroscopic system, the probe and the cantilever, which is finally observed in the measurement system. However, it is very hard to analyze the experimental results without the theoretical supports, because the mechanical, electrical and chemical processes in atomic scale are involved together in the nano-scale region at the top of the probe tip.

In fact, as seen in the various previous researches [1], numerical simulations based on a theory play important roles to analyze the extensive experiments related to the SPM; the SPM images, various spectra, nano-mechanical experiments of bio-materials etc. However, it is difficult for nonspecialists about the theoretical calculation to carry out the theoretical simulation. We have developed the "SPM Simulator" as part of the JST project[1] in order to support the theoretical analyses of the SPM experiments from various measurement techniques and environments. We have developed the commercial version of the simulator for general users since 2013, and continued the promotional activities.

Conventional SPM simulations for research purposes used to occupy the resources of the large scale computer for a long time. However, general nonprofessional users would prefer the simulator with a simple operation and a reliable result even though the result is not so accurate. Our simulator, developed in the "General-purpose SPM Simulator" project, has greatly reduced the computational cost according to their problems so that the brief calculation can be performed by common personal computers or workstations. Moreover, the simulator adopts the graphical user interface (GUI) to support the simple operation for the simulation without high background knowledge. This guidebook aims to explain the contents of the SPM Simulator developed by those projects, and to show how to use the simulator in practice. It is our pleasure for you to use this guidebook as a convenient instruction.

[1] We participated in the first season (2004-2007) and the second season (2009-2012) of Development of Systems and Technologies for Advanced Measurement and Analysis, organized by Japan Science and Technology Agency (JST).

Chapter 2 Outline and Software Composition of SPM Simulator

2.1 Composition of SPM Simulator

As shown above, the numerical simulations based on a theory play important roles to analyze the extensive experiments related to the SPM; the SPM images, various spectra, nano-mechanical experiments of bio-materials etc. We have developed the "SPM Simulator" as part of the JST project1 in order that the general experimetalists can use this simulator with ease. From Chapter 3, we will explain the details of contents and how to use the simulator. We here show, in advance, the composition and the brief outline.

The SPM Simulator is composed of eight solvers (Analyzer, SetModel, GeoAFM, FemAFM, LiqAFM, CG, MD and DFTB) including the sample modeling tool (SetModel), those are listed in Table 1.

Table 1 The list of solvers included in the SPM Simulator.

Solver	Function	Properties
Analyzer	Digital Image Processor of Experimental Data	Preprocessing before simulation. Estimation of tip shape, Removal of tip-shape influence.
SetModel	Modeling of Samples and Tips	Make atomic configurations before simulation.
GeoAFM	Geometrical Mutual AFM Simulator	Resolution is not atomic scale, but meso- or macro-scale.
FemAFM	Finite Element Method AFM Simulator	Resolution is not atomic scale, but meso- or macro-scale. Elastic deformation of samles and tips can be taken into account.
LiqAFM	Soft Material Liquid AFM Simulator	Oscillation analysis of cantilever in liquid. Mechanical calculation of continuous elastic body in liquid.
CG	Geometry Optimizing AFM Image Simulator	Optimization of the atomic configuration by classical force field method. CG-RISM simulates in liquid.
MD	Molecular Dynamics AFM Image Simulator	Molecular Dynamics calculation of the atomic configuration by classical force field method.
DFTB	Quantum Mechanical SPM Simulator	Calculation of the force to the tip and the tunneling current by the quantum mechanics. Calculation of STM/STS, AFM, KPFM.

These solvers are the softwares available on the SPM Simulator, which have been developed to carry out theoretical calculations of various SPM simulations. Figure 1 shows the overall configuration of theoretical calculations available on the SPM Simulator, together with the required solvers.

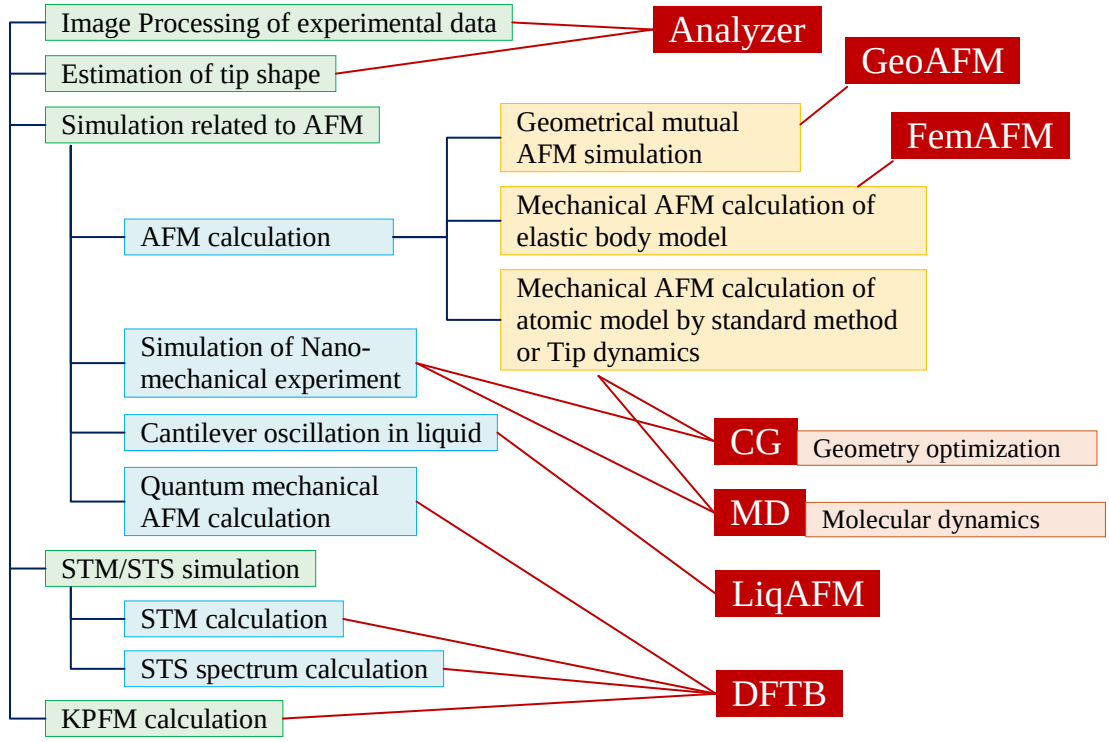

Figure 1 Various calculations available on the SPM Simulator, together with the required solvers.

Before the simulation by the SPM Simulator, we recommend to "analyze the experimental images" in order to compare with the theoretical calculations accurately and to fix obvious human errors and noises of the measured images. Beside, it is usually effective to "estimate the initial tip shape" briefly by the use of the measured SPM image itself. We can perform the theoretical simulation with the estimated tip shape, and then we can obtain the genuine sample structure by the simulation compared with the measured image. The Analyzer, one of the equipped solvers, has such functions.

Next, the SPM Simulator is able to perform "the simulation related to the AFM" such as

(i) "Calculation of AFM images" based on the classical force field,
(ii) "Simulation of Nano-mechanical experiment",
(iii) Numerical analysis of "the cantilever oscillation in liquid",
(iv) "Quantum mechanical AFM calculation".

The AFM simulation (i) based on the classical force field is applicable also to the force spectrum between the tip and the sample.

In "the simulation related to the AFM", we have prepared two kinds of methods: One is based on a calculation of forces between the tip and the sample, the other is a simple geometrical method without calculating forces. The former corresponds to the FemAFM, CG, MD and DFTB solvers, while the latter corresponds to the GeoAFM solver.

The GeoAFM, the simple geometrical method, makes up an AFM image by the contact condition in which the borders of the tip shape and the sample shape are in touch, after those shapes are coarse-grained in a proper scale. The GeoAFM also reconstructs the one out of the other two among three geometrical elements, a tip, a sample material and its AFM image.

On the other hand, the mechanical methods such as FemAFM, CG, MD and DFTB are classified into two groups: CG, MD and DFTB calculate the forces based on atomic models of the tip and the sample, while FemAFM calculates the forces based on the coarse-graining

continuum models. The former is utilized to analyze an AFM image in the atomic resolution, while the latter is utilized when the atomic resolution is not required.

For more detail in case of the atomic models, there are various methods according to the objective of the analysis;

(A) CG and MD solvers are based on the classical force field method, which calculate interatomic forces by the use of the empirical parameters.
(B) DFTB solver calculates interatomic forces based on the quantum mechanical calculation.

There are also several methods how to consider a tip deformation when the tip comes close to the sample:

(a) The tip and the sample are assumed to be rigid bodies so that they do not change their shapes.
(b) They are allowed to change the shapes.
(c) Furthermore, the thermal vibration is taken into account for the atoms contained in the tip and the sample.

FemAFM, CG and MD solvers take (a) and (b) into consideration. (c) is available only for the MD solver. Although (c) is the best approximation, you should choose (a) or (b) when you intend to simulate quickly and effectively.

As you know, in case of a non-contact mode, observed AFM images are not the forces itself, but visualizations of some physical properties influenced by interactions to the cantilever oscillation; such as the frequency shift of the cantilever oscillation, the dissipation of vibration energy etc. These physical properties can be theoretically obtained, once the forces to the tip from the sample are calculated at various tip heights. The simulator has the theoretical formula to obtain those physical properties.

On the other hand, the simulator has another method by calculating the cantilever motion directly with the forces to the tip. Especially, the non-contact AFM simulation in liquid has to reproduce the “cantilever oscillation in liquid” numerically. It requires the fluid dynamics calculation in a wide space including a narrow area between the cantilever and the substrate. The LiqAFM solver has an appropriate method which has been developed to solve such a problem. The LiqAFM solver contains the software to analyze cantilever oscillations with various shaped cantilevers in liquid and to analyze the contact problem with a soft material.

In “STM/STS simulation”, the DFTB solver is able to calculate the tunneling current between the tip and the sample, the STM image, the STS spectrum, the KPFM image etc. Those calculations are derived from electron orbitals based on the quantum mechanics. The Density Functional Based Tight Binding (DFTB) Method, the same as the solver name, is the tight binding method parameterized by the first principle density functional method. The reliability of the DFTB method is guaranteed, and the computational cost is known to be relatively small. The DFTB solver calculates tunneling currents as a basis of the STM and the STS simulation. It is also applicable for AFM image calculations because the tip-sample forces are obtained in consideration of the quantum mechanical interaction.

As mentioned above, you can choose the most appropriate method among various calculation methods equipped in the SPM Simulator corresponding to a variety of SPM experiments, the required physical properties, the required resolution, the accuracy, the resource of a computer, the desired computing time etc. We expect that this guidebook will provide you with a guideline to choose an appropriate method.

2.2 Guideline to decide a solver in SPM Simulator

Figure 2 shows a guideline how a general user should decide an appropriate solver depending on his/her purpose. This is a flowchart to decide a solver from the user's view. We will explain the details soon.

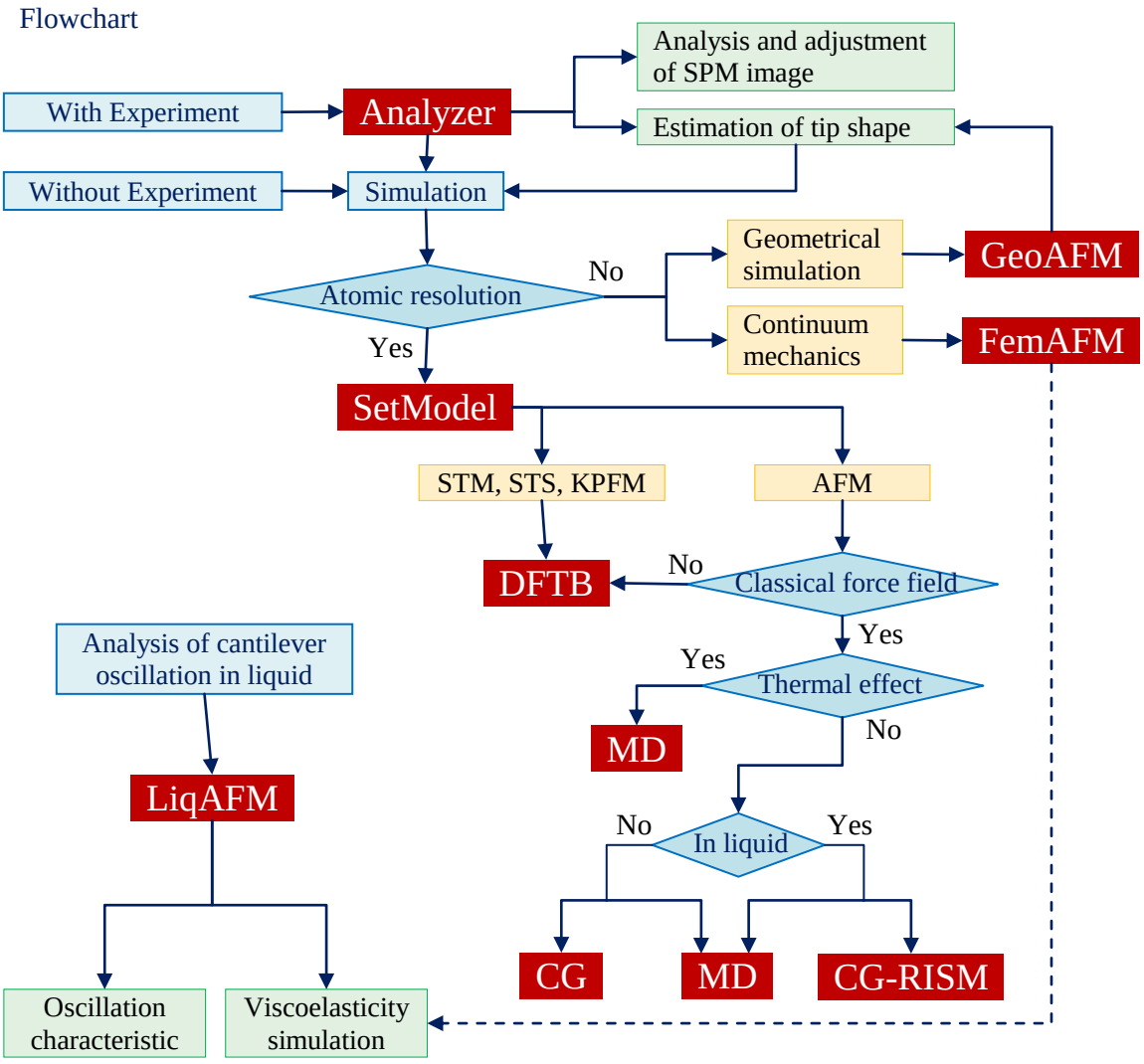

Figure 2 Flowchart to decide a solver.

For example, when a user has an experimental SPM image, the only Analyzer works well in order to reduce the artifacts or analyze the digital image processing. Together with the GeoAFM, the Analyzer can estimate the tip shape at a certain level. In most cases, a simulated image and an observed image may be compared. Thus, the artifacts in an observed image must be removed in advance. The Analyzer is useful for the preparation.

An appropriate solver depends on the resolution; whether the simulation requires meso- to macro-scopic resolution or atomic resolution.

In case of the AFM simulation which does not require the atomic resolution, there are two alternatives;

(A) GeoAFM - to adopt the simple geometrical calculation,
(B) FemAFM - to take into account the interaction forces.

The GeoAFM is recommended when you would like to obtain a result quickly or when a sample is so complicated that the force calculation may take a long time. The GeoAFM also reconstructs the one out of the other two among three geometrical elements, a tip, a sample material and its AFM image. Thus, you will have a clear description from your AFM measurement.

Of course, an AFM image obtained only from the geometrical condition may not be accurate. Therefore, we recommend the FemAFM solver which takes into account interaction forces between the tip and the sample, when you would like more reliable simulation. The FemAFM solver can also simulate the deformation of the sample by a force from the tip, based on the finite element method. It thus provides a higher reliability of an AFM calculation in meso- to macro-scopic system. Note that the computational cost becomes large with the scale of the system. Hence, we recommend using the GeoAFM to estimate the approximate structure of the tip or the sample, before the accurate calculation in a limited area using the FemAFM.

In case of an AFM simulation which requires the atomic resolution, we have to prepare atomic configurations of the sample and the tip. The SetModel solver has such a function. A candidate of a tip structure is made by cutting down from a bulk structure. You can also use your own tip model or the tip models included in the standard database. The SetModel solver provides a sample model of a crystal surface with a periodic structure according to the group theory.

The DFTB solver performs the quantum mechanical calculation based on electronic states of the sample and the tip, so that it can simulate the STM image, the STS spectrum, the KPFM image etc. The AFM image calculations are classified into two methods; the one applies classical force field potentials which were derived empirically for each atom pair, the other applies the quantum mechanical interactions after calculating electronic states. The former corresponds to the CG and the MD solvers, while the latter corresponds to the DFTB solver.

The CG solver adopts the static calculation which does not take the thermal effects into account. But it evaluates atom displacements of the tip and the sample due to their interactions by the use of the optimization method. On the other hand, the MD solver simulates atom motions within the classical mechanics by the numerical integration of the microscopic equation of motion, and then summarizes the whole results to obtain interaction forces between the tip and the sample. Because the interaction force fluctuates rapidly with the time during such a simulation, we decide the interaction force as an averaged value. The MD solver can take the thermal effect into account unlike the CG solver.

In case of an AFM simulation in a liquid environment, we have to calculate an interaction between the tip and the sample affected by solvent molecules moving rapidly. The CG solver includes the CG-RIMS solver, which calculates the distribution function of liquid molecules in the presense of the tip and the sample by the use of the statistic mechanics method called the RISM. It then evaluates a free energy of a system at a specified configuration. The interaction force between the tip and the sample is derived by the gradient of the free energy as a function of their distance. On the other hand, the MD solver can simulate dynamic behaviors of all atoms including solvent molecules, so the MD solver can calculate the tip-sample interaction forces in liquid. Although you may think the MD solver is an all-purpose method, the computational cost becomes huge in case of a large number of atoms of interest.

In case of a non-contact AFM in liquid, we focus on a cantilever oscillation in liquid. The simulation of a cantilever oscillation in liquid plays an effective role in order to find an appropriate experimental condition. It is also required to design an appropriate shape of a cantilever. The LiqAFM solver is available for such problems. The LiqAFM can simulate the oscillation analysis in consideration of the visco-elastic effects to the tip from the sample. Thus, combined with the FemAFM, the LiqAFM can simulate for the AFM in liquid. Besides, the LiqAFM contains software for the contacting system to simulate the visco-elastic sample, as seen in Chapter 5.

References

[1] M.Tsukada, N.Sasaki, M.Gauthier, K.Tagami and S.Watanabe, "Theory of Non-contact Atomic Force Microscopy" in Noncontact Atomic Force Microscopy, Nanoscience and Technology Series of Springer, eds. S.Morita, R.Wisendanger, E.Meyer, (2002) 257-278.

[2] Q.Gao, K.Tagami, M.Fujihira and M.Tsukada, Jpn., J. Appl. Phys. **45** (2006) L929-L931.

[3] A.Masago, S.Watanabe, K.Tagami and M.Tsukada, J. Phys. Conf. Ser. **61** (2007) 785-789.

Chapter 3 Analyzer: the Experimental Image Data Processor

Analyzer is a digital processor for experimental scanning probe microscope (SPM) image data. It imports binary data files, which are output by the SPM during experiments in the laboratory. If we apply varieties of digital processing to experimental SPM image data with the Analyzer, we can obtain new properties of samples that we have not known before. It can compare simulation results and experimental image data obtained with the SPMs, and we can verify whether or not the simulation results are reliable. With these functions of the Analyzer, we can evaluate shapes of surfaces of samples in a proper manner.

We show a flow chart that expresses a concept of the Analyzer in the following figure.

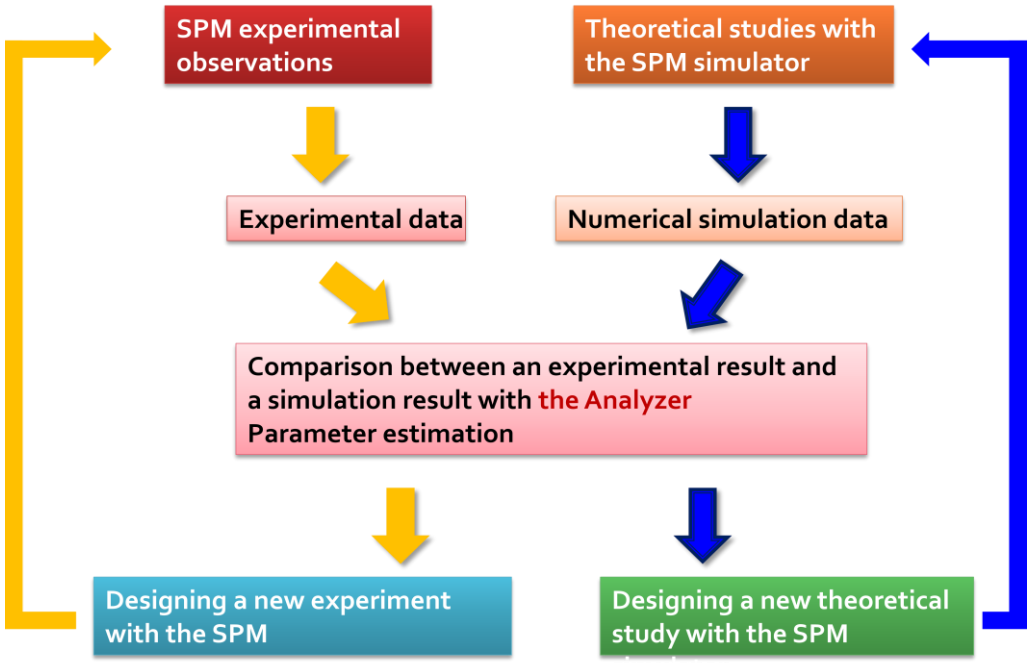

Figure 3 A flow chart expressing a concept of the Analyzer.

How to start the Analyzer is as follows. Let us click [Tool]→[Analyzer] in "Menu Bar" on the GUI of the SPM Simulator. Then, a window for the Analyzer appears.

3.1 How to import the experimental binary data and carry out digital image processing

3.1.a A list of available file formats of the binary image data obtained during SPM experiments

In Table 2, we show available file formats that the Analyzer can imports as experimental SPM image data.

Table 2 File formats that the Analyzer can imports

Formats of binary files	Instrument makers	Extensions of files
Unisoku (.dat, .hdr)	Unisoku	.dat
Scala	Omicron	.par

Asylum Research	Asylum Research	.ibw
Digital Surf	Digital Surf	.sur
JEOL	JEOL	.tif
PicoSPM	Agilent Technologies (Molecular Imaging)	.stp
Nanonis	Nanonis	.sxm
RHK Technology	RHK Technology Inc.	.sm4
RHK Technology	RHK Technology Inc.	.sm3
RHK Technology	RHK Technology Inc.	.sm2
Hitachi(SEIKO)	Hitachi(SEIKO)	.xqd
Shimadzu	Shimadzu Corporation	.*
PSIA	Park Systems Corp.	.tiff
SPIP		.asc
WSxM(ASCII XYZ)		.txt
Gwyddion(ASCII)		.txt
Bitmap		.bmp
JPEG		.jpg, .jpeg
PNG		.png
TIFF		.tif

How to import the SPM image data into the Analyzer is as follows. Let us click [File]→[Open] on "Menu Bar" on the GUI of the Analyzer. Then, a dialog for the "Open File" appears, and you can choose a data file that you want to import into the Analyser with this dialog.

3.1.b Correcting a tilt of a substrate of a sample

In general, a two dimensional plane that a tip of the SPM sweeps does not parallel a substrate where a sample is put. In fact, it is common that the substrate of the sample has a tilt against the plane that the tip of the SPM sweeps. Thus, if the hight caused by the tilt of the substrate is much larger than the height or depth of the sample surface, small ripples and dents of the sample surface become faint and we cannot recognize precise structure of the sample surface.

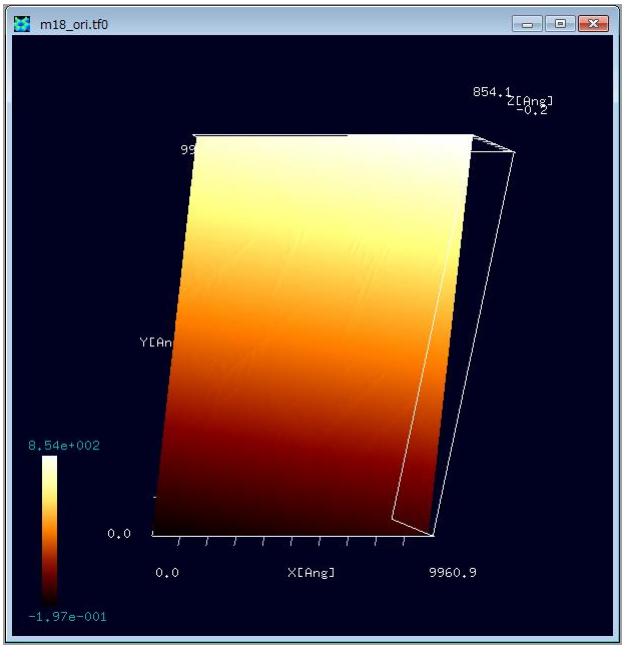

Figure 4 An image obtained with the AFM experiment before correcting its tilt.

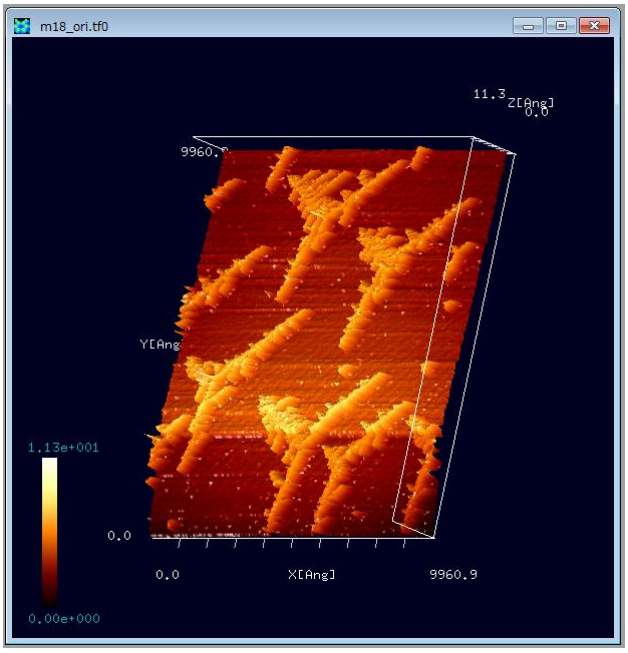

Figure 5 The experimental image of SPM data after correcting the tilt.

To avoid this trouble, the Analyzer has a function for correcting the tilt of the substrate where the sample is put. How to remove the tilt of the substrate is as follows. Let us assume that the image data is displayed on the Analyzer as shown in Figure 4. [This image date is provided by the laboratory of the Professor Fukutani, Institute of Industrial Science, the University of Tokyo. It is obtained by depositing Au atoms on an Ir substrate and annealing them. Au islands form on the Ir substrate in a way of self-organization. S. Ogura et al., Phys. Rev. B 73, 125442 (2006); S. Ogura and K. Fukutani, J. Phys.: Condens. Matter 21 (2009) 474210.] Putting the cursor on the figure displayed, we make a right-click with the mouse. Then, a context menu appears. So, let us click [Correct tilt].

Then, the original image changes into the one whose tilt is corrected as shown in Figure 5. After this process, we can recognize precise structure of the sample surface distinctly.

A theoretical method for correcting the tilt of the substrate is as follows. To estimate the tilt angles around the x and y-axes, we apply the method of the least squares to data on scan lines along the x and y-axes, so that we obtain fitting lines. Taking an average of angles between fitting lines and the xy-plane, we correct the image of experimental data according to the obtained angles.

3.1.c The Fourier analysis of the image data

The Analyzer has functions for the two-dimensional Fourier analysis of experimental image data and filtering a certain frequency components, for example, a high-pass filter and a low-pass filter. If we apply the high-pass filter to the experimental image data, we obtain a sharpened

image with enhancement of edges. By contrast, if we apply the low-pass filter to the experimental image data, we obtain an image on the suitability of identifying the background level.

Here, we explain the two-dimensional Fourier transformation for image data. We assume that the numbers of pixels in the x-axis and the y-axis are equal to N and M respectively in an original imag data. We write the value at the point with coordinates $(x, y) = (n, m)$ as $z(n, m)$.Th evalue of $z(n, m)$ corresponds with the height of the sample surface at the point $(x, y) = (n, m)$. The Fourier transformation of $z(n, m)$ is given as follows:

$$\tilde{z}(u,v) = \frac{1}{NM}\sum_{n=0}^{N-1}\sum_{m=0}^{M-1} z(n,m)\exp[-2\pi i(\frac{nu}{N}+\frac{mv}{M})].$$

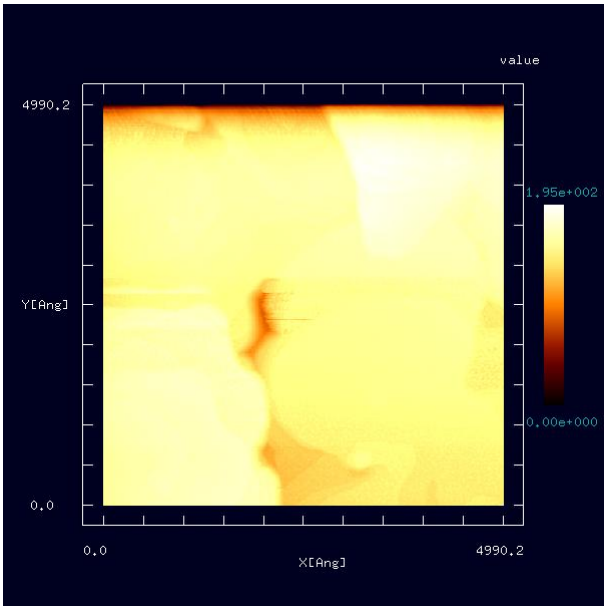

Figure 6 An experimental image obtained with the SPM befor applying the Fourier analysis.

Here, for example, we consider the Fourier analysis of the image data of Figure 6. [The image data of Figure 6 is provided by the laboratory of Professor Fukui, Surface/Interface Chemistry Group in Department of Materials Engineering Science, Osaka Ubniversity.] Putting the cursor on the image displayed, we make a right-click with the mouse. Then, a context menu appears, and we click [Image Processing]. So that, a new window for the Fourier analysis appears and a black and white image is shown in it.

In the window for the Fourier analysis, we can use three modes, [Cartesian], [Fourier] and [Power spectrum] as shown in Figure 7, Figure 8 and Figure 9:

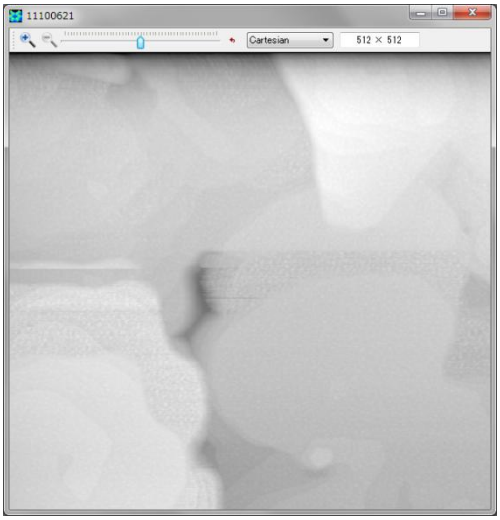

Figure 7 An image of the [Cartesian] mode of the original data obtained with the AFM.

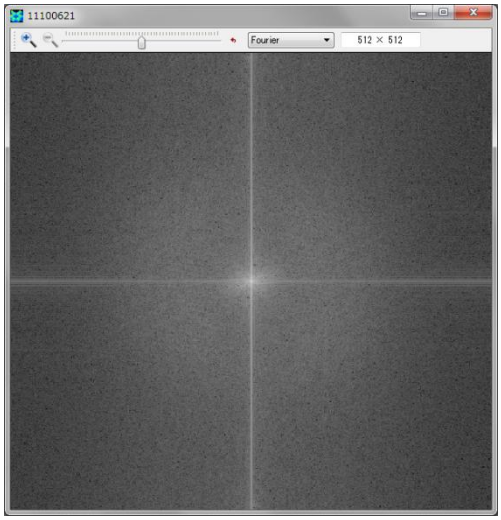

Figure 8 An image of the [Fourier] mode of the original data obtained with the AFM.

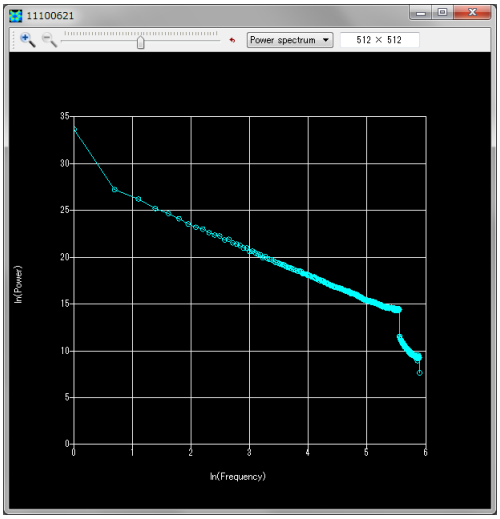

Figure 9 An image of the [Power spectrum] mode of the original data obtained with the AFM.

Adjusting a slider at the top of the window, we can vary the frequency whose component is enhanced. Moving the slider to the right-hand side a little, we obtain an image with the high-pass filter as shown in Figure 10, Figure 11 and Figure 12. Looking at these figures, we notice that we can detect edges easier than the original image.

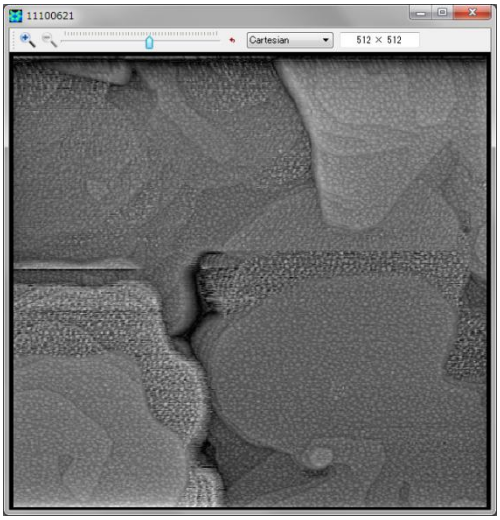

Figure 10 Output of the [Cartesian] mode of the AFM image with the high-pass filter.

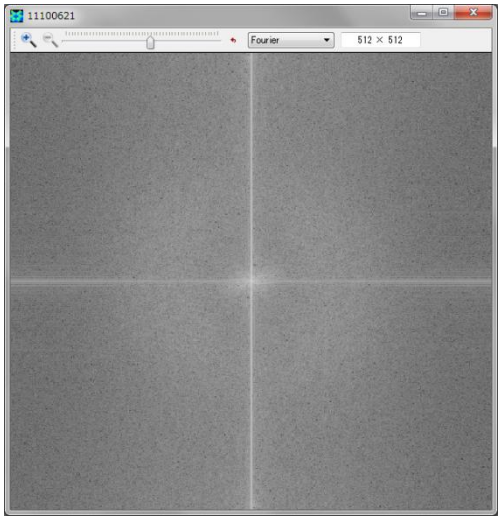

Figure 11 Output of the [Fourier] mode of the AFM image with the high-pass filter.

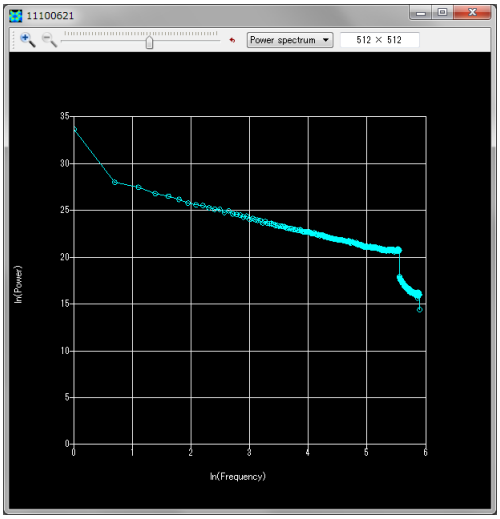

Figure 12 Output of the [Power spectrum] mode of the AFM image with the high-pass filter.

Comparing the graphs of the power spectrumfor the original image and the high-passfiltered image, we notice that a slope of the graph of the power spectrum varies continuously according to the adjustment of the slider at the top of the window. This implies that not only one component of a certain frequency but also the whole Fourier components are changed for generating a continuous adjustment. In other words, the distribution of the power spectrum is interpolated automatically in a wide range of frequencies for keeping consistency.

Moving the slider to the left-hand side a little, we obtain an image with the low-pass filter as shown in Figure 13, Figure 14 and Figure 15. Looking at these figures, we notice that we can identify the background level easier than the original image.

Figure 13 Output of the [Cartesian] mode of the AFM image with the low-pass filter.

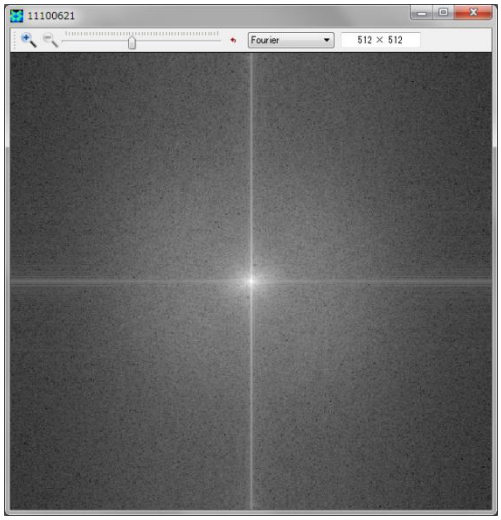

Figure 14 Output of the [Fourier] mode of the AFM image with the low-pass filter.

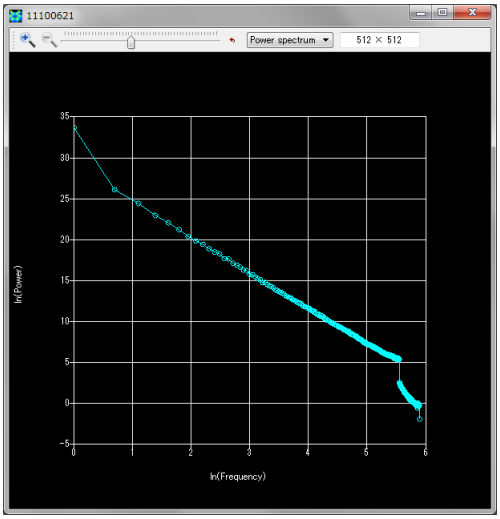

Figure 15 Output of the [Power spectrum] mode of the AFM image with the low-pass filter.

3.1.d Improvement of the subjective quality of the image with the Lanczos interpolation

The Analyzer provides a function for improving the subjective quality of the image with the Lanczos interpolation. It uses the following kernel:

$$L(x) = 1 \quad \text{if} \quad x = 0,$$

$$L(x) = \frac{3\sin(\pi x)\sin(\pi x/3)}{\pi^2 x^2} \quad \text{if} \quad 0 < |x| < 3,$$

$$L(x) = 0 \quad \text{otherwise},$$

$$S(x,y) = \sum_{i=\lfloor x \rfloor - 2}^{\lfloor x \rfloor + 3} \sum_{j=\lfloor y \rfloor - 2}^{\lfloor y \rfloor + 3} s_{ij} L(x-i) L(y-j).$$

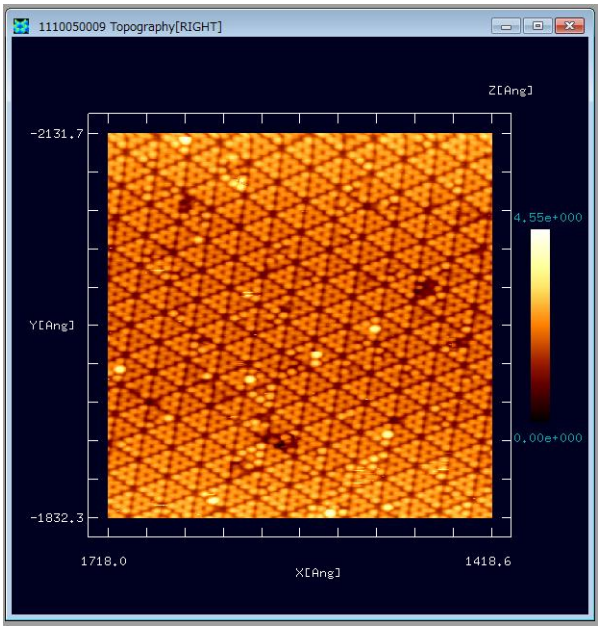

Figure 16 An original image obtained with the SPM experiment before improving with the Lanczos interpolation.

For example, let us improve the quality of an image of experimental data given in Figure 16. (This experimental image data is provided by Professor Hiroyuki Hirayama, Nano-Quantum Physics at Surface & Interface, Department of Materials & Engineering, Tokyo Institute of Technology.)

Putting the cursor on the image displayed, we make a right-click with the mouse. Then, a context menu appears. So that, we choose [Image Processing] and click it. Then, a new window for the Fourier analysis appeares and the black and white image is displayed on it as shown in Figure 17.

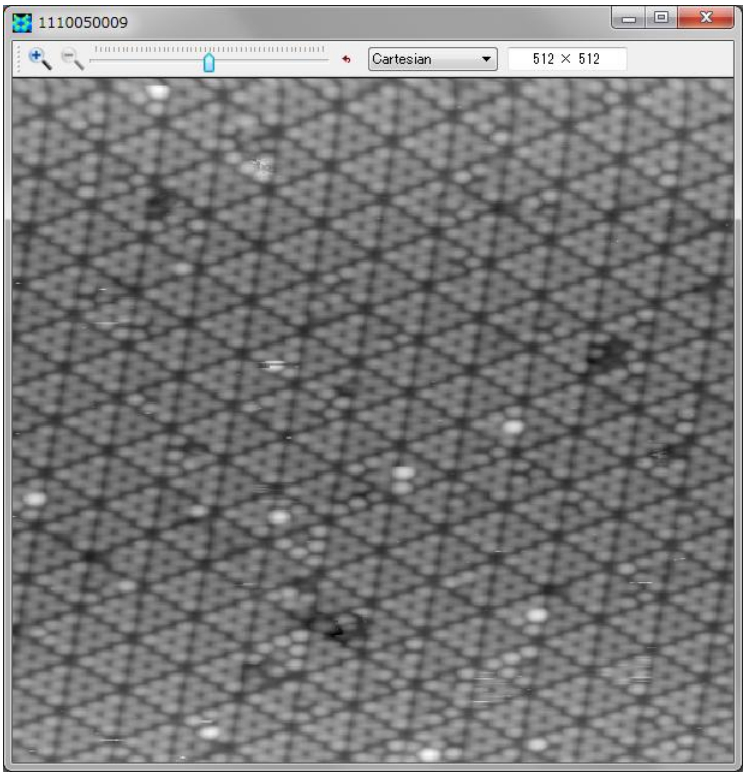

Figure 17 The black and white image obtained with the SPM experiment before making its resolution fine.

Let the resolution of the black and white image shown in Figure 17 be fine. To obtain the higher resolution, we click an icon of the magnifying glass in the upper left corner of the window with the mouse.

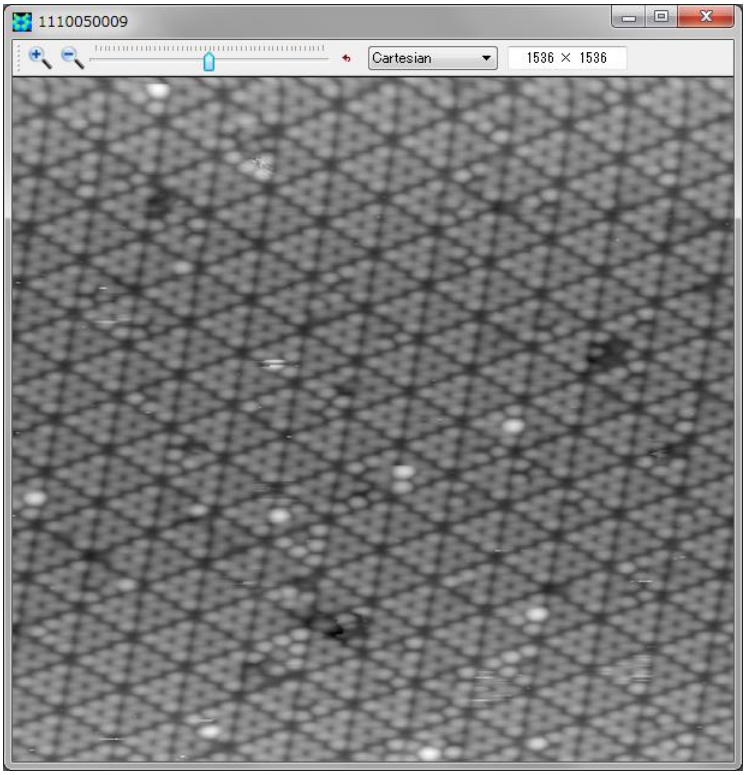

Figure 18 An image obtained with the SPM experiment with high resolution.

Then, we obtain a new image with high resolution as shown in Figure 18.

3.2 Correcting images with the machine learning method realized with the neural network

Let us consider the following problem for example. Carrying out the AFM observation of the collagen (a polymer chain) with a broken double tip, we obtain an experimental image with artifacts. Letting the machine with the neural network learn from this image, we try removing artifacts of the other AFM image obtained with the same broken double tip according to the functions of the machine learning.

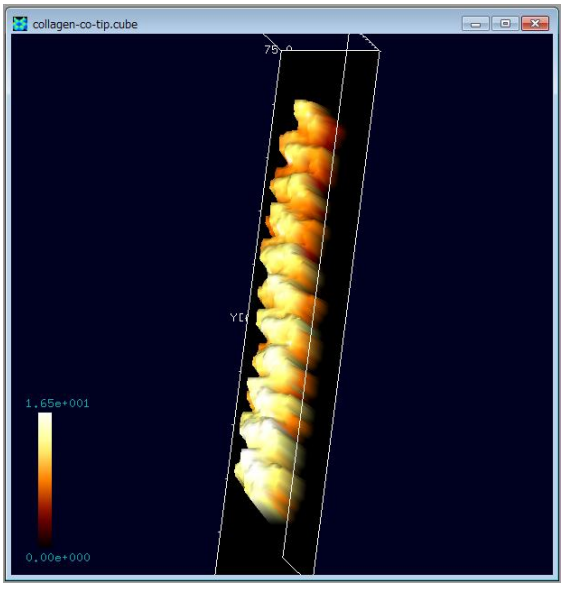

Figure 19 The AFM image of the collagen obtained by simulation using a carbon monoxide (CO) terminated tip (Weregard this image as a nearly ideal and perfect one.)

In Figure 19, we show the AFM image of the collagen obtained by simulation using a carbon monoxide (CO) terminated tip. We derive this image with the solver GeoAFM. Because the carbon monoxide terminated tip is very small and sharp, we can regard the obtained image as a nearly ideal and perfect one.

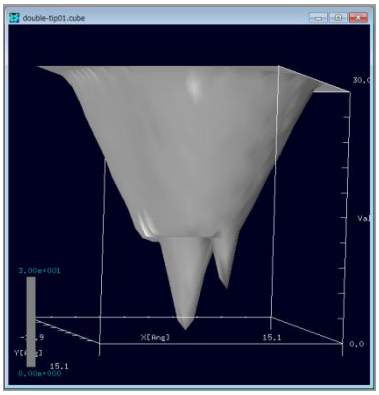

Figure 20 The broken double tip.

Here, we consider the broken double tip as shown in Figure 20.

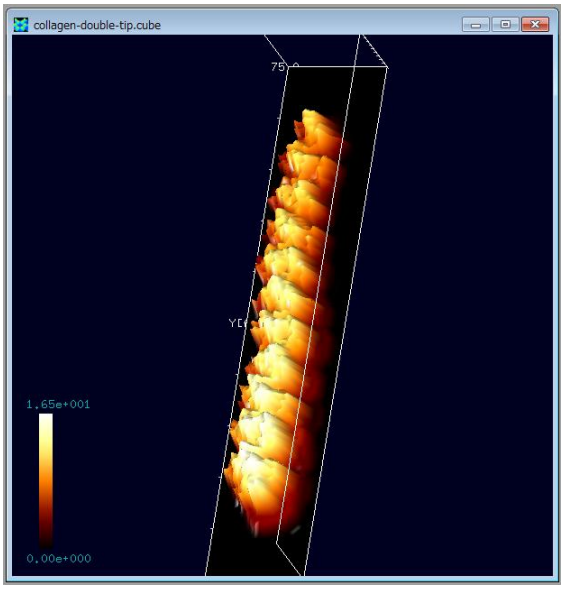

Figure 21 An AFM image of the collagen using the broken double tip.

In Figure 21, we show an AFM image of the collagen obtained by simulation using the broken double tip. We create this image with the GeoAFM. Looking at this AFM image carefully, we notice that the surface of the collagen is rough with artifacts caused by the broken double tip. So that, we try removing these artifacts with the machine learning method realized by the neural network.

How to use the neural network simulator is as follows. At first, let us click [Tool]→[Neuralnet Simulator] in the menu bar of the Analyzer. Then, a window for ”Neuralnet simulator” appears. Next, let us click [File]→[Open] in the menu bar of the window for the ”Neuralnet simulator”.

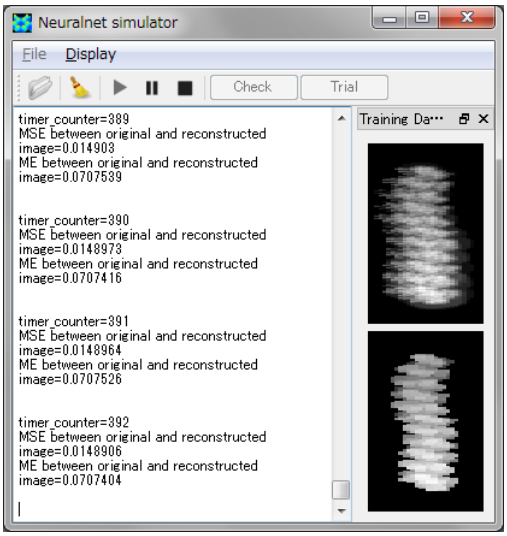

Figure 22 A screenshot of the neural network simulator.

Then, a dialog box of ”Select observed images” appears, so that we choose theAFM image data file of the collagen with the broken double tip. Here, the file format of the AFM image data has to be the “Cube”. Next, a dialog box of ”Select original images” appears, so that we choose the AFM image data file of the collagen with a carbon monoxide (CO) terminated tip as a nearly ideal and perfect image. The file format of this AFM image data has to be the “Cube”, as well. At this moment, we obtain a window as shown in Figure 22.

To start the machine learning with the neural network, we click the triangle-shaped [Start] button, which is put on the toolbar at the top of the window. Then, the machine learning starts.

When the machine learning with the neural network ends, we click the [Pause] button, which is put on the toolbar at the top of the window. To confirm a result of the machine learning, click the [Check] button on the toolbar. Then, three images as shown in Figure 23, Figure 24 and Figure 25 appear.

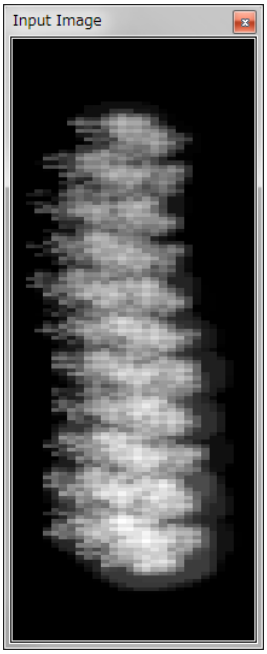

Figure 23 The Input Image for the Neuralnet simulator.

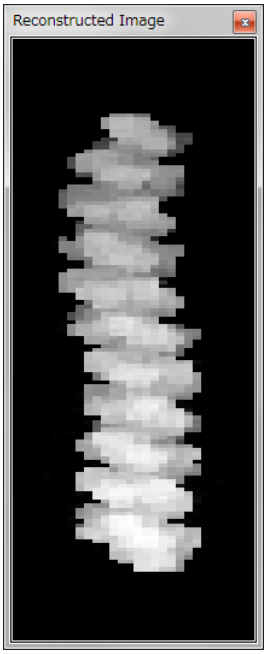

Figure 24 The Reconstructed Image of the Neuralnet simulator.

Figure 25 The Difference Image of the Neuralnet simulator.

Figure 23, Figure 24 and Figure 25 show the ”Input Image”, the “Reconstructed Image” and the “Difference Image”, respectively. The Input Image represents the original input image, which is obtained by the AFM observation of the collagen with the broken double tip. The Reconstructed Image represents the modified image, which is generated according to the results of the machine learning. In other words, the Reconstructed Image is obtained by removing the artifacts from the Inputimage. The Difference Image represents differences between the Input Image and the Reconstructed Image. If there is nothing in the Difference image, the artifacts are removed completely by the machine learning.

We can store the results of the machine learning as a file by clicking [File]→[Save Weight File] on the menu bar.

Finally, we remove artifacts from another new AFM experimental image data by using the results of the machine learning. Clicking the [Trial] button on the tool bar, we choose a cube file of another AFM experimental image data that contains artifacts. Here, for example, we use the AFM image data of a single molecule of Glycoprotein (1clg) on HOPG (Highly Oriented Pyrolytic Graphite) with the same broken double tip. We can create this image with the GeoAFM. Then, Figure 26 and Figure 27 appear.

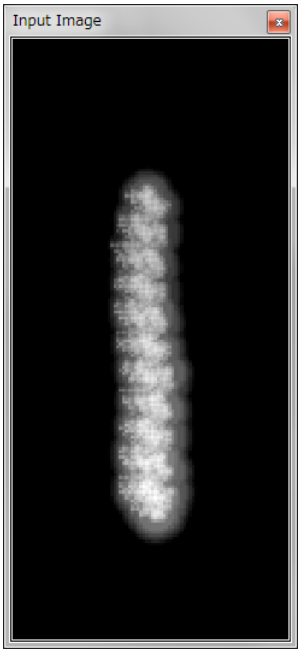

Figure 26 An experimental AFM image of a polymer with the broken double tip.

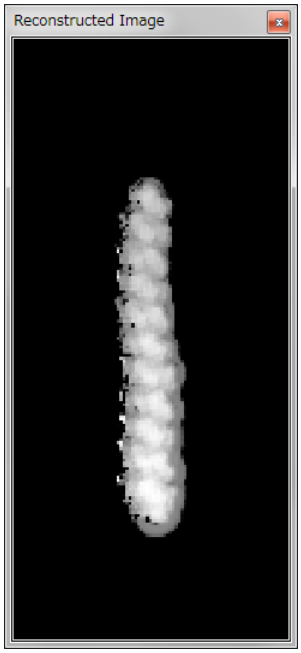

Figure 27 A corrected image that is obtained according to the results of the machine learning with the neural network.

In Figure 26, we show an experimental AFM image of the polymer obtaine with the broken double tip. In Figure 27, we show a modified image , which we can obtain by correcting the image of Figure 26 according to the results of the machine learning with the neural networks. To examine whether the artifacts are removed or not, we display Figure 26 and Figure 27 with the Analyzer as files of the cube format. Let us put the cursor on the figures, make right-clicks with the mouse and choose [Export to Analyzer]. Then, Figure 28 and Figure 29 appear.

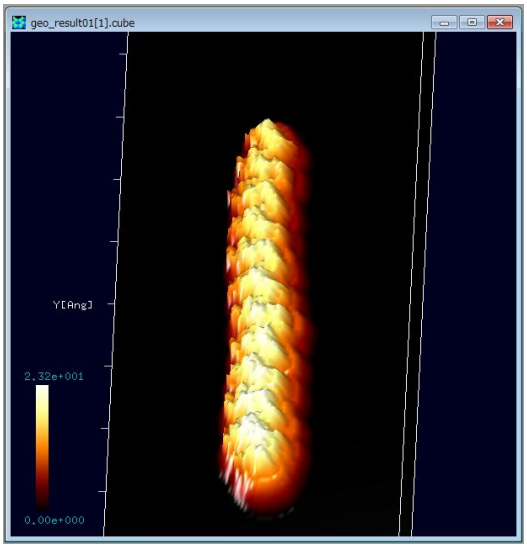

Figure 28 An experimental AFM image of a polymer with the broken double tip.

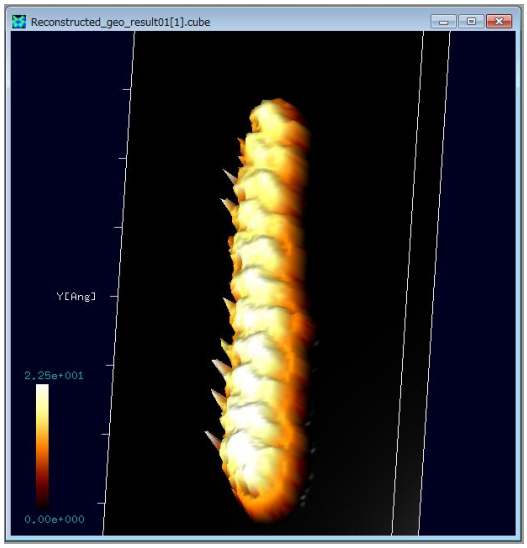

Figure 29 The corrected image of the polymer according to the results of the machine learning with the neural networks.

In Figure 28, we show an experimental AFM image of a polymer with the broken double tip. In Figure 29, we show the corrected image of the polymer according to the results of the machine learning with the neural networks. Looking at Figure 28 and Figure 29, we notice that

the artifacts are removed. However, in Figure 29, we can find some sharp bulges that stick out from the left-hand side of the polymer. This wrong shape of the sample surface occurs because the training data is not enough for the machine learning with the neural networks. To avoid this trouble, we need to give much training data for the machine learning.

3.3 The blind tip reconstruction method and removing the artifacts from experimental images

The blind tip reconstruction method is an algorithm for estimating a shape of the tip from experimental AFM image data in direct. In this section, we explain the blind tip reconstruction method briefly and introduce a method for removing artifacts of an image data obtained with a broken tip.

3.3.a The blind tip reconstruction method

For example, we consider a broken double tip. Let us suppose that we scan the following samples with the broken double tip.
(a) A completely flat sample. (Figure 30)
(b) A sample with some sharp protuberances sticking out from its surface. (Figure 31)
(c) A sample with some blunt protuberances sticking out from its surface. (Figure 32)

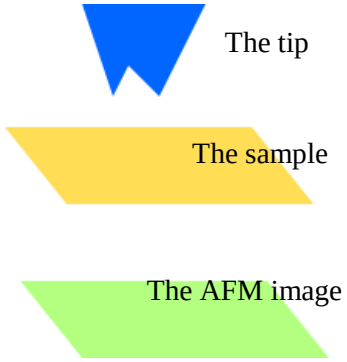

Figure 30 An AFM image of the completely flat sample with the broken double tip.

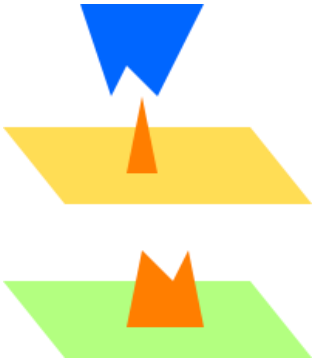

Figure 31 An AFM image of the sample with some sharp protuberances sticking out from its surface using the broken double tip.

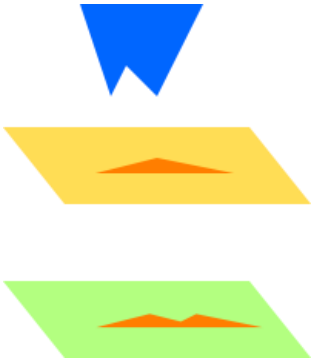

Figure 32 An AFM image of the sample with some blunt protuberances sticking out from its surface using the broken double tip.

Looking at Figure 30, Figure 31 and Figure 32, we notice that the AFM images depend on the shape of the tip. Thus, in the blind tip reconstruction method, we pick some parts of images of the protuberances from the experimental AFM image data. Then, we overlap the pieces of images as shown in Figure 33.

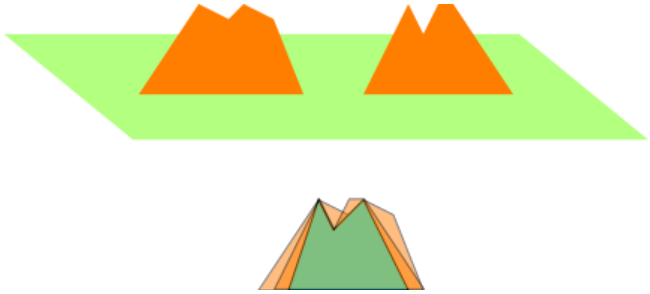

Figure 33 Overlapping two pieces of images of the protuberances sticking out from the sample surface.

Overlapping many pieces of images of the protuberances sticking out from the sample surface, we obtain their intersection. We regard this intersection as an approximation of the shape of the tip. Thus, if we prepare a sample with many protuberances sticking out from its surface, observe it with the AFM and overlap the pieces of images of the protuberances as sample data, we obtain an accurate approximation of the shape of the tip.

We explain this process more precisely in the following. As shown in Figure 34, we take a piece of a image of each protuberance with a certain fixed width from the AFM experimental image data. When we take the piece of the image, we arrange that the highest part of the protuberance is put at the center of the range of the partial image.

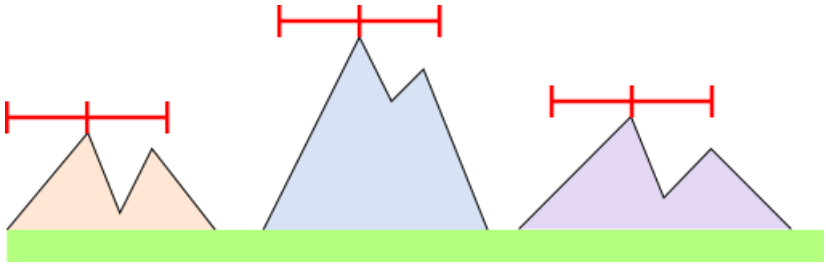

Figure 34 Taking pieces of images of the protuberances with a certain fixed width from the experimental AFM image data.

Next, as shown in Figure 35, we overlap the pieces of the images, which we tear from the experimental AFM image wtith a certain fixed width. Then, we adjust them, so that the highest points of the protuberances are put at the center. Obtaining the intersection of them, we regard it as an approximation of the shape of the tip.

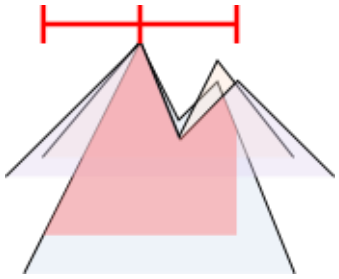

Figure 35 Adjusting the the pieces of the images, which we tear from the experimental AFM image, so that the highest points of the protuberances are put at the center, and obtaining their intersection.

The process explained above is the typical one of the blind tip reconstruction method. Moreover, we can consider a modified version of the blind tip reconstruction method. For the method explained in the above paragraphs, we arrange the torn partial images of the

protuberances of the sample, so that their highest points are put at the center. By contrast, in the modified version, we do not make this arrangement.

In the modified version, we tear the partial images in all possible ways with a certain fixed width from the experimental AFM image, and overlap all of them. For a concrete example, we consider a situation shown in Figure 36. In Figure 36, we take four samples specified with blue short line segments. Although we take samples from the experimental AFM image in all possible ways and overlap all of them, we concentrate on these four samples for a while to make the discussion simple.

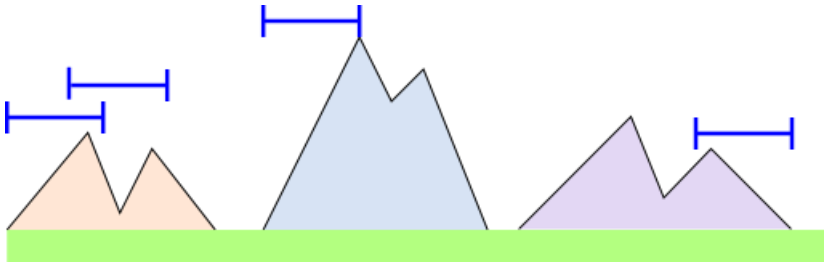

Figure 36 Tearing the partial images in all possible ways with a certain fixed width from the experimental AFM image.

Taking those four samples from the experimental AFM image, we process them as shown in Figure 37. We overlap these samples with arranging that the highest points of the samples are put at the center. Because we put the highest point of the sample at the center, we have to apply a parallel transport to the sample images. This parallel transport makes a gap in the intersection of the overlapped samples. We fill this gap with stuff, whose height is as tall as the part of the center. Overlapping the samples torn from the experimental AFM image in this manner, we obtain their intersection. Then, we regard this intersection as an approximation of the shape of the tip. In general, the approximation of the shape of the tip obtained in this modified method is thinner than that obtained with original blind tip reconstruction method.

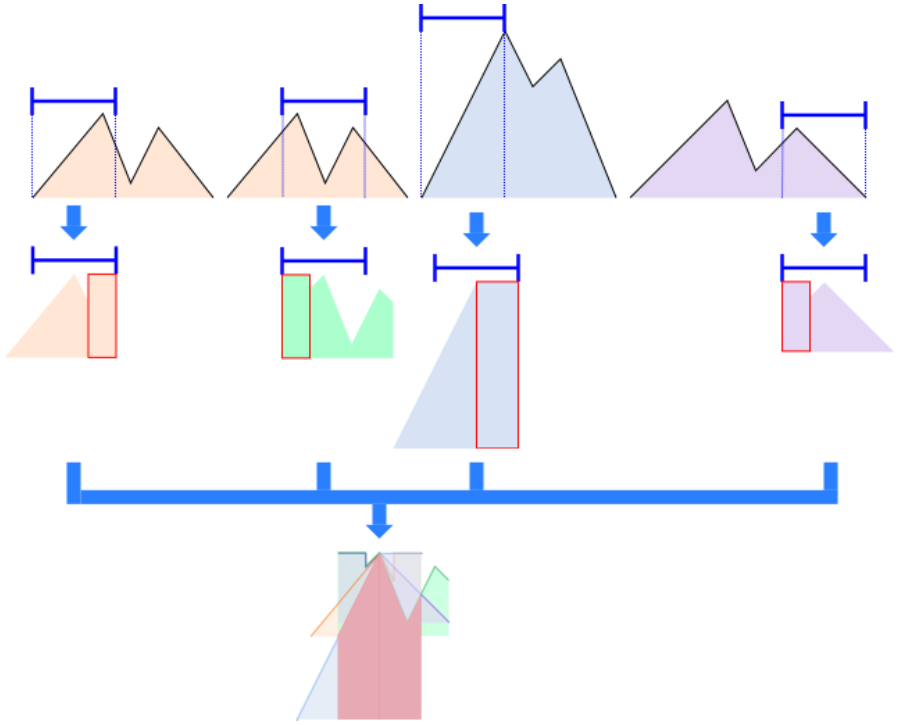

Figure 37 Overlapping samples torn from the experimental AFM image in all possible ways with arranging that the highest points of the samples are put at the center.

From these discussions, we obtain two approximations of the shape of the tip as follows:

1. An approximation of the shape of the tip derived with the original blind tip reconstruction method. (We name this result the approximate shape A.)
2. An approximation of the shape of the tip derived with the modified blind tip reconstruction method, that is to say, with overlapping samples torn from the experimental AFM image in all possible ways. (We name this result the approximate shape B.)

The analyzer has a parameter $x \in [0,1]$ for the blind tip reconstruction method, and we can choose the following options by specifying a value of the parameter x. According to the value of the parameter x, we obtain either the approximate shape A or the approximate shape B. If we set $x = 0$, we obtain the approximate shape A. If we set $x = 1$, we obtain the approximate shape B. if we set $0 < x < 1$, we obtain a superposition of the approximate shape A and the approximate shape B,where the ratio of the shape A to the shape B stands at $(1-x) : x$.

3.3.b Removing the artifacts from the experimental AFM image

If we estimate the shape of the tip from the experimental AFM image data, we can evaluate the original shape of the sample surface, with removing artifacts caused by the broken tip, out of the experimental AFM image data and the data of the approximate shape of the tip. The solver GeoAFM has a function to carry out this process, and we do not explain how it works theoretically in detail here.

In the following paragraphs, with a concrete example, we explain how to obtain an approximate shape of the tip from the experimental AFM image data and evaluate the original shape of the sample surface.

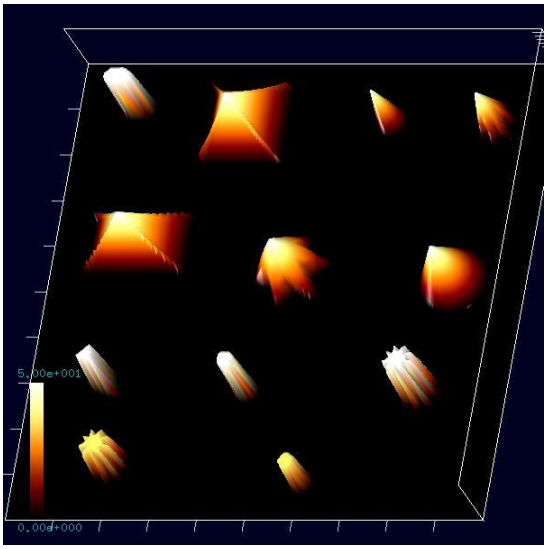

Figure 38 Artificial microstructures for the original sample data.

First, let us think about artificial microstructures for the original sample data as shown in Figure 38.

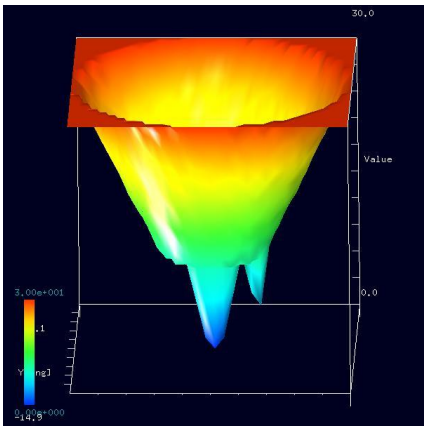

Figure 39 The broken double tip.

Moreover, we prepare the broken double tip as shown in Figure 39.

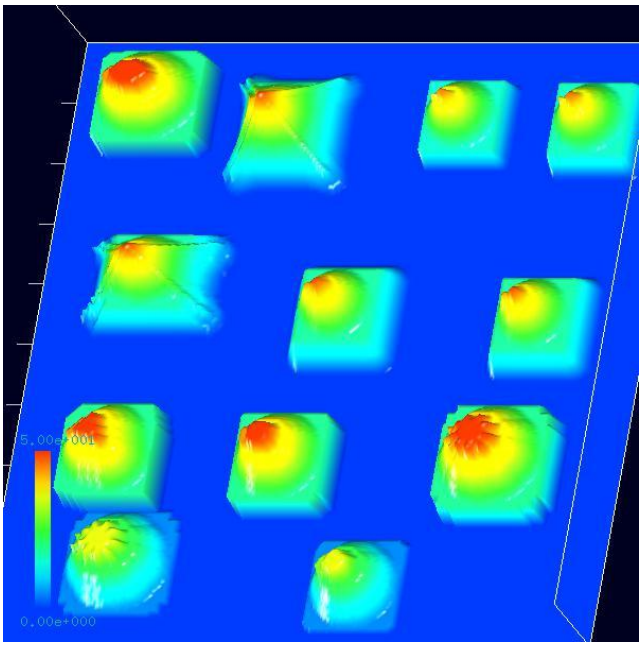

Figure 40 The experimental AFM image obtained by the AFM observation of the artificial microstructures as the sample with the broken double tip.

Performing the AFM observation of the artificial microstructures as the sample with the broken double tip, we obtain the experimental image data shown in Figure 40. In Figure 40, at the tops of protuberances sticking out from the sample surface, we can find artifacts caused by the broken double tip. (We can generate this AFM image with the GeoAFM from the original sample data and the data of the broken double tip.)

From the experimental AFM image data shown in Figure 40, we estimate the shape of the tip. We assume that the experimental AFM image data shown in Figure 40 is stored as the Cube format image file. Clicking [File]→[Open…] on the tool bar of the Analyzer, we can display the AFM experimental image that is stored in the Cube format.

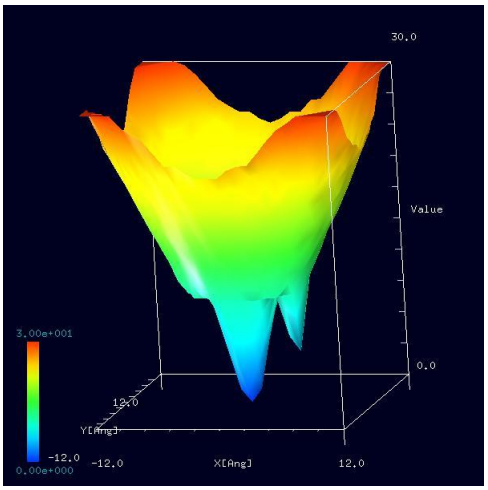

Figure 41 The image of the estimated tip derived with the original blind tip reconstruction method.

Putting the cursor on the window where the image is dislayed, we make a right-click with the mouse. Then, the context menu appears, and we choose [Tip Estimation]. Next, we put 25 for [Tip Nx], 25 for [Tip Ny] and 0.0 for [Parameter]. Then, we obtain the image shown in Figure 41 as the result of the blind tip reconstruction method. In Figure 41, to show the data of the shape of the tip estimated, tip_result.cube, we choose options such as, 3D-View, Rainbow for [Color], and take z-range Normalize off.

In Figure 41, because we put 0.0 for [Parameter] of [Tip Estimation], we obtain an approximation of the shape of the tip for the original blind tip reconstruction method. In fact, the approximate shape of the tip shown in Figure 41 is similar to the original shape of the broken double tip shown in Figure 39.

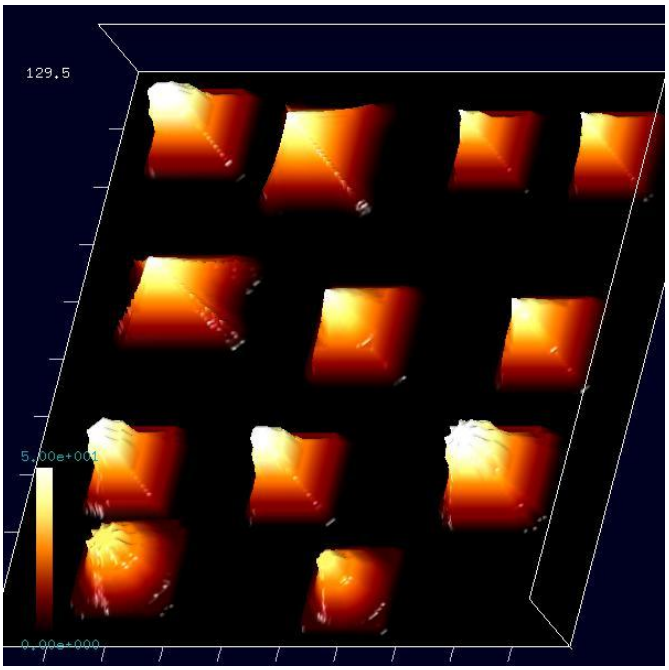

Figure 42 The experimental AFM image in which the artifacts are removed according to the data of the approximate shape of the broken double tip.

We can remove the artifacts from the experimental AFM image as follows. Putting the cursor on the window, wher the AFM image with the artifacts is displayed, we make a right-click with the mouse. Then, the context menu appears, and we choose [Eliminate Tip Effect]. With the dialog of [Select Tip], we select the file "tip_result.cube", which we generate with the blind tip reconstruction method before. Finally, Figure 42 appears.

In Figure 42, we show the experimental AFM image from which we remove the artifacts caused by the broken double tip. In fact, looking at Figure 42, we can confirm that the artifacts are removed from the tops of the protuberances sticking out from the sample surface.

So far, we explain how to perform the original blind tip reconstruction method with putting 0.0 for the parameter. Next, we explain how to perform the modified blind tip reconstruction method with putting 1.0 for the parameter of [Tip Estimation].

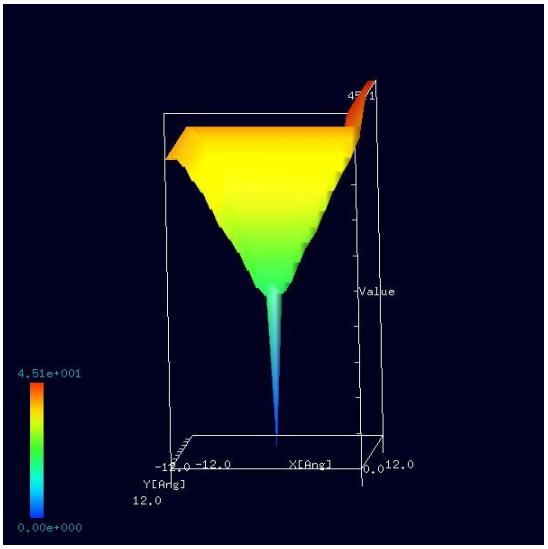

Figure 43 An approximate shape of the tip with putting the parameter 1.0.

In Figure 43, we show an approximate shape of the broken double tip obtained from the experimental AFM image data of the artificial microstructures with putting 1.0 for the parameter of [Tip Estimation]. Looking at Figure 43, we notice that the estimated tip is very sharp.

Assuming this sharp tip, we try removing the artifacts from the experimental AFM image. Then, we obtain Figure 44. Looking at Figure 44, we notice that the artifacts are not removed perfectly from the tops of the protuberances sticking out from the sample surface.

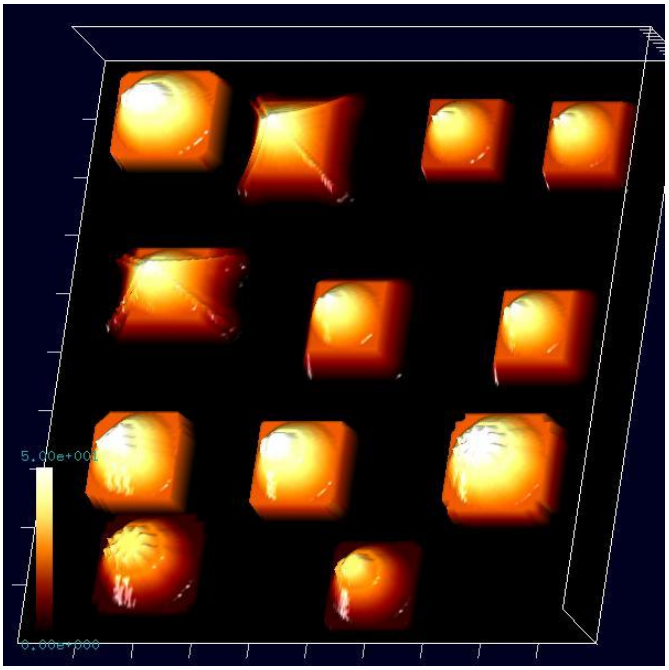

Figure 44 An image obtained with removing the artifacts from the experimental AFM image data according to the estimated shape of the tip with the parameter 1.0.

As discussed above, the value of the parameter of [Tip Estimation] is very important. Thus, we had better choose a suitable value as the parameter of [Tip Estimation] for our own purpose.

3.4 Digital image processing functions for comparing the experimental SPM image data and results of the numerical simulation

The Analyzer has some digital image processing functions for comparing the experimental SPM image data and results of the numerical simulation. Using these functions effectively, we can obtain new knowledge about properties of the physical systems, samples and tips. In this section, we explain them one by one.

3.4.a Thresholding for creating binary images

With the Analyzer, we can apply the thresholding process to the experimental SPM image for creating the binary image, so that we can change the original experimental SPM image into a black-and-white image. We let h_{average} represent an average of the all pixel values, $h_{\max}$ represent the largest pixel value, and $h_{\min}$ represent the smallest pixel value. We pay attention to the fact that the following relation does not always hold in general:

$$h_{\text{average}} = \frac{1}{2}(h_{\max} + h_{\min})$$

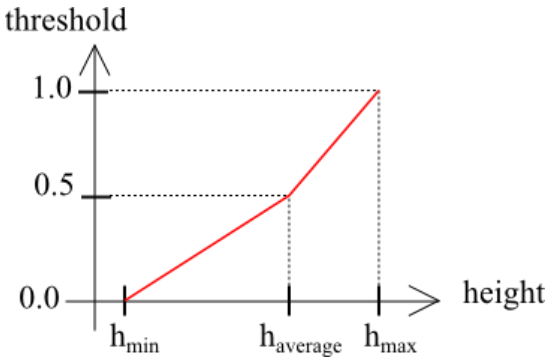

Figure 45 Correspondence between the pixel values and the values of the parameter for thresholding the image data.

Thus, we let the pixel values correspond to the values of a parameter as shown in Figure 45. Specifying the threshold value, we make pixels, whose values are greater than the threshold value, turn white. In a similar way, we make pixels, whose values are smaller than the threshold value, turn black.

In the following paragraphs, we explain how to apply the thresholding process to an experimental SPM image data with the Analyzer actually. The threshold value has to be between 0.0 and 1.0 . By default, the threshould value is set to 0.5.

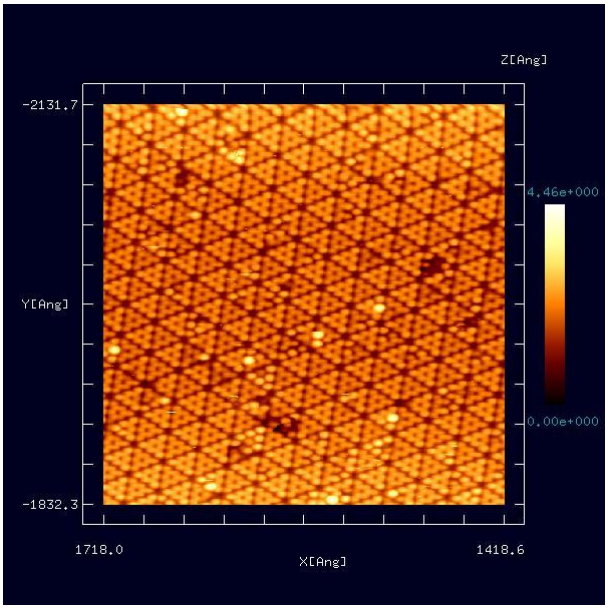

Figure 46 An experimental SPM image that we try to apply the thresholding process

In Figure 46, we show an experimental SPM image. Here, we try to apply the threshoulding process to this image data. We assume that this image is stored as a file with the Cube format and displayed with the Analyzer. (This image is provided by Professor Hiroyuki Hirayama, Nano-Quantum Physics at Surfaces and Interfaces, Department of Materials and Engineering, Tokyo Institute of Technology.)

Putting the cursor on the window where the image of Figure 46 is displayed, we make a right-click with the mouse. Then, a context menu appears, and we choose [Black and white]. Next, a window requiring [Threshold] appears, and we put a preferable value for the threshold.

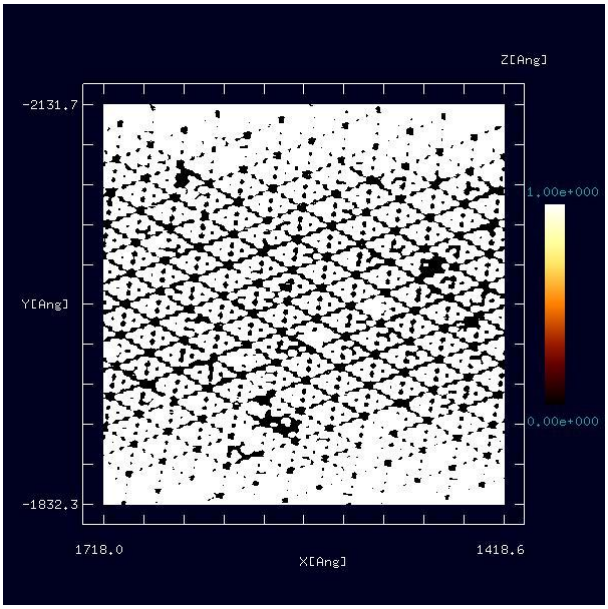

Figure 47 An image obtaine by putting 0.4 for the thresholding value and applying the threshold process to the original experimental SPM image.

Putting 0.4 for the threshold value and applying the thresholding process to the original experimental SPM image, we obtain Figure 47.

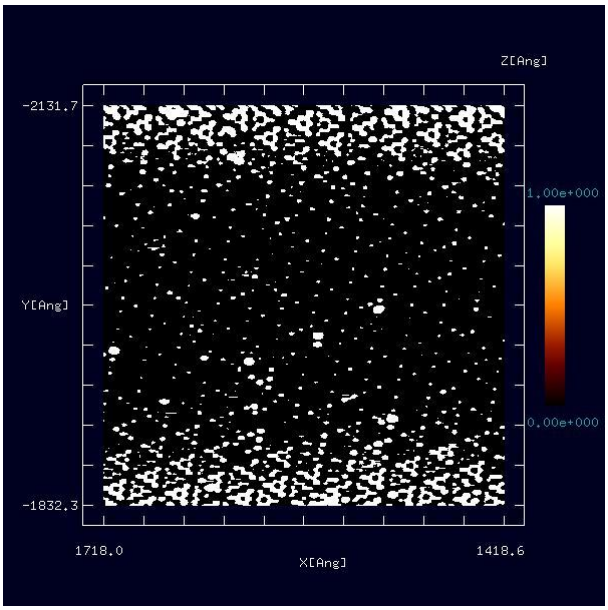

Figure 48 An image obtaine by putting 0.6 for the thresholding value and applying the threshold process to the original experimental SPM image.

Putting 0.6 for the threshold value and applying the thresholding process to the original experimental SPM image, we obtain Figure 48.

3.4.b Adjusting the contrast of the experimental SPM images with the Gamma correction

With the Analyzer, we can adjust the contrast of the experimental SPM images. To change the values of each pixel, we adopt the Gamma correction method. The Gamma correction

adjusts the contrast of the image as follows. First we let $h_{\max}$ represent the largest pixel value and $h_{\min}$ represent the smallest pixel value. We let h represent a value of the pixel at certain point. The Gamma correction changes h into h' according to the following equation:

$$h' = \left(\frac{h - h_{\min}}{\Delta h} \right)^{1/\gamma} \Delta h + h_{\min},$$

where $\Delta h = h_{\max} - h_{\min}$ and γ is a parameter given by the user. In the Analyzer, the parameter is put in the range of $0.25 \le \gamma \le 4$. By default, γ is set to 1.0.

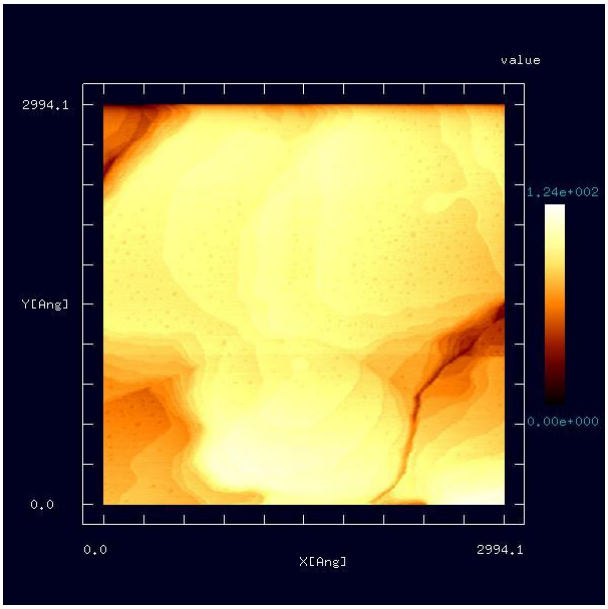

Figure 49 An experimental SPM image whose contrast we try to adjust.

In Figure 49, we show an experimental SPM image. Here, we try to adjust the contrast of this image. We assume that this image is stored as a file with the Cube format and displayed with the Analyzer. (This image is provided by Professor Ken-ichi Fukui, Surface/Interface Chemistry Group, Department of Materials Engineering Science, Osaka University.) In Figure 49, the image is too bright, so that we cannot distinguish small differences of varied surface heights on the sample.

Putting the cursor on the window, where the image of Figure 49 is displayed, we make a right-clickwith the mouse. Then, the context menu appears, and we choose [Contrast adjustment (Gamma correction)]. Next, a window requiring [Gamma] appears, and we put a prefebrable value for [Gamma].

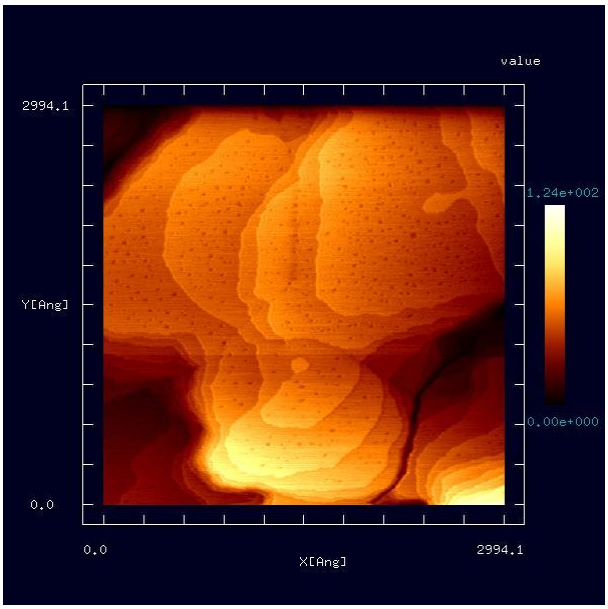

Figure 50 A corrected image obtained with adjusting the contrast of the original experimental SPM image with $\gamma = 0.33$

Adjusting the contrast of the image shown in Figure 49 with $\gamma = 0.33$, we obtain a corrected image shown in Figure 50. Because of the adjustment of the contrast, the image is improved and we can distinguish differences of varied surface heights on the sample well.

3.4.c Edge detection with the Sobel filter

With the Analyzer, we can detect edges of the experimental SPM images.

h(-1,1)	h(0,1)	h(1,1)
h(-1,0)	h(0,0)	h(1,0)
h(-1,-1)	h(0,-1)	h(1,-1)

Figure 51 A 3×3 pixel neighborhood extracted from the experimental SPM image.

An algorithm of the edge detection is as follows. In Figure 51, we show a 3×3 pixel neighborhood extracted from the experimental SPM image. In the following paragraphs, we explain how to apply the Sobel filter to the pixel $h(0,0)$.

1	0	-1
2	0	-2
1	0	-1

Figure 52 A kernel for computing a derivative with respect to x.

We take a weighted sum of values of pixels for the 3×3 pixel neighborhood with a kernel shown in Figure 52. We regard this sum as f_x, a derivative with respect to x.

1	2	1
0	0	0
-1	-2	-1

Figure 53 A kernel for computing a derivative with respect to y.

We take a weighted sum of values of pixels for the 3×3 pixel neighborhood with a kernel shown in Figure 53. We regard this sum as f_y, a derivative with respect to y.

Here, let us compute the following value:

$f' = (f_x^{\,2} + f_y^{\,2})^{1/2}$.

Then, we replace $h(0,0)$ with the derivative f' obtained above. We apply this operation to all pixels of the experimental SPM image.

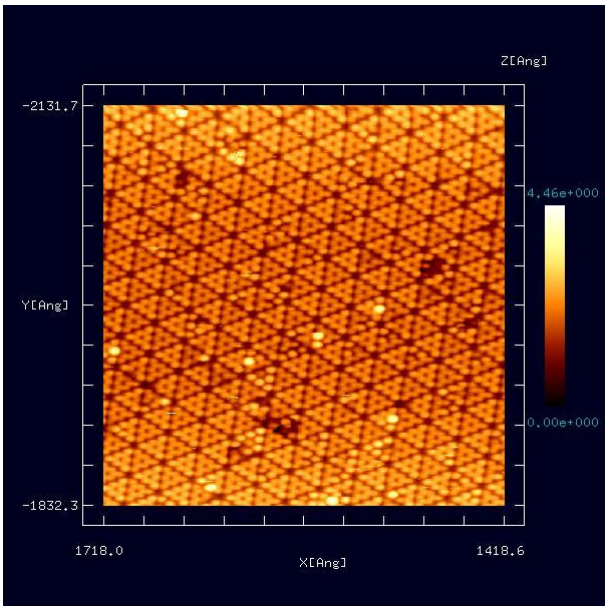

Figure 54 An experimental SPM image, to which we try to apply the edge detection.

In Figure 54, we show an experimental SPM image. Here, we try to apply the edge detection to this image data. We assume that this image is stored as a file with the Cube format and displayed with the Analyzer. (This image is provided by Professor Hiroyuki Hirayama, Nano-Quantum Physics at Surfaces and Interfaces, Department of Materials and Engineering, Tokyo Institute of Technology.)

Putting the cursor on the window, where the image of Figure 54 is displayed, we make a right-click with the mouse. Then, a context menu appears, and we choose [Edge detection (Sobel filter)].

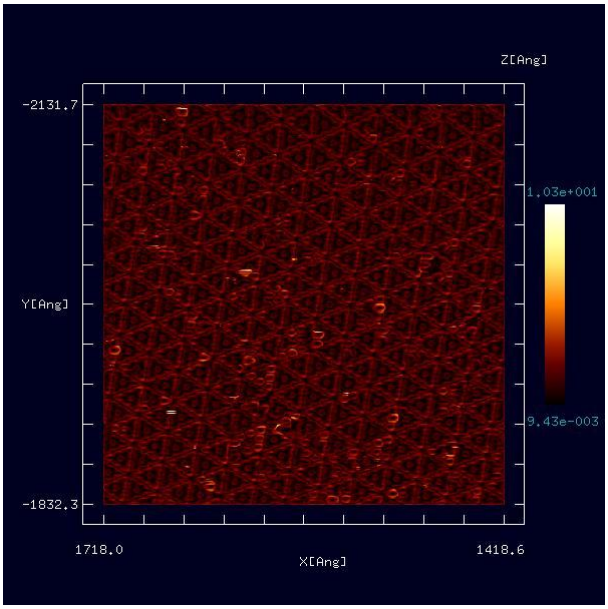

Figure 55 An image obtained with applying the edge detection to the original experimental SPM image.

Applying the edge detection to the original experimental SPM image, we obtain an image shown in Figure 55. Because obtained image is not bright enough, we adjust its contrast.

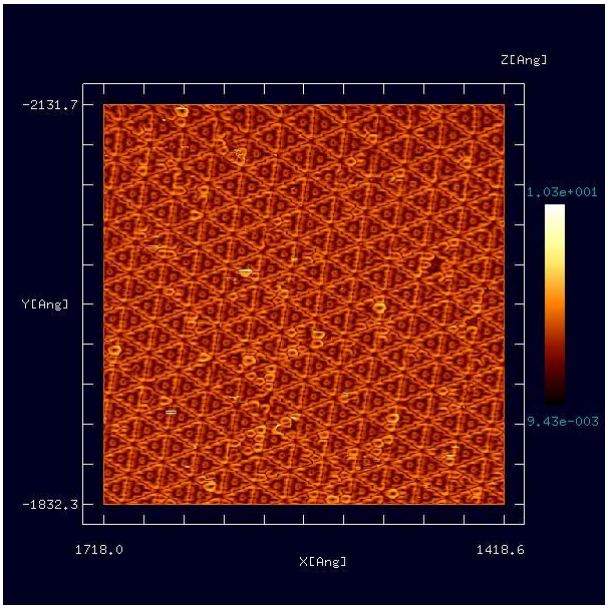

Figure 56 An image obtained by the edge detection and the adjustment of the contrast with $\gamma = 2.0$.

Adjusting the contrast of the image, which is obtained by the edge detection above, with $\gamma = 2.0$, we obtain an image shown in Figure 56. Because of the adjustment of the contrast, the image of Figure 56 is very clear.

3.4.d Noise reduction with the median filter

With the Analyzer, we can remove noises from the experimental SPM image data.

h(-1,1)	h(0,1)	h(1,1)
h(-1,0)	h(0,0)	h(1,0)
h(-1,-1)	h(0,-1)	h(1,-1)

Figure 57 A 3×3 pixel neighborhood extracted from the experimental SPM image.

We explain how to remove noises from the experimental SPM image data as follows. In Figure 57, we show a 3×3 pixel neighborhood extracted from the experimental SPM image. We apply the median filter to the pixel $h(0,0)$ in the following manner. First, we find the median from nine entries in the 3×3 pixel neighborhood. Here, the median is the fifth entry in ascending order of the nine entries. Second, we replace $h(0,0)$ with the median. Third, we carry out this process to all pixels in the experimental SPM image.

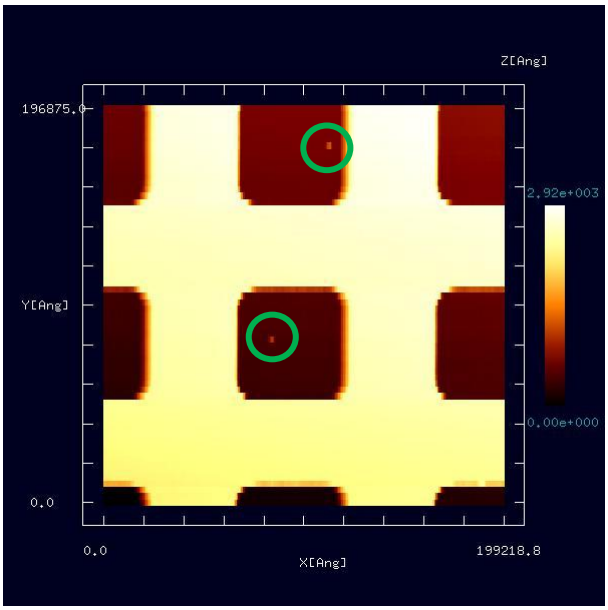

Figure 58 An experimental SPM image, to which we try to apply the noise reduction.

In Figure 58, we show an experimental SPM image. Here, we try to remove noises from this image. We assume that this image is stored as a file with the Cube format and displayed with the Analyzer. (This image is provided by Professor Katsushi Hashimoto, Solid-State Quantum Transport Group, Department of Physics, Graduate School of Science, Tohoku University.) Looking at Figure 58, we notice that there are noises inside a green circle.

Putting the cursor on a window, where the image of Figure 58 is displayed, we make a right-click with the mouse. Then, a context menu appears, and we choose [Noise reduction (median filter)].

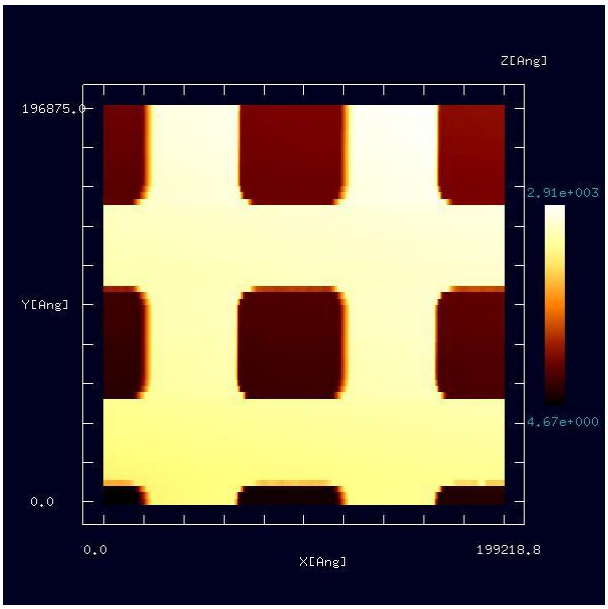

Figure 59 An image obtained with applying the noise reduction to the original experimental SPM image.

In Figure 59, we show an image obtained by applying the noise reduction to the experimental SPM image shown in Figure 58. Looking at the corrected image, we notice that the noises inside the green circles are removed.

3.4.e Displaying cross sections

With the Analyser, specifying two end points on the experimental SPM image, we can display a cross section of sample surface along a line segment between the two end points.

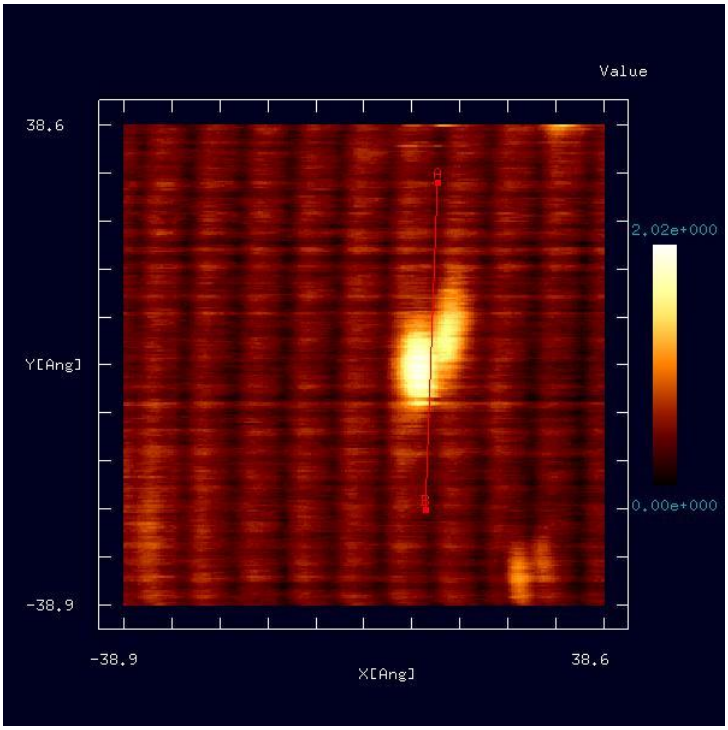

Figure 60 A line segment AB that determines the cross section of the sample surface in the experimental SPM image.

In Figure 60, we show an experimental SPM image. We assume that this image is stored as a file with the Cube format and displayed with the Analyzer. (This image is provided by Fukutani Laboratory, Surface and Vacuum Physics, Institute of Industrial Science, The University of Tokyo.) Here, we explain how to display the cross section of the sample surface in the following paragraphs using the image of Figure 60.

First, let us put the cursor on the image of the window and make a double-click with the mouse. Then, we can specify the end point A on the image. Second, let us move the cursor properly and make a double-click again. Then, we

can specify the end point B, and a line segment between end points A and B appears.

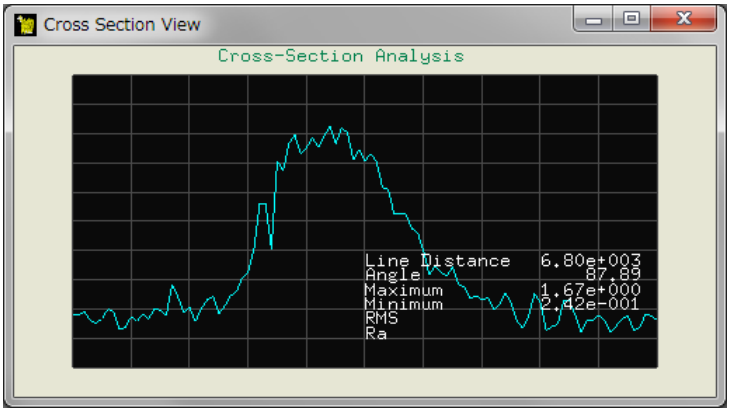

Figure 61 A cross section specified with the line segment AB.

If we determine the line segment AB, a cross section of Figure 61 appears.

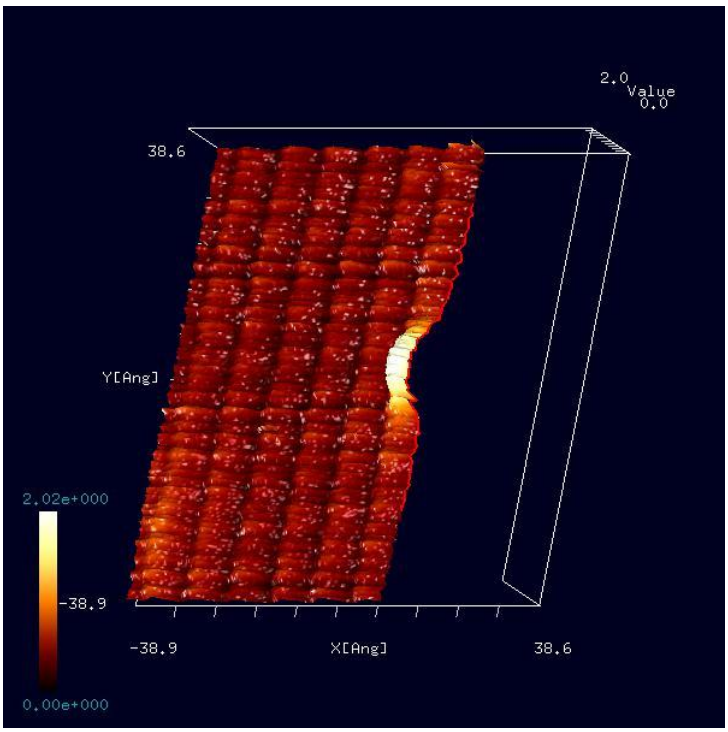

Figure 62 A 3D cross-section view derived from the experimental SPM image.

Moreover, putting the cursor on the window that displays the SPM image, making a right-click, and choosing [3D-View] and [Cross-Section (D-click)]→[Clipping] from the context menu, we obtain a 3D cross-section view as shown in Figure 62.

3.4.f Calculating an angle from three points

With the Analyzer, specifying three points A, B and C on the experimental SPM image, we can obtain lengths of line segments AB and BC and an angle of $\angle ABC$.

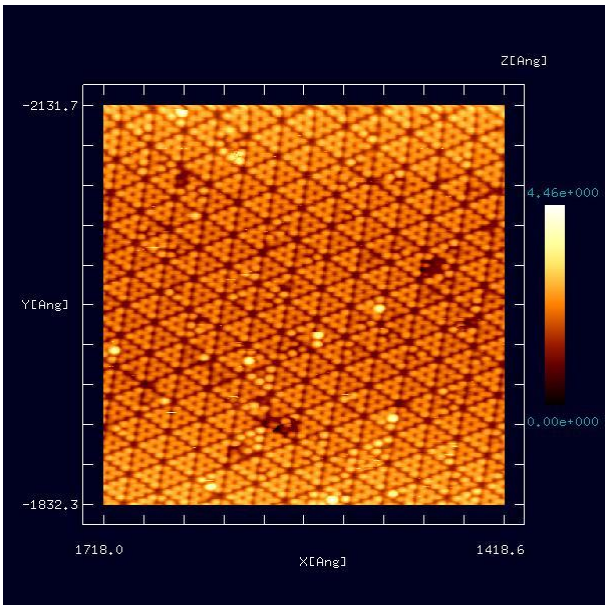

Figure 63 An original experimental SPM image of the structure of Si(111)-(7×7)DAS.

In Figure 63, we show an experimental SPM image. Here, we try to calculate lengths of line segments and an angle from three points on this image data. We assume that this image is stored as a file with the Cube format and displayed with the Analyzer. (This image is provided by Professor Hiroyuki Hirayama, Nano-Quantum Physics at Surfaces and Interfaces, Department of Materials and Engineering, Tokyo Institute of Technology.)

In Figure 63, the structure of Si(111)-(7×7)DAS is shown. Because the image is not clear, we apply the edge detection and the adjustment of the contrast with $\gamma = 2.0$. Moreover, we enlarge the image using the wheel of the mouse and drag the image by moving the mouse with a left-click properly. Finally, we obtain Figure 64.

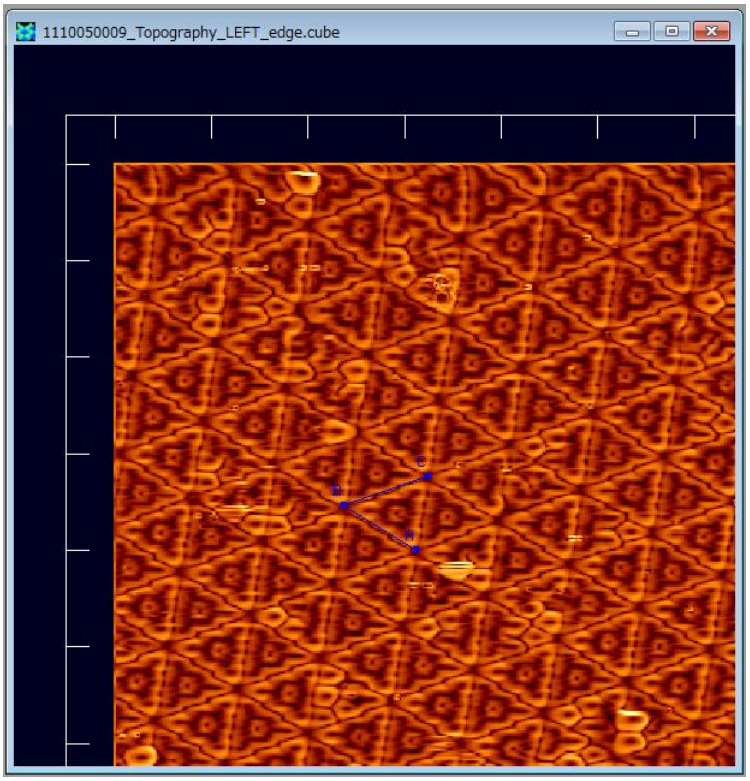

Figure 64 An SPM image of Si(111)-(7×7)DAS structure obtained by the edge detection and the adjustment of the contrast with $\gamma = 2.0$.

Putting the cursor on the window of Figure 64, we make a right-click with the mouse. Then, a context nenu appears, and we choose [Measurement of lines and their angle]. Next, we specify three points A, B and C on the processed SPM image by double-clicks. Then, blue line segments AB and BC appear.

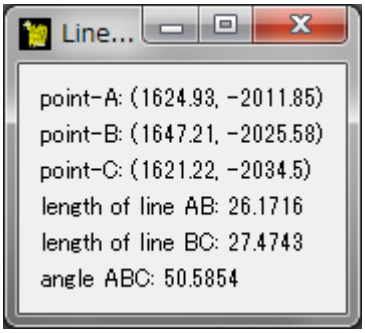

Figure 65 The results of the measurements, lengths of the line segments AB, BC and ∠ABC.

After the above process, a window that shows results of measurements appears as shown in Figure 65. In this example, the results of the measurements are provided as follwos:

The length of the line segment AB: 26.1716 [angstom]
The length of the line segment BC: 26.4743 [angstom]
∠ABC : 50.5854 [degree]

3.5 Examples of practical uses of the Analyzer

Here, we introduce some examples as practical uses of the Analyzer. We compare a simulation result of Si(111)-(7×7)DAS structure obtained with the GeoAFM and an experimental SPM image of Si(111)-(7×7)DAS structure. As shown in Figure 66, we display the simulation result and the experimental image simultaneously on the Analyzer. (This experimental image is provided by Professor Hiroyuki Hirayama, Nano-Quantum Physics at Surfaces and Interfaces, Department of Materials and Engineering, Tokyo Institute of Technology.)

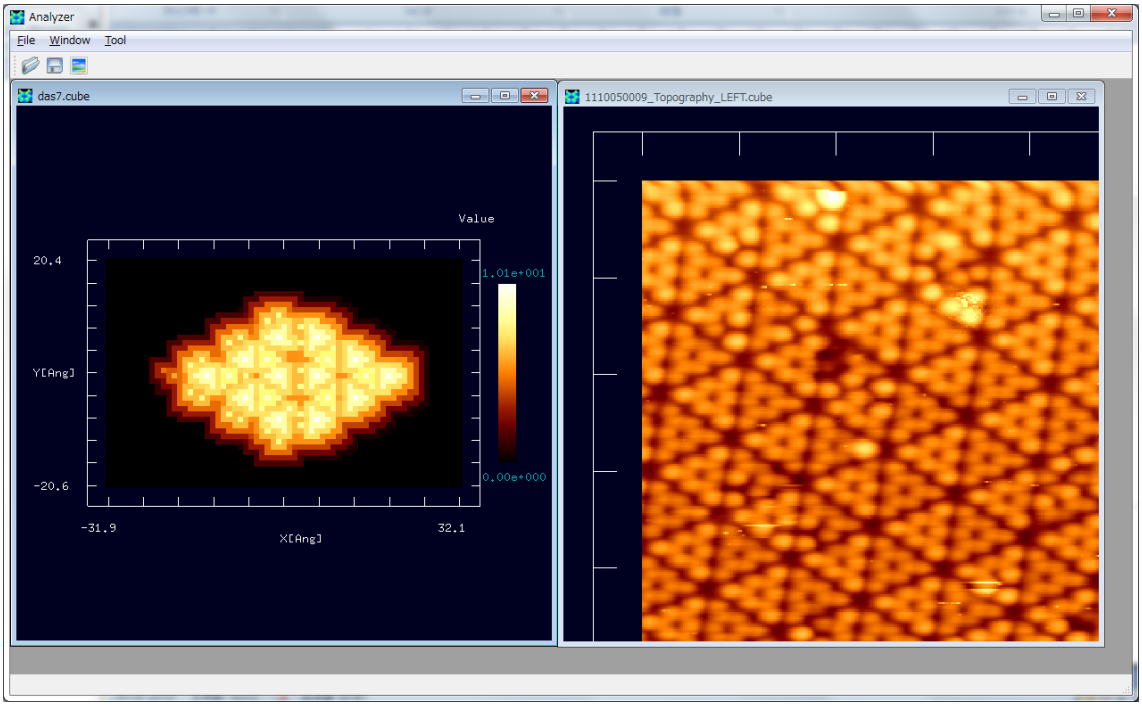

Figure 66 Comparing a simulation result of Si(111)-(7×7)DAS structure obtained with the GeoAFM and an experimental SPM image of Si(111)-(7×7)DAS structure.

To obtain the image of the experimental SPM data shown in Figure 66, we enlarge the image using the wheel of the mouse and drag the image by moving the mouse with a left-click properly.

For both the simulation result and the experimental AFM image, we derive lengths and angles of the Si(111)-(7×7)DAS structure with the function [Measurement of lines and their angle] as shown in Figure 67.

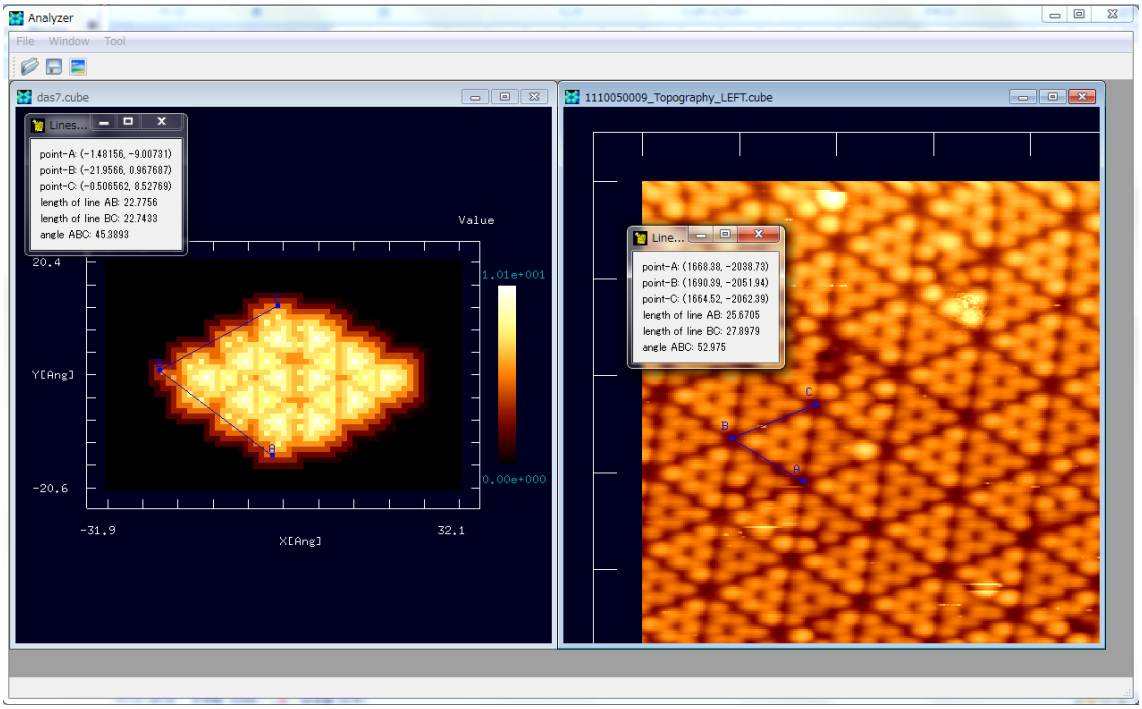

Figure 67 Deriving lengths and angles of the Si(111)-(7×7)DAS structure with the function [Measurement of lines and their angle] for the simulation result obtained with the GeoAFM and an experimental SPM image.

For the simulation result obtained with the GeoAFM, we obtain the following results:
The length of the line segment AB: 22.7756 [angstrom]
The length of the line segment BC: 22.7433 [angstrom]
∠ABC : 45.3893 [degree]

For the experimental image, we obtain the following results:
The length of the line segment AB: 25.6705 [angstrom]
The length of the line segment BC: 27.8979 [angstrom]
∠ABC: 52.975 [degree]

The above results of the measurements are consistent with each other between the result of the simulation and the experimental image.

Moreover, let us use the function of [Cross-Section (D-click)]. As shown in Figure 68, we can compare cross sections of the simulation result and the experimental SPM image.

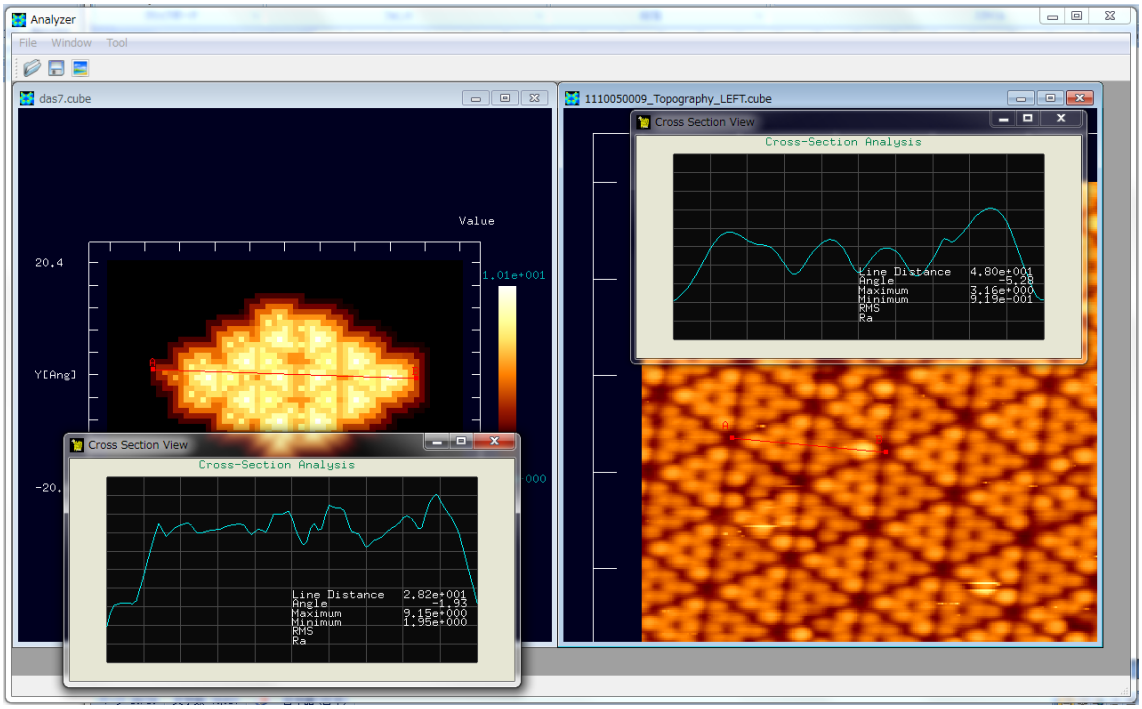

Figure 68 Comparing cross sections of the simulation result and the experimental SPM image of the Si(111)-(7×7)DAS structure using the function [Cross-Section (D-click)].

As explained in this section, using the Analyzer, we can apply various digital processings to the simulation results and the experimental SPM images at will in convenient manners. Thus, you can obtain new knowledge from them.

Chapter 4 Geometrical Mutual AFM Simulator (GeoAFM)

Geometrical Mutual AFM Simulator (GeoAFM) provides users with a kind of a three-way data processor, so that it reconstructs the one out of the other two among three geometrical elements, a tip, a sample material and its AFM image.

A characteristic of this module is that it can only sort out geometrical data of the tip, the sample material and its AFM image. Thus, it never includes the contribution caused by the van der Waals interaction between the tip and the sample material. Moreover, this simulator assumes that the tip and the sample material never suffer from deformation. Hence, the GeoAFM produces a result from only the information of the geometry of the tip, the sample material and the AFM image. Throughout the simulation, this module assumes that the tip always touches the surface of the sample material, so that it scans the surface of the sample in the so-called contact mode.

As mentioned above, the GeoAFM never takes equations of both classical and quantum physics into account. Considering the tip, the sample material and its AFM image to be genuine geometrical objects and assuming the tip and the sample material always to be in the contact mode, this module performs the simulation in a manner of elementary geometry. Thus, this simulator is not suitable for investigating phenomena of the microscopic system, where the quantum effects are significant. In contrast, this module is very suitable for simulating AFM images of semiconductor devices of [μm] scale order and biological macromolecules.

GeoAFM estimates a result from only the information of the geometry of the tip, the sample material and the AFM image. Because the module derives a result without any physical consideration such as an equation of motion, users can obtain simulated results very rapidly, within a few seconds.

4.1 Outline of the mechanism and the computing method in the mutual simulation of the tip, the sample material and the AFM image.

The GeoAFM describes the all data as heights on the two-dimensional xy-plane, where the data include the geometrical data of the tip, the sample material and the AFM image. In other words, the two-dimensional xy-plane is divided into squares (e.g. 1 Å x 1 Å), and then a geometrical data is described by heights on those squares.

In the GeoAFM, we may use a tip of pyramidic shape registered in the database. Then, the pyramidic tip data is described as a discrete solid body on the squares. Thus, the module treats a nearly pyramidic solid shape composed of cuboid blocks.

When a tip or a sample is a crystal or a polymer with a lot of atoms, the solid shape made by the atoms is also considered to be composed of cuboid blocks.

4.1.a Simulation of the AFM image, from the data of the tip and the sample

As seen in

Figure 69 and Figure 70, we define the tip shape data as $T(x,y)$ and the sample shape data as $S(x,y)$.

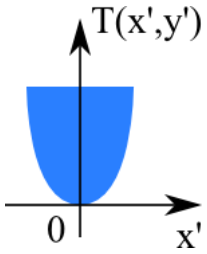

Figure 69 Tip shape data $T(x,y)$.

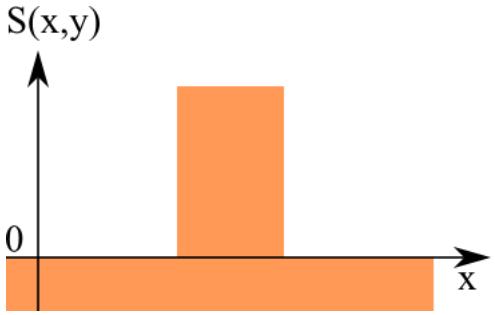

Figure 70 Sample shape data $S(x,y)$.

In this case, when the tip contacts the sample, the position of the top of the tip is apart from the sample surface due to the tip shape itself (Figure 71).

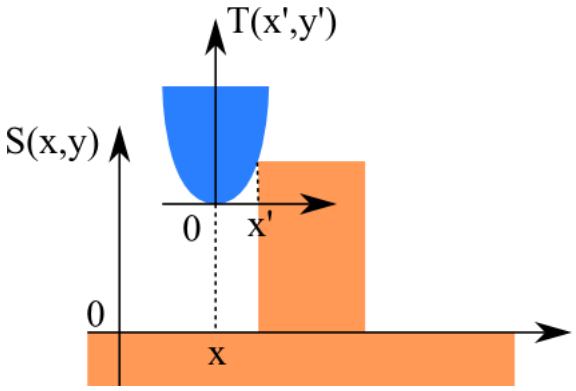

Figure 71 Appearance when the tip contacts the sample.

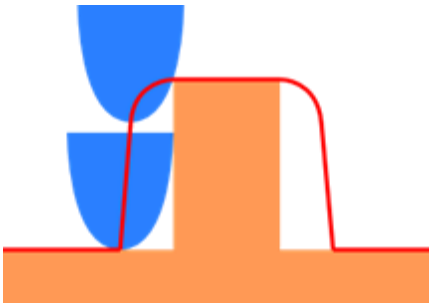

Figure 72 Trajectory of the top of the tip when the tip scans on the sample surface.

Considerting the above effect, the tip scans on the sample surface. Figure 72 shows the trajectory of the top of the tip, which becomes duller than the true shape of the sample surface due to the tip thickness.

In summary, the estimated AFM image $I(x,y)$ is calculated by

$$I(x,y) = \max_{x',y'}[S(x+x',y+y') - T(x',y')].$$

4.1.b Simulation of the sample surface, from the tip data and the observed AFM image

In a similar manner above, the estimated sample shape $S(x,y)$ is calculated by

$$S(x,y) = \max_{x',y'}[I(x-x',y-y') + T(x',y')],$$

usinig the tip shape $T(x,y)$ and the AFM image $I(x,y)$.

4.1.c Simulation of the tip surface, from the sample data and the observed AFM image

In a similar manner above, the estimated tip shape $T(x, y)$ is calculated by

$$T(x, y) = \max_{x', y'}[S(x + x', y + y') - I(x', y')],$$

usinig the sample shape $S(x, y)$ and the AFM image $I(x, y)$.

4.2 Case example of GeoAFM

4.2.a Simulation of the AFM image, from the data of the tip and the sample

As an example, we simulate the estimated AFM image by the use of a pyramidic tip and a "collagen-1clg" data as a sample.

We choose a pyramidic tip shown in Figure 73. Figure 74 shows the molecular structure of a polymer chain of the collagen-1clg.

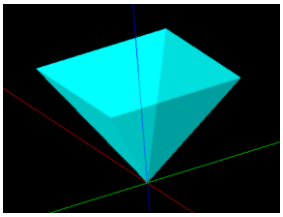

Figure 73 A pyramidic tip.

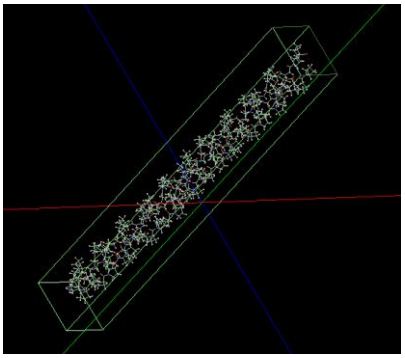

Figure 74 The molecular structure of a polymer chain of the collagen-1clg.

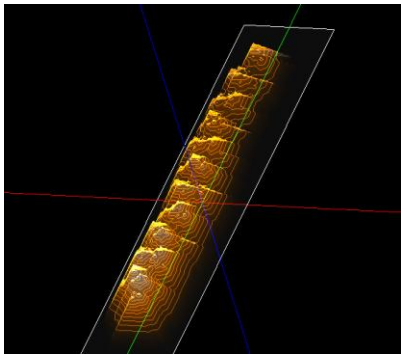

Figure 75 The estimated AFM image.

Using the tip of Figure 73 and the sample of Figure 74, we obtain the estimated AFM image shown inFigure 75.

4.2.b Simulation of the sample surface, from the tip data and the observed AFM image

As an example, we simulate the estimated sample shape by the use of a pyramidic tip and an AFM image which has been obtained in the previous subsection.

We choose a pyramidic tip shown in Figure 76. We choose the AFM image given in the previous subsection shown in Figure 77, as an input AFM image.

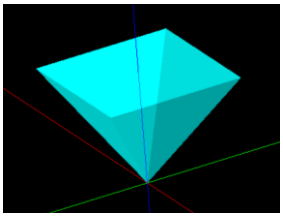

Figure 76 A pyramidic tip.

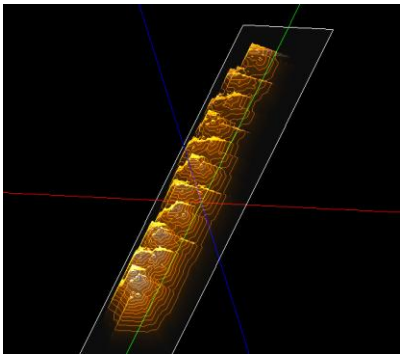

Figure 77 The AFM image of a polymer chain of collagen-1clg.

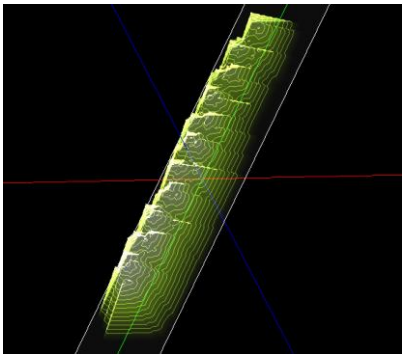

Figure 78 The estimated sample shape.

We obtain the estimated sample shape shown in Figure 78.

4.2.c Simulation of the tip surface, from the sample data and the observed AFM image

As an example, we simulate the estimated tip shape by the use of a sample shape given in the last subsection and an AFM image given in the previous subsection.

We choose the sample shape given in the last subsection shown in Figure 79, as an input sample shape. We choose the AFM image given in the previous subsection shown in Figure 80, as an input AFM image.

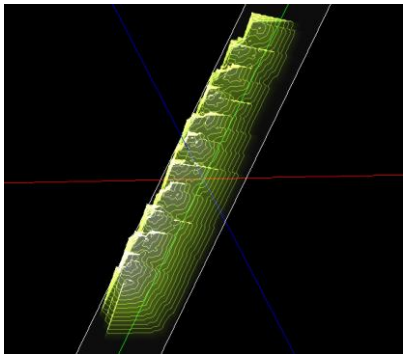

Figure 79 The sample shape of a polymer chain of collagen-1clg.

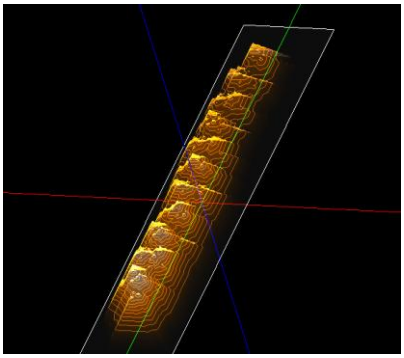

Figure 80 The AFM image of a polymer chain of collagen-1clg.

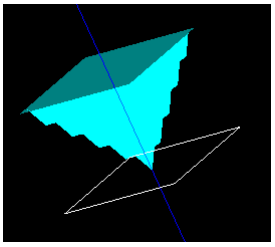

Figure 81 The estimated tip shape.

We obtain the estimated tip shape shown in Figure 81.

4.3 Users guide: how to use GeoAFM

Here we show the concrete operation procedures corresponding to the previous section.

4.3.a Simulation of the AFM image, from the data of the tip and the sample

Table 3 The operation procedure to simulate an AFM image from the tip shape and the sample shape.

Procedure	Input example
Click [File] → [New].	

[Create new project] dialog opens.	Type "geoafm_test001" as [Project name].
Click the [Setup] tab in [Project Editor].	
Right click on the [Component] item, then choose [Add Tip] → [Pyramid].	
Define a parameter of the tip in the [Set Pyramid Angle] dialog.	Type "32.0" as [angle (deg)].
Right click on the [Component] item, then choose [Add Sample] → [Database].	Double-click [collagen-1clg] in the [Sample DB View].
Right click on the main screen to show a context menu.	
Context menu → [GeoAFM] → [Set GeoAFM Resolution]	Type "1.0" [Å] in the [Set Resolution] dialog.
Context menu → [GeoAFM] → [Show Simulated Image]	The estimated AFM image is simulated and displayed on the screen.
Remove a tick from the context menu → [Show Tip]	
Remove a tick from the context menu → [Show Sample]	
Context menu → [GeoAFM] → [Export Simulated Data]	Save the estimated AFM image as "collagen-1clg_afm_image.cube".

4.3.b Simulation of the sample surface, from the tip data and the observed AFM image

Table 4 The operation procedure to simulate a sample surface from the tip shape and the AFM image.

Procedure	Input example
Click [File] → [New].	
[Create new project] dialog opens.	Type "geoafm_test002" as [Project name].
Click the [Setup] tab in [Project Editor].	
Right click on the [Component] item, then choose [Add Tip] → [Pyramid].	
Define a parameter of the tip in the [Set Pyramid Angle] dialog.	Type "32.0" as [angle (deg)].
Right click on the [Component] item, then choose [Add Image]→[File].	Choose "collagen-1clg_afm_image.cube".
Right click on the main screen to show a context menu.	
Context menu → [GeoAFM] → [Set GeoAFM Resolution]	Type "1.0" [Å] in the [Set Resolution] dialog.
Context menu → [GeoAFM] → [Show Simulated Sample]	The estimated sample shaple is simulated and displayed on the screen.
Remove a tick from the context menu → [Show Tip]	
Remove a tick from the context menu → [Show Image]	
Context menu → [GeoAFM] → [Export Simulated Data]	Save the estimated sample shape as "collagen-1clg_sample.cube".

4.3.c Simulation of the tip surface, from the sample data and the observed AFM image

Table 5 The operation procedure to simulate a tip shape from the sample shape and the AFM image.

Procedure	Input example

Click [File] → [New].	
[Create new project] dialog opens.	Type "geoafm_test003" as [Project name].
Click the [Setup] tab in [Project Editor].	
Right click on the [Component] item, then choose [Add Sample] → [File].	Choose "collagen-1clg_sample.cube".
Right click on the [Component] item, then choose [Add Image]→[File].	Choose "collagen-1clg_afm_image.cube".
Right click on the main screen to show a context menu.	
Context menu → [GeoAFM] → [Set GeoAFM Resolution]	Type "1.0" [Å] in the [Set Resolution] dialog.
Context menu → [GeoAFM] → [Show Simulated Tip]	The estimated tip shaple is simulated and displayed on the screen.
Remove a tick from the context menu → [Show Sample]	
Remove a tick from the context menu → [Show Image]	

Chapter 5 A Method for Investigating Viscoelastic Contact Problem

[Caution: Contents of this section concern ongoing research studies. Thus, we may modify the contents of this setion in the future in revised versions of this guidebook.]

5.1 A brief review of the JKR (Johnson-Kendall-Roberts) theory

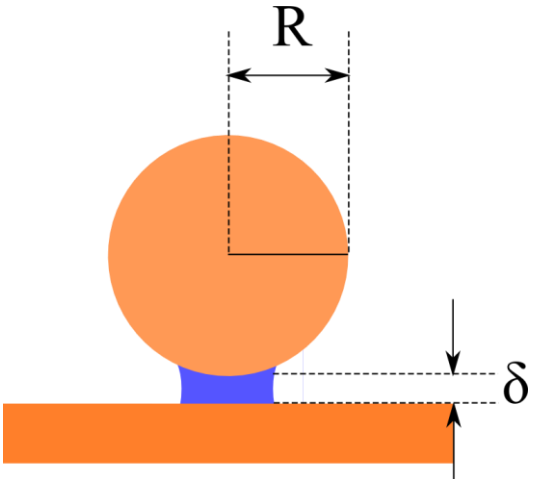

Figure 82 An adhesive force between a sphere of a radius R and an infinite flat surface that belongs to a semi-infinite solid.

At first, we consider an adhesive force betweena sphere of a radius R and an infinite flat surface that belongs to a semi-infinite solid as shown in Figure 82. We assume that the sphere is elastic but it has no viscous characteristic. By contrast, the sem-infinite solid is viscoelastic and its surface tension is given by γ.

According to the JKR theory, we can write down a force F and a distance δ between the sphere and the solid as follows:

$$F = 4F_c(x^3 - x^{3/2}),$$

and

$$\delta = \delta_0(3x^2 - 2\sqrt{x}).$$

A parameter x found in the above two equations represents a dimensionless quantity. It is in proportion to a contact area of the sphere and the solid. Moreover, it satisfies a condition $6^{-2/3} \le x$. This implies that the tip is not in contact with the sample surface under $x < 6^{-2/3} (= 0.303)$.

Furthermore, F_c and δ_0 are given as follows:

$$F_c = 3\pi\gamma R,$$

$$\delta_0 = \frac{a_0^{\,2}}{3R},$$

$$a_0 = \left(\frac{9\pi\gamma R^2}{E^*}\right)^{1/3},$$

$$\frac{1}{E^*} = \frac{1-\sigma_1^{\,2}}{E_1} + \frac{1-\sigma_2^{\,2}}{E_2},$$

where E_1 and E_2 represent Young's moduli of the tip and sample, and σ_1 and σ_2 represent Poisson's ratios of the tip and sample, respectively. Moreover, a_0 represents the contact area at a zero load. That is to say, when the tip goes down below the surface of the sample, and the

adhesive force of the surface tension and the repulsive force of the elasticity cancel each other out with the tip, the area of their contact is equal to a_0.

In fact, the parameter x is given by $x = a/a_0$, where a represents the area of the contact between the tip and the sample surface. Thus, when the force applied to the sphere (the tip) is equal to zero, the relation $x = 1$ holds. Because of these facts, the range of the parameter x is given by $6^{-2/3} \le x \le 1$ under the process of the tip being in contact wity the sample surface.

We show graphs of $F/(4F_c) = x^3 - x^{3/2}$ and $F/(4F_c) = x^3 - x^{3/2}$ as follows.

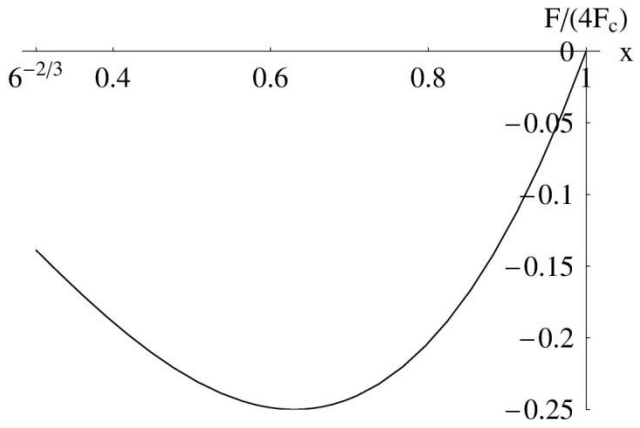

Figure 83 A graph of $F/(4F_c) = x^3 - x^{3/2}$.

Figure 83 shows a graph of $F/(4F_c) = x^3 - x^{3/2}$, where we let the upward force of $F/(4F_c)$ correspond to the positive direction. In the graph of Figure 83, $F/(4F_c)$ is always negative. This implies the following. The force that the semi-infinite solid (the sample) applies to the sphere (the tip) is always attractive.

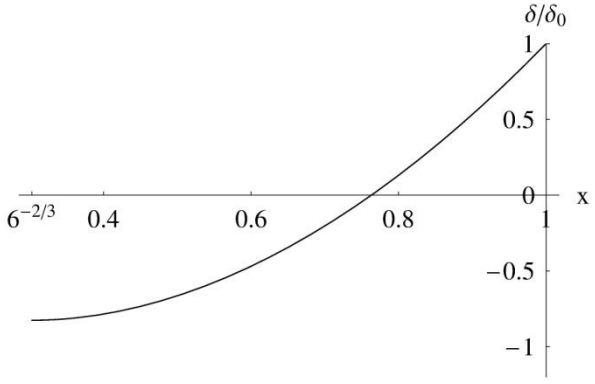

Figure 84 A graph of $\delta/\delta_0 = 3x^2 - 2\sqrt{x}$.

Figure 84 shows a graph of $\delta/\delta_0 = 3x^2 - 2\sqrt{x}$, where we let the downward displacement correspond to the positive direction. Thus $x = 6^{-2/3}$ is a critical point where the sphere (the tip) is contact with the semi-infinite solid (the sample). At this critical point, the surface of the sample rises from its originl level. In contrast, when the relation $x = 1$ holds, the sphere (the tip) sinks deepest into the semi-indefinite solid (the sample).

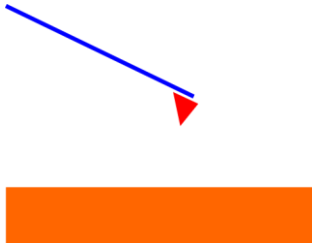

Figure 85 A state where the tip is apart from the sample surface.

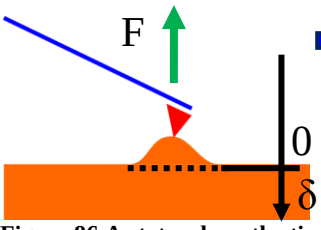

Figure 86 A state where the tip is contact with the sample surface.

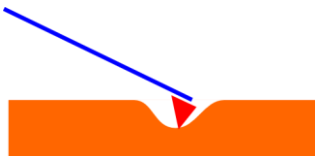

Figure 87 A state where the tip sinks deepest into the sample.

Figure 85, Figure 86 and Figure 87 represent a state where the tip becomes close to the sample surface, a state where the tip is contact with the sample surface, and a state where the tip sinks deepest into the sample, respectively. At the moment when the tip becomes in contact with the sample surface, the sample rises from its original level as shown in Figure 86. Then, the tip sinks into the sample because of the adhesion force that the sample causes. However, as the tip sinks into the sample deeper, the adhesion force becomes weaker. When the adhesion force becomes equal to zero, the tip goes down deepest below the original level of the sample surface.

An outline of the JKR theory, which describes the state of the tip in contact with the sample, is shown above. On the other hand, when the tip is apart from the sample surface, Hamaker's intermolecular force works between the tip and the sample. Therefore, we explain Hamaker's intermolecular force briefly in the following.

To obtain Hamaker's intermolecular force, first, we assume the London-van der Waals potential between two atoms. Second, we carry out an integral of the potential over the macroscopic volume of solids. Then, we obtain the interaction between two solids.

First, we assume that the London-van der Waals is given by

$$-\frac{\lambda}{r^6},$$

where r represents the distance between two atoms. The parameter λ characterizes the strength of the interaction between two atoms, so that λ depends on the kinds of two atoms. As shown above, for the derivation of Hamaker's intermolecular force, we do not consider the repulsive term, which the Lennard-Jones potential includes.

Assuming the above potential between two atoms, we carry out the integral over the macroscopic volume of two solids and we obtain the total energy as follows:

$$E = -\int_{v_1} dv_1 \int_{v_2} dv_2 \frac{q^2\lambda}{r^6},$$

where q represents the number of atoms per unit volume. If we consider a sphere of a radius R and a semi-indefinite body as the two solids, we can evaluate the total energy as follows:

$$E \cong -\frac{A}{12}\frac{D}{d},$$

where $A = \pi^2 q^2 \lambda$ and $D = 2R$. Moreover, d represents the shortest distance betweenthe two solids. In other words, d represents the shortest distance between the surface of the sphere and the surface of the semi-indefinite body. To obtain the above approximation, we assume $D >> d$. According to the above result, we can estimate the attractive force F caused by the interaction between the two solids asfollows:

$$F \cong \frac{A}{12}\frac{D}{d^2}.$$

At last, we introduce the Hamaker constant, which depends on the kind of the material. Writing down the Hamaker constants of the two solids as H_1 and H_2, the following relation holds:

$$A = \sqrt{H_1 H_2}.$$

5.2 Transition between a state where van der Waals force works and a state where the JKR theory is effective

In the previous section, we explain the JKR theory and Hamaker's intermolecular force. Here, we call our attention to the following fact. These models can handle systems in static equilibrium only. In other words, these models can only deal with the tip and the sample in static equilibrium. Because both the models of the JKR theory and Hamaker's intermolecular force do not include time-dependent differential equations, which describe the dynamics of the tip, they can hardly predict time evolution of the system.

Thus, if we discuss the dynamics of the tip and the sample with the models of the JKR theory and Hamaker's intermolecular force, we have to introduce other mechanism for explaining their time evolution. Hence, in the SPM simulator, we assume that the tip moves at a constant velocity while the tip is sinking deep and and going upwards inside the sample.

From now on, we follow the movements of the tip approximately according to the models of the JKR theory and Hamaker's intermolecular force. Here, we define some physical quantities.

- Δ : This variavle represents a displacement of the tip in z direction. We let the downward displacement be positive. Moreover, we assume that a change of this variable is caused by deformation of the cantilever. We can observe this physical quantity in direct during the AFM experiments.
- δ : This variable represents the distance between the tip and the sample. We let a downward change of δ be positive. The interaction between the tip and the sample depends on δ. We cannot observe this physical quantity in direct during the AFM experiments. Thus, to obtain δ, we have to compute it out of other physical variables.

To let discussions be simple, we follow the movement of the tip step by step as follows.

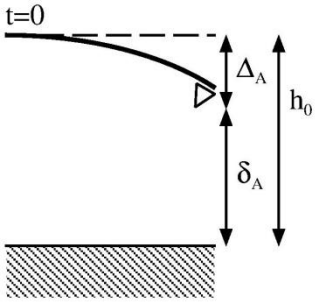

[The first step]

As shown in Figure 88, the tip and the sample are in static equilibrium at $t=0$. A force caused by the elasticity of the cantilever and Hamaker's intermolecular force are balanced. At this step, we write down the displacement of the cantilever as $\Delta_A(>0)$. Moreover, we write down the distance between the tip and the sample as $\delta_A(<0)$.

Figure 88 The first step.

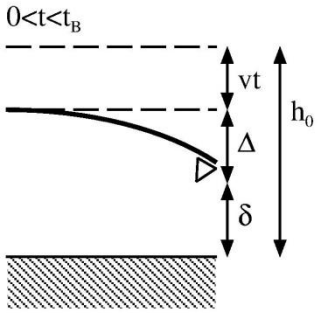

[The second step]

As shown in Figure 89, we let the tip becomes close to the sample gradually after the time $t=0$. During this process, the force caused by the elasticity of the cantilever and Hamaker's intermolecular force are balanced.

Figure 89 The second step.

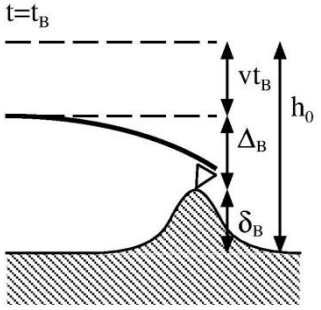

[The third step]

As shown in Figure 90, the tip becomes in contact with the sample surface. We describe the time variable of this moment as t_B. At this moment, we write down the displacement of the cantilever as $\Delta_B(>0)$. Moreover, we write down the rise of the sample from the original level as $\delta_B(<0)$. This rise is caused by the adhesive force , whose origin is the surface tension of the sample.

Figure 90 The third step.

[The fourth step]

The tip is sinking into the sample gradually. During this process, the force caused by the elasticity of the cantilever and Hamaker's intermolecular force are balanced, so that the tip and the sample are in static equilibrium.

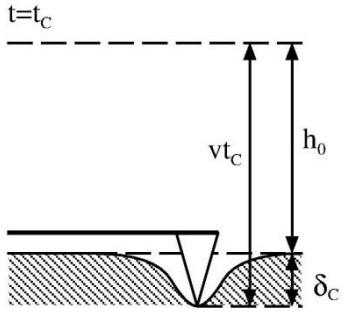

[The fifth step]

As shown in Figure 91, the tip sink deepest into the sample. At this moment, the force caused by the elasticity of the cantilever and Hamaker's intermolecular force cancel each other out, so that the force applied to the tip is equal to zero. We write the time variable at this moment as t_C. Because the force applied to the tip is equal to zero, the relation $\Delta = 0$ holds obviously. We describe the depth of the dent made by the tip sunk into the sample as $\delta_C (> 0)$.

Figure 91 The fifth step.

[The sixth step]

Aftre the time t_C, the tip is pulled off from the sample gradually. Both the force caused by the elasticity of the cantilever and Hamaker's intermolecular force are applied to the tip and the sample.

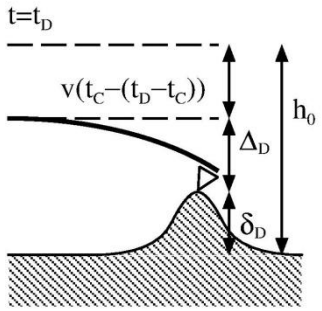

[The seventh step]

As shown in Figure 92, the tip becomes apart from the sample. We describe the time variable at this moment as t_D. At this moment, we write down the displacement of the cantilever as $\Delta_D (> 0)$. Moreover, we write down the rise of the sample from the original level as $\delta_D (< 0)$. This rise is caused by the adhesive force , whose origin is the surface tension of the sample.

Figure 92 The seventh step.

[The eighth step]

From the time t_D, the tip is leaving the surface of the sample gradually. During this process, the force caused by the elasticity of the cantilever and Hamaker's intermolecular force are balanced, so that the tip and the sample are in static equilibrium.

Regarding the whole process as a succession of these eight steps, we understand that the transition between a state where Hamaker's intermolecular force works and a state where the adhesive force works according to the JKR theory occurs at the time t_B and at the time t_D. Thus, we examine the behavior of the tip at the time t_B and at the time t_D precisely.

At first, we consider the behavior of the tip at the time t_B. Let us think the following function $f(t, \delta)$:

$$f(t,\delta) = k\Delta - \frac{AD}{12}\frac{1}{\delta^2} = k(h_0 - vt + \delta) - \frac{AD}{12}\frac{1}{\delta^2}.$$

Just before the tip becoming in contact with the sample surface, the relation $f(t, \delta) = 0$ has to hold. Here, we pay attention to the fact $\delta < 0$. On the other hand, at the time t_B, if the tip becomes in contact with the sample surface because of the adhesive force, the value of δ has

to change to a great extent. The reason why is as follows. The tip sticks to the sample because of the adhesive force, so that δ is determined by the JKR theory. Thus, the value of δ is nothing to do with the condition $f(t,\delta)=0$.

This implies the following. Even if the value of δ changes a little at the time t_{B}, the value of the potential of the interaction between the tip and the sample never changes and it corresponds to a stationary point. From these discussions, we understand that we have to require not only the condition $f(t,\delta)=0$ but also the following condition at the time t_{B}:

$$\frac{\partial}{\partial t} f(t,\delta)=0.$$

We can obtain δ_{B}, which satisfies the above conditions, in an exact expression. From

$$\frac{\partial}{\partial t} f(t,\delta)=k+\frac{AD}{6}\frac{1}{\delta^3}=0,$$

we obtain

$$\delta_{\mathrm{B}}=-\left(\frac{AD}{6k}\right)^{1/3}.$$

Moreover, because of $f(t,\delta_{\mathrm{B}})=0$, we obtain

$$t_{\mathrm{B}}=\frac{h_0}{v}-\frac{6^{2/3}}{4v}\left(\frac{AD}{k}\right)^{1/3}.$$

From now on, we assume that a condition $|\delta_{\mathrm{A}}|>|\delta_{\mathrm{B}}|$ holds in advance. From this condition, the tip has to be apart from the sample at the initial time $t=0$. By contrast, if we assume $|\delta_{\mathrm{A}}|\le|\delta_{B}|$ at $t=0$, the tip is in contact with the sample surface at initial time, so that we cannot carry out numerical simulation.

The value of δ_{B} given by the above equation is a critical distance for the transition between the models of Hamaker's intermolecular force and the JKR theory. Aftre the time t_{B}, the system is governed by the JKR theory with the adhesive force. Thus, the tip has to jump from the distance δ_{B} to the distance $\tilde{\delta}_{\mathrm{B}}$ immediately. In the following paragraphs, we explain how to compute $\tilde{\delta}_{\mathrm{B}}$.

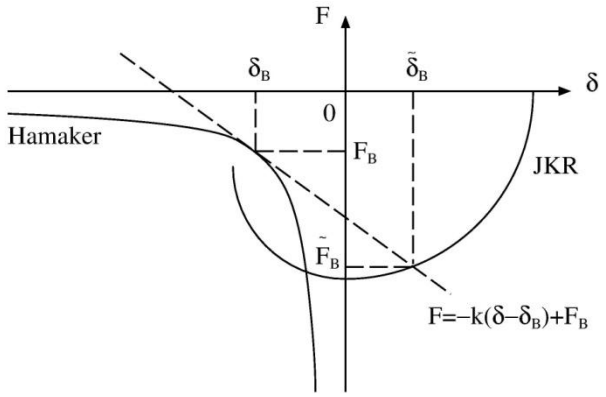

Figure 93 In this figure, we plot Hamaker's intermolecular force and the adhesive force induced by the JKR theory. The horizontal axis represents δ , the distance for the interaction between the tip and the sample. The vertical axis represents F , the interactive force between the tip and the sample.

In Figure 93, we plot Hamaker's intermolecular force and the adhesive force induced by the JKR theory. In Figure 93, the horizontal axis represents δ , the distance for the interaction between the tip and the sample. The vertical axis represents F , the interactive force between the tip and the sample. A moment , when the tip becomes in contact with the sample,corresponds to the coordinates $(\delta_{\mathrm{B}}, F_{\mathrm{B}})$.

Obviously, the point $(\delta_{\mathrm{B}}, F_{\mathrm{B}})$ is on the curve of Hamaker's intermolecular force. Here, we consider a tangent line to the curve of Hamaker's intermolecular force at the point $(\delta_{\mathrm{B}}, F_{\mathrm{B}})$. The condition $(\partial/\partial t) f(t,\delta) = 0$ lets the slope of the tangent line be equal to $-k$. Hence, we obtain the equation of the tangent line as

$$F = -k(\delta - \delta_{\mathrm{B}}) + F_{\mathrm{B}}.$$

Moreover, we describe the point $(\tilde{\delta}_{\mathrm{B}}, \tilde{F}_{\mathrm{B}})$, where this tangent line and the curve of the JKR theory intersect. Then, we understand that the tip jumps from δ_{B} to $\tilde{\delta}_{\mathrm{B}}$ immediately when the tip becomes in contact with the sample. The reason why is that the elastic force of the cantilever $-k(\delta - \delta_{\mathrm{B}})$ cancels out the the difference of the forces between F_{B} and $\tilde{F}_{\mathrm{B}}$ exactly. This fact tells us that the change of the interaction between the tip and the sample depends on the slope of the tangent line $-k$.

We have just given a discussion, which explains the transition from the model of Hamaker's intermolecular force into the model of the JKR theory at time t_{B} , when the tip becomes in contact with the sample. We can apply a similar discussion to the transiton from the model of the JKR theory into the model of Hamaker's intermolecular force at t_{D} , when the tip leaves the sample surface.

At the moment when the tip leaves the sample surface, the behavior of the tangent line, whose slope $-k$ causes the transition of the interaction, relies on whether the spring constant k is large or not. In other words, the behavior of the tip depends largely on whether the cantilever is soft or hard. In the following section, we explain this fact with concrete examples and numerical calculations.

5.3 In the case where the cantilever is soft

In this section, we examine the behavior of the tip and the sample surface with a soft cantilever. We follow the time evolution of the tip and the sample with numerical calculations.

First, we pay attention to the following fact. When experimental researchers observe softmaterials with the AFM , for example, molecules of proteins and DNA, they prefer soft cantilevers whose spring constants are less than 0.5[N/m]. The reason why is to prevent damaging samples like cells and other soft materials with the tip. Thus, instruments makers aggressively provide soft silicon nitride cantilevers whose spring constants are in the range of 0.02 to 0.08[N/m].

If we let the spring constant of the cantileber be small, we face the problem that a frequency of the cantilever oscillation becomes small. Although the instrument makers try to develop high-Q cantilevers, which have small spring constants and high resonant frequencies, they do not still succeed in making such high-Q cantilevers.

From the above discussions, we understand that we have to assume the cantilever of the small spring constant for the AFM experiment of the viscoelaticity of the soft materials. In Table 6, we show typical physical quantities for the AFM experiments with a soft cantilever and a soft material, for example, a molecular of a protein.

Table 6 Typical physical quantities for the AFM experiments with a soft cantilever and a soft material, for example, a molecular of a protein.

Physical quantities	Values
A distance between the tip and the sample at $t=0$	$h_0 = 5.0\times10^{-9}[\mathrm{m}]$
A velocity of the cantilever	$v = 4.5\times10^{-6}[\mathrm{m/s}]$
A density of the tip (with assuming SiO_2)	$\rho = 2.2\times10^{3}[\mathrm{kg/m^3}]$
A radius of the tip	$R = 2.5\times10^{-8}[\mathrm{m}]$
A spring constant of the cantilever (with assuming the soft cantilever)	$k = 0.5[\mathrm{N/m}]$
Hamaker constant (The tip: with assuming SiO_2)	$H_1 = 5\times10^{-20}[\mathrm{J}]$
Hamaker constant (The sample: with assuming: SiO_2)	$H_2 = 5\times10^{-20}[\mathrm{J}]$
A surface tension (The sample: one and a half times larger than water)	$\gamma = 0.108[\mathrm{N/m}]$
Young modulus (The tip: with assuming SiO_2)	$E_1 = 7.65\times10^{10}[\mathrm{N/m^2}]$
Young modulus (The sample: with assuming SiO_2)	$E_2 = 7.65\times10^{10}[\mathrm{N/m^2}]$
Poisson's ratio (The tip: with assuming SiO_2)	$\sigma_1 = 0.22$
Poisson's ratio (The sample: with assuming SiO_2)	$\sigma_2 = 0.22$

From now on, we follow the eight steps, which we define in the previous section, one by one. Here, to understand the discussions at ease, we plot the graphs of (δ, F) for Hamaker's intermolecular force and the adhesive force of the JKR theory in Figure 94.

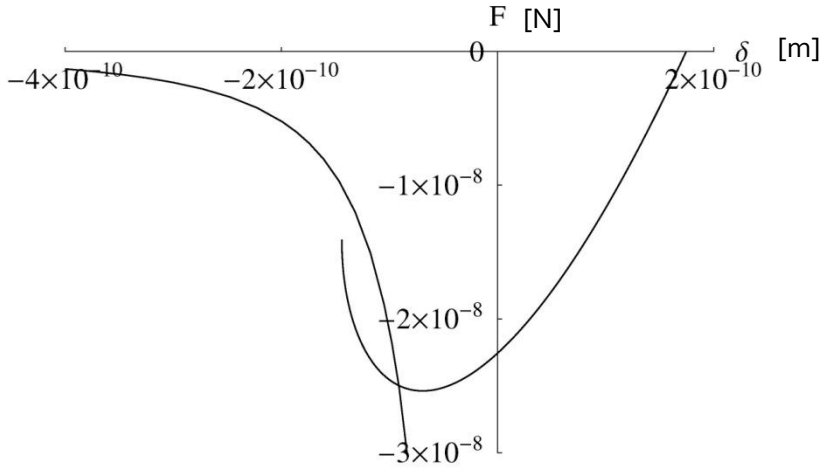

Figure 94 The graphs of (δ, F) for Hamaker's intermolecular force and the adhesive force of the JKR theory.

To let the graphs of Hamaker's intermolecular force and the adhesive force of the JKR theory overlap each other properly as shon in Figure 94, we have to adjust the Hamaker constants H_1, H_2 and the surface tension γ precisely. This fact implies that we cannot choose preferable values as H_1, H_2 and γ at will for the simulation. If we choose the values of H_1, H_2 and γ without adjusting them, the graphs of Hamaker's intermolecular force and the adhesive force of the JKR theory hardly overlap each other properly as shon in Figure 94. Therefore, when we carry out the simulation, it is possible that we have to adjust these physical quantities H_1, H_2 and γ by trial and error many times.

For the first step, we compute Δ_{A} and δ_{A} at $t = 0$. Remenbering the function $f(t, \delta)$ that we define in the previous section, we derive δ which satisfies $f(0, \delta) = 0$ at $t = 0$. Thus, what we have to do is just only computing δ which satisfies $f(0, \delta) = 0$ with numerical calculations. However, because the equation $f(0, \delta) = 0$ may have two or more roots for δ, we have to be careful for choosing a suitable root.

If the variable of the distance δ has two or more real roots, we have to choose the one whose absolute value is largest as δ_{A}. Thus, if we apply Newton's method for deriving δ numerically to the equation $f(0, \delta) = 0$, we may not notice the true δ_{A}. Therefore, when we solve the equation $f(0, \delta) = 0$ for obtaining δ numerically, we have to come up with new ideas for the numerical algorithms. In this example, we obtain

$\delta_{\mathrm{A}} = -4.98 \times 10^{-9}[\mathrm{m}]$,

and

$\Delta_{\mathrm{A}} = h_0 + \delta_{\mathrm{A}} = 1.68 \times 10^{-11}[\mathrm{m}]$.

Next, leaving aside the second step, we consider the third step. We mention in the previous section that we can describe δ_{B} and t_{B} in algebraic exact expressions, where δ_{B} and t_{B} correspond to the tip becoming in contact with the sample. Thus, substituting physical quantities of Table 6 into these exact algebraic expressions, we obtain

$\delta_{\mathrm{B}} = -9.41\times10^{-10}[\mathrm{m}]$,

and

$t_{\mathrm{B}} = 7.97\times10^{-4}[\mathrm{s}]$.

Moreover, because $f(t_{\mathrm{B}},\delta_{\mathrm{B}})=0$ holds at the time t_{B} for the function $f(t,\delta)$ defined in the previous section, we obtain

$\Delta_{\mathrm{B}} = 4.71\times10^{-10}[\mathrm{m}]$.

Looking at the values of δ_{A} and δ_{B} obtained above, we confirm that therelation $|\delta_{\mathrm{A}}|>|\delta_{\mathrm{B}}|$ holds. Thus, at the initial time $t=0$, the tip has to be apart from the sample surface. To let the condition $|\delta_{\mathrm{A}}|>|\delta_{\mathrm{B}}|$ hold, we have to carefully adjust the initial distance between the tip and the sample h_0 and the spring constant of the cantilever k. If we choose a soft cantilever, whose spring constant k is too small, we have to let the value of h_0 large enough or else the cantilever bends badly and touches the sample surface at initial time.

Here, we compute the $\tilde{\delta}_{\mathrm{B}}$, which is obtained by the transition of interactions at time t_{B}, according to the last figure shown in the previous section. This implies that we solve the following equations:

$$-k(\tilde{\delta}_{\mathrm{B}}-\delta_{\mathrm{B}})-\frac{AD}{12}\frac{1}{{\delta_{\mathrm{B}}}^2}=4F_c(x^3-x^{3/2}),$$

$$\tilde{\delta}_{\mathrm{B}}=\delta_0(3x^2-2\sqrt{x}),$$

and

$6^{-2/3}\le x\le 1$.

We substitute the numerical value of δ_{B} obtaine before into the above equations. From some numerical calculations, we obtain

$x_{\mathrm{B}} = 0.995$,

and

$\tilde{\delta}_{\mathrm{B}} = 1.70\times10^{-10}[\mathrm{m}]$.

Moreover, we obtain $\tilde{\Delta}_{\mathrm{B}}$ as

$\tilde{\Delta}_{\mathrm{B}} = h_0 - vt_{\mathrm{B}} + \tilde{\delta}_{\mathrm{B}} = 1.58\times10^{-9}[\mathrm{m}]$.

Here, we go back to the second step. From the above calculations, what we have to do is just numerically computing the value of δ, which satisfies

$f(t,\delta)=0 \quad (0\le\forall t\le t_{\mathrm{B}})$,

where the function $f(t,\delta)$ is given in the previous section. We pay attention to the following fact. If there are two or more real roots for δ, we choose the one whose absolute value is lagest.

Next, we consider the fourth step. At the time t_B, the tip becomes in contact with the sample surface. Here, we examine the process of the tip sinking into the inside of the sample. Let us define the following function $g(t,x)$:

$$g(t,x)$$
$$= k\Delta + 4F_c(x^3 - x^{3/2})$$
$$= k(h_0 - vt + \delta) + 4F_c(x^3 - x^{3/2})$$
$$= k[h_0 - vt + \delta_0(3x^2 - 2\sqrt{x})] + 4F_c(x^3 - x^{3/2})$$

for $t \geq t_B$ and $x_B \leq x \leq 1$.

For a given value of the time t, we compute numerically the variable x, which satisfies $g(t,x) = 0$. If we obtain the value of the parameter x numerically, we can compute F and δ, which are described in algebraic exact expressions of x in the previous section. Here, we pay attention to the following fact. For a given certain value of t, the equation $g(t,x) = 0$ may have two or more roots for the variable x. If there are two or more roots for x, we choose the one that is larger than $x_B (= 0.995)$ obtained before.

We describe the time, when $x = 1$ holds, as t_C. This value of the time t_C corresponds to the sixth step. At the time t_C, the force applied to the cantilever is equal to zero. Thus, after the time t_C, the cantilever rise upwards at the constant velocity $-v$. From numerical calculations, we obtain

$t_C = 1.15 \times 10^{-3}$[s],

and

$\delta_C = 1.75 \times 10^{-10}$[m].

Moreover, obviously, we obtain $\Delta_C = 0$. Here, we plot the time evolution of the cantilever for $0 \leq t \leq t_C$ in the following figure.

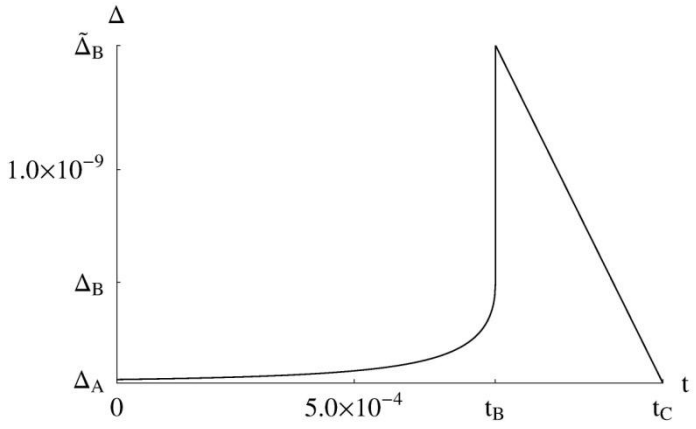

Figure 95 shows a graph of the time evolution of Δ for $0 \leq t \leq t_C$.

Figure 95 A graph of the time evolution of Δ for $0 \leq t \leq t_C$.

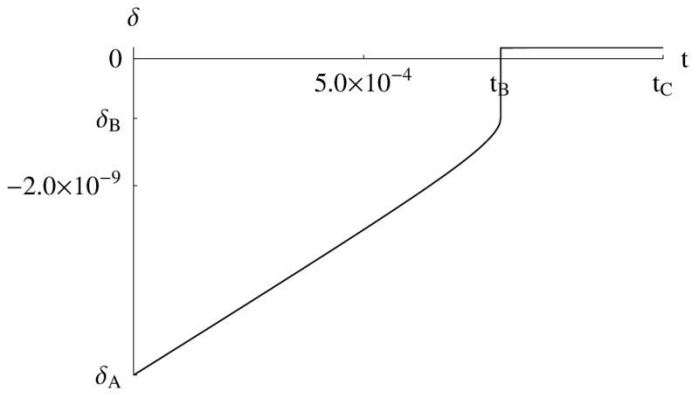

Figure 96 shows a graph of the time evolution of δ for $0 \le t \le t_C$.

Figure 96 A graph of the time evolution of δ for $0 \le t \le t_C$.

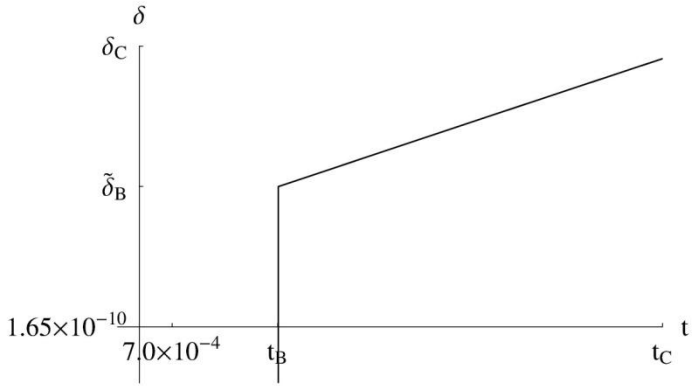

Figure 97 shows an enlarged graph of the time evolution of δ for $t_B \le t \le t_C$.

Figure 97 An enlarged graph of the time evolution of δ for $t_B \le t \le t_C$.

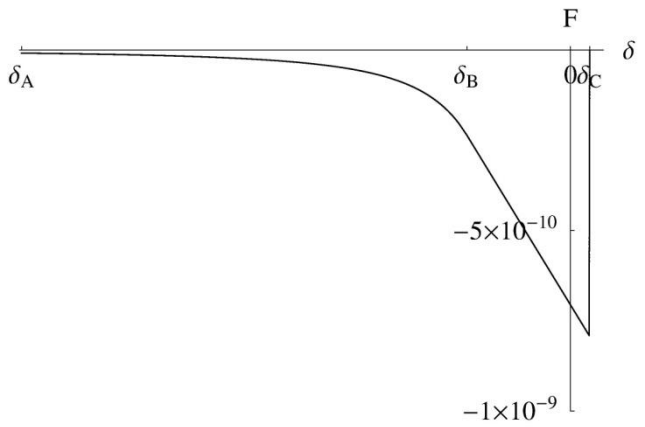

Figure 98 shows a graph of the time evolution of (δ, F) for $0 \le t \le t_C$.

Figure 98 A graph of the time evolution of (δ, F) for $0 \le t \le t_C$.

Because the interactive force applied to the cantilever by the sample is always equal to $-k\Delta$, we can regard the graph of the time evolution of Δ for $0 \le t \le t_C$ as the graph of the time evolution of the interactive force applied to the cantilever by the sample. Looking at the

above graphs of the time evolution of δ for $0 \le t \le t_C$, we feel that δ hardly changes during $t_B \le t \le t_C$ when the adhesive force is dominant for the interaction between the tip and the sample. However, looking at the enlarged graph of the time evolution of δ for $t_B \le t \le t_C$, we notice that δ becomes larger gradually with the tip sinking into the sample deeper.

Next, we consider the seventh step. For the time $t \ge t_C$, we numerically compute x that satisfies the condition $g(t,x) = 0$, where the function $g(t,x)$ is given before. Here, we pay attention to the following fact. If there are two or more roots for x, we choose the largest one as a proper solution.

If we compute x numerically as letting the time variable t be larger than t_C gradually, we find a certain time t_D after which , that is to say $t(> t_D)$, we cannot find a root of x for the equation $g(t,x) = 0$. Thus, at the time t_D, the tip becomes apart from the sample surface. From numerical calculations, we obtain

$t_D = 1.25 \times 10^{-2}$[s],

$x_D = 0.663$,

$\delta_D = -6.79 \times 10^{-11}$[m],

and

$\Delta_D = 5.08 \times 10^{-8}$[m].

Here, we show the movement of the cantilever for $0 \le t \le t_D$ as graphs.

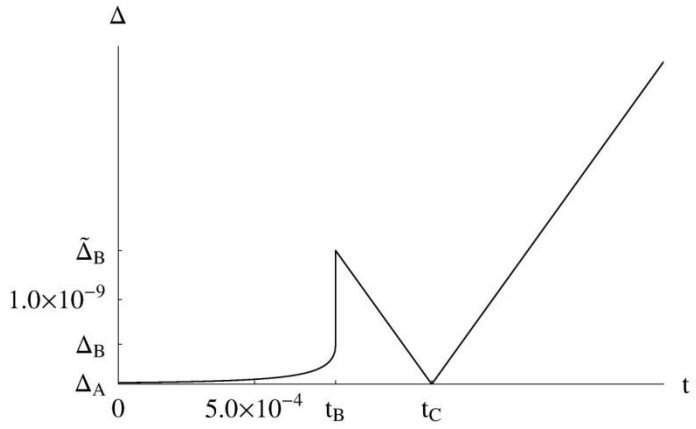

Figure 99 shows a graph of the time evolution of Δ for $0 \le t \le t_D$.

Figure 99 A graph of the time evolution of Δ for $0 \le t \le t_D$.

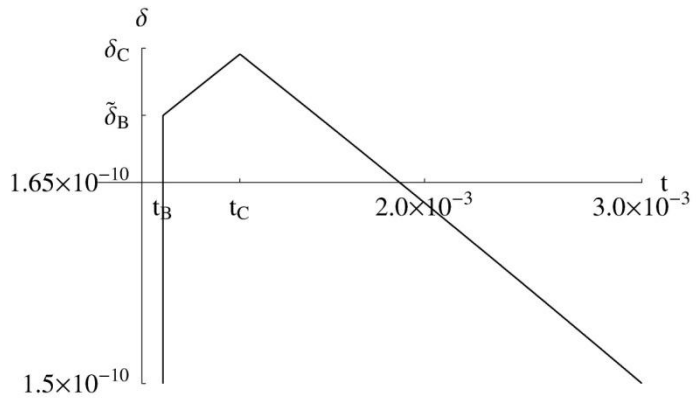

Figure 100 shows a graph of the time evolution of δ for $0 \le t \le t_D$.

Figure 100 Agraph of the time evolution of δ for $0 \le t \le t_D$.

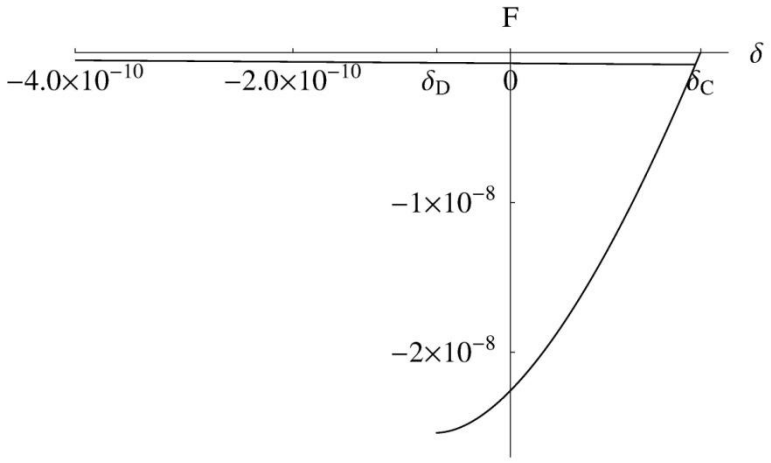

Figure 101 shows a graph of the time evolution of (δ, F) for $0 \le t \le t_D$.

Figure 101 A graph of the time evolution of (δ, F) for $0 \le t \le t_D$.

The above graph of (δ, F) for $0 \le t \le t_D$ coincides with experimental results well. Thus, we can consider that our model is a good approximation and it describes the behavior of the tip sinking into the sample and rising upwards out of the viscoelastic sample exactly.

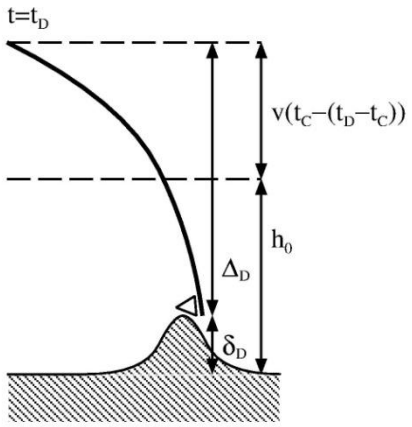

Figure 102 An example where the tip cannot leave the sample surface.

However, thinking about the value of Δ_D obtained by numerical calculations, we understand that our model hardly describe the process of the tip being detached from the viscoelastic sample surface. In fact, our model cannot follow the phenomena of detachments of the tips at all. This is because we obtain $\Delta_D = 5.08\times10^{-8}[\mathrm{m}]$ numerically and it is much larger than the initial distance of the tip and the sample $h_0 = 5.0\times10^{-9}[\mathrm{m}]$. Figure 102 represents this situation of the cantilever, the tip and the sample at the time t_D. Looking at Figure 102, we notice that the cantilever rises up far beyond the initial position. This implies that we cannot let the tip become apart from the sample surface under the framework of our model.

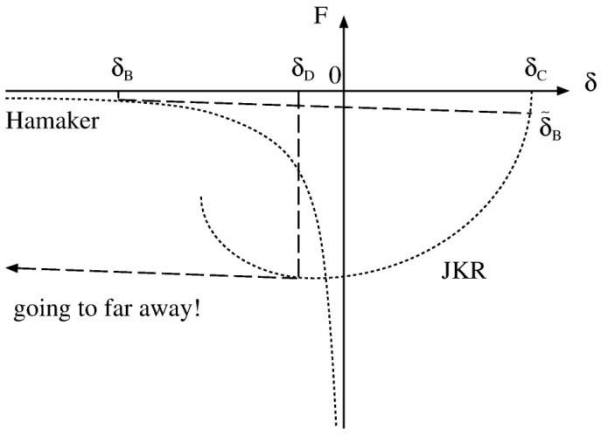

Figure 103 An example where the transition hardly occurs from the adhesive force of the JKR theory to Hamaker's intermolecular force.

Let us discuss this point more precisely. In Figure 103, we describe the transition of the interactive force between Hamaker's intermolecular force and the adhesive force of the JKR theory. At the time t_B, the tip jumps from δ_B to $\tilde{\delta}_B$ according to the tangent line whose slope is equal to $-k$. Here, we pay attention to the following fact. Because the slope $-k$ is very small now, the tangent line is nearly equal to the horizontal line. Thus, at the time t_D, the tip jump from δ_D to $\tilde{\delta}_D$, which is very far from δ_D. Therefore, the tip has to go far away at the time t_D.

The above things are the reasons why our model hardly describes the detachment of the tip from the sample surface. Looking at Figure 103, we notice that the problem is caused only by geometrical arrangements of the graphs of Hamaker's intermolecular force, the adhesive force of the JKR theory and the tangent line with slope of the spring constant k.

To avoid this problem, the solvers FemAFM and LiqAFM take the following treatments for the simulation of the dynamics of the viscoelasticity between the tip and the sample:

- The FemAFM stops the simulation at the time t_D and at the displacement of the sample surface δ_D. Thus, the FemAFM never compute $\tilde{\delta}_D$ numerically.
- The LiqAFM computes the successive displacement $\tilde{\delta}_D$ at the time t_D and at the displacement of the sample surface δ_D. If the displacement $\tilde{\delta}_D$ is not larger than the

initial distance h_0, the LiqAFM includes $\tilde{\delta}_D$ in the results of the simulation. However, if $\tilde{\delta}_D$ is larger than the initial distance h_0, the LiqAFM stops the simulation at δ_D.

5.4 In the case where the cantilever is hard

In the previous section, we consider the case where the cantilever is soft and point out that the following problem may occur. That is to say, the tip cannot leave the sample surface. By contrast, if the cantilever is hard enough and its spring constant is large enough, the problem never occurs and the tip always leaves the sample surface in our model. Thus, if we use a hard cantilever, it is safe to say the whole process of the tip and the sample is consistent and we do not need to worry about the problem mentioned before.

Indeed, using the physical parameters shown in Table 7, we obtain the graph of (δ, F) as shown in Figure 104 and we understand that our model is consistent. In Figure 104, the transitions from δ_B to $\tilde{\delta}_B$ and from δ_D to $\tilde{\delta}_D$ is realized with the tangent line whose absolutevalue of the slope is quite large. Thus, as shown in Figure 104, if the absolute value of the slope of the tangent line $-k$ is large enough, our model of the tip and the sample never causes the problem.

Table 7 Typical physical quantities for the AFM experiments with a hard cantilever and a soft material.

Physical quantities	Values
A distance between the tip and the sample at $t=0$	$h_0 = 5.0\times10^{-9}$[m]
A density of the tip (It is slightly larger than that of SiO_2.)	$\rho = 2.57\times10^{3}$[kg/m^3]
A radius of the tip	$R = 2.5\times10^{-8}$[m]
A spring constant of the cantilever (with assuming the hard cantilever)	$k = 100.0$[N/m]

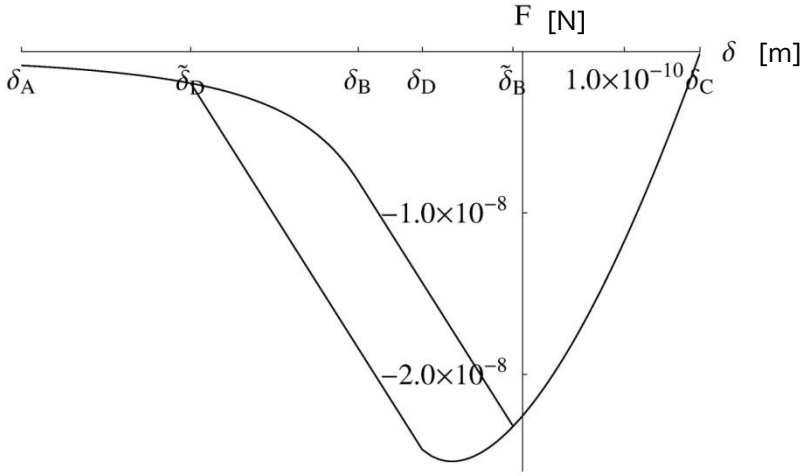

Figure 104 A graph of (δ, F) using a hard cantilever.

5.5 Difficulty of adjusting physical parameters

So far, we discuss the model that describes the dynamics of viscoelaticity between the tip and the sample according to Hamaker's intermolecular force and the adhesive force of the JKR theory. In our model, it is difficult for adjusting the physical parameters properly. For example, if we choose the values of the Hamaker constants and the surface tension without any adjustment of them and plot (δ, F), we obtain a graph as shown in Figure 105. In Figure 105, graphs of Hamaker's intermolecular force and the adhesive force of the JKR theory do not overlap each other properly. Then, if we draw the tangent line with the slope of $-k$ at δ_B, it never intersects with the curve of the adhesive force of the JKR theory, so that the tip cannot become in contact with the sample surface.

The reason why this problem occurs is that the curve of Hamaker's intermolecular force and the curve of the adhesive force of the JKR theory are independent of each other. Both the curves are determined with the physical constants H_1, H_2 and γ, and these constants are independent of each other. Because there is no dependence between Hamaker constants H_1, H_2 and the surface tension γ, we can choose any values of them at will. Thus, we cannot predict geometrical arrangement of graphs of Hamaker's intermolecular force and the adhesive force of the JKR theory at all, when we make their (δ, F) plots.

Therefore, if we carry out the simulation of the dynamics of the viscoelaticity with the solvers FemAFM and LiqAFM, we have to adjust them by trial and error many times and find their suitable values.

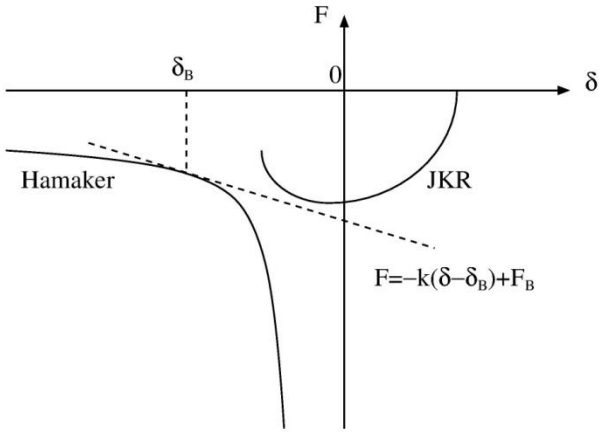

Figure 105 Graphs of Hamaker's intermolecular force and the adhesive force of the JKR theory, which do not overlap each other properly.

5.6 Improving the treatments of the dynamics of the viscoelaticity: a prospective method

As explained above, if we draw the tangent line with the slope $-k$ to the curve of Hamaker's intermolecular force, it cannot intersect with the curve of the adhesive force of the JKR theory in general. Thus, the tip cannot become in contact with the sample surface. To overcome this problem, we consider the model show Figure 106.

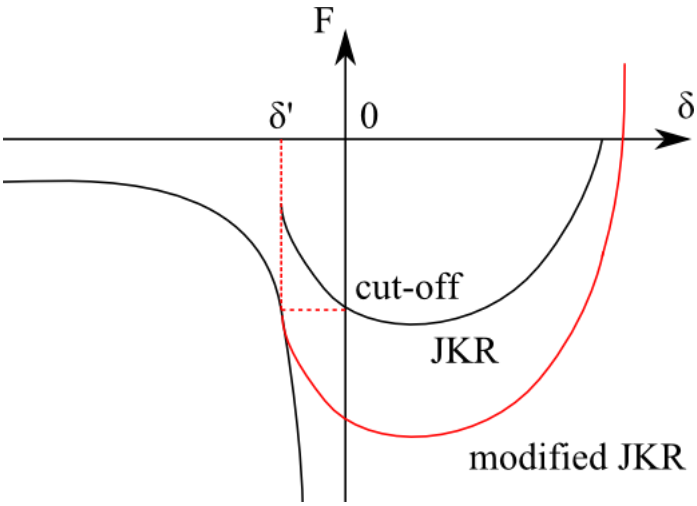

Figure 106 A model with the curve of the adhesive force according to the modified JKR theory.

Because Hamaker's theory and the JKR theory are independent of each other, we cannot join them together without coming up with new ideas.

First, let us think about the curve of Hamaker's intermolecular force. This curve shows that only an attractive force works between molecules both on macroscopic and microscopic scales. This behavior is proper when the sample is very far from the tip. However, when the sample becomes close to the tip on an atomic scale, Hamaker's intermolecular force is not valid for real physical phenomena.

Thus, we try to think about the modified Hamaker's intermolecular force. We assume that the intermolecular force becomes constant and never strengthens when the tip becomes close to the sample surface in the range of the atomic scale. This implies that we introduce the cut-off length in Hamaker's intermolecular force. This modified Hamaker's intermolecular force seems to describe real physical phenomena well. Then, we consider how to join the curve of the modified Hamaker's intermolecular force and the curve of the adhesive force of the JKR theory together.

As shown in Figure 106, at the moment when the tip become apart from the sample according to the curve of the adhesive force of the JKR theory, we regard the distance between the tip and the sample as the cut-off length. Then, we add the strength of Hamaker's intermolecular force at this caut-off length to the adhesive force of the original JKR theory, and we obtain a new curve of the adhesive force. In Figure 106, we draw this new curve of the modified adhesive force as a red curve named the "modified JKR" force.

If we use this new model, we may avoid the problems mentioned in the previous sections. Implementation of this model to the SPM simulator remains to be solved in the future.

Chapter 6 Finite element method AFM simulator (FemAFM)

6.1 A model of continuous elastic medium

The solver FemAFM is software for simulating the atomic force microscope (AFM) with approximating the sample and the tip as models of continuous elastic medium. In the simulation, we regard each of the sample and the tip as continuous elastic medium consisting of a single material and assume that the van der Waals foce works between elements of the continuous elastic medium. By solving the linearly elastic constitutive equations numerically, we examine total interactive forces between the tip and the sample.

Keywords of theoretical physics that represent simulation methods of the FemAFM are the van der Waals foce and the linearly elastic constitutive equations. Thus, the FemAFM treat problems with phenomelogical force fields according to the classical mechanics. The price of this typical feature is that the FemAFM does not consider effects of quantu mechanical dynamics.

When we use the FemAFM, we have to consider each of the sample and the tip to be continuous elastic medium consisting of a single material. Thus, even if we want to treat a complex polymer as a sample, we have to treat it as elastic medium of a single material. We have to neglect its atomic structure. What we can do with the FemAFM is to obtain average dynamical properties over the elastic medium with numerical calculations. However, the FemAFM has the following advantage. It can investigate macroscopic changes of shapes of the tip and the sample, which are affected by the van der Waals forces, with solving the linearly elastic constitutive equations numerically.

From these reasons, the FemAFM is suitable for examining macroscopic properties of samples. However, the FemAFM cannot carry out microscopic simulations. For example, the FemAFM cannot simulate AFM images of atomic structures on the sample surfaces. If we want to simulate SPM images of atomic structures, we need the CG, the MD and the DFTB. The FemAFM provides us with convenient tools for simulating macroscopic AFM images of biopolymers and semiconductor devices, for example.

The FemAFM has the following three simulation modes.

- [femafm_Van_der_Waals_force]
  Using this mode, we can carry out simulation of general non-contact AFM images. In this mode, we can let the tip scan the sample surface with constant hight, plot the interactive force, from which the tip suffers, on the two-dimensional plane, and obtain an experimental AFM image. At each point plotted on the two-dimensional plane, the FemAFM solves the linearly elastic constitutive equations numerically and estimate changes of the shapes of the tip and the sample caused by the van der Waals forces under static equilibrium. Plotting the interactive forces between the tip and the sample under this static equilibrium, we obtain an experimental AFM image as a result of the simulation.
- [femafm_frequency_shift]
  Using this mode, we can carry out simulation of non-contact frequency modulation AFM (FM-AFM) with obtaining the frequency shift of the oscillating cantilever. In this mode, we let the cantilever and the tip be oscillating at a certain frequency, scan the sample surface, and plot the shift of the resonant frequency, which is caused by the interaction between the tip and the sample, on the two-dimensional plane. During the simulation, we assume that the tip is not in contact with the sample surface. If the tip become in contact with the

sample surface, the simulation stops immediately.

- [femafm_JKR]
  Using this mode, we can carry out simulation of the contact mechanics between the tip and the viscoelastic sample. At the ceratin point on the sample surface, we let the tip go down towards the sample gradually, sink into the sample, and pull it upwards. In this mode, we can simulate successive processes such as making the tip become in contact with the sample surface, making the tip be stuck with the sample by the adhesive force, letting the tip be pushed back upwards outside the sample, and letting the tip leave the sample surface. During the simulation, we can obtain the vertical displacement of the tip and the interactive force between the tip and the sample as output data. If the tip is apart from the sample, we assume that the van der Waals force works. If the tip is in contact with the sample surface, we assume that we can describe the dynamics with the Johnson-Kendall-Roberts (JKR) theory.

The user can choose one of the above three simulation modes according to the user's purpose.

6.2 Describing the continuous elastic medium with the finite element method

As explained in the previous section, to carry out the simulation, the FemAFM treat the tip and the sample as the continuous elastic medium and solve its linearly elastic constitutive equations numerically. The femAFM makes use of the finite element method for solving the linearly constitutive equations numerically.

How to create FEM meshes of the tip and the sample is as follows. We assume that the tip and the sample are given as data of molecular structures. First, we let the lowest atom in the molecules be located at the origin of the Cartesian coordinate system (x, y, z). Second, we create the projection of the object (the tip or the sample) on the xy plane, so that we obtain a region, which the object occupies. Third, we perform mesh discretization of the region with a square lattice, whose edge length is equal to 1.0[angstrom]. Fourth, to each unit cell on the square lattice of the xy plane, we give height of the object. Then, we obtain a surface mesh model of the object on the two-dimensional lattice of the xy plane.

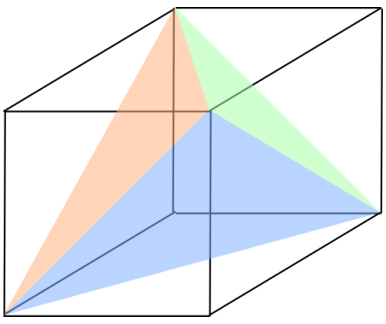

Figure 107 Dividing a cube into five tetrahedrons

Next, we apply discretization to the height of each unit cell on the xy plane with a space step of 1.0[angstrom]. Then, we obtain a three-dimensional mesh of the object with cubes, whose edge length is equal to 1.0[angstrom]. Finally, we divide each unit cube of side 1.0[angstrom] into five tetrahedrons as shown in Figure 107. Thus, we obtain a three-dimensional finite element mesh of the object with tetrahedrons.

If an object is given with other data format, which is not data of molecular structures, we can apply similar process to it and we can obtain a three-dimensional finite element mesh of the object with tetrahedrons.

6.3 Calculating the interactive forces between the tip and the sample and changes of their shapes with the finite elemet method

The FemAFM computes the long-range interactive force between the tip and the sample as the van der Waals force, which is given by

$$\vec{f}(\vec{r}_1) = C_1\rho_1 C_2\rho_2 dV_1 \sum_{\vec{r}_2} dV_2 \left[\frac{6}{r_{12}^{\,6}} \left(1 - \frac{R_{\text{rep}}^{\,6}}{r_{12}^{\,6}} \right) \frac{\vec{r}_{12}}{r_{12}^{\,2}} \right],$$

where

$$C_1\rho_1 = \frac{\sqrt{H_1}}{\pi},$$

$$C_2\rho_{21} = \frac{\sqrt{H_2}}{\pi},$$

H_1, H_2 represent the Hamaker constants with unit of [J], and R_{rep} represents the van der Waals radius that determines the repulsive force in the short range. In the FemAFM, we set $R_{\text{rep}} = 5a_0$, where $a_0 = 0.529 \times 10^{-10}[\text{m}]$ represents the Bohr radius. Moreover, defining $R_{\text{cutoff}} = 50a_0$, we do not let the van der Waals force work in the case where r_{12} is longer than R_{cutoff}. The introduction of R_{cutoff} prevents the divergence to infinity for the van der Waals force and lets results of numerical calculations be stable.

The linearly elastic constitutive equations are given as follows:

$$\frac{1}{1+\nu}\frac{E}{2}\Delta\vec{u} + \frac{1}{1+\nu}\frac{1}{1-2\nu}\frac{E}{2}\vec{\nabla}(\vec{\nabla}\cdot\vec{u}) + \frac{1}{dV}\vec{f} = 0,$$

where E represents Young's modulus in unit $[\text{N}/\text{m}^3]$ and represents Poisson's ratio.

The FemAFM solves the above two equations simultaneously and obtains displacements of infinitesimally small volume elements $\vec{u}$ and forces acting throughout infinitesimally small volume elements $\vec{f}$ numerically. We can evaluate a total force that acts on the tip as sum of all forces acting through the all volume elements of the tip. From this process, we can simulate an experimental AFM image. The simulation mode [femafm_Van_der_Waals_force] basically follows this procedure.

6.4 Estimating the frequency shift of the cantilever under the model of the continuous elastic medium: using a standard formula

In the mode [femafm_frequency_shift], the FemAFM can carry out simulation of non-contact frequency modulation AFM (FM-AFM) image with obtaining the frequency shift of the cantilever. We explain how to estimate the frequency shift in the following paragraphs.

If we want to evaluate the frequency shift, we have to consider two external forces acting on the tip. The first one is the force caused by the oscillation of the cantilever. The second one is the interactive van der Waals force between the tip and the sample. Thus, we obtain the following equation of motion for the tip:

$$\ddot{z} = -A_0\Omega^2 \sin(\Omega t) - \frac{k}{m}(z - z_0) + \frac{F_{\text{ts}}}{m},$$

where A_0 represents the amplitude of the oscillation of the cantilever, Ω represents the circular frequency of the oscillation of the cantilever, k represents the spring constant of the cantilever, m represents the mass of the tip and F_{ts} represents the total external force acting between the tip and the sample. In concrete terms, F_{ts} is a sum of the interactive van der Waals force between the tip and every volume element of the sample. The constant position z_0 represents the equilibrium position where the spring force of the cantilever and the total van der Waals force between the tip and the sample cancel out without cantilever's oscillation.

The total external force F_{ts} varies as time proceeds according to the distance between the tip and the sample and the changes of the shapes of the tip and the sample caused by their elasticity. Thus, to solve the equation of motion for the tip numerically, we have to perform the following procedure. We apply the finite difference method for solving the equation of motion for the tip numerically. Thus, we discretize the time variable with the difference in time Δt. At each time step, we solve the linearly elastic constitutive equations of the tip and the sample. Then, we include the effects of changes of the shapes of the tip and the sample in the calculation of the finite difference method for solving the equation of motion for the tip. This treatment is valid under the condition that the changes of the shapes of the tip and the sample occurs quickly and its time scale is much shorter than the period Δt.

Moreover, we assume the following fact. The van der Waals force between the tip and the sample is weak enough, so that we consider it to be the first-order perturbation for the dynamics of the oscillation of the cantilever. Thus, we assume that the tip never becomes in contact with the sample surface. If the tip becomes in contact with the sample surface, the FemAFM stops the simulation immediately. To judge whther the tip becomes in contact with the sample surface or not, we utilize some notions explained in Sec.5, "A method of investigating contact problem".

To estimate the frequency shift $\Delta\nu$, we use the following formula [N. Sasaki and M. Tsukada, Jpn. J. Appl. Phys. Vol. 39 (2000) pp. L1334-L1337, Part 2, No. 12B, 15 December 2000]:

$$\Delta\nu = -\frac{1}{2\pi a k}\frac{\omega_0}{2\pi}\int_0^{2\pi} F_{\mathrm{ts}}(z)\frac{z-z_0}{a}\,d\psi ,$$

$$z - z_0 = a\cos\psi ,$$

where z represents the distance between the tip and the sample surface, $a = (z_{\max} - z_{\min})/2$ represents a half of the amplitude of the tip's actual oscillation, $\omega_0 = \sqrt{k/m}$ represents the resonant frequency of the cantilever and $F_{\mathrm{ts}}(z)$ represents the interactive force between the tip and the sample for the distance z.

To calculate the frequency shift $\Delta\nu$ with the above formula, we rewrite the integral as the following discrete sum. First of all, we divide the period of the oscillation of the cantilever into N equal intervals as follows:

$$t_i = \frac{2\pi}{\Omega}\frac{i}{N}.$$

We describe the displacement of the tip at each descrete time as

$$z_i = z(t_i) = z\left(\frac{2\pi}{\Omega}\frac{i}{N}\right).$$

From the above preparations, we can write down $\Delta\nu$ as

$$\Delta\nu = -\frac{1}{2\pi ak}\frac{\omega_0}{2\pi}\sum_{i=0}^{N-1}F_{\mathrm{ts}}(z_i)\frac{z_i - z_0}{a}\frac{2\pi}{N} = -\frac{1}{2\pi a^2 k}\frac{\omega_0}{N}\sum_{i=0}^{N-1}F_{\mathrm{ts}}(z_i)(z_i - z_0).$$

Using the above equation and solving the equation of motion for the tip with the finite difference method, we can compute $\Delta\nu$ at ease.

The FemAFM repeats the above procedure for obtaining $\Delta\nu$ at each point on the two-dimensional xy-plane with scanning the sample surface and eventually generates a frequency shift AFM image.

6.5 Simulating the contact mechanics between the tip and the viscoelastic sample under the model of continuous elastic medium

In the mode of [femafm_JKR], the FemAFM can carry out the simulation of the contact mechanics between the tip and the viscoelastic sample. In the following paragraphs, we explain how to realize this simulation numerically.

In the mode of the [femafm_JKR], the FemAFM examines the contact mechanics between the tip and the viscoelastic sample at a certain fixed point on the sample surface. A method of numerical calculations is similar to that of the mode [femafm_frequency_shift], in which the frequency shift is estimated. While we solve the equation of motion of the tip with the finite difference method numerically, we solve the linearly elastic constitutive equations for the tip and the sample at each time step and we examine the equilibrium states of elastic materials.

If the dynamics of the tip and the sample makes a transition from the theory of van der Waals force to the JKR theory, the tip sinks into the sample with the adhesive force at a constant velocity. We assume that this velocity is nearly equal to the typical velocity of the oscillation of the cantilever.

After the system of the tip and the sample makes the transition to the JKR theory, its dynamics is governed as explained in Sec.5, “A method for investigating viscoelastic contact problem”.

In the mode of the [femafm_JKR], the FemAFM stops calculations just before the tip leaves the sample surface. Then, it outputs a data file “femafm_simulation_tip_delta_force.csv”. The time variations of the displacement of the tip along the z-axis and the z-component of the interactive force between the tip and the sample are recorded in this file.

6.6 Some examples of simulations

In the following sections, we show some examples of simulations carried out by the FemAFM.

6.6.a A simulation in the mode of [femafm_Van_der_Waals_force]

In Figure 108, Figure 109 and Figure 110, we explain results of an AFM simulation of a single molecule of Glycoprotein (1clg) on HOPG (Highly Oriented Pyrolytic Graphite) with a pyramid tip.

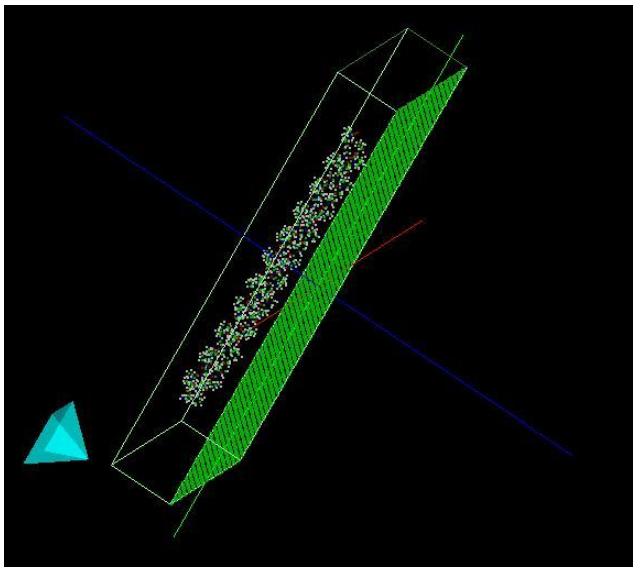

Figure 108 A pyramid tip and a single molecule of Glycoprotein (1clg) on HOPG (Highly Oriented Pyrolytic Graphite)

In Figure 108, we show molecular structure data of a single molecule of Glycoprotein (1clg) on HOPG (Highly Oriented Pyrolytic Graphite). We carry out the AFM simulation for this molecular structure data with the FemAFM.

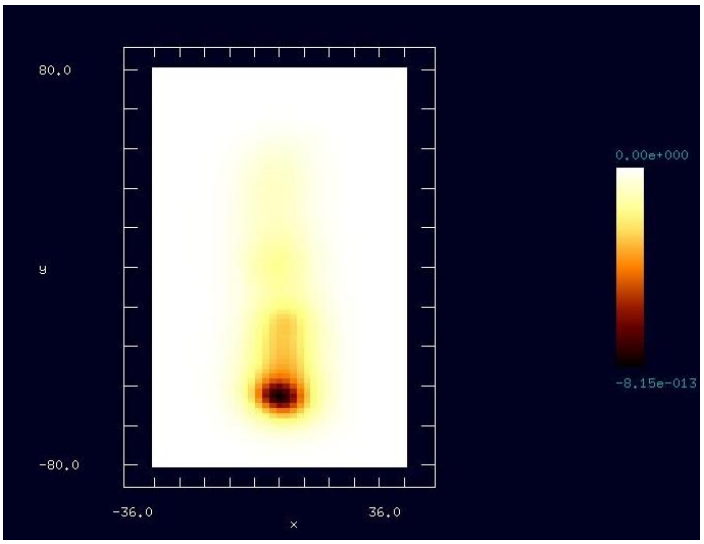

Figure 109 An AFM simulation image of a single molecule of Glycoprotein (1clg) on HOPG (Highly Oriented Pyrolytic Graphite) with two-dimensional view

In Figure 109, we show an AFM simulation image obtained with the FemAFM in the mode of [femafm_Van_der_Waals_force]. On the two-dimensional plane, the interactive van der Waals forces between the tip and the sample are plotted. Looking at Figure 109, we notice that the van der Waals foce becomes extremely strong in the area where the tip is quite close to the sample surface.

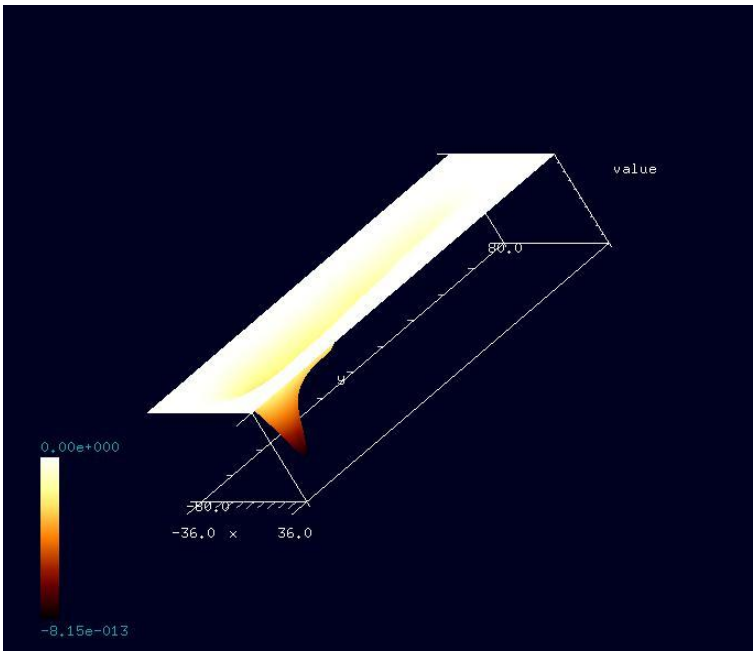

Figure 110 An AFM simulation image of a single molecule of Glycoprotein (1clg) on HOPG (Highly Oriented Pyrolytic Graphite) with three-dimensional view

In Figure 110, we show an AFM simulation image obtained with the FemAFM in the mode of [femafm_Van_der_Waals_force] with three-dimensional view. Looking at Figure 110, we notice that the van der Waals force becomes extremely strong with being proportional to the molecular distance at the power of six in the area where the tip is quite close to the sample surface.

6.6.b A simulation in the mode of [femafm_frequency_shift]

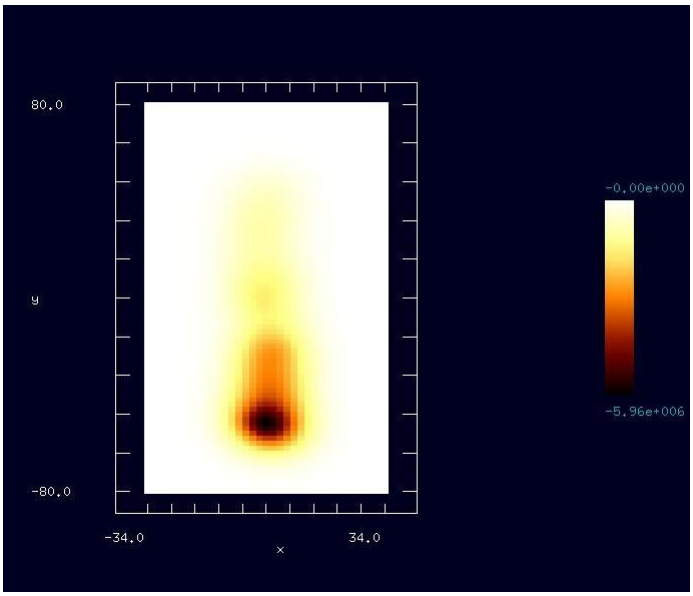

Figure 111 A frequency shift AFM image of a single molecule of Glycoprotein (1clg) on HOPG (Highly Oriented Pyrolytic Graphite) with two-dimensional view

In Figure 111 and Figure 112, we explain simulation results of a frequency shift AFM for a single molecule of Glycoprotein (1clg) on HOPG (Highly Oriented Pyrolytic Graphite) with a pyramid tip.

In Figure 111, we show a frequency shift AFM image obtained by simulation with two-dimensional view. In this simulation, we assume that the cantilever oscillates at 500[MHz]. Looking at Figure 111, we notice that the maximum value of the frequency shift is about 5.96[MHz].

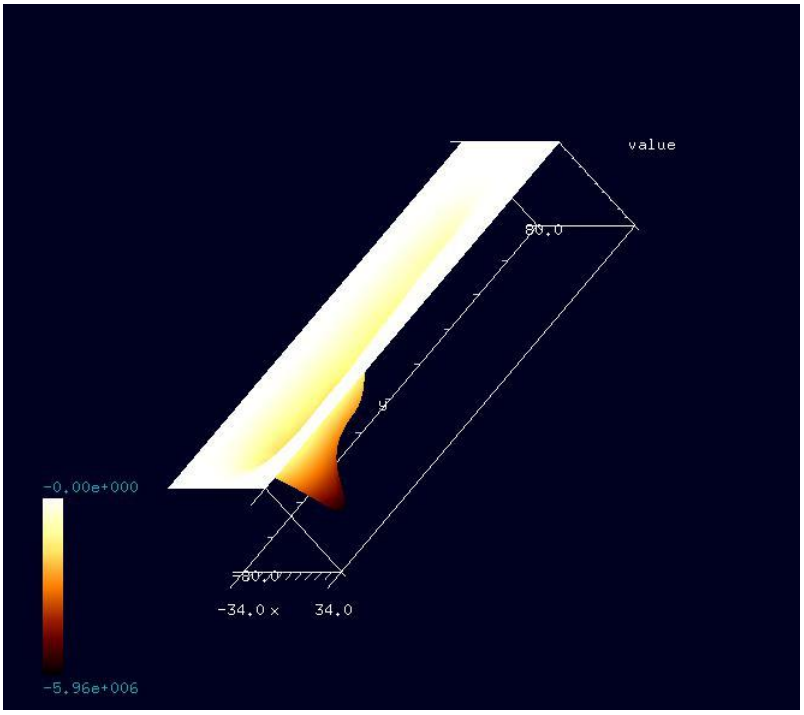

Figure 112 A frequency shift AFM image of a single molecule of Glycoprotein (1clg) on HOPG (Highly Oriented Pyrolytic Graphite) with three-dimensional view

In Figure 112, we show a frequency shift AFM image obtained by simulation with three-dimensional view.

6.6.c A simulation in the mode of [femafm_JKR]

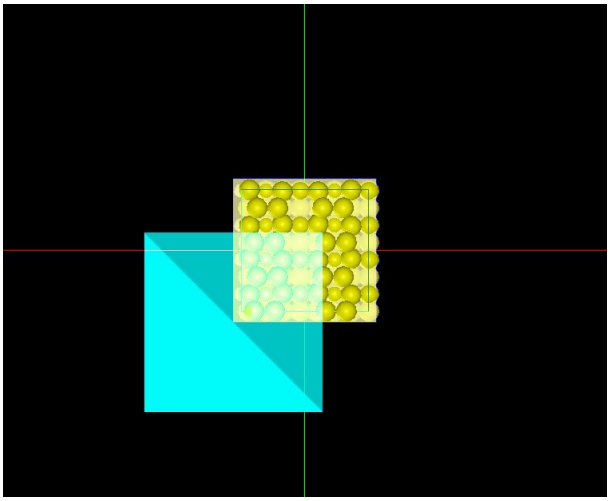

Figure 113 A pyramid tip and Si(001) substrate

In Figure 113 and Figure 114, we explain simulation results of contact mechanics between the pyramid tip and the viscoelastic Si(001) substrate at a certain fixed point on its surface.

In Figure 113, we show atomic structure of Si(001) substrate.

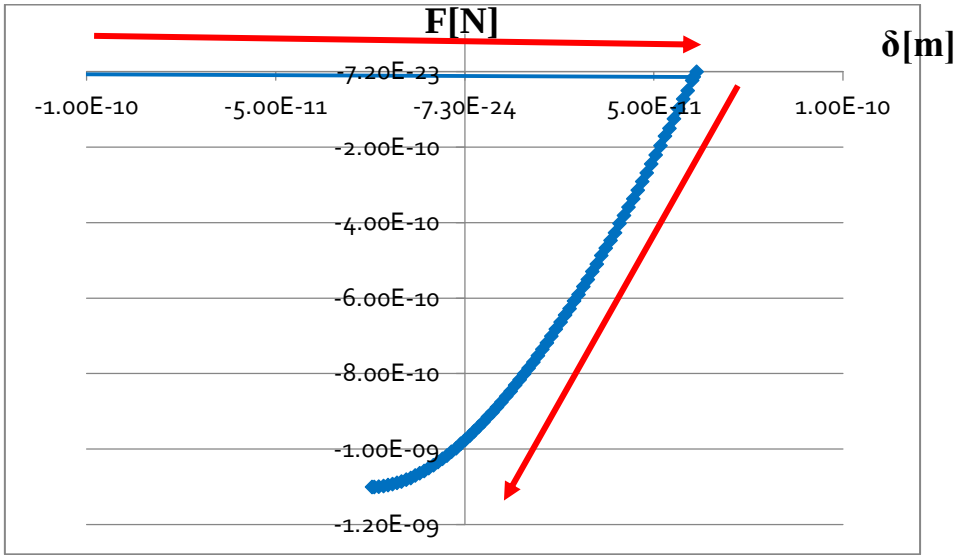

Figure 114 A graph of the interactive force between the tip and the sample against the displacement of the tip. The horizontal axis represents the displacement of the tip. The vertical axis represents the interactive force between the tip and the sample.

In Figure 114, we show a graph of the interactive force between the tip and the sample against the displacement of the tip as a result of simulation. The horizontal axis represents the displacement of the tip. The vertical axis represents the interactive force between the tip and the sample. Because the ranges of both the replacement and the interactive force are too large, we enlarge a part of original graph as $-1.0\times10^{-10} \le \delta \le 1.0\times10^{-10}$ [m] and $-1.2\times10^{-9} \le F \le 1.0\times10^{-10}$ [N] to examine the contact mechanics of the tip and the sample precisely.

How to interpret Figure 114 is as follows. We assume that the tip moves along red arrows. First, the tip moves downwards and becomes in contact with a round part that sticks out from sample surface. Second, the tip sinks into the sample because of the adhesive force. Third, the tip sinks into the sample deepest and the adhesion force become equal to zero. Fourth, the tip moves upwards. The FemAFM simulates the movement of the tip numerically just before it leaves the sample surface.

In the above example, because the spring constant of the cantilever is too small, a slope of the tangent line to the curve of the JKR theory is very small and it is nearly horizontal, so that it cannot induce the transition from the curve of the JKR theory to the curve of the van der Waals force. The FemAFM does not simulate how the tip leaves the sample surface. This is because the transition from the JKR theory to the model of the van der Waals force is often invalid. In fact, if the spring constant of the cantilever is too small, the tip leaves the sample surface and move upwards far away.

6.7 Users guide: how to use FemAFM

6.7.a How to simulate in the mode [femafm_Van_der_Waals_force]

Table 8 Procedures for carrying out simulation in the mode [femafm_Van_der_Waals_force]

Procedures	Examples for input fields
Click [File]➔[New].	
The box [Create new project] appears.	Input "test-femafm100" for [Project name].
Click the tab of [Setup] in [Project Editor].	
Put the cursor on [Component], make a right-click with the mouse and choose [Add Tip].	Choose [Pyramid].
The angle (deg) is required.	Use the default value 32.0 (deg) and choose [OK].
Choose [Add Sample]→[Database].	Choose [1clg-HOPG].
Choose the tab of [FEM] in [Project Editor].	
Choose [simulation]→[resolution].	Put 2[angstrom].
Look at [Sample][Size] in the tab of [Setup].	Confirm the size of the sample: width w: 66.861[angstrom], depth d: 156.464[angstrom], height h: 23.152[angstrom].
Input values for [Tip][Position] in the tab of [Setup].	Input x=”-36”, y=”-80” and z=”30” for [Position].
Input values for [Tip][ScanArea] in the tab of [Setup].	Input w=”72”, d=”160” and h=”0” for [ScanArea].
With the mouse, put the cursor on the window displaying the images of the tip and the sample properly and make a right-click. Next, a context menu appears, so that put a check mark on the item [Show Scan Area]. Then, the area for scanning is shown in the window.	
Put values for Young’smoduli [GPa], Poisson’s ratios [dimensionless] and Hamaker constants [zJ] for [Tip][Property] and [Sample][Property] in the tabs of [Setup].	Use the default values, [young] 76.5[GPa], [poisson] 0.22 and [hamaker] 50[zJ].
Put the number for [OpenMP_threads] in the tab of [FEM].	Put the number of CPUs for parallel calculations. (The default number of CPUs for parallel calculations is equal to 1.)
Choose [simulation_mode].	Choose the mode of ”femafm_Van_der_Waals_force”.
Click a triangle button for [Calculation] of [FEM].	Start the simulation.
Choose [Display]➔[Result].	Display results of the simulation.

6.7.b How to simulate in the mode [femafm_ frequency_shift]

Table 9 Procedures for carrying out simulation in the mode [femafm_ frequency_shift]

Procedures	Examples for input fields
Click [File]➔[New].	
The box [Create new project] appears.	Input "test-femafm200" for [Project name].
Click the tab [Setup] in [Project Editor].	
Make a right-click on [Component], and [Add Tip] appears.	Choose [Pyramid].
The angle (deg) is required.	Use the default value 32.0 (deg) and choose [OK].
Choose [Add Sample]→[Database].	Choose [si001].

Choose the tab [FEM] in [Project Editor].	
Choose [simulation]→[resolution].	Put 2[angstrom].
Look at [Sample][Size] in the tab of [Setup].	Confirm the size of the sample: width w: 14.28665 [angstrom], depth d: 13.52978 [angstrom], height h: 8.16468 [angstrom].
Input values for [Tip][Position] in the tab of [Setup].	Input x=”-8”, y=”-8” and z=”26” for [Position].
Input values for [Tip][ScanArea] in the tab of [Setup].	Input w=”16”, d=”16” and h=”0” for [ScanArea].
With the mouse, put the cursor on the window displaying the images of the tip and the sample properly and make a right-click. Next, a context menu appears, so that put a check mark on the item [Show Scan Area]. Then, the area for scanning is shown in the window.	
Put values for Young’smoduli [GPa], Poisson’s ratios [dimensionless] and Hamaker constants [zJ] for [Tip][Property] and [Sample][Property] in the tabs of [Setup].	Use the default values, [young] 76.5[GPa], [poisson] 0.22 and [hamaker] 50[zJ].
Put values for [density] and [spring_constant] for [Tip][Property] in the tab of [FEM].	Use the default values, [density]2329.0[kg/m3]and [spring_constant]0.05[n/m].
Put a value of [surface_tension] for [Sample][Property] in the tab of [FEM].	Use the default value, [surface_tension]0.108[N/m].
Put values of [amplitude] and [frequency] for [simulation] in the tab of [FEM].	Input [amplitude]150[angstrom] and [frequency]0.5[GHz].
Put the number of [OpenMP_threads] in the tab [FEM].	Input the number of CPUs for parallel calculations. (The default number of CPUs for parallel calculations is equal to 1.)
Choose [simulation_mode].	Choose the mode of ”femafm_frequency_shift”.
Click a triangle button for [Calculation] of [FEM].	Start the simulation.
Choose [Display]➔[Result].	Display results of the simulation.

6.7.c How to simulate in the mode [femafm_ JKR]

Table 10 Procedures for carrying out simulation in the mode [femafm_ JKR]

Procedures	Examples for input fields
Click [File]➔[New].	
The box [Create new project] appears.	Input "test-femafm300" for [Project name].
Click the tab [Setup] in [Project Editor].	
Make a right-click on [Component] and choose [Add Tip].	Choose [Pyramid].
The angle (deg) is required.	Use the default value 32.0 (deg) and choose [OK].
Choose [Add Sample]→[Database].	Choose [si001].
Choose the tab [FEM] in [Project Editor].	
Choose [simulation]→[resolution].	Put 2[angstrom].
Look at [Sample][Size] in the tab of [Setup].	Confirm the size of the sample: width w: 14.28665 [angstrom], depth d: 13.52978 [angstrom], height h: 8.16468 [angstrom].

Input values for [Tip][Position] in the tab of [Setup].	Input x=”-8”, y=”-8” and z=”6” for [Position].
Input values for [Tip][ScanArea] in the tab of [Setup].	Input w=”16”, d=”16” and h=”0” for [ScanArea].
With the mouse, put the cursor on the window displaying the images of the tip and the sample properly and make a right-click. Next, a context menu appears, so that put a check mark on the item [Show Scan Area]. Then, the area for scanning is shown in the window.	
Put values for Young’smoduli [GPa], Poisson’s ratios [dimensionless] and Hamaker constants [zJ] for [Tip][Property] and [Sample][Property] in the tabs of [Setup].	Use the default values, [young] 76.5[GPa], [poisson] 0.22 and [hamaker] 50[zJ].
Put values for [density] and [spring_constant] for [Tip][Property] in the tab of [FEM].	Use the default values, [density]2329.0[kg/m3]and [spring_constant]0.05[n/m].
Put a value of [surface_tension] for [Sample][Property] in the tab of [FEM].	Use the default value, [surface_tension]0.108[N/m].
Put values of [amplitude] and [frequency] for [simulation] in the tab of [FEM].	Input [amplitude]150[angstrom] and [frequency]0.5[GHz].
Put numbers for [ix] and [iy] of [JKR_position] in the tab [FEM].	Input 5 for [ix] and 1 for [iy].
Put the number for [OpenMP_threads] in the tab [FEM].	Input the number of CPUs for parallel calculations. (The default number of CPUs for parallel calculations is equal to 1.)
Choose [simulation_mode].	Choose the mode of ”femafm_JKR”.
Click a triangle button for [Calculation] of [FEM].	Start the simulation. (Results of the simulation are stored in an output file “femafm_simulation_tip_delta_force.csv”.)

Chapter 7 Soft Material Liquid AFM Simulator (LiqAFM)

Soft Material Liquid AFM Simulator (LiqAFM) is the solver which simulates AFM experiments in liquid. By using LiqAFM, We can simulate oscillation of a cantilever in liquid, and compute a resonance frequency. We can also simulate a contact between a viscoelastic sample and a tip, and can compute a force curve.

7.1 Calculation method for simulation of cantilever oscillation in liquid

7.1.a Modeling of cantilever (one dimensional elastic beam model)

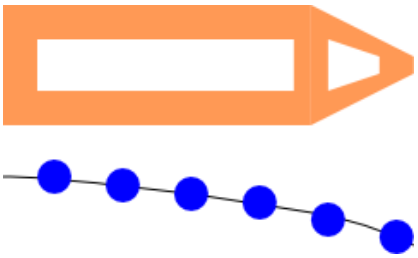

Figure 115 One dimensional elastic beam.

In LiqAFM, we treat a cantilever as a one dimensional elastic beam, illustrated by Figure 115. The beam extends in the longitudinal direction of cantilever, and we assume that the cantilever moves in two ways, that is, oscillates in the vertical direction and rotates around the longitudinal axis.

The reason that we approximate the cantilever by such a simplified model is explained below.

- The cantilever used in AFM experiment is elongate, and thickness and width is tiny in comparison with length.
- In actual AFM experiment, motion of cantilever is ristricted to oscillation in the vertical direction and rotation around the longitudinal axis.

It may be thought that when we examine motion of cantilever in this model, it is not necessary to consider a perforated cantilever. But it is not true. Considering the structure of a cantilever is necessary for calculation of fluid dynamics, as we explain detail at following section. So we adopt the methid that we consider liquid as incompressible viscous fluid, discretize the cantilever and surrouding space, and then solve fluid dynamics equation numerically.

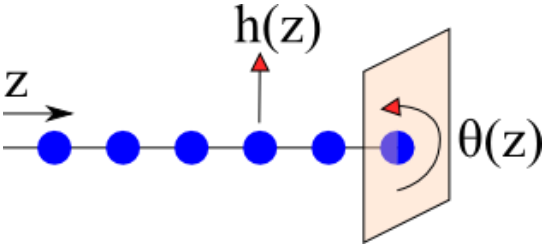

Figure 116 Flexibility of one dimensional elastic beam.

We examine equations of one dimensional elastic beam below. The position of the cantilever in the longitudinal direction is denoted by z. Displacement of beam in the vertical direction at a position z is denoted by $h(z)$, and rotation angle in the direction of counterclockwise is denoted by $\theta(z)$. So $h(z)$ expresses vertical oscillation of the beam, and $\theta(z)$ expresses rotational oscillation.

Equations of motion about a variable $h(z)$ and a variable $\theta(z)$ are given next.

$$\rho S(z)\frac{\partial^2}{\partial t^2}h(z) = -\frac{\partial^2}{\partial z^2}\left[EI(z)\frac{\partial^2}{\partial z^2}h(z)\right] - \gamma\rho S(z)\frac{\partial}{\partial t}h(z) + F^{\mathrm{liq}}(z)$$

$$\rho I(z)\frac{\partial^2}{\partial t^2}\theta(z) = GI(z)\frac{\partial^2}{\partial z^2}\theta(z) + T^{\mathrm{liq}}(z)$$

ρ stands for density of cantilever's material, and $S(z)$ stands for cross section of the cantilever at the position z. When $w(z)$ stands for horizontal width and $d(z)$ stands for vertical thickness at positin z, a following relation holds.

$$S(z) = w(z)d(z)$$

E stands for modulus of longitudinal elasticity (Young's modulus) of cantilever's material, G stands for modulus of transverse elasticity, and γ stands for damping ratio. The dimension of γ is reciprocal of time. $I(z)$ stands for second moment of area of the cantilever at position z, and given by following relation.

$$I(z) = \frac{1}{2}w(z)d(z)^3$$

$F^{\mathrm{liq}}(z)$ stands for a sum of fluid resistance at position z and contact force which a tip recieves from a sample. $F^{\mathrm{liq}}(z)$ is given as force per unit length. $T^{\mathrm{liq}}(z)$ stands for a sum of fluid resistance at position z and torque of contact force which a tip recieves from a sample. $T^{\mathrm{liq}}(z)$ is given as moment per unit length.

Cantilever is forced to vibrate with base excitation in simulation.

7.1.b Modeling of fluid (two dimensional incompressible viscous fluid)

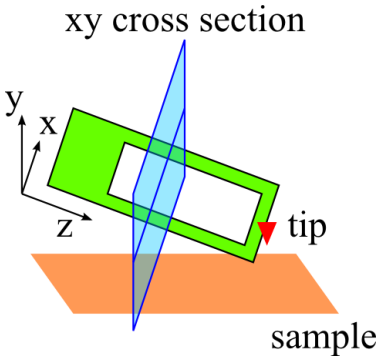

Figure 117 z axis is along the longitudinal direction. xy plane is perpendicular to the z axis.

In LiqAFM, fluid is treated as two dimensional incompressible viscous fluid. We consider fluid to be restricted to xy plane which is perpendicular to z axis, which is along longitudinal direction. (x axis is horizontal direction, and y axis is vertical direction.) We consider effect of viscosity in addition, and approximate fluid as stokes flow.

The reason that we approximate the fluid by such a simplified model is explained below.

- Motion of fluid is considered to be restricted to the plane perpendicular to the cantilever, because cantilever which drives fluid is uniformly constructed in the horizontal direction.
- Fluid can be regarded as incompressible because flow speed is sufficiently smaller than sonic speed.

- Fluid can be regarded as stokes flow because a scale of fluid is in the order of 100[μm] and a viscosity term is dominant as compared with a inertia term in fluid motion.

We examine the equation of motion which dominates motion of fluid. First of all, we consider Navier-Stokes equation of incompressible fluid in a two dimensional space.

$$\frac{\partial \vec{v}}{\partial t} + (\vec{v} \cdot \vec{\nabla})\vec{v} = -\frac{1}{\rho}\vec{\nabla} p + \nu \Delta \vec{v} ,$$

$$\vec{\nabla} \cdot \vec{v} = 0$$

$\vec{v}(x, y) = (v_x(x, y), v_y(x, y))$ stands for a velocity vector field in the xy plane, $p(x, y)$ stands for a pressure field, ρ stands for fluid density and ν stands for kinematic viscosity. The kinematic viscosity ν has following relation with viscosity μ and density ρ.

$$\nu = \frac{\mu}{\rho}$$

We consider the viscosity term $\nu \Delta \vec{v}$ is dominant as compared with the inertia term $(\vec{v} \cdot \vec{\nabla})\vec{v}$, and approximate the Navier-Stokes equation by a following Stokes equation.

$$\frac{\partial \vec{v}}{\partial t} = -\frac{1}{\rho}\vec{\nabla} p + \nu \Delta \vec{v} ,$$

$$\vec{\nabla} \cdot \vec{v} = 0$$

Equation of two demensional incompressible fluid can be simplified with use of a stream function ψ and vorticity ω.

$$v_x = \frac{\partial \psi}{\partial y}, \quad v_y = -\frac{\partial \psi}{\partial x},$$

$$\omega = \partial_x v_y - \partial_y v_x$$

Here the equations below hold.

$$\frac{\partial \omega}{\partial t} = \nu \Delta \omega ,$$

$$\Delta \psi = -\omega$$

The fluid is assumed to be static in an initial state on simulation. A boundary condition is set up so that a velocity of fluid coincides with a velocity of cantilever on the surface of the cantilever where cantilever contacts fluid. The fluid is assumed to be static on the surface of a substrate and at infinity. We solve the equation of motion in fluid numerically at the condition. [reference：M.Tsukada, N.Watanabe, Jpn. J. Appl. Phys. 48 (2009)035001]

The equation of motion of a cantilever and the equation of motion of fluid explained above are solved, by being discretized about time and space in simulation. A domain of a cantilever and fluid is spatially divided into cubic meshes, and a time variable is divided at equal intervals.

7.2 Oscillation of a tabular cantilever in liquid

In this section, we explain a simulation of movement of fluid and a cantilever at the time the tabular cantilever is forced to vibrate in liquid. And we also explain the way to find resonance frequency of a cantilever by simulating repeatedly, varying frequency of forced vibration. In addition, we examine what kind of relation holds between a shape of cantilever and effective viscosity by making holes on a cantilever. It should be noted that viscoelastic contact dynamics between a cantilever and a sample is not taken into account in this section.

7.2.a A characteristc oscillation analysis and a resonance peak

Figure 118 A cantilever without a hole.

We think a cantilever of a shape illustrated in Figure 118. Length, width and thickness of the cantilever is assumed to be 400[μm], 100[μm] and 4[μm] respectively. We vibrate this cantilever in a liquid of density 200.0[kg/m^3] and kinematic viscosity 0.25×10^{-6} [m^2/s]. Here fluid is assumed to be more rarefied than water for easy calculation.

Figure 119 is the graph that shows the amplitude change of the caltilever over time when the cantilever is vibrated on frequency 4.0[kHz] in the liquid. The graph shows that amplitude of the cantilever converges to a value with time.

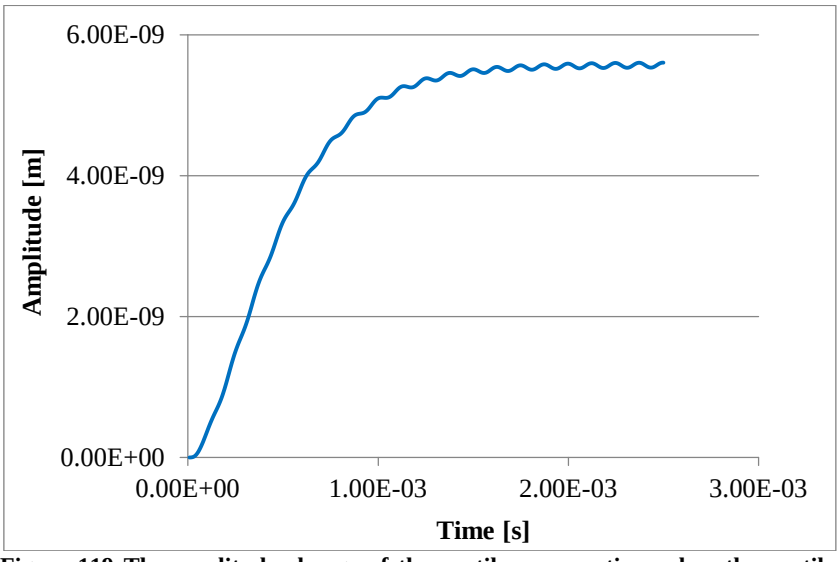

Figure 119 The amplitude change of the cantilever over time when the cantilever is forced to vibrate in a liquid.

So we vary frequency of forced vibration of the cantilever and plot convergence values of the cantilever's amplutide. Figure 120 is this graph. This graph shows that resonance frequency of the cantilever is about 18.0[kHz].

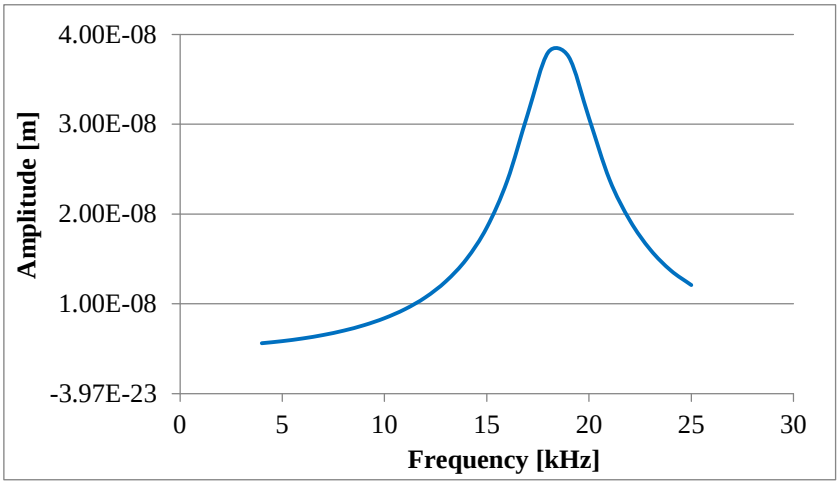

Figure 120 The graph on which convergence value of cantilever's amplitude is plotted over frequency of forced vibration of the cantilever.

7.2.b Effect of cantilever's holes and effective viscosity

In this section we will argue by simulation calculation about a change of effective viscosity which a cantilever feels from liquid by perforating a cantilever.

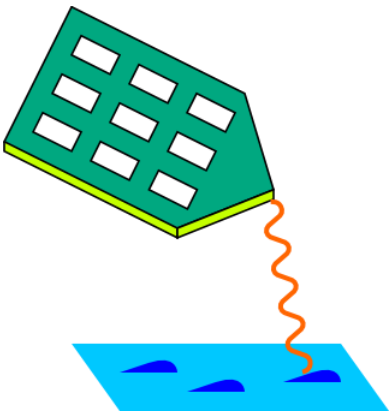

Figure 121 A polymer chain is attached on the apex of the cantilever and AFM experiment is conducted with this tip.

Here we assume the following situation. We attach a polymer chain on the apex of the cantilever and conduct AFM experiment with this polymer chain tip as Figure 121. We want to investigate properties of the polymer chain such as a modulus of elasticity. Such experiments are actually conducted in research in which soft materials are investigated by AFM.

When such an experiment is conducted, it is expected that viscous resistance force which the cantilever feels becomes noise and disturbs the result. Hence a cantilever of small viscous resistance force is needed. So we come to the idea that what is necessary is reducing the effective viscosity which the cantilever feels by making many holes on the cantilever.

The following is the analysis procedure for finding a modulus of viscous resistance force by simulation of perforated cantilever's oscillation in liquid. First, we think the following equation as the equation of motion for a rigid sphere in luquid which is attached to spring.

$$m\ddot{z} = -kz - cR\eta\dot{z} + F_0 \cos\omega t$$

k stands for a spring constant, c stands for a dimensionless coefficient, R stands for a radius for a rigid sphere, η stands for viscosity of liquid and $F_0 \cos\omega t$ is the external force term.

Here we introduce Q-value with the following.

$$cR\eta = \frac{m\omega_0}{Q}$$

At this time a solution of the equation of motion for a rigid sphere in an appropriate initial condition is given by the following.

$$z = \frac{F_0}{(k - m\omega^2)^2 + (\frac{m\omega_0\omega}{Q})^2}[(k - m\omega^2)\cos\omega t + \frac{m\omega_0\omega}{Q}\sin\omega t]$$

ω_0 in the previous equation stands for resonance angular frequency and the following relation is thought to be hold.

$$\omega_0 = \sqrt{\frac{k}{m}}$$

We can understand from the previous equation that the spring constant is gained from the resonance angular frequency. In addition the coefficient of viscous resistance force is gained from Q-value as follows.

$$cR\eta = \frac{\sqrt{mk}}{Q}$$

Now we examine the cantilever in the previous section. Length, width and thickness of the cantilever is 400[μm], 100[μm] and 4[μm] respectively. We make one hole, two holes, four holes and ten holes on the caltilever as illustrated in Figure 122, Figure 123, Figure 124 and Figure 125 respectively. And these cantilevers are oscillated in luquid of density 200.0[kg/m^3] and kinematic viscosity 0.25×10^{-6} [m^2/s].

Figure 122 The cantilever with one hole.

Figure 123 The cantilever with two holes.

Figure 124 The cantilever with four holes.

Figure 125 The caltilever with ten holes.

The five cantilevers illustrated in Figure 118, Figure 122, Figure 123, Figure 124 and Figure 125 are vibrated in liquid. Figure 126 is the graph on which the convergence values of cantilever's amplitude with time is plotted with respect to frequency of forced vibration of the cantilever.

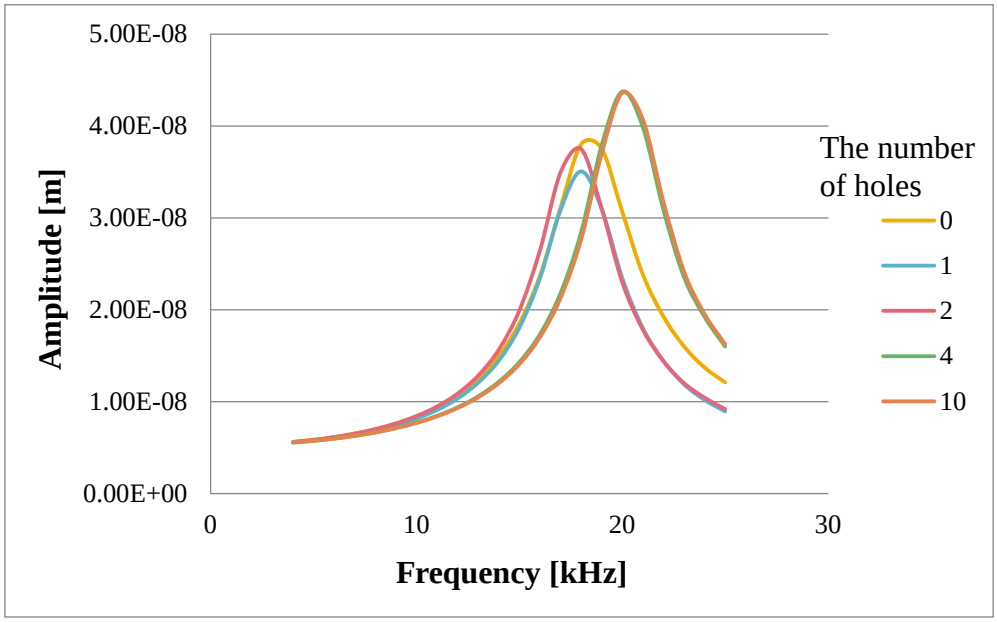

Figure 126 The graph on which the convergence values of cantilever's amplitude with time is plotted for the five kinds of cantilever, varying frequency of cantilever's forced vibration.

Table 11 is obtained by reading resonance angular frequency ω_0 and Q-value from Figure 126 and calculating the coefficient of viscous resistance force. Mass m is calculated considering density of the cantilever's material as 2330[kg/m^3].

Table 11 Mass, spring constants, Q-values and coefficients of viscous resistance force for the five kinds of cantilever.

The numberof holes	0	1	2	4	10
m [kg]	3.73×10^{-10}	2.75×10^{-10}	2.75×10^{-10}	2.75×10^{-10}	2.75×10^{-10}
k [N/m]	4.77	3.52	3.52	4.34	2.17
Q	6.78	6.30	6.70	7.89	7.87
$cR\eta$ [kg/s]	6.22×10^{-6}	4.93×10^{-6}	4.64×10^{-6}	4.38×10^{-6}	3.10×10^{-6}

Figure 127 Variation of a spring constant to the number of cantilever's holes.

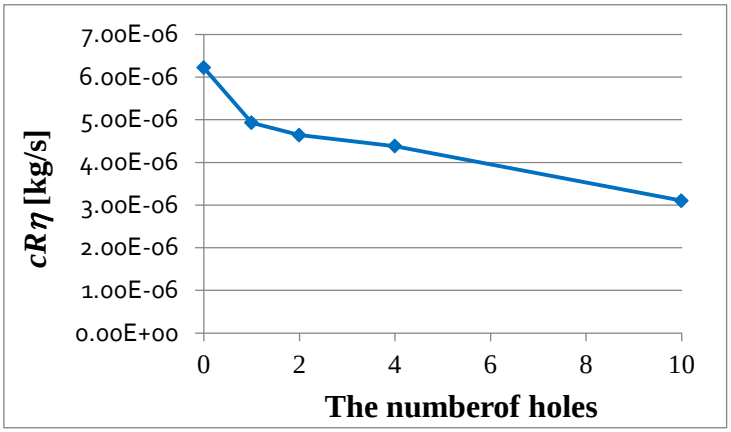

Figure 128 Variation of coefficient of viscous resistance force to the number of cantilever's holes.

It is understood from Figure 128 that the coefficient of viscous resistance force decreases as holes increase.

GUI is shown in Figure 129 on which the oscillation of a cantilever which has ten holes is simulated.

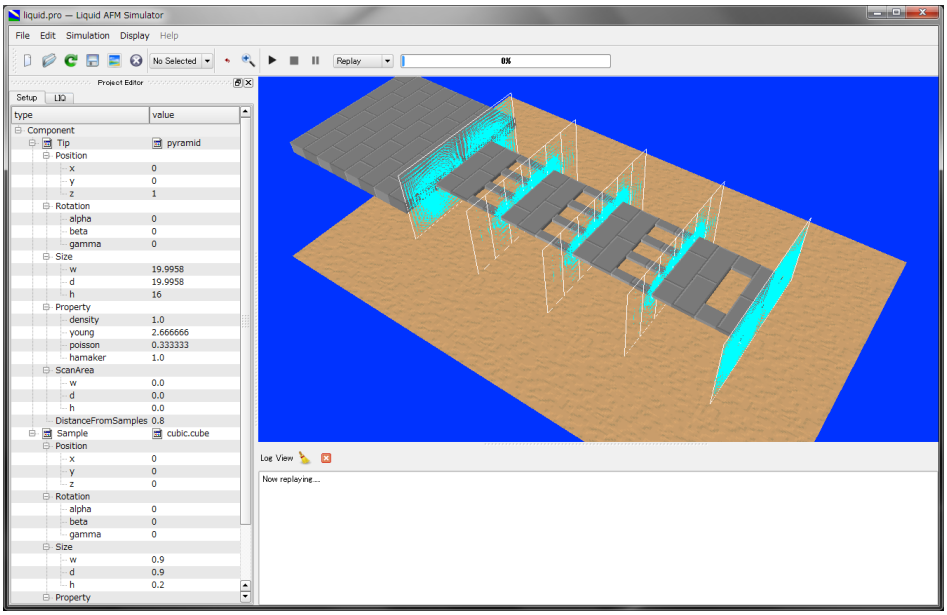

Figure 129 GUI on which the vibration of a cantilever which has ten holes is simulated.

7.3 The calculation method of viscoelastic contact dynamics between a cantilever in liquid and a sample surface

LiqAFM provides an option for simulating viscoelastic contact dynamics between a tip and a sample. This option is activated by the "viscoelasticity" button in the "LIQ-Mode setting" tab which is located in the "ProjectEditor" window on the left of the GUI. Off is selected by default in this button. And by switching on the button, simulation of viscoelastic contact dynamics can be carried out.

A state of viscoelastic contact is examined at a designated point of a sample surface on the viscoelastic contact dynamics simulation of the LiqAFM. The method of numeric calculation is as follows. The equation of motion of a cantilever and the Stokes equation of fluid are numerically calculated by the difference method while the distance between a tip and a sample is calculated at each step of time. The tip is assumed to be in contact with the sample when the tip reaches a fixed distance.

When the tip slips in the region of JKR theory from the region of Van der Waals force, the tip is drawn in the inside of the sample with uniform velocity by adhesion force from the sample. The velocity of the tip in this situation is set up almost similarly to the typical velocity of a tip excited by a cantilever.

Motion of a tip which slips in the region of JKR theory is as explained in the chapter 5 “A method for investigating viscoelastic contact problem”.

The simulation is set to be stopped when the tip leaves from the sample. The file named delta_tipforce.csv is output as calculation result data. Displacements of a tip in the z axis and z -components of force which interacts from a sample to a tip is writed out in the file.

Three concrete examples of computation are introduced below. The each value of properties and parameters in this simulation is explained in section 7-4.

7.3.a In the case of a cantilever of a large spring constant in vacuum

We think the simulation on which a cantilever with a large spring constant is in contact with a viscoelastic sample in a vacuum. Figure 130 is the graph on which displacements of the tip and external force to a tip are plotted. In order to display this graph, it is needed to extend the region $-2.0\times10^{-9} \le z \le 5.0\times10^{-10}$ [m], $-1.0\times10^{-7} \le F \le 0$ [N] to the total region of the graph which is gained from the data of delta_tipforce.csv. The curve on the graph is drawn with time evolution in the direction of the arrows.

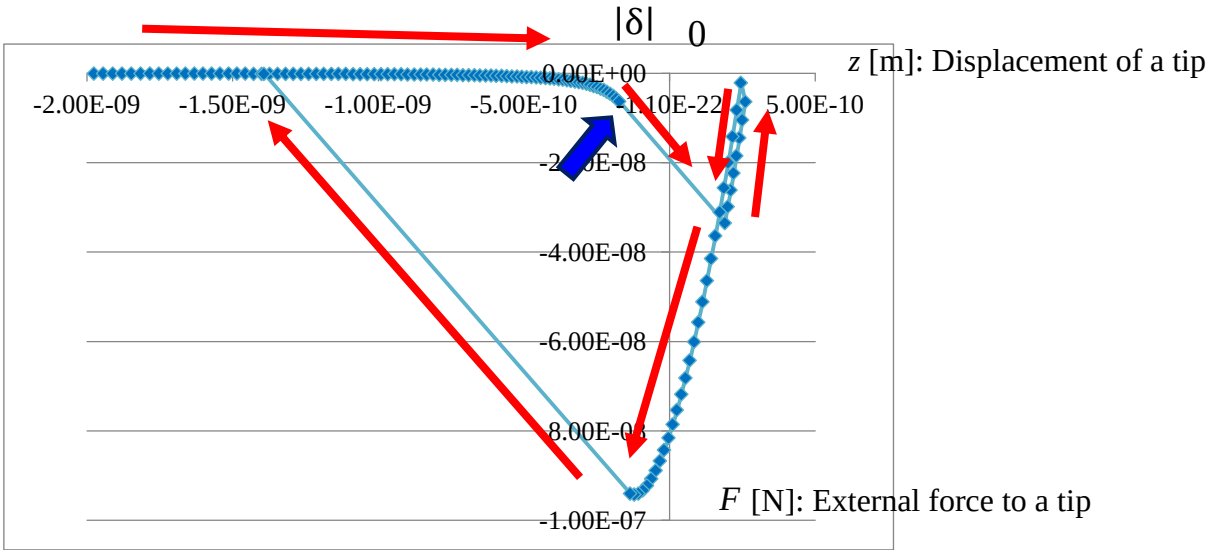

Figure 130 The graph on which displacements of a tip and external force applied to a tip is plotted which is gained from simulating a contact between a cantilever with a large spring constant and a viscoelastic sample in a vacuum.

Here z is positive in the vertical downward direction, and F is positive in the vertical upward direction as descripted in Figure 131. In the upper graph, the adhesion which is applied to a tip when a tip is in contact with a sample is about 80~100[nN]. This value is valid.

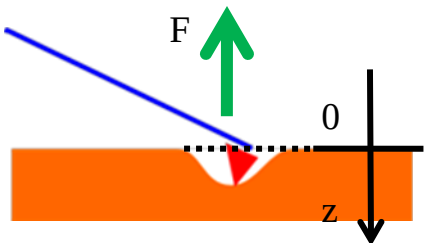

Figure 131 The direction of variable z, F

We view Figure 130 as follows. First the tip comes in contact with the sample above the surface and is pushed into the interior of the sample. Once the tip is pushed into a position where adhesion becomes zero, the tip is in turn pulled back in the direction away from the sample. Calculation is carried out till the tip leaves the sample on the simulation.

Height of the position where a tip is in contact with a sample is descripted as follows.

$$|\delta| = \left(\frac{AD}{6k}\right)^{1/3}$$

Here A stands for a Hamaker constant, k stands for a spring constant and D stands for a diameter of a tip.

7.3.b In the case of a cantilever of a small spring constant in vacuum

We think the simulation on which a cantilever with a small spring constant is in contact with a viscoelastic sample in a vacuum. The following is the graph on which displacements of the tip and external force to a tip are plotted. In order to display this graph, it is needed to extend the region $-1.0\times10^{-9} \le z \le 6.0\times10^{-10}$, $-1.0\times10^{-7} \le F \le 0$ to the total region of the graph which is gained from the data of delta_tipforce.csv. The curve on the graph is drawn with time evolution in the direction of the arrows.

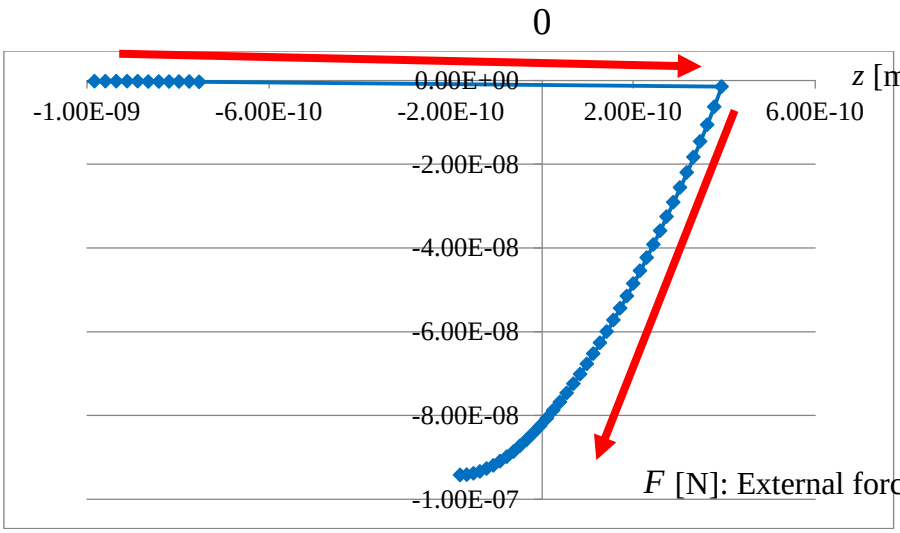

Figure 132 The graph on which displacements of a tip and external force applied to a tip is plotted which is gained from simulating a contact between a cantilever with a small spring constant and a viscoelastic sample in a vacuum.

On the graph of Figure 132, the slope of the curve at the time the tip slips in the region of JKR theory from the region of Van der Waals force, is small and almost horizontal because the spring constant of the cantilever is small. In addition, the process of a tip leaving a sample is not reproduced in the simulation. This is because the spring constant is too small that the tip can not overcome adhesion and can not leave the sample. (If a spring constant is small, a tip is often flown to a nearly infinity position in the process that the tip slips out from the region of JKR theory to the region of Van der Waals force.)

7.3.c In the case of a cantilever of a large spring constant in liquid

We think the simulation on which a cantilever with a large spring constant is in contact with a viscoelastic sample in liquid. Figure 133 is the graph on which displacements of the tip and external force to a tip are plotted. In order to display this graph, it is needed to extend the region $-2.0\times10^{-9} \le z \le 5.0\times10^{-10}$, $-1.0\times10^{-7} \le F \le 0$ to the total region of the graph which is gained from the data of delta_tipforce.csv. The curve on the graph is drawn with time evolution in the direction of the red arrows. It is observed that motion of the tip is influenced by fluid in the process of contact between the tip and the sample.

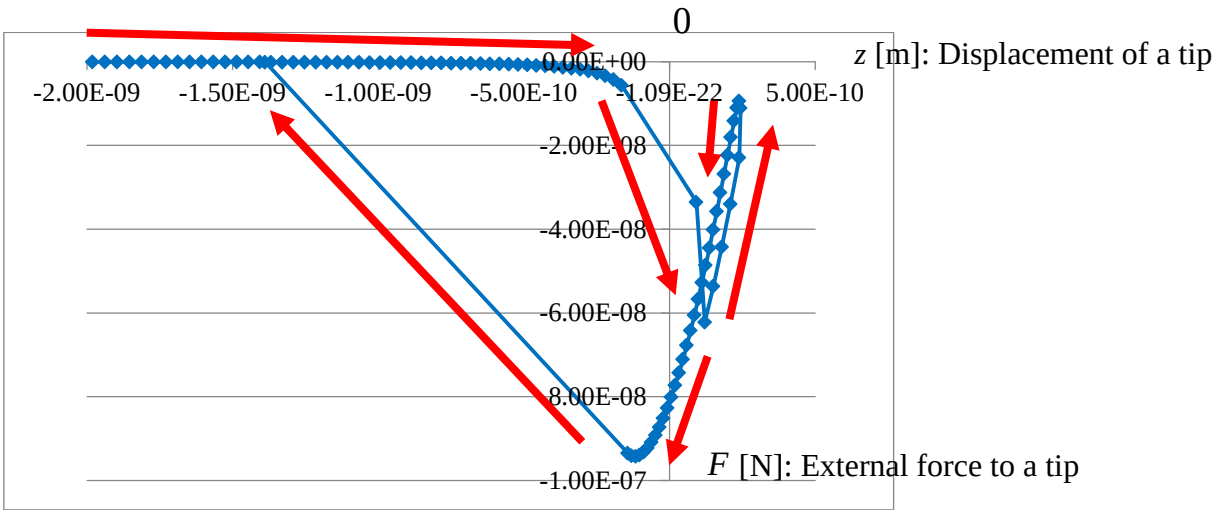

Figure 133 The graph on which displacements of a tip and external force applied to a tip is plotted which is gained from simulating a contact between a cantilever with a large spring constant and a viscoelastic sample in liquid.

7.4 Users guide: how to use LiqAFM

In this section, it is explained how values of property and values of parameters should be set up when LiqAFM is actually used.

7.4.a Simulation of a cantilever with many holes in liquid

First, we explain how to carry out the simulation of section 7.2 on which the cantilever with many holes is vibrated in liquid. The project file actually used in this simulation is shown as follows.

```
<Project>
  <Setup headers="type,value">
    <Component>
  <Tip charge="" radius="0" type="model" free="" angle="32">pyramid
    <Position><x>0</x>
                <y>0</y>
                <z min="0">1</z>
        </Position>
        <Rotation><alpha min="-180" max="180">0</alpha>
                <beta min="-180" max="180">0</beta>
                <gamma min="-180" max="180">0</gamma>
        </Rotation>
        <Size><w ctrl="label">19.9958192610985</w>
            <d ctrl="label">19.9958192610985</d>
            <h ctrl="label">16</h>
        </Size>
        <Property><density unit="a.u.">1.0</density>
                <young unit="a.u.">2.666666</young>
                <poisson>0.333333</poisson>
                <hamaker unit="a.u.">1.0</hamaker>
        </Property>
        <ScanArea><w min="-1000" max="1000">0.0</w>
                <d min="-1000" max="1000">0.0</d>
                <h min="-1000" max="1000">0.0</h>
        </ScanArea>
        <DistanceFromSamples unit="nm">0.8</DistanceFromSamples>
  </Tip>
      <Sample charge="" type="grid" free="">cubic.cube
    <Position><x>0</x>
                <y>0</y>
                <z min="0">0</z>
        </Position>
        <Rotation><alpha min="-180" max="180">0</alpha>
                <beta min="-180" max="180">0</beta>
                <gamma min="-180" max="180">0</gamma>
        </Rotation>
        <Size><w ctrl="label">0.9</w>
            <d ctrl="label">0.9</d>
            <h ctrl="label">0.2</h>
        </Size>
        <Property><density unit="a.u.">1.0</density>
                <young unit="a.u.">2.666666</young>
                <poisson>0.333333</poisson>
                <hamaker unit="a.u.">1.0</hamaker>
        </Property>
      </Sample>
    </Component>
  </Setup>
  <LIQ headers="name,value,unit,descriptions">
    <fluid>
  <material><kviscosity unit="m^2/s" unitgrp="m^2/s">0.25e-06</kviscosity>
            <density unit="kg/m^3" unitgrp="kg/m^3, g/cm^3">200.0</density>
            <impulse unit="N/ms" unitgrp="N/ms">0.0e-06</impulse>
      </material>
    </fluid>
    <bar>
  <material><density unit="kg/m^3" max="10000.0">2330.0</density>
            <young unit="GPa" max="1000.0">130.0</young>
            <poisson>0.28</poisson>
      </material>
      <structure><length unit="um" max="1000.0">400.0</length>
            <width unit="um" max="1000.0">100.0</width>
            <depth unit="um">4.0</depth>
            <angle unit="degree" max="89.9">0.0</angle>
            <twist unit="degree" min="-89.9" max="89.9">0.0</twist>
            <sections>17</sections>
            <tip><position unit="um" max="1000.0">400.0</position>
                <width unit="um">0.0</width>
                <radius unit="nm">1.0</radius>
            </tip>
            <spotlight display="false"><position display="false" unit="um">400.0</position>
```

```
                                                <distance display="false" unit="um">1000.0</distance>
                                                <angle display="false" unit="degree">0.0</angle>
                        </spotlight>
                        <body display="false"><section display="false">0.0 1.0 1.0</section>
                                                <section display="false">1.0 1.0 1.0</section>
                        </body>
                        <split display="false"><section display="false">0.125 0.0 0.1</section>
                                                <section display="false">0.25 0.0 0.1</section>
                        </split>
                        <split display="false"><section display="false">0.125 0.2 0.4</section>
                                                <section display="false">0.25 0.2 0.4</section>
                        </split>
                        <split display="false"><section display="false">0.375 0.0 0.1</section>
                                                <section display="false">0.5 0.0 0.1</section>
                        </split>
                        <split display="false"><section display="false">0.375 0.2 0.4</section>
                                                <section display="false">0.5 0.2 0.4</section>
                        </split>
                        <split display="false"><section display="false">0.625 0.0 0.1</section>
                                                <section display="false">0.75 0.0 0.1</section>
                        </split>
                        <split display="false"><section display="false">0.625 0.2 0.4</section>
                                                <section display="false">0.75 0.2 0.4</section>
                        </split>
                        <split display="false"><section display="false">0.875 0.0 0.3</section>
                                                <section display="false">0.9375 0.0 0.3</section>
                        </split>
            </structure>
            <motion><frequency unit="kHz" max="1000.0">5.0</frequency>
                        <amplitude unit="nm">5.0</amplitude>
                        <baseheight unit="um">50</baseheight>
            </motion>
          </bar>
          <sample>
        <material>
          <point><young unit="GPa" max="10000000000.0">1.0e+05</young>
                        <damper unit="Ns/um">0.0</damper>
                        <tension unit="uN">0.0</tension>
                        <touch unit="nm">1.5</touch>
                        <detach unit="">1.0</detach>
              </point>
            </material>
            <structure>
          <surface display="false">
            <section display="false" unit="um">0.0 0.0</section>
                  <section display="false" unit="um">1.0 0.0</section>
              </surface>
            </structure>
          </sample>
          <simulation><resolution display="false" unit="nm">0.1</resolution>
                        <time><steps_per_cycle max="2048.0">1024</steps_per_cycle>
                                <cycles_per_resolution step="smooth">8</cycles_per_resolution>
                        </time>
                        <convergence>
                      <criterion>0.0</criterion>
                        </convergence>
          </simulation>
          <Output>
        <Directory ctrl="label">.\output
          <height where="head" interval="32" displaytype="2D" ctrl="label">height.dat</height>
                <height_amplitude where="head" interval="32" displaytype="2D"
ctrl="label">height_amplitude.dat</height_amplitude>
                <twist where="head" interval="32" displaytype="2D" ctrl="label">twist.dat</twist>
                <tipforce where="head" interval="32" displaytype="2D" ctrl="label">tipforce.dat</tipforce>
                <Movie displaytype="movie" ctrl="label">movie1.mvc</Movie>
                <bar_motion displaytype="movie" ctrl="label">barmotion.bar</bar_motion>
            </Directory>
          </Output>
        </LIQ>
      </Project>
```

The project file descripted as above is created and edited as a text file with the extension .pro. The folder named SampleProjects is prepared in the folder where executable files of SPM simulator are put. The samples of the project files are contained in the folder. So you may refer to it.

We explain the items of the project considered to be important below.

First a shape of a cantilever is set up by the description below which belongs to the tag named <bar><structure>.

```
    <body display="false"><section display="false">0.0 1.0 1.0</section>
<section display="false">1.0 1.0 1.0</section>
    </body>
    <split display="false"><section display="false">0.125 0.0 0.1</section>
<section display="false">0.25 0.0 0.1</section>
    </split>
    <split display="false"><section display="false">0.125 0.2 0.4</section>
<section display="false">0.25 0.2 0.4</section>
    </split>
    <split display="false"><section display="false">0.375 0.0 0.1</section>
<section display="false">0.5 0.0 0.1</section>
    </split>
    <split display="false"><section display="false">0.375 0.2 0.4</section>
<section display="false">0.5 0.2 0.4</section>
    </split>
    <split display="false"><section display="false">0.625 0.0 0.1</section>
<section display="false">0.75 0.0 0.1</section>
    </split>
    <split display="false"><section display="false">0.625 0.2 0.4</section>
<section display="false">0.75 0.2 0.4</section>
    </split>
    <split display="false"><section display="false">0.875 0.0 0.3</section>
<section display="false">0.9375 0.0 0.3</section>
    </split>
```

The shape of the cantilever set up by the description above becomes like Figure 134.

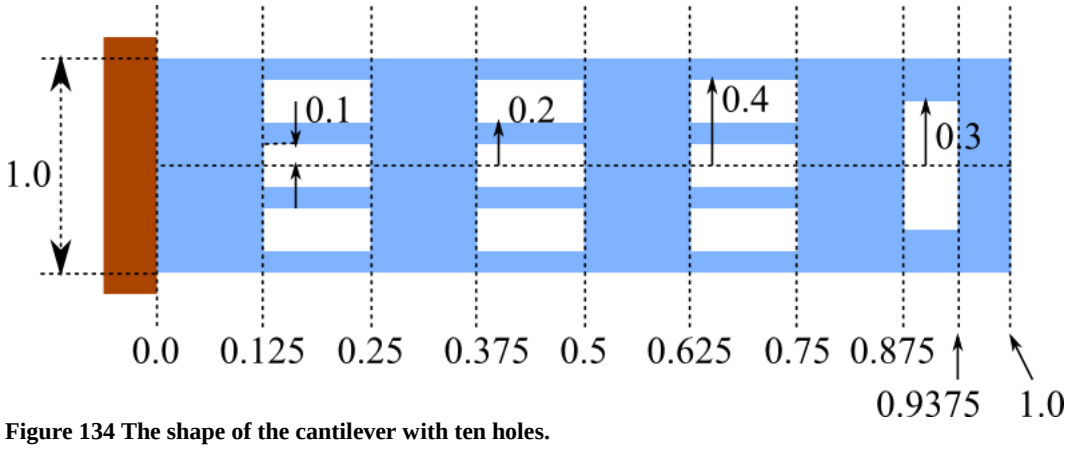

Figure 134 The shape of the cantilever with ten holes.

The important items descripted in a project file are the following.

Table 12 The important items descripted in a project file in LiqAFM.

<LIQ><fluid><material><kviscosity>	Kinematic viscosity of the fluid (unit="m^2/s")

<LIQ><fluid><material><density>	Density of fluid (unit="kg/m^3")
<LIQ><fluid><material><impulse>	Impulse of force that molecules give to the fluid at random (unit="N/ms")
<LIQ><bar><material><density>	Density of material used for making the cantilever (unit="kg/m^3")
<LIQ><bar><material><young>	Young's modulus of material used for making the cantilever (unit="GPa")
<LIQ><bar><material><poisson>	Poisson's ratio of material used for making the cantilever (dimensionless)
<LIQ><bar><material><friction>	Coefficient of friction of material used for making cantilever (dimensionless)
<LIQ><bar><material><hamaker>	Hamaker constant of material used for making the cantilever (unit="J")
<LIQ><bar><structure><tip><radius>	Radius of the tip of the cantilever (unit="nm")
<LIQ><bar><motion><frequency>	Frequency of the oscillation of the cantilever with external force (unit="kHz")
<LIQ><bar><motion><amplitude>	Amplitude of the oscillation of the cantilever with external force (unit="nm")
<LIQ><bar><motion><baseheight>	Distance between the surface of the sample and the center of the cantilever in the initial position (unit="nm") (To let the tip of the cantilever touch the surface of the sample, it has to be nearly equal to the amplitude of the oscillation of the cantilever.)
<LIQ><bar><DistanceFromSamples>	Put the value which is equal to <baseheight> (unit="nm")
<LIQ><sample><material><point><young>	Young's modulus of the sample (unit="GPa")
<LIQ><sample><material><point><poisson>	Poisson's ratio of the sample (dimensionless)
<LIQ><sample><material><point><damper>	Damping coefficient of the sample (unit="Ns/m") (This coefficient is made use of to generate the damping force, which is linearly dependent upon the velocity.)
<LIQ><sample><material><point><tension>	Tension between the tip of the cantilever and the sample when they touch (unit="uN")

<LIQ><sample><material><point><touch>	Distance between the surface of the sample and the tip of the cantilever in the initial position (It has to be less than zero. Multiply the value of <baseheight> by (-1) and put it.) (unit="nm")
<LIQ><sample><material><point><detach>	Distance between the point where the tip is released from sample and the initial position of the tip of the cantilever (It has to be less than zero. Put the value being equal to the value of <touch>.) (unit="nm")
<LIQ><sample><material><point><hamaker>	Hamaker constant of the sample (unit="J")
<LIQ><sample><material><point><adhesive>	The surface tension of the sample (unit="N/m")
<LIQ><simulation><time><max_cycles step="smooth">1.6	A period of the cycle of the cantilever's oscillation caused by the external force during the whole simulation (dimensionless. A suitable value of this quantity is 1.6 around.)
<LIQ><Output><Directory><delta_tipforce where="head" interval="1" displaytype="1D" ctrl="label">delta_tipforce.csv	Time evolution of a distance and forces of attraction and repulsion between the cantilever's tip and the sample is output into a file, "delta_tipforce.csv".

7.4.b Simulation of a cantilever with a large spring constant in vacuum

The project file of "In the case of a cantilever of a large spring constant in a vacuum" which is simulated at the section 7.3.a is the following.

```
<Project>
  <Setup headers="type,value">
    <Component>
  <Tip charge="" radius="0" type="model" free="" angle="32">pyramid
    <Position><x>0</x>
                <y>0</y>
                <z min="0">0</z>
        </Position>
        <Rotation><alpha min="-180" max="180">0</alpha>
                <beta min="-180" max="180">0</beta>
                <gamma min="-180" max="180">0</gamma>
        </Rotation>
        <Size><w ctrl="label">19.9958192610985</w>
              <d ctrl="label">19.9958192610985</d>
              <h ctrl="label">16</h>
        </Size>
        <Property><density unit="a.u.">1.0</density>
                  <young unit="a.u.">2.666666</young>
                  <poisson>0.333333</poisson>
                  <hamaker unit="a.u.">0.0</hamaker>
        </Property>
        <ScanArea><w min="-1000" max="1000">0.0</w>
                <d min="-1000" max="1000">0.0</d>
                <h min="-1000" max="1000">0.0</h>
        </ScanArea>
```

```
            <DistanceFromSamples unit="nm">30.0</DistanceFromSamples>
          </Tip>
          <Sample charge="" type="grid" free="">cubic.cube
       <Position><x>0</x>
                        <y>0</y>
                        <z min="0">0</z>
          </Position>
          <Rotation><alpha min="-180" max="180">0</alpha>
                        <beta min="-180" max="180">0</beta>
                        <gamma min="-180" max="180">0</gamma>
          </Rotation>
          <Size><w ctrl="label">0.0</w>
                  <d ctrl="label">0.0</d>
                  <h ctrl="label">0.0</h>
          </Size>
          <Property><density unit="a.u.">1.0</density>
                        <young unit="a.u.">2.666666</young>
                        <poisson>0.333333</poisson>
                        <hamaker unit="a.u.">0.0</hamaker>
          </Property>
        </Sample>
      </Component>
    </Setup>
    <LIQ headers="name,value,unit,descriptions">
<!--
      <fluid>
        <material><kviscosity unit="m^2/s">0.25e-06</kviscosity>
                  <density unit="kg/m^3">200.0</density>
                  <impulse unit="N/ms">0.0e-6</impulse>
        </material>
      </fluid>
-->
      <bar>
    <material><density unit="kg/m^3" unitgrp="kg/m^3" max="10000.0">2200.0</density>
                  <young unit="GPa" unitgrp="GPa,MPa,kPa,Pa" max="1000.0">6000.0</young>
                  <poisson>0.22</poisson>
                  <friction>0.</friction>
                  <hamaker unit="J">5.0e-20</hamaker>
        </material>
        <structure><length unit="um" unitgrp="um,nm" max="1000.0">400</length>
                    <width unit="um" unitgrp="um,nm" max="1000.0">50</width>
                    <depth unit="um" unitgrp="um,nm">4</depth>
                    <angle unit="deg" max="89.9">0.0</angle>
                    <twist unit="deg" min="-89.9" max="89.9">0.0</twist>
                    <sections max="500">17</sections>
                    <tip><position unit="um" max="1000.0">400</position>
                          <width unit="um">0.0</width>
                          <radius unit="nm">25.0</radius>
                    </tip>
                    <spotlight><position unit="um" max="1000.0">400</position>
                                <distance unit="um" max="10000.0">1000.0</distance>
                                <angle unit="deg">0.0</angle>
                  </spotlight>
                        <body><section display="false">0.0 1.0 1.0</section>
                              <section>1.0 1.0 1.0</section>
                        </body>
        </structure>
        <motion><frequency unit="kHz" unitgrp="kHz,MHz,Hz">1.0</frequency>
                  <amplitude unit="nm" unitgrp="nm,um,ang">30.0</amplitude>
                  <baseheight unit="nm" unitgrp="nm,um,mm,ang">30.0</baseheight>
        </motion>
        <DistanceFromSamples unit="nm" unitgrp="nm,um,ang,mm">30.0</DistanceFromSamples>
      </bar>
      <sample unit="">
    <material>
      <point><young unit="GPa" unitgrp="GPa,MPa,kPa,Pa" max="100000.0">76.5</young>
                  <poisson>0.22</poisson>
                  <damper unit="Ns/m" unitgrp="Ns/um,Ns/m">0.0</damper>
                  <tension unit="uN" unitgrp="uN,nN,N">0.0</tension>
                  <touch unit="nm" unitgrp="um,nm,ang">-30.0</touch>
                  <detach unit="nm">-30.0</detach>
```

```
                        <hamaker unit="J">5.0e-20</hamaker>
                        <adhesive unit="N/m">0.4</adhesive>
                </point>
              </material>
          <structure>
            <surface display="false">
              <section display="false" unit="um">0.0 0.0</section>
                    <section display="false" unit="um">1.0 0.0</section>
                </surface>
              </structure>
            </sample>
            <simulation>
          <time><steps_per_cycle max="2048.0">2048</steps_per_cycle>
                    <max_cycles step="smooth">1.6</max_cycles>
              </time>
              <convergence>
            <criterion min="0.0" max="0.99">0.0</criterion>
              </convergence>
            </simulation>
            <Output>
          <Directory ctrl="label">.\output
            <resonance_curve displaytype="1D" ctrl="label">resonance.csv</resonance_curve>
                <height where="head" interval="1" displaytype="1D" ctrl="label">height.csv</height>
                <height_amplitude where="head" interval="8" displaytype="1D"
ctrl="label">height_amplitude.csv</height_amplitude>
                <tipforce where="head" interval="1" displaytype="1D" ctrl="label">tipforce.csv</tipforce>
                <bending where="head" interval="1" displaytype="1D" ctrl="label">bending.csv</bending>
                <delta_tipforce where="head" interval="1" displaytype="1D" ctrl="label">delta_tipforce.csv</delta_tipforce>
                <Movie interval="8" displaytype="movie" ctrl="label">movie1.mvc</Movie>
                <bar_motion interval="8" displaytype="movie" ctrl="label">barmotion.bar</bar_motion>
              </Directory>
            </Output>
          </LIQ>
        </Project>
```

It is ruled that parts surrounded by "<!--" and "-->" in the project file is skipped. In the project file above, the part of <fluid> is invalidated and simulation in vacuum is carried out.

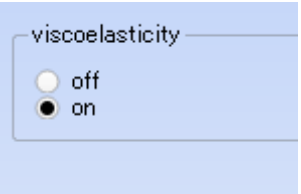

Figure 135 "viscoelasticity" button in "LIQ-Mode setting" tab.

In addition when you carry out simulation with viscoelastic contact dynamics, you should switch on the button "viscoelasticity", shown in Figure 135, in the "LIQ-Mode setting" tab which is located in the "ProjectEditor" window on the left of th GUI. (This button is switched off by default.)

7.4.c simulation of a cantilever with a small spring constant in vacuum

The project file of "In the case of a cantilever of a small spring constant in a vacuum" which is simulated at the section 7.3.b is the following.

```
    <Project>
  <Setup headers="type,value">
    <Component>
      <Tip charge="" radius="0" type="model" free="" angle="32">pyramid
        <Position><x>0</x>
                    <y>0</y>
                    <z min="0">0</z>
              </Position>
```

```
            <Rotation><alpha min="-180" max="180">0</alpha>
                        <beta min="-180" max="180">0</beta>
                        <gamma min="-180" max="180">0</gamma>
            </Rotation>
            <Size><w ctrl="label">19.9958192610985</w>
                    <d ctrl="label">19.9958192610985</d>
                    <h ctrl="label">16</h>
            </Size>
            <Property><density unit="a.u.">1.0</density>
                        <young unit="a.u.">2.666666</young>
                        <poisson>0.333333</poisson>
                        <hamaker unit="a.u.">0.0</hamaker>
            </Property>
            <ScanArea><w min="-1000" max="1000">0.0</w>
                        <d min="-1000" max="1000">0.0</d>
                        <h min="-1000" max="1000">0.0</h>
            </ScanArea>
            <DistanceFromSamples unit="nm">30.0</DistanceFromSamples>
          </Tip>
          <Sample charge="" type="grid" free="">cubic.cube
      <Position><x>0</x>
                        <y>0</y>
                        <z min="0">0</z>
            </Position>
            <Rotation><alpha min="-180" max="180">0</alpha>
                        <beta min="-180" max="180">0</beta>
                        <gamma min="-180" max="180">0</gamma>
            </Rotation>
            <Size><w ctrl="label">0.0</w>
                    <d ctrl="label">0.0</d>
                    <h ctrl="label">0.0</h>
            </Size>
            <Property><density unit="a.u.">1.0</density>
                        <young unit="a.u.">2.666666</young>
                        <poisson>0.333333</poisson>
                        <hamaker unit="a.u.">0.0</hamaker>
            </Property>
          </Sample>
        </Component>
    </Setup>
    <LIQ headers="name,value,unit,descriptions">
<!--
        <fluid>
          <material><kviscosity unit="m^2/s">0.25e-06</kviscosity>
                    <density unit="kg/m^3">200.0</density>
                    <impulse unit="N/ms">0.0e-6</impulse>
          </material>
        </fluid>
-->
        <bar>
    <material><density unit="kg/m^3" unitgrp="kg/m^3" max="10000.0">2200.0</density>
                    <young unit="GPa" unitgrp="GPa,MPa,kPa,Pa" max="1000.0">76.5</young>
                    <poisson>0.22</poisson>
                    <friction>0.</friction>
                    <hamaker unit="J">5.0e-20</hamaker>
          </material>
          <structure><length unit="um" unitgrp="um,nm" max="1000.0">400</length>
                  <width unit="um" unitgrp="um,nm" max="1000.0">50</width>
                      <depth unit="um" unitgrp="um,nm">4</depth>
                      <angle unit="deg" max="89.9">0.0</angle>
                      <twist unit="deg" min="-89.9" max="89.9">0.0</twist>
                      <sections max="500">17</sections>
```

```
                        <tip><position unit="um" max="1000.0">400</position>
                            <width unit="um">0.0</width>
                            <radius unit="nm">25.0</radius>
                        </tip>
                        <spotlight><position unit="um" max="1000.0">400</position>
                                <distance unit="um" max="10000.0">1000.0</distance>
                                <angle unit="deg">0.0</angle>
                        </spotlight>
                    <body><section display="false">0.0 1.0 1.0</section>
                            <section>1.0 1.0 1.0</section>
                        </body>
    </structure>
        <motion><frequency unit="kHz" unitgrp="kHz,MHz,Hz">1.0</frequency>
                <amplitude unit="nm" unitgrp="nm,um,ang">30.0</amplitude>
                <baseheight unit="nm" unitgrp="nm,um,mm,ang">30.0</baseheight>
        </motion>
        <DistanceFromSamples unit="nm" unitgrp="nm,um,ang,mm">30.0</DistanceFromSamples>
      </bar>
      <sample unit="">
    <material>
      <point><young unit="GPa" unitgrp="GPa,MPa,kPa,Pa" max="100000.0">76.5</young>
                <poisson>0.22</poisson>
                <damper unit="Ns/m" unitgrp="Ns/um,Ns/m">0.0</damper>
                <tension unit="uN" unitgrp="uN,nN,N">0.0</tension>
                <touch unit="nm" unitgrp="um,nm,ang">-30.0</touch>
                <detach unit="nm">-30.0</detach>
                <hamaker unit="J">5.0e-20</hamaker>
                <adhesive unit="N/m">0.4</adhesive>
          </point>
        </material>
        <structure>
      <surface display="false"><section display="false" unit="um">0.0 0.0</section>
                                <section display="false" unit="um">1.0 0.0</section>
          </surface>
        </structure>
      </sample>
      <simulation>
    <time><steps_per_cycle max="2048.0">2048</steps_per_cycle>
            <max_cycles step="smooth">1.6</max_cycles>
        </time>
        <convergence>
      <criterion min="0.0" max="0.99">0.0</criterion>
        </convergence>
      </simulation>
      <Output>
    <Directory ctrl="label">.\output<resonance_curve displaytype="1D" ctrl="label">resonance.csv</resonance_curve>
          <height where="head" interval="1" displaytype="1D" ctrl="label">height.csv</height>
          <height_amplitude where="head" interval="8" displaytype="1D"
ctrl="label">height_amplitude.csv</height_amplitude>
          <tipforce where="head" interval="1" displaytype="1D" ctrl="label">tipforce.csv</tipforce>
          <bending where="head" interval="1" displaytype="1D" ctrl="label">bending.csv</bending>
          <delta_tipforce where="head" interval="1" displaytype="1D" ctrl="label">delta_tipforce.csv</delta_tipforce>
          <Movie interval="8" displaytype="movie" ctrl="label">movie1.mvc</Movie>
          <bar_motion interval="8" displaytype="movie" ctrl="label">barmotion.bar</bar_motion>
        </Directory>
      </Output>
    </LIQ>
  </Project>
```

7.4.d simulation of a cantilever with a large spring constant in liquid

The project file of "In the case of a cantilever of a large spring constant in liquid" which is simulated at the section 7.3.c is the following.

```
<Project>
  <Setup headers="type,value">
    <Component>
  <Tip charge="" radius="0" type="model" free="" angle="32">pyramid
    <Position><x>0</x>
                    <y>0</y>
                    <z min="0">0</z>
        </Position>
        <Rotation><alpha min="-180" max="180">0</alpha>
                    <beta min="-180" max="180">0</beta>
                    <gamma min="-180" max="180">0</gamma>
        </Rotation>
        <Size><w ctrl="label">19.9958192610985</w>
                <d ctrl="label">19.9958192610985</d>
                <h ctrl="label">16</h>
        </Size>
        <Property><density unit="a.u.">1.0</density>
                    <young unit="a.u.">2.666666</young>
                    <poisson>0.333333</poisson>
                    <hamaker unit="a.u.">0.0</hamaker>
        </Property>
        <ScanArea><w min="-1000" max="1000">0.0</w>
                    <d min="-1000" max="1000">0.0</d>
                    <h min="-1000" max="1000">0.0</h>
        </ScanArea>
        <DistanceFromSamples unit="nm">30.0</DistanceFromSamples>
      </Tip>
      <Sample charge="" type="grid" free="">cubic.cube
    <Position><x>0</x>
                    <y>0</y>
                    <z min="0">0</z>
        </Position>
        <Rotation><alpha min="-180" max="180">0</alpha>
                    <beta min="-180" max="180">0</beta>
                    <gamma min="-180" max="180">0</gamma>
        </Rotation>
        <Size><w ctrl="label">0.0</w>
                <d ctrl="label">0.0</d>
                <h ctrl="label">0.0</h>
        </Size>
        <Property><density unit="a.u.">1.0</density>
                    <young unit="a.u.">2.666666</young>
                    <poisson>0.333333</poisson>
                    <hamaker unit="a.u.">0.0</hamaker>
        </Property>
      </Sample>
    </Component>
  </Setup>
  <LIQ headers="name,value,unit,descriptions">
    <fluid>
      <material><kviscosity unit="m^2/s">0.25e-06</kviscosity>
                <density unit="kg/m^3">200.0</density>
            <impulse unit="N/ms">0.0e-6</impulse>
      </material>
    </fluid>
    <bar>
  <material><density unit="kg/m^3" unitgrp="kg/m^3" max="10000.0">2200.0</density>
```

```
                        <young unit="GPa" unitgrp="GPa,MPa,kPa,Pa" max="1000.0">6000.0</young>
                        <poisson>0.22</poisson>
                        <friction>0.</friction>
                        <hamaker unit="J">5.0e-20</hamaker>
            </material>
            <structure><length unit="um" unitgrp="um,nm" max="1000.0">400</length>
                    <width unit="um" unitgrp="um,nm" max="1000.0">50</width>
                        <depth unit="um" unitgrp="um,nm">4</depth>
                        <angle unit="deg" max="89.9">0.0</angle>
                        <twist unit="deg" min="-89.9" max="89.9">0.0</twist>
                        <sections max="500">17</sections>
                        <tip><position unit="um" max="1000.0">400</position>
                                <width unit="um">0.0</width>
                                <radius unit="nm">25.0</radius>
                    </tip>
                        <spotlight><position unit="um" max="1000.0">400</position>
                                    <distance unit="um" max="10000.0">1000.0</distance>
                                    <angle unit="deg">0.0</angle>
                        </spotlight>
                        <body><section display="false">0.0 1.0 1.0</section>
                                <section>1.0 1.0 1.0</section>
                    </body>
            </structure>
            <motion><frequency unit="kHz" unitgrp="kHz,MHz,Hz">20.0</frequency>
                    <amplitude unit="nm" unitgrp="nm,um,ang">30.0</amplitude>
                    <baseheight unit="nm" unitgrp="nm,um,mm,ang">30.0</baseheight>
            </motion>
            <DistanceFromSamples unit="nm" unitgrp="nm,um,ang,mm">30.0</DistanceFromSamples>
          </bar>
          <sample unit="">
        <material>
          <point><young unit="GPa" unitgrp="GPa,MPa,kPa,Pa" max="100000.0">76.5</young>
                        <poisson>0.22</poisson>
                        <damper unit="Ns/m" unitgrp="Ns/um,Ns/m">0.0</damper>
                        <tension unit="uN" unitgrp="uN,nN,N">0.0</tension>
                        <touch unit="nm" unitgrp="um,nm,ang">-30.0</touch>
                        <detach unit="nm">-30.0</detach>
                        <hamaker unit="J">5.0e-20</hamaker>
                        <adhesive unit="N/m">0.4</adhesive>
              </point>
            </material>
            <structure>
          <surface display="false"><section display="false" unit="um">0.0 0.0</section>
                                        <section display="false" unit="um">1.0 0.0</section>
              </surface>
            </structure>
          </sample>
          <simulation>
        <time><steps_per_cycle max="2048.0">1024</steps_per_cycle>
                    <max_cycles step="smooth">1.6</max_cycles>
            </time>
            <convergence>
          <criterion min="0.0" max="0.99">0.0</criterion>
            </convergence>
          </simulation>
          <Output>
        <Directory ctrl="label">.\output<resonance_curve displaytype="1D" ctrl="label">resonance.csv</resonance_curve>
                <height where="head" interval="1" displaytype="1D" ctrl="label">height.csv</height>
                <height_amplitude where="head" interval="8" displaytype="1D"
ctrl="label">height_amplitude.csv</height_amplitude>
                <tipforce where="head" interval="1" displaytype="1D" ctrl="label">tipforce.csv</tipforce>
                <bending where="head" interval="1" displaytype="1D" ctrl="label">bending.csv</bending>
```

```
            <delta_tipforce where="head" interval="1" displaytype="1D" ctrl="label">delta_tipforce.csv</delta_tipforce>
            <Movie interval="8" displaytype="movie" ctrl="label">movie1.mvc</Movie>
            <bar_motion interval="8" displaytype="movie" ctrl="label">barmotion.bar</bar_motion>
          </Directory>
        </Output>
      </LIQ>
    </Project>
```

Chapter 8 Geometry Optimizing AFM Image Simulator (CG)

8.1 Classical Force Field

We will explain atomic scaled AFM image simulator based on classical mechanics from the eighth chapter to the tenth chapter. Structures such as a tip and a substitute which is used for AFM measurement and a sample which is a measuring object are aggrigates of atoms, so a value of force applied to a structure and deformation of a structure can be predicted by taking all interactions between atoms into account. For a system for which this simulation is applied, the model is needed which expresses covalent bonds as proper as possible because atoms of a structure often is covalently bonded such as in a solid surface and in a molecule. A classical force field is a model which is constructed for classical mechanical treatment, and various models about classical force field are developed according to purposes and kinds of target structures.

This simulator adopts the MM3 force field model which is developed by Allinger et al. [Allinger1989]. Geometry optimizing AFM image simulator treats the following nine kinds of interaction among atoms.

1. Bond Stretching (the equation (1) in the reference [Allinger1989])
2. Angle Bending (the equation (2) in [Allinger1989])
3. Torsion (the equation (3) in [Allinger1989])
4. Stretch-Bend Interaction (the equation (4) in [Allinger1989])
5. Torsion-Stretch Interaction (the equation (5) in [Allinger1989])
6. Bend-Bend Interaction (the equation (6) in [Allinger1989])
7. Coulomb Interaction (when electric polarization exists.)
8. Dipole-Dipole Interaction
9. van der Waals' Interaction (the equation (7) in [Allinger1989]) based on Buckingham potential (exp-6)

The interactions from first to sixth of above work among bonded atoms. We can choose the following interaction, which is highly used in classical atomic simulation, instead of van der Waals's Interaction based on exp-6 potential.

9'. van der Waals' Interaction based on Lennard-Jones 6-12 potential

References

[Allinger1989] N. L. Allinger, Y. H. Yuh, and J.-H. Lii, J. Am. Chem. Soc., **111**(23), (1989) 8551.

8.2 Geometry optimizing

The interactions listed in the preceding section only depend on the position of atoms. So total potential energy U of a system is described as a function $U = U(\mathbf{r}_1, \mathbf{r}_2, \ldots, \mathbf{r}_N)$ whose inputs are only atomic coordinates $\{\mathbf{r}_i\}$ (Here $i = 1, \ldots, N$ and N is the number of atoms in the system). It can be assumed that a structure is deformed to a stable shape instantly if the temperature of the system is low and time scale of tip's movement is smaller enough than that of geometry optimization. In other words, the atoms are rearranged instantly to the coorinates which minimizes the total potential energy. Geometry optimizing AFM image simulator treats deformation of a structure based on this assumption, and calculates force applied to a tip model.

There are some calculation algorithm which finds a minimum of a multivariable function and a set of inputs which minimize the function. The conjugate gradient method is used in this simulator. An abbreviation of this simulator CG comes from this method. We explain outline of conjugate gradient method below.

Suppose there is a 3N-dimensional space. We express a point of the space as $\mathbf{x} = \{\mathbf{r}_1, \mathbf{r}_2, \ldots, \mathbf{r}_N\}$ and assume the energy $U = U(\mathbf{x})$ of a system as a function on the space. When we take an arbitrary point $\mathbf{x}^{(0)}$, the energy of this point $U^{(0)} = U(\mathbf{x}^{(0)})$ in general is not a minimum value. Starting from this point, we search coordinates of the point which minimize the energy. The procedure may be concieved that minimum points of the energy along a downward gradient direction of the energy at a preceding point are stepped repeatedly to reach the minimum point of energy.

$$\mathbf{x}^{(n)} \rightarrow \mathbf{x}^{(n+1)} = \mathbf{x}^{(n)} - f^{(*)}\nabla U(\mathbf{x}^{(n)})$$

($f^{(*)}$ is the minimizing point of $U^{(n+1)} = U(\mathbf{x}^{(n)} - f\nabla U(\mathbf{x}^{(n)}))$ with respect to the value f.)

This method, which is called gradient descent, is known to be inefficient. The reason is that the direction of a step is orthogonal to that of the preceding step, so that the direction of a step often is away from the direction for the global minimum of the energy.

In the conjugate gradient method, which improves this weakness, the conjugate direction vector is made to search the minimizing coordinate in each step. Here we introduce the method of Polak-Ribiere [Polak1971], which we adopt for this simulator. We express the vector of the search direction from $\mathbf{x}^{(n)}$ as $\mathbf{h}^{(n)}$. And we express gradient descent vectors at $\mathbf{x}^{(n)}$ as follows.

$$\mathbf{g}^{(n)} = -\nabla U(\mathbf{x}^{(n)})$$

It is natural to set the inital value $\mathbf{h}^{(0)} = \mathbf{g}^{(0)}$. The vector of the search direction at the next point $\mathbf{x}^{(n+1)}$ is decided as follows.

$$\mathbf{h}^{(n+1)} = \mathbf{g}^{(n+1)} + \gamma^{(n)}\mathbf{h}^{(n)}$$

Here the following condition holds.

$$\gamma^{(n)} = \frac{(\mathbf{g}^{(n+1)} - \mathbf{g}^{(n)}) \cdot \mathbf{g}^{(n+1)}}{\mathbf{g}^{(n)} \cdot \mathbf{g}^{(n)}}$$

The way how to get

$$\mathbf{g}^{(n+1)} = -\nabla U(\mathbf{x}^{(n+1)})$$

is that we take $\mathbf{x}^{(n+1)}$ as the minimizing point in the following condition.

$$U(\mathbf{x}^{(n+1)}) = U(\mathbf{x}^{(n)} + \lambda^{(n)}\mathbf{h}^{(n)})$$

By this method we can search without calculating second order differential coefficients of $U(\mathbf{x})$. It is known that when energy function has quadratic form, the minimizing point can be reached by steps of the space dimension times (3N times in this case) in this method.

It should be noted that some atoms which constitutes a structure need to be fixed at positions on the space. If all atoms which constitutes a tip model are set at the geometry optimizing coordinates, the force applied to the tip, which is the sum of the force applied to the atoms of the tip, becomes zero and the significant information can not be gained.

References

[Polak1971] Polak, E., 1971, Computational Methods in Optimization (New York: Academic Press), §2.3.

8.3 Calculation of tip-sample interaction

After calculating geometry optimizing shape of all the structures with the fixed position of the tip using the method of preceding section, the interaction between the tip and the sample is gained by computing the sum of the force applied to all the atoms which constitutes the tip. This force is assumed to be the force the tip feels in this simulator. Based on this assumption, a force curve can be gained by calculating force while changing the position of the tip along a vertical direction, and a force map can be gained by calculating force while changing the position of the tip in the plane parallel to the sample surface. The force considered in this calculation is force between two structures, that is, van der Waals' Interaction and Coulomb Interaction (if charge polarization exists).

8.4 Calculation of an AFM image - using formula -

Cantilever's motion which drives a tip is not taken into account in this simulator as it is understood from the explanations up to here. But there is a simple relation between influence on the tip's oscillation and a force curve if the tip and the sample interact only slightly with each other. Concretely a shift amount of resonance oscillation frequency, that is, difference from a oscillation frequency with no sample, is described as follows [Sasaki2000].

$$\Delta f = -\frac{f_0}{2\pi kA}\int_0^{2\pi} F_{\mathrm{TS}}(z_0 + A\cos\theta)\cos\theta d\theta$$

Here f_0 stands for resonance frequency in the case the force applied to the tip is zero, k stands for a spring constant of the cantilever, A stands for oscillation amplitude of the tip, $F_{\mathrm{TS}}(z)$ stands for the vertical component of the force applied to the tip at the z position of the tip, z_0 stands for the z-component of the oscillation center and θ stands for a phase of the oscillation. A phase is defined to be zero when the tip is in the top position. A frequency shift image is calculated by using this formula in this simulator.

References

[Sasaki2000] N. Sasaki and M. Tsukada, Jpn. J. Appl. Phys. **39** (2000) L1334.

8.5 Energy dissipation

Energy dissipates by cantilever oscillation in AFM observation. The major causes are internal friction of the cantilever, friction between the cantilever and surrounding fluid (in the case of measurement in liquid), deformation of the tip and the sample and thermal oscillation of the atoms which constitutes the tip and the sample. The first two causes are beyond the scope of the application of the calculation model in this simulator. First, we consider the energy dissipation from deformation of the tip and the sample. The effect of the thermal oscillation of the atoms can be taken into account [Gauthier2000] by a molecular dynamics method explained

in the MD's chapter or by treatment of Brownian motion. But this effect does not taken into account in this simulator because its dissipation is not so large.

There is a dissipation formula under the condition that the interaction between the tip and the sample is weak enough as in the case of frequency shift calculation. Dissipation energy in one cycle of the oscillation is as follows [Sasaki2000].

$$\Delta E = A\int_0^{2\pi} F_{\mathrm{TS}}(z_0 + A\cos\theta)\sin\theta d\theta$$

The symbols mean the same as in the previous section. It is read from this equation that energy dissipation become zero when force of tip's certain height is same whether the tip approaches the sample or departs from the sample. In other words, hysteresis of the force applied to the tip is needed for non zero energy dissipation.

References

[Gauthier2000] M. Gauthier and M. Tsukada, Phys. Rev. Lett. **85** (2000) 5348.
[Sasaki2000] N. Sasaki and M. Tsukada, Jpn. J. Appl. Phys. **39** (2000) L1334.

8.6 Users guide: how to use CG

We explain how to use CG with an example of frequency shift image calculation of a pentacene molecule. The calculation procedure is described below. The measured frequency shift image of a pentacene molecule can be reproduced well in this calculation which is first measured by Gross et al. in 2009.

Table 13 The procedure of calculating a frequency shift image of a pentacene molecule.

	Description	Procedure
	To execute GUI of SPM Simulators	
1	To create a new simulation project	1. Click [new] from [File] in Menu bar. 2. Enter a project file name you like in the [project file] text box. 3. Change the directory if needed, then click "OK".
2	To select a tip model	Right-click the area of [Component] in the Project Editor. Then click the [add tip] > [file]. The dialog [Import file] will be displayed. For this time, select "co.txyz".(*1)
3	To select a sample model	Right-click the area of [Component] in the Project Editor. Then click the [add sample] > [file]. The dialog [Import file] will be displayed. For this time, select "pentacene_opti.txyz".(*1)
4	To set the initial position of the tip at (-9, -5, 4.5)	Enter "-9", "-5" and "4.5" in the cell of [x], [y] and [z] respectively in the [Component] > [Tip] > [Position].

5	To set size of scan area of the tip at (18, 10, 1.1)	Enter "18", "10", "1.1" in the cell of [w], [d] and [h] respectively in the [Component] > [Tip] > [ScanArea] in the Project Editor.
6	To select the CG solver	1. Select "CG" and "Calculation" in the box on the top of GUI, respectively. 2. Select the [CG] tab in the project editor.
7	To select in vacuum calculation mode	Select “CG” in the [AFMmode] in the Project Editor.
8	To select the NC-AFM frequency shift calculation mode as a scan mode	Select "ncAFMConstZ" in [Tip_Control] > [scanmode] box. (*2)
9	To set the value of the step size of the tip to 0.2 Ang	Enter "0.2" in [Tip_Control] > [delta_xy] box in the Project Editor.
10	To set the input parameters of the frequency shift calculation mode	Set the parameters (*2) in [Tip_Control] > [NC_Mode_Setting] in the Project Editor. 1. Input "10" in [ThetaStepNumber] (The number of partitions in the z-axis direction.) 2. Input "0.6" in [TipZamplitude] (Amplitude of tip's oscillation. The unit is angstrom.) 3. Input "200" in [SpringConst] (A spring constant of the cantilever. The unit is N/m.) 4. Input "23.165" in [ResoFreq] (Resonance frequency of the cantilever. The unit is kHz.)
11	To save	Click the [File] - [Save] at the menu bar on the top of the window.
12	To run	Click the [Simulation] - [Start] at the menu bar on the top of the window.(Calculation takes some time to complete.)
13	To view the result	1. Click the [Display] - [Result View] at the menu bar on the top of the window. 2. Select "cgafm_frq.csv" in the [Result View] window.
*1	There are files of tip and sample model at [data¥] in the installed directory. For instance, if you install the simulator at [C:¥Program Files¥SpmSimurator¥], the files are at [C:¥Program Files¥SpmSimulator¥data¥]. The file "co.txyz" and the file "pentacene_opti.txyz" are directly under the directory [data¥Sample¥Mol¥CGMDsample¥].	
*2	Refer the manual of this simulator for more information about the parameters for each scan mode.	

Chapter 9 Atomic-scale liquid AFM simulator (CG-RISM)

9.1 Reference Interaction Site Model (RISM) theory

In the previous chapter, we discuss how to simulate the AFM-based force measurements in vacuum environments with the solver CG (the Geometry optimizing AFM image simulator included in the Classical Force Field AFM Simulator). However, the CG can also simulate the AFM-based measurements in liquid environments. If the sample and the tip are in liquid, the interaction between the liquid, the sample and the tip let the free energy of the whole system be different from that in the vacuum. Then, a derivative of the free enrgy with respect to the position variable causes the force acting on the tip. To compute variances of the free energy, we need to derive correlation functions between a pair of atoms, which construct the sample, the tip and the liquid. To derive the correlation functions, we adopt Reference Interaction Site Model (RISM) theory. (Strictly speaking, we adopt the one-dimensional RISM theory.) In this section, we explain the RISM theory.

9.2 The RISM equation and the closure relation

First of all, we introduce the Ornstein-Zernike equation, which gives a relation of density correlation functions of simple liquid. Here, the term "simple liquid" means a many-body system of classical point particles. The Ornstein-Zernike equation is given by

$$h(\mathbf{r},\mathbf{r}') = c(\mathbf{r},\mathbf{r}') + \int d\mathbf{r}'' c(\mathbf{r},\mathbf{r}'')\rho(\mathbf{r}'')h(\mathbf{r}'',\mathbf{r}') , \qquad \ldots(1)$$

where $h(\mathbf{r},\mathbf{r}')$ represents the total correlation function between positions $\mathbf{r}$ and $\mathbf{r}'$, $c(\mathbf{r},\mathbf{r}')$ represents the direct correlation function between positions $\mathbf{r}$ and $\mathbf{r}'$ and $\rho(\mathbf{r})$ represents the density at the position $\mathbf{r}$. The physical meaning of this equation is as follows. The left-hand side of the equation implies the density-density correlation between two points $\mathbf{r}$ and $\mathbf{r}'$. This left –hand term is equal to a sum of the first term and the second term in the right-hand side of the equation. The first term in the right-hand side of the equation gives a contribution induced by the dirct correlation. The second tern in the right-hand side of the equation gives contributions caused by all of the possible indirect weighted correlations.

In general, shapes of molecules, of which real liquid consists, are more complicated than those of the simple liquid. Thus, sometimes the Ornstein-Zernike equation does not describe the real liquid properly. For example, we cannot treat the direction of the molecule with the above Ornstein-Zernike equation. However, if we adopt the generalized coordinates $(\mathbf{R},\boldsymbol{\Omega})$, which include the position and the direction of the molecule, we can deal with the real liquid. Here, we use the following notation. If we write down the generalized coordinates $(\mathbf{R},\boldsymbol{\Omega})$ rigidly, the equation becomes too complex. Thus, we write a simple symbol "1" instead of the generalized coordinates $(\mathbf{R}_1,\boldsymbol{\Omega}_1)$. Hence, the generalized Ornstein-Zernike equation is given by

$$h(1,2) = c(1,2) + \frac{\rho}{\Omega}\int d3c(1,3)h(3,2) .$$

In the above equation, we put the density outside the integral because we can consider it to be nearly constant. Moreover, Ω that is not written with a bold font represents a normalization constant for the integral with respect to the angular coordinates.

However, because the above equation is too general, it is difficult for us to perform anlyses with it. Thus, we stop considering the correlation function between the molecules. Alternatively, we concentrate on the correlation function between atoms that belong to the molecule. We can relate these correlation functions as the following equation:

$$h_{\alpha\gamma}(r) = \frac{1}{\Omega^2}\int d1d2\delta(\mathbf{R}_1 + \mathbf{l}_1^{\alpha})\delta(\mathbf{R}_2 + \mathbf{l}_2^{\gamma} - \mathbf{r})h(1,2)$$

where $\mathbf{R}_i$ represents the position of the molecule i, $\mathbf{l}_i^{\alpha}$ represents the relative position that is a vector from the position $\mathbf{R}_i$ to the position of an atom α belonging to the molecule i and $\delta(\cdots)$ represents the delta function. Thus, the avobe function implies the following. We assume that the atom α belonging to the molecule 1 exists at the origin of the coordinates. Moreover, we assume that the atom γ belonging to the molecule 2 exists at the position $\mathbf{r}$. Under these assumptions, we average the total correlation function $h(1,2)$ between the molecules. Then obtained average is equal to the total correlation function for the point $\mathbf{r}$, which is described in the left-hand side of the above equation. Because we assume that the system has the spatial translational symmetry, an argument of the function in the left-hand side of the above equation is given by the absolute value of $\mathbf{r}$.

To let the above equation be tractable, we try to rewrite its right-hand side in the other form. We can rewrite the generalized Ornstein-Zernike equation according to the perturbation method as follows:

$$h(1,2) = c(1,2) + \frac{\rho}{\Omega}\int d3c(1,3)c(3,2) + \left(\frac{\rho}{\Omega}\right)^2\int d3d4c(1,3)c(3,4)c(4,2) + \cdots$$

Moreover, we assume that the direct correlation function between the molecules is equal to a sum of all the direct correlation functions between points where the interaction acts as follows:

$$c(1,2) = \sum_{\alpha,\gamma} c_{\alpha\gamma}(|\ \mathbf{r}_1^{\alpha} - \mathbf{r}_2^{\gamma}\ |)$$

From these equations and the Fourier integral representation of the delta function, with tough calculations, we obtain

$$h_{\alpha\gamma}(r) = \frac{1}{(2\pi)^3}\int d\mathbf{k}\exp(i\mathbf{k}\cdot\mathbf{r})\left[\hat{\mathbf{w}}\hat{\mathbf{c}}(\mathbf{1} - \boldsymbol{\rho}\hat{\mathbf{c}}\hat{\mathbf{w}})^{-1}\hat{\mathbf{w}}\right]_{\alpha\gamma}$$

where

$$\hat{w}_{\alpha\gamma}(\mathbf{k}) = \frac{1}{\Omega}\int d\boldsymbol{\Omega}_1\exp[i(\mathbf{l}_1^{\alpha} - \mathbf{l}_1^{\gamma})\cdot\mathbf{k}]$$

and $\hat{c}_{\alpha\gamma}(\mathbf{k})$ represents the Fourier transformation of $c_{\alpha\gamma}(\mathbf{r})$. Symbols described with the bold font inside $[\cdots]_{\alpha\gamma}$ represent matrices. In these matrices, we omit arguments of wave vectors $\mathbf{k}$. For example, $\hat{\mathbf{c}}$ represents the matrix $\hat{c}_{\alpha\gamma}(\mathbf{k})$ whose row and column are given by indices α and γ respectively. Thus, the rank of the matices is equal to the number of points, where the interaction acts on, in the liquid. In other words, the rank of the matrices is equal to the total number of atoms in the molecule of the liquid. Moreover, $\mathbf{1}$ represents the unit matrix and $\boldsymbol{\rho} = \rho\mathbf{1}$ holds. The above is called the RISM equation, that we have to solve.

However, because $h_{\alpha\gamma}$ and $c_{\alpha\gamma}$ are unknown functions, we cannot obtain a solution from the above equation only. Thus, we introduce the closure relation. Then, we can obtain a solution from the RISM equation and the closure relation. The Hyper Netted Chain (HNC) closure relation is often used,

$$h_{\alpha\gamma}(r) = \exp[-\beta u_{\alpha\gamma}(r) + h_{\alpha\gamma}(r) - c_{\alpha\gamma}(r)] - 1$$

where $\beta = 1/k_{\mathrm{B}}T$ represents the inverse of the temperature and $u_{\alpha\gamma}(r)$ represents the potental energy for atoms α and γ with distance r. Assuming the initial values of correlation functions, using the RISM equation and the closure relation, we carry out self-consistent numerical calculations many times until $h_{\alpha\gamma}$ or $c_{\alpha\gamma}$ converges at a certain form of the function. Finally, we obtain the correlation functions between the positions where the interaction acts. [Kovalenko1999]。

Reference:
[Kovalenko1999] A. Kovalenko, S. Ten-no, and F. Hirata, J. Comput. Chem. **20**(9), (1999) 928-936.

9.3 Equations in liquid environment and variation of the free energy

So far, we consider the liquid composed of only one type of the molecule. However, if we consider the AFM measurements in liquid environment, the tip and the sample are in the liquid. Thus, we need to know equations that describe a physical system including the liquid. In this section, we examine a model of the solution in which the densities of the solutes are iinfintely small and its RISM equation.

If we rewrite the RISM equation for the simple pure liquid, which is given in the previous section, with the Fourier components, we obtain

$$\hat{\mathbf{h}} = \hat{\mathbf{w}}\hat{\mathbf{c}}(\mathbf{1} - \boldsymbol{\rho}\hat{\mathbf{c}}\hat{\mathbf{w}})^{-1}\hat{\mathbf{w}}\,.$$

Furthermore, we can rewrite this equation as

$$\hat{\mathbf{h}} = \hat{\mathbf{w}}\hat{\mathbf{c}}\hat{\mathbf{w}} + \hat{\mathbf{w}}\hat{\mathbf{c}}\boldsymbol{\rho}\hat{\mathbf{h}}$$

From the discussions given in the previous section, if we treat the physical system including the liquid, we can regard the indices of the matrices correspond to both atoms in the molecules of the solutes and atoms in the molecules of the solvent. To let the discussion be simple, it is convenient to deal with small matrices, for example, a matrix of the correlation function between atoms in the molecule of the solvent, a matrix of the correlation function between an atom of molecule in the solute and an atom of the molecule in the solvent. (Because we consider the densities of the solutes to be infinitely small, we do not need to think about a matrix of the correlation function between atoms in the molecule of the solutes.) Hence, we obtain the RISM equations as

$$\hat{\mathbf{h}}^{\mathrm{VV}} = \hat{\mathbf{w}}^{\mathrm{V}}\hat{\mathbf{c}}^{\mathrm{VV}}\hat{\mathbf{w}}^{\mathrm{V}} + \hat{\mathbf{w}}^{\mathrm{V}}\hat{\mathbf{c}}^{\mathrm{VV}}\boldsymbol{\rho}^{\mathrm{V}}\hat{\mathbf{h}}^{\mathrm{VV}}$$

and

$$\hat{\mathbf{h}}^{\mathrm{UV}} = \hat{\mathbf{w}}^{\mathrm{U}}\hat{\mathbf{c}}^{\mathrm{UV}}\hat{\mathbf{w}}^{\mathrm{V}} + \hat{\mathbf{w}}^{\mathrm{U}}\hat{\mathbf{c}}^{\mathrm{UV}}\boldsymbol{\rho}^{\mathrm{V}}\hat{\mathbf{h}}^{\mathrm{VV}}\,.$$

The indices of rows and columns of matices, V and U, correspond to atoms of molecules in the solvent and the solutes. Because matrices $\hat{\mathbf{w}}$ and $\boldsymbol{\rho}$ are block diagonal and symmetric, we gave them only one index.

In a similar way, we obtain the closure relations as

$$h_{\alpha\gamma}^{\mathrm{VV}}(r) = \exp[-\beta u_{\alpha\gamma}^{\mathrm{VV}}(r) + h_{\alpha\gamma}^{\mathrm{VV}}(r) - c_{\alpha\gamma}^{\mathrm{VV}}(r)] - 1$$

$$h_{\alpha\gamma}^{\mathrm{UV}}(r) = \exp[-\beta u_{\alpha\gamma}^{\mathrm{UV}}(r) + h_{\alpha\gamma}^{\mathrm{UV}}(r) - c_{\alpha\gamma}^{\mathrm{UV}}(r)] - 1\,.$$

We can carry out the simulation in the following manner. At first, from the RISM equations, we evaluate the correlation functions between atoms in the molecules of the solvent, for example $h_{\alpha\gamma}^{\mathrm{VV}}(r)$, with self-consistent numerical calculations. Next, using results of these calculations, we evaluate the correlation functions between an atom in the molecules of the solutes and an atom in the molecules of the solvent, for example $h_{\alpha\gamma}^{\mathrm{UV}}(r)$, with self-consistent numerical calculations.

Even if the densities of the solutes are infinitely small, the free energy of the solution is not equal to that of the pure liquid because of non-zero correlation functions, $h_{\alpha\gamma}^{\mathrm{UV}}(r)$ and $c_{\alpha\gamma}^{\mathrm{UV}}(r)$. In Reference [Singer1985], a formula for estimating the difference of these free energies for a single solute is given as follows:

$$\Delta\mu = -4\pi k_{\mathrm{B}} T \rho_{\mathrm{V}} \sum_{\alpha\subset \mathrm{U}} \sum_{\gamma\subset \mathrm{V}} \int_0^\infty dr r^2 \left\{ c_{\alpha\gamma}^{\mathrm{UV}}(r) - \frac{1}{2}\left[h_{\alpha\gamma}^{\mathrm{UV}}(r)\right]^2 + \frac{1}{2} h_{\alpha\gamma}^{\mathrm{UV}}(r) c_{\alpha\gamma}^{\mathrm{UV}}(r) \right\} \qquad \ldots(4)$$

where ρ_{V} represents the number density of the solvent.

Reference:
[Singer1985] S. J. Singer and D. Chandler, Mol. Phys. **3** (1985) 621.

9.4 Evaluation of the interactive force between the tip and the sample

To apply the RISM method to the physical system of the AFM measurement, we regard a compound of the tip and the sample as the solutes in the solvent for the RISM method. The compound of the tip and the sample is the only matter in the solvent, we can assume that the densities of the solutes are infinitely small as discussed in the previous section.

The interactive force acting on the tip is equal to a sum of the following two interactive forces as explained in the previous section. The first one is the interactive force between the tip and the sample through the vacuum environment. The second one is the interactive force between the tip and the sample through the liquid environment. However, we cannot estimate the the interactive force between the tip and the sample through the liquid environment in a direct manner. Thus, we evaluate the derivative of the free energu given by Eq. (4) and we regard it as the interactive force through the liquid environment. Hence, to obtain its derivative, we evaluate the free energy twice with moving the tip slightly. From the difference of the free energies and a distance of the tip's movement, we calculate the derivative numerically [Koga1997].

Reference:
[Koga1997] K. Koga, X. C. Zeng and H. Tanaka, J. Chem. Phys. **106**(23), (1997) 9781-9792.

9.5 How to carry out simulation with the RISM method actually

Here, we show an example for introducing how to calculate the force-distance curve. In this example, we choose a carbon nanotube for the tip and a grapheme sheet for the sample. We let the tip be close to the sample in pure water and examine the force-distance curve. Using the RISM method, we can simulsate oscillation of the force-distance curve under the influence of

salvation around the grapheme sheet in the water. We can carry out the simulation in the following way.

Table 14 How to calculate the force-distance curve with choosing a carbon nanotube for the tip and a grapheme sheet for the sample and letting the tip be close to the sample.

	What to do	Procedures
	Start SPM Simulator.	
	Create a project file.	1. Click [File] - [New] on the tool bar. 2. Input a name for the project file as "Project name". 3. Click "OK" button, after change your directory if you need.
	Choose a model for the tip.	Making a right-click on "Component" in the Project Editor and choosing [Add Tip] - [File], make a doble-click on "Nanotube-10x0-Height12A.txyz". (*1)
	Choose a model for the sample.	Making a right-click on "Component" in the Project Editor and choosing [Add Sample] - [File], make a double-click on "hopg_a50_20x20.txyz". (*1)
	Let the initial position of the tip be (0[angstrom], 0[angstrom], 13[angstrom]).	Input [0] for “x”, [0] for “y” and [13] for “z” in "Component" - "Tip" - "Position" of the Project Editor.
	Let the scan area for the tip be (0[angstrom], 0[angstrom], 10[angstrom]).	Input [0] for “w”, [0] for “d” and [10] for “h” in "Component" - "Tip" - "ScanArea" of the Project Editor.
	Choose the tab for [CG], the geometry optimizing AFM image simulator, in order to input parameters of (CG).	1. Choose [CG] and [Calculation] from the box for selecting the simulator. 2. Choose the tab of [CG] in the Project Editor.
	Let the calculation mode be [CG-RISM] for liquid environment.	Select [CG-RISM] for "AFMmode" in the Project Editor.
	Chosse [ForceCurve] for the scan mode.	Choose [ForceCurve] for "Tip_Control" - "scanmode" in the Project Editor. (*2)
	Let the distance for each step of the movement of the tip be 0.1[angstrom] in the direction of the z-axis.	1. Input [0.0] for "Tip_Control" - "delta_xy" of the Project Editor. 2. Input [0.1] for "Tip_Control" - "delta_z" of the Project Editor.
0	Let the movement of the tip for scanning in the direction of the z-axis be one-way.	Put [Yes] for "Tip_Control" - "OneWayForceCurve" in the Project Editor.
1	Save the input parameters and the settings.	Click [File] - [Save] on the tool bar.
2	Start the simulation.	Click [Simulation] - [Start] on the tool bar. (Sometimes, it takes long time for obtaining the results.)
3	Display the results of the simulation.	1. Click [Display] - [Result View] on the tool bar. 2. Choose [cgafm_fz.csv] from the box.
*1	The file of molecular structure is stored in a subfolder of the [data¥], which is a subfolder of the installation directory for the SPM Simulator. For example, if the installation folder is [C:¥Program Files¥SpmSimurator¥], the file of the molecular structure is saved in the subfolder of [C:¥Program Files¥SpmSimulator¥data¥]. Then, the file “Nanotube-10x0-Height12A.txyz” is stored in the folder [data¥Tip¥], and the file “hopg_a50_20x20.txyz” is stored in the folder	

	[data¥Sample¥Surface¥CGMDsurface¥].
* 2	To obtain information about required parameters for each scan mode, refer to Section 4 in the Reference Manual.

Chapter 10 Molecular Dynamics AFM Image Simulator (MD)

10.1 Principle of the molecular dynamics calculation

In Chapter 8, the Geometry Optimizing AFM Image Simulator (CG) assumes that the time scale of the tip motion is much longer than the time scale of the relaxation of the atomic configuration, so that the atomic configurations of tips or samples have transfered in the stable states for a given initial configuration. On the other hand, when the time scale of the tip motion is short, we had better to calculate the atomic motions of constituents based on the equation of motion. Such a method is able to take a thermal effect into account. In this chapter, we introduce the Molecular Dynamics AFM Image Simulator (MD), which has been designed to calculate the atomic motion according to the classical mechanics. The module solves the Newton's equation of motion

$$m_i \frac{d^2\mathbf{r}_i}{dt^2} = \mathbf{F}_i = -\frac{\partial}{\partial \mathbf{r}_i} U(\mathbf{r}_1, \mathbf{r}_2, \ldots, \mathbf{r}_N),$$

where $i = 1, \ldots, N$ and N is the total number of atoms in the system.

You know, there are various numerical algorithms to solve the ordinary differential equation. Our simulator is based on the velocity Verlet method, which is widely applied in the classical molecular dynamics. The velocity Verlet method follows the difference equation shown below, and calculates the time evolution of the position and the velocity of each atom once given the initial positions and the initial velocities:

$$\mathbf{r}_i(t+h) = \mathbf{r}_i(t) + h\mathbf{v}_i(t) + \frac{h^2}{2m_i}\mathbf{F}_i(t),$$

$$\mathbf{v}_i(t+h) = \mathbf{v}_i(t) + \frac{h}{2m_i}\left[\mathbf{F}_i(t+h) + \mathbf{F}_i(t)\right],$$

where h is the time step specified by the user. The appropriate value is about 1 fs in case of the atomic scale simulation. If the time scale is too large, the simulation will break down. The computing procedure of the time evolution is as follows,

- It calculates $\mathbf{r}_i(t+h)$ for all i.
- It then calculates $\mathbf{F}_i(t+h)$ for all i according to the given $\mathbf{r}_i(t+h)$.
- It then calculates $\mathbf{v}_i(t+h)$ for all i.

Those procedures are repeated until it reaches the desired time.

When the molecular dynamics calculation is performed for a molecule like a protein, the hydrogens in a molecule does not contribute to the result so much even though the hydrogens have a shorter time scale of motion than the other atoms. Hence, this module keeps the bond length constant between hydrogen and the other atoms, so that we can specify a fairly long time step when solving the equation of motion. We adopted the RATTLE algorithm to solve the differential equation with constraint condition [Andersen1983].

References

[Andersen1983] H. C. Andersen, J. Comput. Phys. **52** (1983) 24-34.

10.2 Classical atomic force field model

The Molecular Dynamics AFM Image Simulator adopts the MM3 (molecular mechanics force field) model as in the Geometry Optimizing AFM Image Simulator. In order to improve the computing speed, we now consider only five kinds of interactions as follows;

1. Bond stretching interaction (Eq. (1) in [Allinger1989])
2. Angle bending interaction (Eq. (2) in [Allinger1989])
3. Torsion interaction (Eq. (3) in [Allinger1989])
4. Dipole-dipole interaction
5. van der Waals interaction of the (exp-6) funcion by Buckingham (Eq. (7) in [Allinger1989])

The formulae are the same as in the Geometry Optimizing AFM Image Simulator.

References

[Allinger1989] N. L. Allinger, Y. H. Yuh, and J.-H. Lii, J. Am. Chem. Soc., **111**(23), (1989) 8551.

10.3 Thermal effect

There are seveal algorithms to keep the temperature in typical classical molecular dynamics. We adopt the highly simplified velocity rescaling method. The velocities are rescaled by $\mathbf{v}_i(t) \rightarrow \lambda \mathbf{v}_i(t)$ before every time step, where

$$\lambda = \sqrt{(N-1)3k_{\mathrm{B}}T_{\mathrm{input}} \Big/ \sum_{i=1}^{N} m_i v_i^2} \ .$$

Under such a condition, we presume that the temperature will be kept constant.

10.4 Forces due to the tip-sample interaction

The calculation method of the force to the tip is the same as the Geometry Optimizing AFM Image Simulator. However, note that the tip movement is not always synchronized with the atomic motion from the molecular dynamics. Thus, the module supplies the averaged force during the N_t time steps of the time evolution while the tip stays at a certain position;

$$\left\langle \mathbf{F}_{\mathrm{tip}} \right\rangle = \frac{1}{N_t} \sum_{i=1}^{N_t} \mathbf{F}_{\mathrm{tip},i} \ .$$

The force map and the force curve are also derived from this equation.

In the present MD solver, the tip moves in the same manner as the CG solver. After the time evolution of N_t steps based on the equation of motion, the whole tip goes up/down with a finite height. Then the module performs the time evolution of N_t steps again at the new tip position. If we intend to solve also the tip movement by the equation of motion, we have to perform the time evolution in consideration of the external force to the tip model. The latter manner will be shown in the next section.

10.5 Simulation of the AFM Image -Tip Dynamics-

[The simulator will be equipped with the contents of this section in the future.]

When we consider more realistic tip motion, we should solve the equation of motion with the external force from the cantilever to the atoms of the tip. The external force from the cantilever seems to be a sine curve, written by $\boldsymbol{F}_{\mathrm{ex}} \sin(2\pi f_0 t + \theta_0)$. We assume that the direction of $\boldsymbol{F}_{\mathrm{ex}}$ is parallel to the z-axis. While taking that force into account, we perform the simulation until the tip comes back to the initial position. Then, we can estimate the period and the amplitude f of the tip motion, and we have the frequency shift $\Delta f = f - f_0$. We will obtain the frequency shift AFM image after we calculate Δf 's on the two-dimensional xy-plane.

Note that the present MD solver can simulate the frequency shift AFM image based on the formula introduced in section 8.4.

In the description above, we assumed that we could simulate "until the tip comes back to the initial position". However, the tip model may be deformed due to the thermal motion and the interaction with the sample. Thus we are not sure that we can simulate "until the tip comes back to the initial position". Alternatively, it may go well if we assume that the tip model is never deformed.

10.6 Simulation in liquid

[The simulator will be equipped with the contents of this section in the future.]

When we perform the in-liquid simulation based on the molecular dynamics, we put the solvent constituents such as molecules and ions properly around the tip and the sample, and we follow the motion of all the atoms according to the equation of motion. While the simulation, in general, the periodic boundary conditions are imposed on the boundary of the calculation area, so that the density of molecules and ions keeps constant. Such a condition implies that the molecules and the ions exist in the unlimited space periodically. We have to calculate the forces from the infinite number of atoms scattered in the space, when the long range interaction forces such as the Coulombic force and the van der Walls' force are taken into account. There is the effective algorithm to calculate the interactions from those infinite numbers of atoms if the periodic boundary conditions are imposed along all the direction, and if the interaction energy between two atoms is described as a function of the power of their distance. For example, both the Coulombic force and the London dispersion force satisfy that condition; the former is propotional to the inverse of the distance, and the latter is propotional to the distance to the power of minus six. Our module makes the use of that algorithm to calculate the long range force and is possible to perform the in-liquid simulation.

The 3D-Ewald method is known as the effective technique to calculate the Coulombic potential in the periodic boundary condition. We will take such a technique into consideration in the future development and improvement [Essmann1995].

References

[Essmann1995] U. Essmann *et al.*, J. Chem. Phys. **103**(19), (1995) 8577-8593.

10.7 Case example of MD

[The results of the case examples in this section were obtained by the prototype simulator, while the latest simulator does not reproduce those results. The simulator will be improved to achieve them in the future.]

10.7.a Compression simulation of apoferritin

As the first example of the molecular dynamics AFM image simulator, we show the force curve calculation while the AFM tip is compressing a spherical protein called apoferritin. We show three figures; the snapshots during the simulation in Figure 136, the simulated force curve in Figure 137, and the force curve measured by the SPM device in Figure 138. The diameter of the apoferritin is about 13 nm. In the measured force curve, we see repulsive forces below around 12 nm, the distance between the tip and the substrate. When we continue compressing by 3 nm (until the distance comes to 9 nm), we see an elastic behavior. Further compression gives discrete relaxations.

In the simulated result, we see the starting of the repulsive force and the next elastic behavior. But we do not have the discrete relaxations as seen in the measurement. The difference between the experiment and the simulation may be caused by that the simulation does not take into account the effects of the environment in liquid, and that the apoferritin stays on the substrate steadily in the simulation.

We also find the difference between the simulation and the experiment about the magnitude of the forces. The simulated force is about ten times larger than the measured force. It is believed that the difference is caused by the compression speed in the simulation or the experiment.

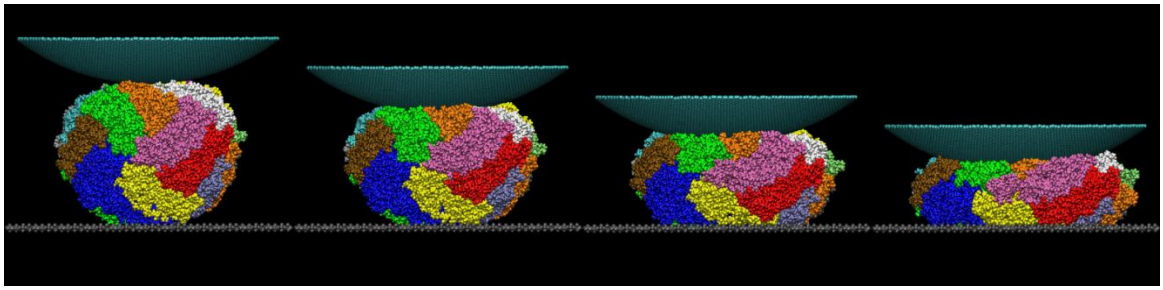

Figure 136 The simulation images while the AFM tip is compressing a spherical protein, apoferritin [Tagami2006].

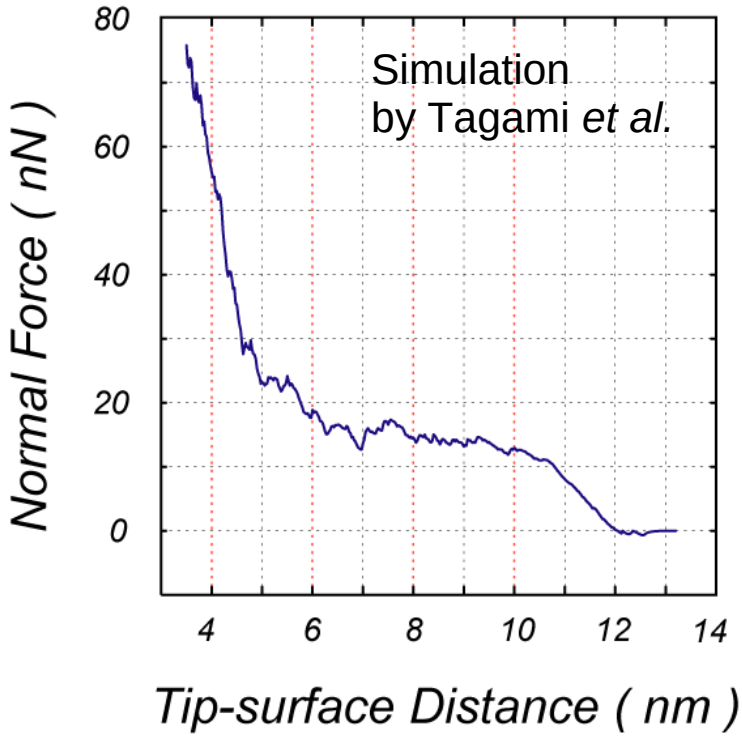

Figure 137 The simulated force curve while the AFM tip is compressing a spherical protein, apoferritin [Tagami2006].

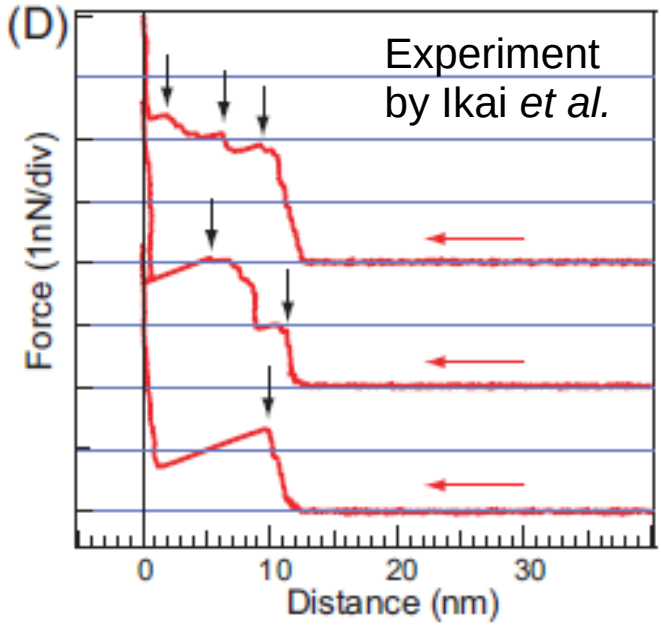

Figure 138 The measured force curve while the AFM tip is compressing a spherical protein, apoferritin [Tagami2006].

References

[Tagami2006] K. Tagami, M. Tsukada, R. Afrin, H. Sekiguchi and A. Ikai, e-J. Surf. Sci. Nanotech. 4, 552-558 (2006).

10.7.b Force map on the surface of muscovite mica in water

As the other example, we show the simulation of the surface of the muscovite mica in the water [Tsukada2010]. The target is the single layered muscovite mica surface with the honeycomb structure (shown in Figure 139), which is composed of aluminum (green), silicon (yellow) and oxygen (red) atoms. We assumed the potassium atoms are dissolved in the water as ions.

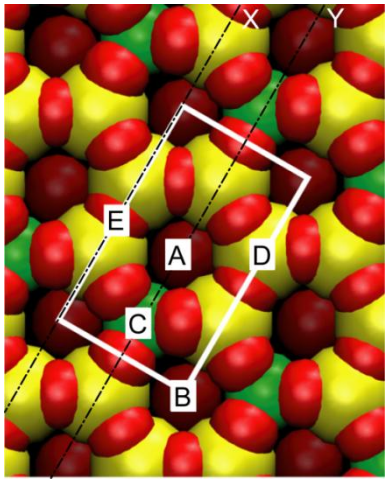

Figure 139 The single layered muscovite mica surface with the honeycomb structure. Green, yellow and red spheres stand for aluminum, silicon and oxgen atoms, respectively.

We used the capped (10, 0)-single walled carbon nanotube as a tip. In Figure 140, we have calculated the forces to the tip at each position on a plane which is perpendicular to the mica surface. We see the strong repulsive force near the surface. Apart from the surface, we find the oscillatory behavior of the forces: Attractive and repulsive forces alternately appear. It may be because that the water forms the layered structure (hydration structure) near the mica surface. We have found an interesting behavior of the force map on the other plane perpendicular to the mica surface. The repulsive force is strong at the hollow site on the surface, which is unexpected behavior according to the atomic configuration. This may be also due to the hydration structure. In fact, those features are implied by measurements, which indicate the validity of our simulator.

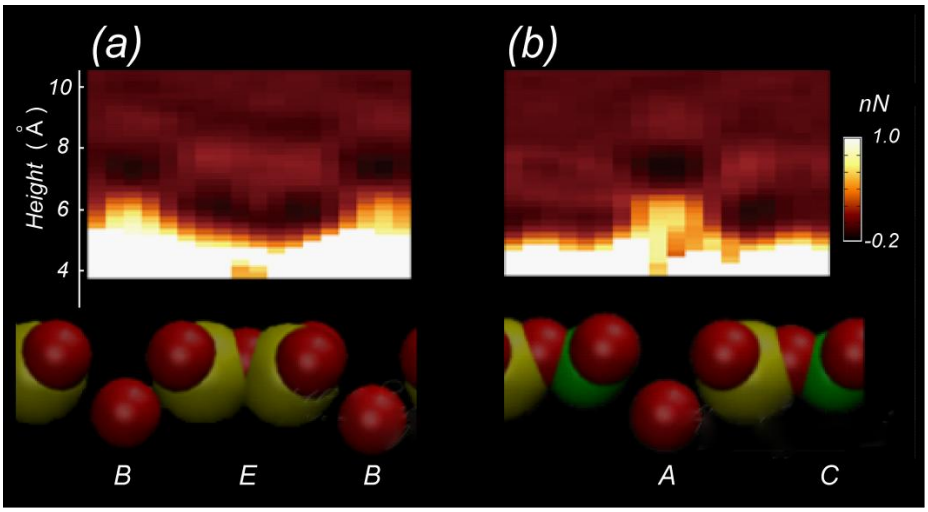

Figure 140 Visualization of the force map where we calculated the forces to the tip at each position on two planes which are perpendicular to the mica surface.

References

[Tsukada2010] M. Tsukada, N. Watanabe, M. Harada and K. Tagami, J. Vac. Sci. Technol. B **28** (2010) C4C1.

10.8 Users guide: how to use MD

Here we show the concrete operation procedure to simulate the force curve of a system composed of four octane molecules. Let us try the following procedure.

Table 15 The operation procedure to simulate the force curve of a system composed of four octane molecules.

	Description	Procedure
1	Make a project file.	1. Click [File] → [New] on the menu bar. 2. Type a project name as you like at [Project name] in the [Create new project] dialog. 3. Change the directory that you would like to save the project, then click [OK].
2	Set the tip model.	1. Right click on the [Component] item. Next, choose [Add Tip] → [File]. Then select "Nanotube-10x0-Height12A.txyz" (*1). 2. Set the initial tip position below [Component] → [Tip] → [Position]: Type "2.8", "2.8", "20" at [x], [y], [z], respectively.
3	Set the first molecule as the sample.	1. Right click on the [Component] item. Next, choose [Add Sample] → [File]. Then select "octane.txyz" (*1). 2. Set the position below [Component] → [Sample] → [Position]: Type "0", "0", "0" at [x], [y], [z], respectively. 3. Set the direction below [Component] → [Sample] → [Rotation]: Type "-90", "-11", "-84" at [alpha], [beta], [gamma], respectively.

4	Set the second molecule as the sample.	1. Right click on the [Component] item. Next, choose [Add Sample] → [File]. Then select "octane.txyz" (*1). 2. Set the position below [Component] → [Sample] → [Position]: Type "5.6", "0", "0" at [x], [y], [z], respectively. 3. Set the direction below [Component] → [Sample] → [Rotation]: Type "-90", "-11", "-84" at [alpha], [beta], [gamma], respectively.
5	Set the third molecule as the sample.	1. Right click on the [Component] item. Next, choose [Add Sample] → [File]. Then select "octane.txyz" (*1). 2. Set the position below [Component] → [Sample] → [Position]: Type "0", "5.6", "0" at [x], [y], [z], respectively. 3. Set the direction below [Component] → [Sample] → [Rotation]: Type "-90", "-11", "-84" at [alpha], [beta], [gamma], respectively.
6	Set the fourth molecule as the sample.	1. Right click on the [Component] item. Next, choose [Add Sample] → [File]. Then select "octane.txyz" (*1). 2. Set the position below [Component] → [Sample] → [Position]: Type "5.6", "5.6", "0" at [x], [y], [z], respectively. 3. Set the direction below [Component] → [Sample] → [Rotation]: Type "-90", "-11", "-84" at [alpha], [beta], [gamma], respectively.
7	Assign the movement flag for each atom. The five bottommost atoms are to be fixed.	1. Right click on the [Sample] item below [Component]. Next, choose [Show Data] to display the "Data View". 2. Type "0" at the [Relax] column at 1, 2, 9, 10 and 11-th rows. Otherwise, type "1". Then, click [OK]. 3. Repeat those procedures for each octane.
8	Set the scan area by 10 [Å] down from the initial tip position.	Set the scan area below [Component] → [Tip] → [ScanArea]: Type "0", "0", "10" at [w], [d], [h], respectively.
9	Select the MD solver.	1. Select [MD] and [Calculation] in the simulator selection boxes on the toolbar. 2. Click the [MD] tab in the [Project Editor].
10	Select the force curve mode.	Select "ForceCurve" below [Tip_Control] → [scanmode].
11	Set the interval of the scan area as 0.5 Å.	Type "0.5" at [Tip_Control] → [delta_z].
12	Set the time step as 1.0 fs.	Type "1.0" at [MD_Setting] → [TimeStep].
13	Set the number of steps at each tip position as 4000.	Type "4000" at [MD_Setting] → [StepNumber].
14	Set the temperature at 300 K.	Type "300" at [MD_Setting] → [Temperature].
15	Save the contents.	Click [File] → [Save] on the menu bar.
16	Run the simulation.	Click [Simulation] → [Start] on the menu bar.
17	View the result of the force curve simulation.	1. Click [Display] → [Result View] on the menu bar. 2. On the [Result view] window, select "MD_Fz.csv" in the selection box.
*1	There are molecular structure files below [data¥] folders in the installed folder. For instance, if you have installed the simulator at [C:¥Program Files¥SpmSimurator¥], there is the data folder at [C:¥Program Files¥SpmSimulator¥data¥]. The tip data, "Nanotube-10x0-Height12A.txyz", is prepared just below [data¥Tip¥]. The sample data, "octane.txyz", is prepared just below [data¥Sample¥Mol¥CGMDsurface¥].	

Chapter 11 Quantum Mechanical SPM Simulator

Quantum Mechanical SPM Simulator calculates electronic states of the system by quantum mechanics, and computes a tunneling current image, an image of scanning tunneling spectroscopy, a frequency shift image of AFM and a local contact potential difference image of KPFM. DFTB (Density Functional based Tight Binding) Method is adopted, and it is suitable for analyzing a SPM image with an atomic resolution. It is also the feature of Quantum Mechanical SPM Simulator that it has a function of calculating an image of scanning tunneling spectroscopy and a local contact potential difference image of kelvin probe force microscopy.

11.1 Outline of the DFTB method

11.1.a Density functional theory

In quantum mechanics describing an equation which determines electronic states of a system is comparatively easy, but determining electronic states by solving the equation is not easy. Even if you calculate numerically, a wave function $\psi(\mathbf{r}_1,\mathbf{r}_2,\cdots,\mathbf{r}_N)$ has inputs of N electron coordinates $\{\mathbf{r}_j\}$, and has a dimension of 3N. To solve this problem is very difficult. Various calculation methods for finding electronic states are developed, and density functional theory is the one of them [29].

Fundamental conception of density functional theory is to treat electron density $\rho(\mathbf{r})$ which is only three dimensional instead of a wave function $\psi(\mathbf{r}_1,\mathbf{r}_2,\cdots,\mathbf{r}_N)$ which is 3N dimensional for describing states of a system. And physical properties such as energy and so on are described as a functional of electron density like E[p]. It saves huge calculation cost that a state of a system is described by electron density only instead of a wave function which has 3N variables.

A wave function $\psi(\mathbf{r}_1,\mathbf{r}_2,\cdots,\mathbf{r}_N)$ can not be reproduced from density $\rho(\mathbf{r})$ in general. But it is ensured by the Hohenberg-Kohn theorems [1] that taking into account density $\rho(\mathbf{r})$ only is sufficient if you do not take into account an uninteresting "additive constant potential" and you treat only a ground state of a system. It is also shown [1] that energy E is considered to be a functional of density $E(\rho)$ formally and we can find a ground state by searching the density ρ which minimizes $E(\rho)$.

But a concrete form of $E(\rho)$ is not found. Although $E(\rho)$ can be described as a concrete form by approximation methods [2][3], the forms does not have adequate accuracy.

So in order to perform calculation which withstands practical use, we relinquish the original method of describing a system with density $\rho(\mathbf{r})$ only. And instead we adopt the model that each of N electrons is described as one particle wave function $\{\psi_j(\mathbf{r})\}$ and interact with each other. Then the wave functions satisfy the following Kohn-Sham equations [4].

$$V_{eff}(\mathbf{r}) = V_{ext}(\mathbf{r}) + \int d\mathbf{r}' \frac{\rho(\mathbf{r}')}{|\mathbf{r}-\mathbf{r}'|} + V_{XC}(\mathbf{r}) \qquad \ldots(1)$$

$$\left(-\frac{1}{2}\Delta + V_{eff}(\mathbf{r}) - \varepsilon_j\right)\psi_j = 0 \qquad \ldots(2)$$

$$\rho(\mathbf{r}) = \sum_{j=1}^{N} |\psi_j(\mathbf{r})|^2 \qquad \ldots(3)$$

$$V_{XC}(\mathbf{r}) = \frac{d}{d\rho}\rho E_{XC}(\rho)\Big|_{\rho=\rho(\mathbf{r})} \qquad \ldots(4)$$

The Kohn-Sham equations take in the influence of electron-electron interaction with a exchange-correlation potential V_{XC}. Average interaction among electron clouds is expressed by the right side of the equation (4). The procedure of calculation is as follows. First initial density $\rho_0(\mathbf{r})$ is given. A effective potential $V_{eff}(\mathbf{r})$ is calculated by the equation (1). N wave functions $\{\psi_j(\mathbf{r})\}$ is calculated by the equation (2). Density $\rho(\mathbf{r})$ is calculated by the equation (3). The ground state and the energy of a system are found by repeating the steps until the energy E converges. $V_{ext}(\mathbf{r})$ denotes a potential of external force, and is a Coulomb potential in this case. E_{xc} denotes exchange-correlation energy, and is calculated by a approximation method such as Local Density Approximaton (LDA). The exchange-correlation potential $v_{xc}(\mathbf{r})$ is a functional derivative of E_{xc}.

Physical properties such as a lattice constant and a bulk modulus are reproduced precisely [5] with a smaller calculation cost by local density approximation (LDA). However at the same time LDA has a weakness such as underestimation of a band gap of a semiconductor and difficulty of Van der Waals force calculation. Methods of improving LDA for these problems are developed, but we omit the explanation.

11.1.b Pseudo-atomic orbital and Bloch sum

Wave functions are expanded in an infinite series of bases functions, but wave functions are described as a linear combination of finite bases on numerical calculation. A set of bases can be taken as plane waves, gaussian functions, pseudo-atomic orbitals and so on, and each set of bases has their own features.

A pseudo-atomic orbital is imitation of an electron orbital of an atom, and is a pseudo wave function like an s-orbital, a p-orbital or a d-orbital for each element. Though it is possible to deal with the all electrons of an atom, chemically unimportant core electrons are often treated as a potential of an atomic nucleus, so that only the chemically important valence electrons are dealt with explicitly. If optimized pseudo-atomic orbitals are used as a set of bases, precise calculation can be performed with a small number of bases.

Quantum Mechanical SPM Simulator mainly treats a surface with a periodic boundary condition as a sample. So, pseudo-atomic orbitals are replaced with bases which are reflected by periodical structure.

$\{P_i(\mathbf{r})\}$ denotes pseudo-atomic orbital of an orbital of an atom, and we adopt a Bloch sum

$$b_i(\mathbf{k},\mathbf{r}) = \frac{1}{\sqrt{N}} \sum_{\mathbf{t}}^{N} e^{i\mathbf{k}\bullet\mathbf{t}} P_i(\mathbf{r} - (\mathbf{R}_a + \mathbf{t})) \qquad \ldots(5)$$

as a set of bases which satisfies the condition of Bloch's theorem [6].

$$u_{\mathbf{k}}(\mathbf{r} + \mathbf{t}) = u_{\mathbf{k}}(\mathbf{r})$$

$$\psi_{\mathbf{k}}(\mathbf{r}) = e^{i\mathbf{k}\bullet\mathbf{r}} u_{\mathbf{k}}(\mathbf{r})$$

N denotes the number of translational vectors, **t** denotes a translation vector of the crystal, "a" denotes the atom which a pseudo-atomic orbital P_i belongs to, $\mathbf{R}_a$ denotes the position vector of an atom "a". $\mathbf{k}$ denotes a wave vector and corresponds to electron momentum of a crystal. An electronic state is expanded by $b_i(\mathbf{r}) = b_i(\mathbf{0},\mathbf{r})$, where $\mathbf{k} = \mathbf{0}$, when we do not take states of non zero momentum into account. When we want to take states of non zero momentum into account, we take several $\mathbf{k}$ and expand a state $\psi(\mathbf{k},\mathbf{r})$ of wave vector $\mathbf{k}$ with $b_i(\mathbf{k},\mathbf{r})$. In the STM mode and in the STS mode, Quantum Mechanical SPM Simulator deals with states of a sample which has non zero momentum, but electronic states of a tip is expanded not with Bloch sums but with pseudo-atomic orbitals.

Quantum Mechanical SPM Simulator reads translational vectors of sample's periodic boundary condition not from a sample's structure file but from setting items of a project file. So be careful whether a set of input translational vectors is valid or not.

11.1.c DFTB method

DFTB method (Density-Functional based Tight-Binding method) is a tight-binding method with optimized atomic orbitals based on the density functional theory. The method expands a state of a system with a pseudo-atomic orbital or a Bloch sum, based on the density functional theory. The total energy of a system in the density functinal theory is described as follows [7].

$$E_{DFT} = \sum_n f_n \left\langle \psi_n \right| -\frac{\Delta}{2} + V_{ext}(\mathbf{r}) + \frac{1}{2}\int d\mathbf{r}' \frac{\rho(\mathbf{r}')}{|\mathbf{r} - \mathbf{r}'|} \left| \psi_n \right\rangle + E_{xc}[\rho] + \frac{1}{2}\sum_{a \neq b} \frac{Z_a Z_b}{|\mathbf{R}_a - \mathbf{R}_b|} \qquad \ldots(6)$$

Atomic units are used. $|\psi_n\rangle$ denotes a state of one particle in the Kohn-Sham equation, f_n denotes the occupation number of a state $|\psi_n\rangle$, V_{ext} denotes the external force field which comes from a Coulomb potential of an atomic nucleus and of a core electron, ρ denotes electron density, and E_{xc} denotes exchange-correlation energy. Z_a denotes the charge of the atomic core of an atom "a" at the position of the atomic nucleus, that is, the sum of the nuclear charge and the core electron's charge. Temparature effect is taken into consider with occupation numbers f_n. When charge ρ is separeted into the initial charge and the fluctuation like

$$\rho(\mathbf{r}) = \rho_0(\mathbf{r}) + \delta\rho(\mathbf{r})$$

, then the equation (6) can be written as follows.

$$E = \sum_n f_n \langle \psi_n | -\frac{\Delta}{2} + V_{ext}(\mathbf{r}) + \int d\mathbf{r}' \frac{\rho_0(\mathbf{r}')}{|\mathbf{r}' - \mathbf{r}|} + v_{XC}[\rho_0] | \psi_n \rangle$$

$$-\frac{1}{2}\int d\mathbf{r}' d\mathbf{r} \frac{\rho_0(\mathbf{r}')(\rho_0(\mathbf{r}) + \delta\rho(\mathbf{r}))}{|\mathbf{r}' - \mathbf{r}|} - \int d\mathbf{r} v_{XC}[\rho_0](\rho_0(\mathbf{r}) + \delta\rho(\mathbf{r}))$$

$$+\frac{1}{2}\int d\mathbf{r}' d\mathbf{r} \frac{\delta\rho(\mathbf{r}')(\rho_0(\mathbf{r}) + \delta\rho(\mathbf{r}))}{|\mathbf{r}' - \mathbf{r}|} + E_{XC}[\rho_0 + \delta\rho] + E_{ii},$$

$$E_{ii} = \frac{1}{2}\sum_{a \neq b} \frac{Z_a Z_b}{|\mathbf{R}_a - \mathbf{R}_b|}$$

In addition, expanding energy at ρ to second order in fluctuation $\delta\rho$, the following holds.

$$E = \sum_n f_n \langle \psi_n | H_0 | \psi_n \rangle + E_2 + E_{rep}$$

$$H_0 = -\frac{\Delta}{2} + V_{ext}(\mathbf{r}) + \int d\mathbf{r}' \frac{\rho_0(\mathbf{r}')}{|\mathbf{r}' - \mathbf{r}|} + v_{XC}[\rho_0]$$

$$E_2 = \frac{1}{2}\int d\mathbf{r}' d\mathbf{r} \left(\frac{1}{\|\mathbf{r}' - \mathbf{r}\|} + \frac{\delta^2 E_{XC}}{\delta\rho(\mathbf{r}')\delta\rho(\mathbf{r})}\bigg|_{\rho_0} \right) \delta\rho(\mathbf{r}')\delta\rho(\mathbf{r}) \qquad \ldots(7)$$

$$E_{rep} = -\frac{1}{2}\int d\mathbf{r}' d\mathbf{r} \frac{\rho_0(\mathbf{r}')\rho_0(\mathbf{r})}{|\mathbf{r}' - \mathbf{r}|} + E_{XC}[\rho_0] - \int d\mathbf{r} v_{XC}[\rho_0]\rho_0(\mathbf{r}) + E_{ii}$$

E_{rep} is called repulsive energy term. H_0 and E_{rep} do not depend on $\delta\rho$. E_2 term treats effects of charge transfer explicitly.

From here, using tight-binding approximation, we expand a wave function with Bloch sums.

$$\psi_n(\mathbf{r}) = \sum_i c_{in} b_i(\mathbf{r})$$

And using the Mulliken population analysis [8], the charge of an atom "a" is assumed to be as follows.

$$q_a = \frac{1}{2}\sum_n f_n \sum_{i \in a}\sum_j \left(c^*_{in} S_{ij} c_{jn} + c^*_{jn} S_{ji} c_{in} \right) \qquad \text{---(8)}$$

Here

$$S_{ij} = \langle b_i | b_j \rangle$$

and * means complex conjugate. Difference from initial charge q_a^0 is described as follows.

$$\Delta q_a = q_a - q_a^0$$

Then the second term E_2 of energy in the equation (7) is described as follows [9].

$$E_2 = \frac{1}{2}\sum_{a,b \in atom} \gamma_{ab} \Delta q_a \Delta q_b$$

$$\gamma_{ab} = \frac{1}{R} - \left[e^{-\tau_a R}\left(\frac{\tau_b^4 \tau_a}{2(\tau_a^2 - \tau_b^2)^2} - \frac{\tau_b^6 - 3\tau_b^4\tau_a^2}{(\tau_a^2 - \tau_b^2)^3 R} \right) + e^{-\tau_b R}\left(\frac{\tau_a^4 \tau_b}{2(\tau_b^2 - \tau_a^2)^2} - \frac{\tau_a^6 - 3\tau_a^4\tau_b^2}{(\tau_b^2 - \tau_a^2)^3 R} \right) \right]$$

$$R = |\mathbf{R}_a - \mathbf{R}_b|$$

$$\tau_a = \frac{16}{5} U_a$$

Here U_a denotes chemical hardness of an atom "a" and can be calculated from ionization energy and electron affinity [10].

In order to find the minimum of the energy in equation (7), we use the variational principle under the condition,

$$N = \int d\mathbf{r}\rho(\mathbf{r})$$

and we get the following relations.

$$\sum_j c_{jn}\left(H_{ij} - \varepsilon_n S_{ij}\right) = 0$$

$$H_{ij} = H_{ij}^0 + H_{ij}^1$$

$$H_{ij}^0 = \left\langle b_i \middle| H_0 \middle| b_j \right\rangle \qquad \ldots(9)$$

$$H_{ij}^1 = \frac{1}{2} S_{ij} \sum_g \left(\gamma_{ag} + \gamma_{bg}\right)\Delta q_g$$

By using the approximation of considering only two-body problem, H_0 is described as follows.

$$H_{ij}^0 = \begin{cases} \varepsilon_i^{neutral\ \ free\ \ atom}, (i = j) \\ \left\langle b_i \middle| T + V_0^a + V_0^b \middle| b_j \right\rangle, (a \neq b) \\ 0, otherwise \end{cases}$$

Here a and b denotes the atom which the orbital i and j belongs to respectively, V_0^a denotes the potential of atom "a" at the time the charge of "a" is initial charge q_a^0 and $\varepsilon_i^{neutral\ \ free\ \ atom}$ denotes the energy of orbital i.

The procedure of finding electronic state is as follows. Initial charge $\left\{q_a^0\right\}_a$ is input and the secular equation of (9) is solved. States $\psi_n(\mathbf{r})$ and eigenvalues ε_n is gained as the solution. By applying the Fermi-Dirac distribution function to the distribution of the eigenvalues ε_n, the occupation numbers f_n and the Fermi level E_F is calculated. The charges are calculated from the states $\psi_n(\mathbf{r})$ and the occupation numbers f_n by using the equation (8). And the equation (9) is solved from the charge. These steps are repeated until the energy in the equation (7) converges. When the energy converges, the states is what we want to find. This procedure is called the self-consistance calculation. It is not needed to consider the repulsive energy E_{rep} of the equation (7) during a self-consistant calculation because the repulsive energy does not vary by charge transfer. So it is enough to calculate repulsive energy once and to add the repulsive energy to the calculated energy after the self-consistance calculation. The concrete calculation method is detailed in [7].

11.2 Simulation of STM

When the scanning tunneling microscope (STM) is invented in the early 1980s, there are uncomprehended fundamental issues. Why a surface image with atomic resolution is observed with a probe whose curvature radius is larger than 100 angstrom? How an image is affected by the effect of a probe such as material and structure? Theoretical simulations have played important roles in these fundamental issues. A STM image reflects electronic states of a surface sensitively, and structure of a surface is observed through electronic states only. Though atomic structure of a surface is determined by a STM image in some cases, a large atom in a surface is concealed or a bright area does not coincide with an atom in other cases. So in order to comprehend STM images, theoretical simulation based on quantum mechanics is especially important. In this chapter we show examples of STM and explain the simulation method of STM and STS which is adopted in this simulator.

11.2.a Electronic states of a surface and band structure

A surface of a solid is an interface between bulk which forms a crystal and external space. Because translational symmetry in the vertical direction is lost, various unusual situations occur so that unique structure and functions of a surface are yielded. When bulk of a crystal is ideally cut in a plane, the atoms of the surface lose neighboring bonded atoms, that is, dangling bonds are generated, and the surface become unsteady. So the atoms of the surface change themselves by finding chemically stable states, and the atoms are arranged differently from in the bulk. This phenomenon is called surface reconstruction. Periodic structure of a reconstructed surface becomes different from that of an ideal surface in some cases. Though periodic structure of a surface can be measured with LEED (Low-Energy Electron Diffraction), but LEED can not determine atomic positions. Surface reconstruction causes change of electronic states and, as a result, change of chemical properties. There are Si(111)-7x7 structure [11] (Figure 141) and Au(100)-26x5 structure [12] (Figure 142) as a sample of surface reconstruction.

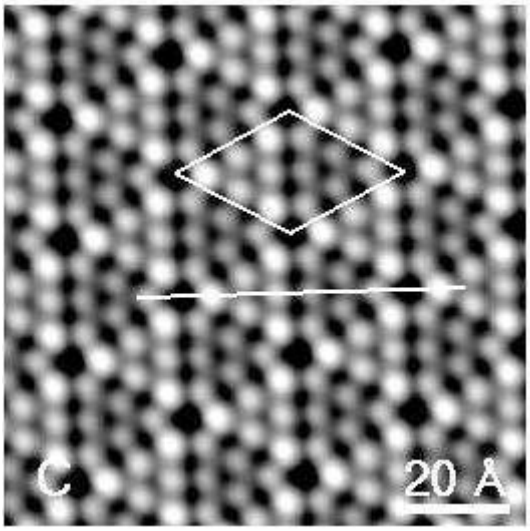

Figure 141 The STM image of Si(111)-7x7 [13].

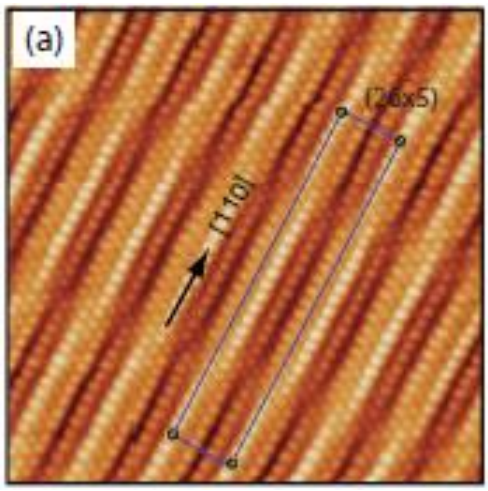

Figure 142 The STM image of Au(100)-26x5 [12].

Electronic states in a crystal is illustrated as band structure. An electron bound to an atom has discrete energies in the frame of quantum mechanics. But when atoms are arranged periodically like in a crystal or on a surface, energy forms continuous distribution (band structure). An energy is determined if a wave number $\mathbf{k}$ is determined, which correnponds to momentum of the electron in the crystal. So we can plot energies $E(\mathbf{k})$ to wave numbers $\mathbf{k}$

(extended zone scheme). But the following scheme (reduced zone scheme) is often used that the domain of the energy $E(\mathbf{k})$ is restricted to the first Brillouin zone B_1 by translating energies with reciprocal vectors where the reciprocal vectors and the first Brillouin zone is calculated from the periodic boundary condition. The first Brillouin zone is three dimensional in a crystal and two dimensional in a surface plane. The band structure is characterized by plotting $E(\mathbf{k})$ along some line segments which connects a representative point to another representative point in the first Brillouin zone as illustrated in Figure 143 and Figure 144.

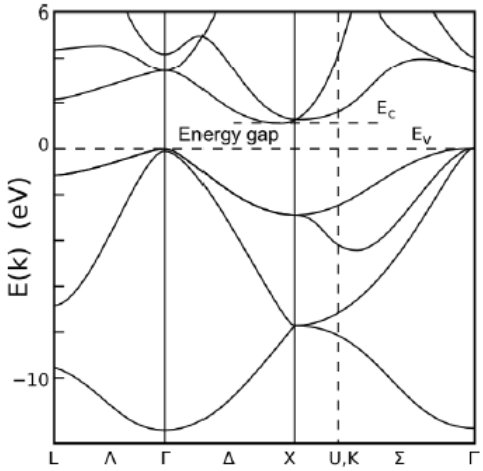

Figure 143 The band structure of the single crystal silicon [15].

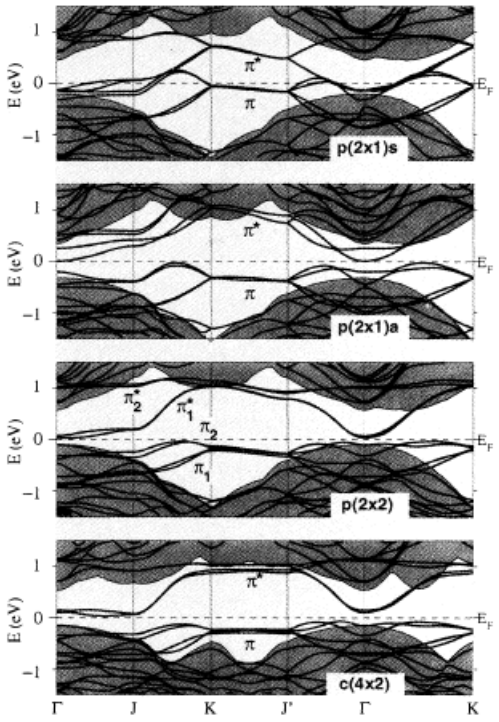

Figure 144 The band structure of the surface silicone [16]. The band structure of surface reconstructions differ each other.

11.2.b Calculation of tunneling current

The calculation model of tunneling current is based on the Bardeen's tunneling theory [17]. We explain the outline below. We introduce the Hamiltonian of the system as $H = T + V_S + V_T$ in order to find electron transition probability between the tip and the sample later. Here T denotes a kinetic energy operator and V_S and V_T denotes a potential energy operator of sample space Ω_S and tip space Ω_T each other. We assume the localization of the tip and the sample as follows.

$$\begin{aligned} H\left|\psi_\nu\right\rangle &\approx (T+V_T)\left|\psi_\nu^T\right\rangle = E_\nu^T\left|\psi_\nu^T\right\rangle \quad in \quad \Omega_T \\ H\left|\psi_\mu(\mathbf{k})\right\rangle &\approx (T+V_S)\left|\psi_\mu^S(\mathbf{k})\right\rangle = E_\mu^S\left|\psi_\mu^S(\mathbf{k})\right\rangle \quad in \quad \Omega_S \end{aligned} \qquad \ldots(10)$$

Because we can consider V_S to be zero in the domain Ω_T and similar in the domain Ω_S. The total domain is described as $\Omega = \Omega_T + \Omega_S$. It is assumed in the equation (10) that a

voltage is not applied externally and the Fermi level of the tip and of the sample is the same value E_F.

When the voltage V is applied to the tip, the potential, the energy and the Fermi level of the tip become $\tilde{V}_T(\mathbf{r}) = V_T(\mathbf{r}) - eV$, $\tilde{E}_\nu^T = E_\nu^T - eV$ and $\tilde{E}_F^T = E_F - eV$ respectively (refer to Figure 145 and Figure 146).

The transition probability from a state $\left|\psi_\mu^S(\mathbf{k})\right\rangle$ to a state $\left|\psi_\nu^T\right\rangle$ is described as follows by the perturbation theory of quantum mechanics (Fermi's golden rule).

$$P = P_{(\mu,\mathbf{k})\to\nu} = \frac{2\pi}{\hbar}\delta\left(\tilde{E}_\nu^T - E_\mu^S(\mathbf{k})\right)\left|\left\langle\psi_\nu^T\left|H - H^S\right|\psi_\mu^S(\mathbf{k})\right\rangle\right|^2$$

Here $H^S = T + V_S$, and $\tilde{V}_T = H - H^S$ is the perturbation. Transition of a state is made from an occupied state to an unoccupied state. So using the the Fermi-Dirac distribution function,

$$f_{E_F}(E) = \frac{1}{1+\exp\left(\frac{E-E_F}{k_bT}\right)}$$

the total amount of the current is described as follows.

$$\begin{aligned}
I &= I^{T\to S} - I^{S\to T} \\
&= e\sum_{\mu,\nu}\frac{1}{vol(B)}\int_{\mathbf{k}\in B}dk\left\{f_{E_F}\left(E_\mu^S(\mathbf{k})\right)\left(1 - f_{\tilde{E}_F^T}\left(\tilde{E}_\nu^T\right)\right)P - f_{\tilde{E}_F^T}\left(\tilde{E}_\nu^T\right)\left(1 - f_{E_F}\left(E_\mu^S(\mathbf{k})\right)\right)P\right\} \\
&= \frac{2\pi e}{\hbar}\sum_{\mu,\nu}\frac{1}{vol(B)}\int_{\mathbf{k}\in B}dk\left(f_{E_F}\left(E_\mu^S(\mathbf{k})\right) - f_{E_F}\left(E_\nu^T\right)\right) \\
&\times\delta\left(E_\nu^T - eV - E_\mu^S(\mathbf{k})\right)\left|\left\langle\psi_\nu^T\left|H - H^S\right|\psi_\mu^S(\mathbf{k})\right\rangle\right|^2 \qquad \ldots(11) \\
&= \frac{2\pi e}{\hbar}\sum_{\mu,\nu}\frac{1}{vol(B)}\int_{\mathbf{k}\in B}d\mathbf{k}\int_{E\in\mathbf{R}}dE\left(f_{E_F}(E) - f_{E_F}(E+eV)\right) \\
&\times\delta\left(E_\nu^T - eV - E\right)\delta\left(E_\mu^S(\mathbf{k}) - E\right)\left|\left\langle\psi_\nu^T\left|H - H^S\right|\psi_\mu^S(\mathbf{k})\right\rangle\right|^2
\end{aligned}$$

Here B denotes the first Brillouin zone, $vol(B)$ denotes the volume of the first Brillouin zone, e denotes the elementary charge and k_b denotes the Boltzmann constant. Decomposition of Dirac delta function is applied.

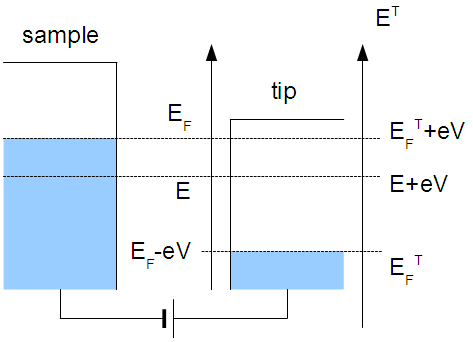

Figure 145 The conceptual diagram of energy level with applied tip's voltage V.

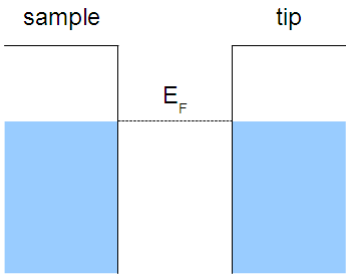

Figure 146 The conceptual diagram of energy level without applied voltage.

Then the state $\left|\psi_\mu^S(\mathbf{k})\right\rangle$ and the state $\left|\psi_\nu^T\right\rangle$ is expanded by the Bloch sums and by the pseudo-atomic orbital respectively as follows.

$$\left|\psi_\mu^S(\mathbf{k})\right\rangle = \sum_j C_{j,\mu}^S(\mathbf{k})\left|b_j^S(\mathbf{k})\right\rangle$$

$$\left|\psi_\nu^T\right\rangle = \sum_i C_{i,\nu}^T\left|b_i^T\right\rangle$$

The content of the absolute value in the equation (11) is described as follows.

$$\left\langle\psi_\nu^T\left|H-H^S\right|\psi_\mu^S(\mathbf{k})\right\rangle = \sum_{i,j}\left(C_{i,\nu}^T\right)^* C_{j,\mu}^S(\mathbf{k})J_{j,i}(\mathbf{k})$$

$$J_{j,i}(\mathbf{k}) = \left\langle b_i^T\left|H-H^S\right|b_j^S(\mathbf{k})\right\rangle \qquad \ldots(12)$$

$$= \int d\mathbf{r}\left(b_i^T(\mathbf{r})\right)^* H b_j^S(\mathbf{k},\mathbf{r}) - \varepsilon_j\int d\mathbf{r}\left(b_i^T(\mathbf{r})\right)^* b_j^S(\mathbf{k},\mathbf{r})$$

Here "*" means complex conjugate and ε_j denotes the eigenvalue of the sample's atomic orbital.

An energy spectrum of a tip is discrete because a tip is approximately treated as an atom cluster with a small size. But because the eigenvalues are widened by the influence of the bulk part of the tip's root [18, 19], we replace the δ function for the tip in the equation (11) with the Lorentzian function of width 1.0 eV. Please refer to the reference [19] for more detailed derivation of the equation, especially the grounds for using the Lorentzian function. The resulting equation of the tunneling current is as follows.

$$I = \frac{2\pi e}{\hbar}\sum_{\mu,\nu}\frac{1}{vol(B)}\int_{\mathbf{k}\in B} d\mathbf{k}\left\{\left|\left\langle\psi_\nu^T\left|H-H^S\right|\psi_\mu^S(\mathbf{k})\right\rangle\right|^2\right.$$
$$\left.\times\int_{E\in\mathbf{R}} dE\left(f_{E_F}(E)-f_{E_F}(E+eV)\right)L_\Gamma\left(E_\nu^T-eV-E\right)\delta\left(E_\mu^S(\mathbf{k})-E\right)\right\} \qquad \ldots(13)$$

Here L_Γ denotes the Lorentzian of with Γ.

As is shown in the equation (13), the integration which includes the delta function with respect to energy is needed, and the integration is treated as follows in this solver. We take some k points in the first Brillouin zone and calculate electronic states of the sample at the k points. At each k point we consider the μ-th eigenvalue $\left\{E_\mu^S(\mathbf{k})\right\}_{\mathbf{k}\in B}$ from the bottom as energy which belongs to the μ-th band from the bottom. We set the maximum energy and minimum energy in the μ-th band to be the top and the bottom of the band respectively, and we widen

eigenvalues $E_\mu^S(\mathbf{k})$ with the Lorentzian of width Γ_μ so that all two energies are connected each other in the band. Delta function is written as follows.

$$\delta\left(E_\mu^S(\mathbf{k})-E\right)\approx\frac{1}{\pi}\frac{\Gamma_\mu}{\left(E-E_\mu^S(\mathbf{k})\right)^2+\Gamma_\mu^2}$$

We force the outer part of the band to be zero. Though some part of the density of states is cut off, the scale does not change seriously. Width Γ_μ of Lorentzian, which is calculated for each band μ, is based on the maximum interval of the ordered energy $\left\{E_\mu^S(\mathbf{k})\right\}_{\mathbf{k}\in B}$ as follows.

$$\max\left\{\Delta E_i = E_{i+1}-E_i\right\}$$

There are two major method of measurement in the STM experiment, that is, the method which scans distance between a tip and a sample as the tunneling current is kept to be constant and the method which scans current as distance between a tip and a sample is kept to be constant. Quantum Mechanical SPM Simulator adopts the model of constant height experiment. Please take notice that pseudo-atomic orbitals by which electronic states are expanded are cut off on the outside of a distance, so a tunneling current image which you want can not be gained unless distance between a tip and a sample is adjusted in some cases.

11.2.c A example of calculation of a tunneling current image

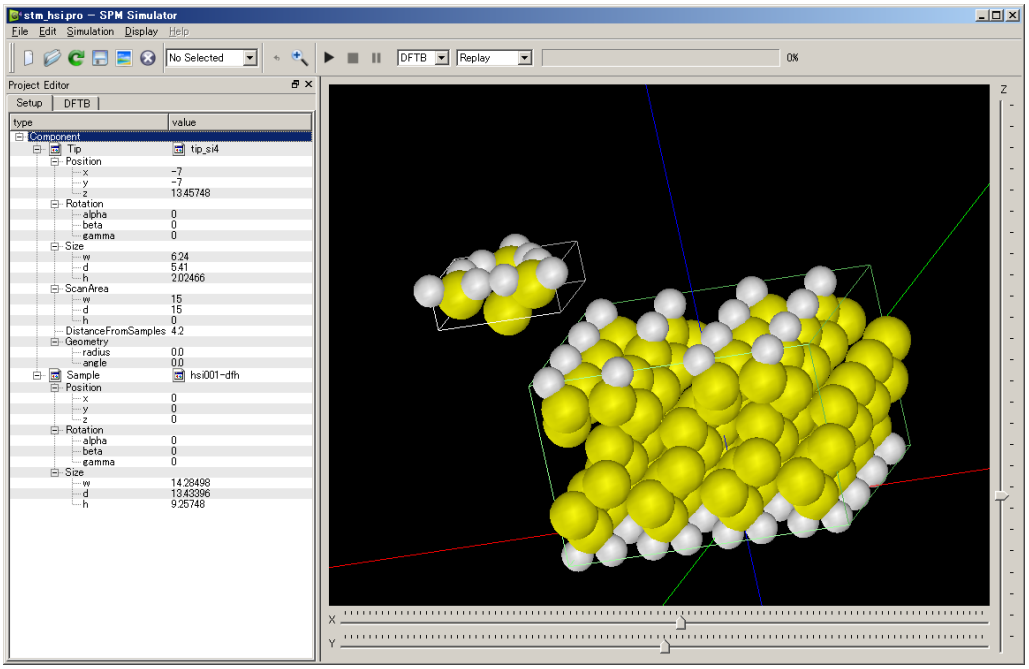

Figure 147 GUI on which calculation of tunneling current is set. The sample is one hydrogen eliminated surface from a hydrogen-terminated Si(001) surface.

We calculate the system illustrated above as an example. The tip is made of silicon, and the sample is the surface which one hydrogen is eliminated from a hydrogen-terminated Si(001) surface. The result is shown in Figure 148.

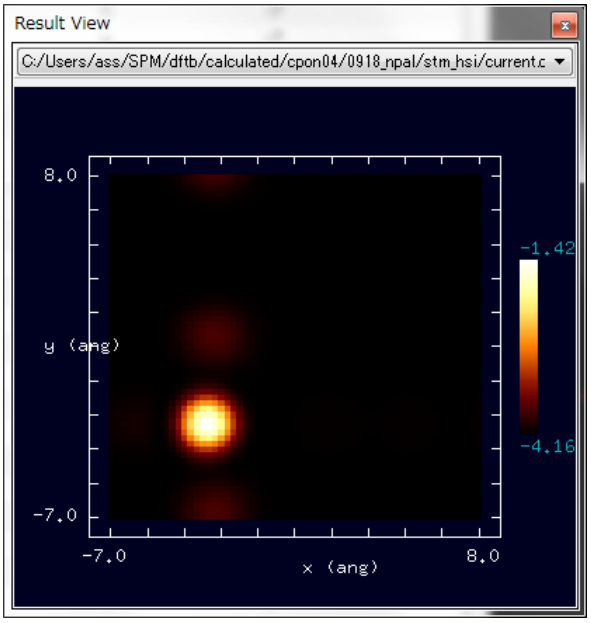

Figure 148 The tunneling current image of the calculation of Figure 147.

This is read that a large current flows in the hydrogen-eliminated position.

11.3 Simulation of STS

A tunneling current image of STM reflects not a position of a surface atom but local density of states (LDoS) of an electron on the surface. In view of the fact, local density of states directly under a tip can be measured with the method that we draw a current-voltage curve by measuring current in the fixed tip position and differentiate the curve. This is STS (Scanning Tunneling Spectroscopy).

When a tip is supposed to be one point $\mathbf{X}$ only, the following relation holds from the equation (12).

$$\left\langle \psi_\nu^T \left| H - H^S \right| \psi_\mu^S(\mathbf{k}) \right\rangle = \int d\mathbf{r} d\mathbf{r}' \left(\psi_\nu^T(\mathbf{r})\right)^* \left\langle \mathbf{r} \left| \tilde{V}_T(\mathbf{r}') \right| \mathbf{r}' \right\rangle \psi_\mu^S(\mathbf{k},\mathbf{r}')$$

$$\approx \left(\psi_\nu^T(\mathbf{x})\right)^* \left(V_T(\mathbf{x}) - eV\right) \psi_\mu^S(\mathbf{k},\mathbf{x})$$

The equation (11) is transformed to the following equation.

$$I \approx \frac{2\pi e}{\hbar} \int_{E\in\mathbf{R}} dE \left(f_{E_F}(E) - f_{E_F}(E+eV)\right) \left(V_T(\mathbf{x}) - eV\right)^2$$

$$\times \sum_\nu \left\{ \delta\left(E_\nu^T - eV - E\right) \left|\psi_\nu^T(\mathbf{x})\right|^2 \right\} \sum_\mu \left\{ \frac{1}{vol(B)} \int_{\mathbf{k}\in B} d\mathbf{k}\, \delta\left(E_\mu^S(\mathbf{k}) - E\right) \left|\psi_\mu^S(\mathbf{k},\mathbf{r})\right|^2 \right\}$$

$$\approx \frac{2\pi e}{\hbar} \left(V_T(\mathbf{x}) - eV\right)^2 \int_{E=E_F-eV}^{E_F} dE \cdot LDoS^T(\mathbf{x}, E+eV) \cdot LDoS^S(\mathbf{x}, E)$$

$$LDoS^T(\mathbf{x}, E+eV) = \sum_\nu \left\{ \delta\left(E_\nu^T - eV - E\right) \left|\psi_\nu^T(\mathbf{x})\right|^2 \right\}$$

$$LDoS^S(\mathbf{x}, E) = \sum_\mu \left\{ \frac{1}{vol(B)} \int_{\mathbf{k}\in B} d\mathbf{k}\, \delta\left(E_\mu^S(\mathbf{k}) - E\right) \left|\psi_\mu^S(\mathbf{k},\mathbf{r})\right|^2 \right\}$$

Here the Fermi-Dirac distribution function is replaced with a step function for simple argument. And $LDoS^T$ and $LDoS^S$ denotes the local density of states of a tip and a sample respectively. (For simple argument we ignore g-factor.) The derivation of the above equatin is as follows.

$$\frac{dI}{dV} \approx \frac{2\pi e^2}{\hbar}\Big[\big(V_T(x)-eV\big)^2 LDoS^T\big(x,E_F\big)\cdot LDoS^S\big(x,E_F-eV\big)$$

$$+2\big(eV-V_T(x)\big)\int_{E=E_F-eV}^{E_F} dE\cdot LDoS^T\big(\mathbf{x},E+eV\big)\cdot LDoS^S\big(\mathbf{x},E\big)$$

$$+\big(V_T(x)-eV\big)^2\int_{E=E_F-eV}^{E_F} dE\cdot \frac{dLDoS^T}{dE}\big(\mathbf{x},E+eV\big)\cdot LDoS^S\big(\mathbf{x},E\big)\Big]$$

And further the equation devided by I/V is as follows.

$$\frac{\dfrac{dI}{dV}}{\dfrac{I}{V}} \approx e\cdot\frac{LDoS^T\big(x,E_F\big)\cdot LDoS^S\big(x,E_F-eV\big)+A(V)}{B(V)}$$

$$A(V)=\frac{2}{\big(eV-V_T(x)\big)}\int_{E=E_F-eV}^{E_F} dE\cdot LDoS^T\big(\mathbf{x},E+eV\big)\cdot LDoS^S\big(\mathbf{x},E\big)$$

$$+\int_{E=E_F-eV}^{E_F} dE\cdot\frac{dLDoS^T}{dE}\big(\mathbf{x},E+eV\big)\cdot LDoS^S\big(\mathbf{x},E\big)$$

$$B(V)=\frac{1}{V}\int_{E=E_F-eV}^{E_F} dE\cdot LDoS^T\big(\mathbf{x},E+eV\big)\cdot LDoS^S\big(\mathbf{x},E\big)$$

Here $A(V)$ and $B(V)$ is expected to vary slowly to bias voltage V. Therefore ((dI/dV)/(I/V)) is often used as an index of local density of states.

In an actual calculation, derivative of current with respect to voltage

$$\frac{dI}{dV}=-\frac{2\pi e^2}{\hbar}\sum_{\mu,\nu}\frac{1}{vol(B)}\int_{\mathbf{k}\in B}d\mathbf{k}\Big[\Big|\big\langle\psi_\nu^T\big|H-H^S\big|\psi_\mu^S(\mathbf{k})\big\rangle\Big|^2$$

$$\times\int_{E\in\mathbf{R}}dE\,\delta\big(E_\mu^S(\mathbf{k})-E\big)\Big\{\frac{df_{E_F}}{dE}\big(E+eV\big)L_\Gamma\big(E_\nu^T-eV-E\big)$$

$$+\big(f_{E_F}(E)-f_{E_F}(E+eV)\big)\frac{dL_\Gamma}{dE}\big(E_\nu^T-eV-E\big)\Big\}\Big]$$

is calculated, and the spectrum is calculated as a ratio to I/V. But it is known that when we divide a derivative dI/dV by I/V in the tunneling spectroscopy calculation, this calculation diverges around a band gap because the value I/V is too small. In order to prevent divergence there is a numerical treatment [20] that the denominator I/V is replaced by the following value.

$$\sqrt{\left(\frac{I}{V}\right)^2+\varepsilon^2}$$

We think a system illustrated in Figure 149 as an example.

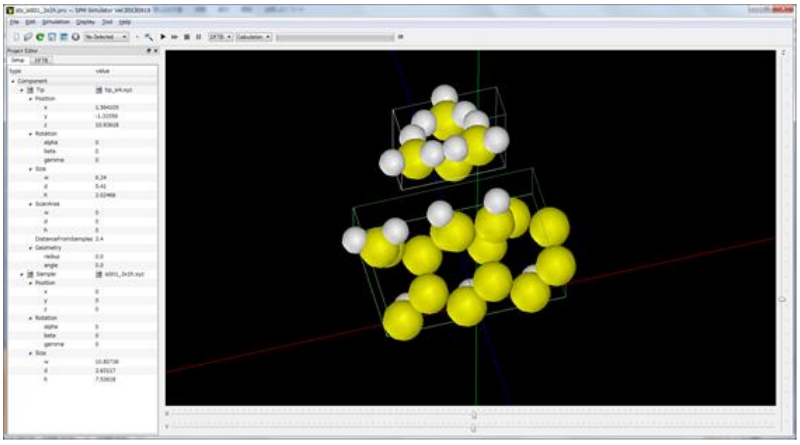

Figure 149 GUI on which STS calculation of the Si(001)-3x1:H surface to the silicon tip is set.

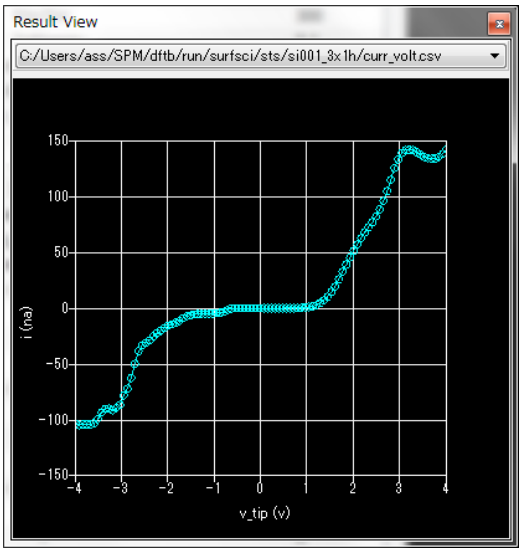

Figure 150 The I-V curve.

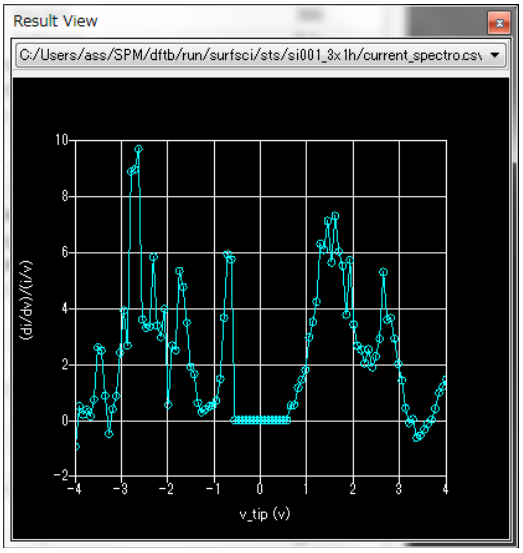

Figure 151 The spectral curve ((dI/dV)/(I/V)).

Figure 150 and Figure 151 are the calculation results in the simulator and Figure 152 is a result from a preceding paper.

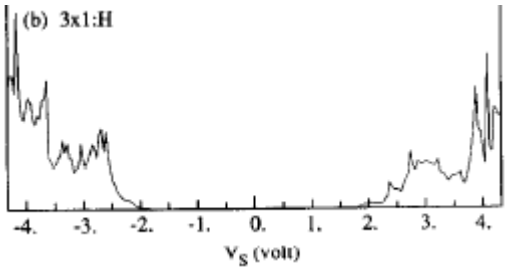

Figure 152 The dI/dV curve [18].

It is read that existence of a band gap is reproduced. But the band gap is underestimated because this calculation is based on the density functional theory.

11.4 Simulation of AFM

It is difficult to calculate Van der Waals force in the frame of the density functional theory. This Quantum Mechanical SPM Simulator calculates force from a sample surface to a tip as the sum of chemical force based on the DFTB method and Van der Waals force.

11.4.a Chemical force

In order to calculate chemical force from a sample surface to a tip it is enough to calculate force applied to an atom of a tip and to take a summation over the total atoms of a tip. Force applied to each atom "a" of a tip is calculated as a gradient of energy with respect to the positin vector $\mathbf{R}_a$ of an atom "a".The gradient of energy of equation (7) is calculated as follows.

$$\mathbf{F}_a = -\frac{\partial E_{DFTB}}{\partial \mathbf{R}_a}$$

$$= -\sum_n f_n \sum_{i,j} (c_{in})^* c_{jn} \left[\left(\frac{\partial H^0_{ij}}{\partial \mathbf{R}_a} - \varepsilon_n \frac{\partial S_{ij}}{\partial \mathbf{R}_a} \right) + \frac{H^1_{ij}}{S_{ij}} \frac{\partial S_{ij}}{\partial \mathbf{R}_a} \right]$$

$$- \Delta q_a \sum_b \frac{\partial \gamma_{ab}}{\partial \mathbf{R}_a} \Delta q_b - \frac{\partial}{\partial \mathbf{R}_a} \sum_{b \neq g} E_{rep,bg}$$

Force applied to a tip is calculated as the summation of a z-component of the force applied to an atom.

$$\sum_{a \in tip} F_{a,z}$$

11.4.b Van der Waals force

Quantum Mechanical SPM Simulator calculates force applied to a pyramidal tip, a conical tip, a parabolic tip and a spherical tip by using formulae in the paper [21].

$$F^{vdw}_{Pyramidal} = -\frac{2A_H \tan^2(\alpha/2)}{3\pi} \left(\frac{1}{z} - \frac{1}{z+H} - \frac{H}{(z+H)^2} - \frac{H^2}{(z+H)^3} \right)$$

$$F^{vdw}_{conical} = -\frac{A_H \tan^2(\alpha/2)}{6} \left(\frac{1}{z} - \frac{1}{z+H} - \frac{H}{(z+H)^2} - \frac{H^2}{(z+H)^3} \right)$$

$$F^{vdw}_{Parabolic} = -\frac{A_H R}{6} \left(\frac{1}{z^2} + \frac{1}{(z+H)^2} - \frac{2H}{(z+H)^3} \right)$$

$$F^{vdw}_{Spherical} = -\frac{A_H R}{6} \left(\frac{1}{z^2} - \frac{1}{(z+H)^2} - \frac{2}{H} \left(\frac{1}{z} - \frac{1}{z+H} \right) \right)$$

Here A_H, α, H and R denotes the Hamaker constant, the tip apex angle, the height of the tip and the curvature radius of the tip apex respectively. For the spherical tip, $H = 2R$.

11.4.c NC-AFM and a frequency shift image

Quantum Mechianical SPM Simulator in AFM calculation mode simulates noncontact atomic force microscopy (NC-AFM) in which a tip does not contact with a sample surface. In noncontact AFM a vibrated tip scans a sample surface and frequency shift or phase shift with respect to a tip's position is imaged which is caused by the force from a sample surface to a tip. There are two ways of measuring variation of oscillation, that is, AM-AFM which measures the change in amplitude of the oscilation and FM-AFM which measures the change in resonant frequency of the oscillation. It is said that FM-AFM is more sensitive than AM-AFM and can perform a measurement with higher resolution. Quantum Mechanical SPM Simulator simulates FM-AFM, which measures the change in frequency, and outputs a frequency shift image.

Equation of motion about the hight of a tip is as follows.

$$m\frac{d^2z}{dt^2}+2m\gamma(z,\dot{z})\frac{dz}{dt}+k(z-u_0+h)-F_{TS}(z)=kl\cos(\omega t)$$

From this equation, a frequency shift $\Delta\nu$ is described as follows [22].

$$\Delta\nu=-\frac{\nu_0}{2\pi ak}\int_0^{2\pi}F_{TS}(z(\theta))\cos(\theta)d\theta$$

Here γ, k, h, F_{TS}, ν_0 and a denotes the general friction coefficient, the cantilever spring constant, the tip length, the tip-sample interaction force, the resonance frequency and the amplitude of the oscillation.

11.4.d A example of calculation of a frequency shift image

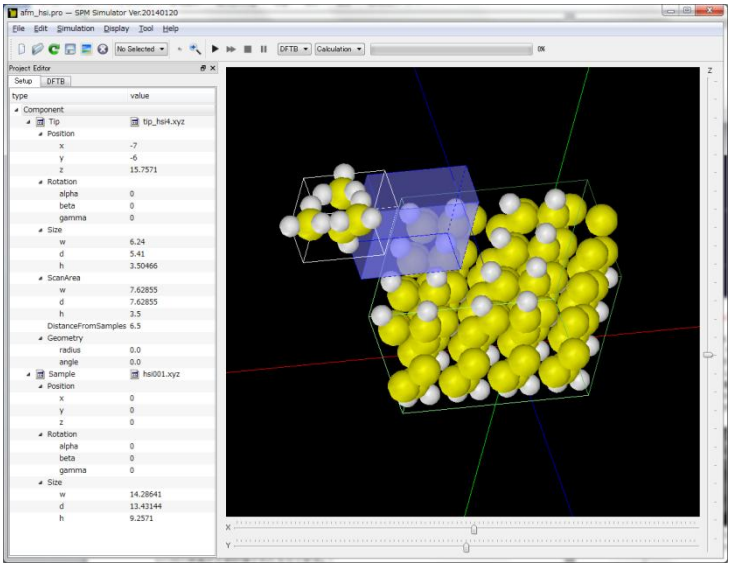

Figure 153 GUI on which simulation of a frequency shift image with a sample of hydrogen-terminated Si(001) surface is set.

We calculate a system of Figure 153 as an example of frequency shift image simulation. The sample is the hydrogen-terminated Si(001) surface. The tip scans surface while oscillating in the range of the blue cube. The result is shown in Figure 154. It is read that absolute value of the frequency shift around the position of hydrogen atoms is larger than the others.

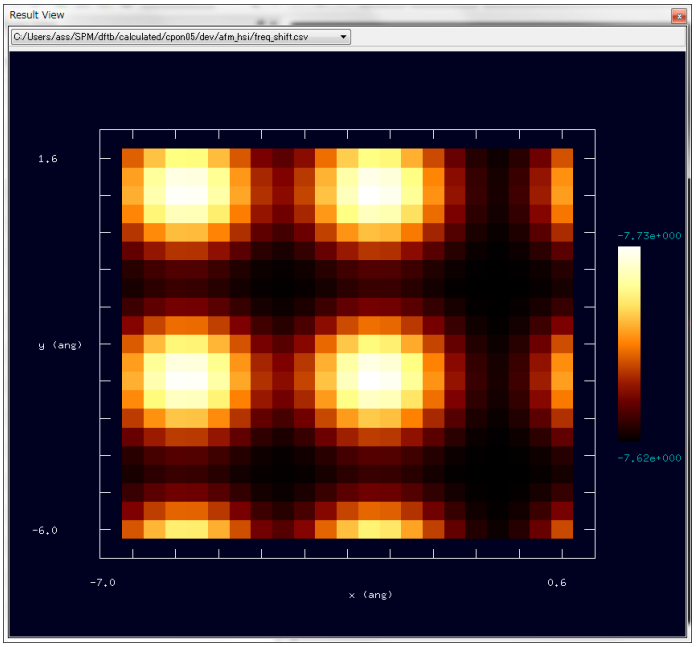

Figure 154 The frequency shift image of hydrogen-terminated Si(001) sample surface.

11.5 Simulation of KPFM

After the invention of STM by Binning various kinds of scanning microscopy have been developed as an extention of STM. Kelvin probe force microscopy (KPFM) is one of them and is useful technique for measuring a distribution of work functions on a surface at microscale, or more properly, a distribution of local contact potential difference. Minimum energy needed to remove an electron from a surface material is called a work function. A work function is strongly influenced not only by a type of the atoms but also by a crystal orientation and by an absorbed atom. Because KPFM measures not a macroscopic work function but microscopic distribution of local contact potential difference, KPFM is key technique for surface science development that, for example, evaluates properties of semiconductor and evaluates charge transfer by absorbed metal catalyst.

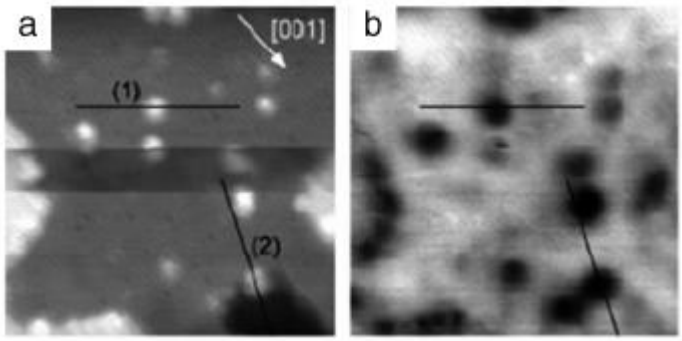

Figure 155 (a) the AFM image (b) the KPFM image, of Pt evaporated TiO_2 surface [23]. (a) Open (b) Filled, circles are obtained on the Pt nanostructures.

11.5.a Kelvin probe and work function

KPFM is based on Kelvin probe method and AFM. Kelvin probe is the method which evaluates a work function by measuring contact potential difference and this method is based on the principle below.

Suppose there are two metal plates A and B, and a work function of them is Φ_A and Φ_B respectively. Φ_A and Φ_B corresponds to the difference between vacuum energy level and Fermi level of A and B respectively. When these two metals are electrically connected each other or are close to each other, charge transfers between the metal A and the metal B so that two Fermi levels match each other and each metal is charged. Next, we eliminate the electrostatic charge by applying appropriate voltage between two metals. This applied voltage

$$\Delta V = \frac{\Phi_B - \Phi_A}{e}$$

is contact potential difference. This value is measured in the condition that oscillating electrical force is nullified while gradually increasing DC voltage and AC voltage is applied. Here e denotes elementary charge.

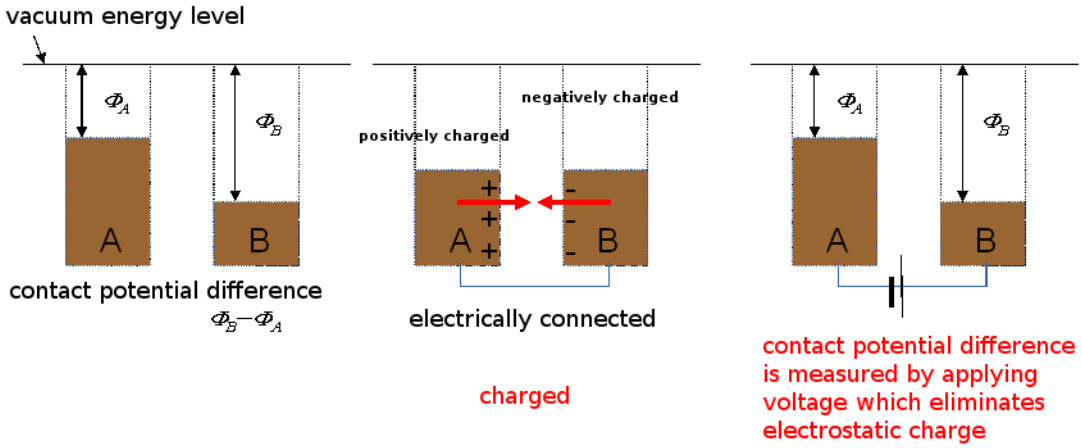

Figure 156 Diagram which explains Kelvin probe.

11.5.b KPFM and local contact potential difference

Kelvin probe is a macroscopic observation method. And KPFM is a method which measures microscopic local contact potential difference between a tip and a sample by applying Kelvin probe to AFM. When a tip is scanning on a surface in AFM, applying voltage between the tip and the sample causes change of tip's charge and sample surface's charge. Here electrical interaction between the tip and the region of the sample near the tip determines the distribution of charge. In other words, distribution of charge on the tip and the local domain of sample near the tip is influenced by quantum mechanical interaction each other and as a result distribution of charge depends on a position of the tip. It should be noted that measurement is usually performed under the condition tunneling current does not occur. This charge distribution causes electrostatic force between the tip and the sample. Gradually varying applied voltage, we measure the voltage which minimizes interaction between the tip and the sample. This voltage corresponds to local contact potential difference at the position of the tip [27], [28]. In KPFM local contact potential difference (LCPD) at the time a tip scans on a sample surface is output as a image to a position of tip.

11.5.c Calculation method of KPFM with partitioned real-space density functional based tight binding method

In order to calculate local contact potential difference with DFTB method, we adopt partitioned real-space density functional based tight binding method. The principle of this method is below. Suppose charge Δq transfers from a sample to a tip by applying voltage V between the tip and the sample. Charge of the tip increases by Δq and charge of the sample decreases by Δq. With a fixed charge transfer Δq, electronic states of the tip and the sample is calculated by partitioned real-space density functional based tight binding method. Here electronic states of the tip is influenced by the potential of the sample, and electronic states of the sample is influenced by the potential of the tip. Because charge transfer Δq is fixed, Fermi level of the tip and the sample is determined by the each number of electron after the charge transfer. Difference of these Fermi levels is divided to be a potential difference between the electrodes to the charge transfer. So we search the charge transfer which minimizes tip-sample interaction, varying the charge transfer, and the potential difference between the electrodes at this time is local contace potential difference [27], [28]. The calculation explained bove can be performed as an extention of DFTB.

11.5.d Examples of local contact potential difference image

We take a system below as examples of local contact potential difference. Samples are Si(001) surface and one silicon atom in the fourth-layer is replaced by nitrogen atom in Figure 158 [27], [28].

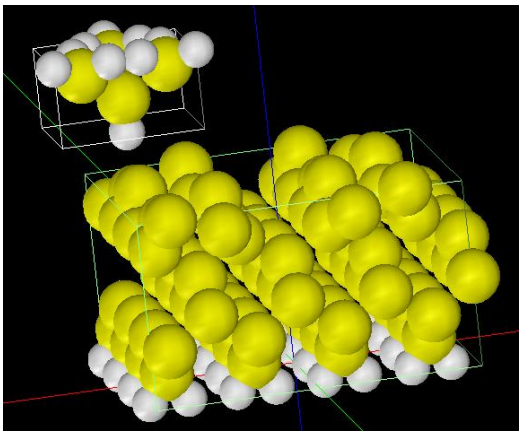

Figure 157 Clean Si(001) sample surface.

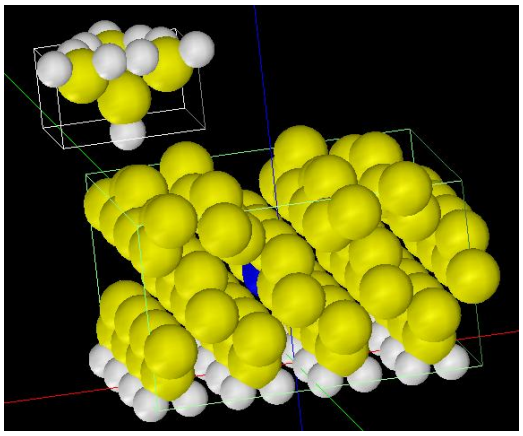

Figure 158 N-doped Si(001) sample surface in which one of the fourth-layer atoms is replaced by nitrogen atom.

The following pictures are the local contact potential difference (LCPD) images gained by simulation. The right image is the LCPD image of N-doped surface. The positions of topmost silicon atoms are featured in both left and right image. We can read brown gradient around the position of the doped nitrogen atom in the right image. Though the dopant is in the deep position from the surface, local contact potential difference significantly shift negative.

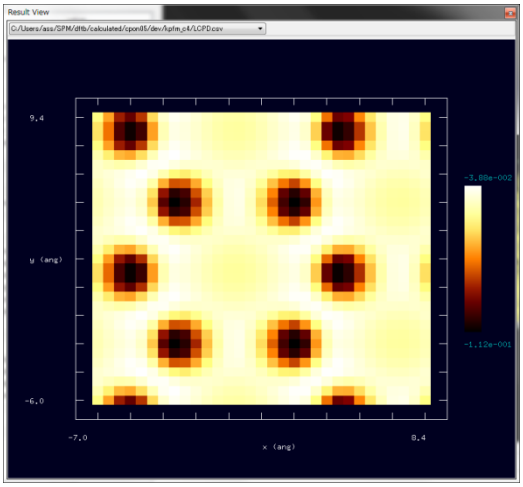

Figure 159 The LCPD image of clean Si(001) surface.

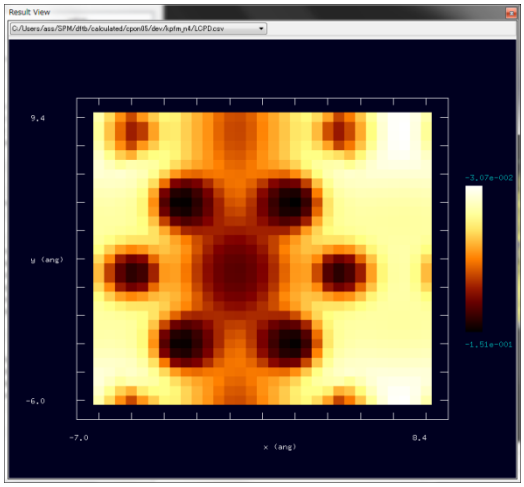

Figure 160 The LCPD image of N-doped Si(001) surface.

11.6 Users guide: how to use DFTB

We explain procedures for calculation in this section.

11.6.a Operation procedure for a tunneling current image

The table below is the operation procedure which calculates the tunneling current image, the result image is put in the STM section, of the hydrogen-terminated Si(001) surface without one hydrogen. As is mentioned in 11-1-2, translational vectors of sample's periodical structure is read not from a sample's structure file but from setting items in "translational_vector" of a project file.

Table 16 Operation procedure which calculates the tunneling current image of the hydrogen-terminated Si(001) surface without one hydrogen.

Description	Procedure
To execute GUI of SPM Simulators	Double click the icon.
To create the new simulation project	Select "new" from "File" in Menu bar. Enter a project name, then click "OK".
To select tip apex model	After right click "Component" in Project Editor, click [Add Tip] > [Database] menu. Then, double click "tip_si4".
To select surface model	After right click "Component" in Project Editor, click [Add Sample] > [Database] menu. Then, double click "hsi001-dfh".
To set the initial position of the tip	1. Enter "-7" in two cells of "Component" > "Tip" > "Position" > "x" and "y". 2. Enter "3.8" in the cell of "Component" > "Tip" > "DistanceFromSamples".

To set size of scan area of the tip	Enter "15", "15", "0" in the cells of "Component" > "Tip" > "ScanArea" > "w", "d", "h", respectively. (If you want to see this area graphically, check "show scan area" in the right click menu of Main View.)
To select a suitable solver	Select "DFTB" and "Calculation" in the boxes on the top of GUI, respectively.
To change to the parameter tab for Quantum Mechanical SPM Simulator	Select "DFTB" tab in Project Editor.
To select the calculation mode	Select the value of "DFTB_STM" for "mode".
To select the two_body_parameter_folder	Select the value of "h-c-si" for "two_body_parameter_folder".
To set the pixel numbers for calculation image	Enter "60" in two cells of "tip" > "Ndiv" > "X" and "Y", and enter "0" in the cell for "Z".
To set the tip bias voltage	Enter "-1.0" in two cells of "tip_bias_voltage"-"minimum" and "maximum".
To set the number of k-points	Input "4" in the cell of "Ndiv_kpoints".
To set translational vectors	Input "15.35014", "15.35014" and "100" in the cells of "a" - "X", "b" - "Y" and "c" - "Z" in the "translational_vector" and input "0" in the others in the "translational_vector".
To start calculation	Push the ▶ button on the top of GUI. (When the confirmation dialog box popped up, please click "Save" button.)
To display the result	Select [Display] > [Result View] in Menu bar. Choose the item including the string "current.csv" from the combo box.

11.6.b Operation procedure for a tunneling current spectroscopy curve

The table below is the operation procedure which calculates tunneling current spectroscopy of Si(001)-3x1:H surface, the result of which is put in the STS section.

Table 17 Operation procedure which calculates the tunneling current spectroscopy of Si(001)-3x1:H surface.

Description	Procedure
To execute GUI of SPM Simulators	Double click the icon.
To create the new simulation project	Select "new" from "File" in Menu bar. Enter a project name, then click "OK".
To select tip apex model	After right click "Component" in Project Editor, click [Add Tip] > [Database] menu. Then, double click "tip_si4".
To select surface model	After right click "Component" in Project Editor, click [Add Sample] > [Database] menu. Then, double click "si001_3x1h".

To set the initial position of the tip	1. Enter "1.5" and "-1.5" in the cell of "Component" > "Tip" > "Position" > "x" and "y", respectively. 2. Enter "3.4" in the cell of "Component" > "Tip" > "DistanceFromSamples".
To select a suitable solver	Select "DFTB" and "Calculation" in the boxes on the top of GUI, respectively.
To change to the parameter tab for Quantum Mechanical SPM Simulator	Select "DFTB" tab in Project Editor.
To select the calculation mode	Select the value of "DFTB_STS" for "mode".
To select the two_body_parameter_folder	Select the value of "h-c-si" for "two_body_parameter_folder".
To set the tip bias voltage	Enter "-4.0", "+4.0" and "100" in the cell of "tip_bias_voltage"-"minimum", "maximum" and "Ndiv", respectively.
To set the number of k-points	Input "4" in the cell of "Ndiv_kpoints".
To set translational vectors	Input "11.51877", "3.83959" and "100" in the cells of "a" - "X", "b" - "Y" and "c" - "Z" in the "translational_vector" and input "0" in the others in the "translational_vector".
To start calculation	Push the ▶ button on the top of GUI. (When the confirmation dialog box popped up, please click "Save" button.)
To display the result	Select [Display] > [Result View] in Menu bar. Choose the item including the string "curr_volt.csv" or "current_spectro.csv" from the combo box.

11.6.c Operation procedure for a frequency shift image

The table below is the operation procedure which calculates the frequency shift image, the result image is put in the AFM section, of the hydrogen-terminated Si(001) surface. AFM calculation and KPFM calculation often returns error unless translational vectors is sufficiently larger than a size of a tip.

Table 18 Operation procedure which calculates the frequency shift image of the hydrogen-terminated Si(001) surface.

Description	Procedure
To execute GUI of SPM Simulators	Double click the icon.
To create the new simulation project	Select "new" from "File" in Menu bar. Enter a project name, then click "OK".
To select tip apex model	After right click "Component" in Project Editor, click [Add Tip] > [Database] menu. Then, double click "tip_hsi4".
To select surface model	After right click "Component" in Project Editor, click [Add Sample] > [Database] menu. Then, double click "hsi001".

To set the initial position of the tip	1. Enter "-7" and "-6" in the cell of "Component" > "Tip" > "Position" > "x" and "y". 2. Enter "6.5" in the cell of "Component" > "Tip" > "DistanceFromSamples".
To set size of scan area of the tip	Enter "7.628550", "7.628550", "3.5" in the cells of "Component" > "Tip" > "ScanArea" > "w", "d", "h", respectively. (If you want to see this area graphically, check "show scan area" in the right click menu of Main View.In AFM mode, scan area is three dimensional cube which consider the tip's vibration.)
To select a suitable solver	Select "DFTB" and "Calculation" in the boxes on the top of GUI, respectively.
To change to the parameter tab for Quantum Mechanical SPM Simulator	Select "DFTB" tab in Project Editor.
To select the calculation mode	Select the value of "DFTB_AFM" for "mode".
To select the two_body_parameter_folder	Select the value of "h-c-si" for "two_body_parameter_folder".
To set vibration of the tip	Enter "160", "41" and "172" in the cell of "amplitude", "k_cantilever" and "resonant_freq" in the content "tip".
To set the pixel numbers for calculation image	Enter "20" in two cells of "tip" > "Ndiv" > "X" and "Y", and enter "10" in the cell for "Z".
To set Van der Waals force	Select the value of "conical" for "tip_shape" and Input "0.22", "120", "1000" and "1.00" in the cell of "Hamaker_const", "apex_angle", "tip_height" and "radius_of_tip_apex" in the "Fvdw" content respectively.
To set translational vectors	Input "15.35014", "15.35014" and "100" in the cells of "a" - "X", "b" - "Y" and "c" - "Z" in the "translational_vector" and input "0" in the others in the "translational_vector".
To start calculation	Push the ▶ button on the top of GUI. (When the confirmation dialog box popped up, please click "Save" button.)
To display the result	Select [Display] > [Result View] in Menu bar. Choose the item including the string "freq_shift.csv" from the combo box.

11.6.d Operation procedure for a local contact potential difference image

The table below is the operation procedure which calculates the local contact potential difference image, the result image is put in the KPFM section, of the nitrogen doped Si(001) surface. As is mentioned in the 11-5-3 section, in KPFM force is calculated in the condition that charge Δq is transfered from a sample to a tip. And the charge transfer which minimizes electrostatic force is searched by varying Δq. Item "tip_charge_neutrality" sets how to vary this charge transfer Δq.

Table 19 Operation procedure which calculates the local contact potential difference image of the nitrogen doped Si(001) surface.

Description	Procedure
To execute GUI of SPM Simulators	Double click the icon.
To create the new simulation project	Select "new" from "File" in Menu bar. Enter a project name, then click "OK".
To select tip apex model	After right click "Component" in Project Editor, click [Add Tip] > [Database] menu. Then, double click "tip_hsi4".
To select surface model	After right click "Component" in Project Editor, click [Add Sample] > [Database] menu. Then, double click "surf_si001n".
To set the initial position of the tip	1. Enter "-7" and "-6" in the cell of "Component" > "Tip" > "Position" > "x" and "y". 2. Enter "4" in the cell of "Component" > "Tip" > "DistanceFromSamples".
To set size of scan area of the tip	Enter "15.350140", "15.350140", "0" in the cells of "Component" > "Tip" > "ScanArea" > "w", "d", "h", respectively.
To select a suitable solver	Select "DFTB" and "Calculation" in the boxes on the top of GUI, respectively.
To change to the parameter tab for Quantum Mechanical SPM Simulator	Select "DFTB" tab in Project Editor.
To select the calculation mode	Select the value of "DFTB_KPFM" for "mode".
To select the two_body_parameter_folder	Select the value of "h-n-si" for "two_body_parameter_folder".
To set the pixel numbers for calculation image	Enter "30" in two cells of "tip" > "Ndiv" > "X" and "Y", and enter "0" in the cell for "Z".
To set charge transfer from a sample to a tip	Input "-0.1", "+0.1" and "4" in the cell of "minimum", "maximum" and "Ndiv" in the "tip_charge_neutrality" content.
To set translational vectors	Input "15.35014", "15.35014" and "100" in the cells of "a" - "X", "b" - "Y" and "c" - "Z" in the "translational_vector" and input "0" in the others in the "translational_vector".
To start calculation	Push the ▶ button on the top of GUI. (When the confirmation dialog box popped up, please click "Save" button.)
To display the result	Select [Display] > [Result View] in Menu bar. Choose the item including the string "LCPD.csv" from the combo box.

Reference

[1] P. Hohenberg and W. Kohn, Phys. Rev., **136** (1964) B864.
[2] L. H. Thomas, Proc. Camb. Phil. Soc. **23** (1927) 542.
[3] E. Fermi, Atti. Accad. Nazl. Lincei **6** (1927) 602.

[4] W. Kohn and L. J. Sham, Phys. Rev. **140** (1965) A1133.
[5] M. Y. Chou, P. K. Lam, and M. L. Cohen, Phys. Rev. B **28** (1983) 4179.
[6] Charles Kittel, "Introduction to Solid State Physics".
[7] P. Koskinen and V. Makinen, Computational Materials Science **47** (2009) 237-253.
[8] R. S. Mulliken, J. Chem. Phys. **23** (1955) 1833.
[9] M. Elstner, D. Porezag, G. Jungnickel, *et al*., Phys. Rev. B **58** (1998) 7260.
[10] R. G. Parr and R. G. Pearson, J. Am. Chem. Soc. **105** (1983) 7512.
[11] G. Binnig, H. Rohrer, Ch. Gerber, and E. Weibel, Phys. Rev. Lett. **50** (1983) 120.
[12] S. Bengio *et al*. Phys. Rev. B **86** (2012) 045426.
[13] R. Erlandsson and L. Olsson, Appl. Phys. A **66** (1998) S879.
[15] J. R. Chelikowsky and M. L. Cohen, Phys. Rev. B **10** (1974) 5095.
[16] A. Ramstad *et al*., Phys. Rev. B **20** (1994) 51.
[17] J. Bardeen, Phys. Rev. Lett. **6** (1961) 57.
[18] T. Uchiyama and M. Tsukada, Surf. Sci. **313** (1994) 17-24.
[19] M. Tsukada, Analytical Sci., **27** (2011) 121-127.
[20] A. Naitabdi and B. Roldan Cuenya, Appl. Phys. Lett. **91** (2007) 113110.
[21] N. Sasaki and M. Tsukada, Appl. Phys. A **72** (2001) S39.
[22] N. Sasaki and M. Tsukada, Jpn. J. Appl. Phys. **39** (2000) L1334.
[23] A. Sasahara, C. L. Pang, and H. Onishi, J. Phys. Chem. B **110** (2006) 17584.
[24] Sascha Sadewasser, Thilo Glatzel, eds., "Kelvin Probe Force Microscopy: Measuring and Compensating Electrostatic Forces (Springer Series in Surface Sciences)", Heidelberg: Springer, 2012, ISBN: 978-3-642-22565-9.
[25] K. Matsunami, T. Takeyama, T. Usunami, S. Kishimoto, K. Maezawa, T. Mizutani, M. Tomizawa, P. Schmid, K. M. Lipka, E. Kohn, Solid-State Electron. **43** (1999) 1547.
[26] N. Nakaoka, K. Tada, S. Watanabe, *et al*., Phys. Rev. Lett. **86** (2001) 540.
[27] A. Masago, M. Tsukada and M. Shimizu, Phys. Rev. B **82** (2010) 195433.
[28] M. Tsukada, A. Masago and M. Shimizu, J. of Phys.: Condensed Matter **24** (2012) 084002.
[29] J. Callaway and N. H. March, "Solid State Physics vol 38", Academic Press, 1984, p135.

Chapter 12 Sample Modeling (SetModel)

12.1 Introduction to sample modeling

Before using the SPM Simulator, we have to prepare the atomic models of a tip and a sample. In case of a crystal surface as a sample, it is very hard to construct the model with tens of or hundreds of atoms (element, coordinate, etc.). To reduce the boring work, the SPM Simulator includes the Modeling Tool. We can make a model of a thin film with an ideal surface by using the tool. We can also modify the surface, make a defect on the surface, and make a probe tip model. The working models are displayed on 3D-view. We may edit the models intuitively; e.g. we can select an atom on the 3D-view.

This chapter shows the basic concepts to construct a lattice model and the concrete examples how to use the Modeling Tool. On the other hand, the Modeling Tool is not adequate to make a molecular model without the translational symmetry. When we intend to make an organic molecule, we recommend using other software whose usage will be shown later.

12.2 Modeling of samples

Before explaining about a crystal, we define the lattice points. Every lattice point has the same environment. There may or may not be an atom on a lattice point. A parallelepiped configured by the lattice points is called the unit cell. Especially, the primitive unit cell has only one lattice point in the unit cell. There is a basic structure with one or more atoms around a lattice point. The lattice points are extended infinitely in three dimensions using the translational symmetry, which we call the lattice. The basic structure and the lattice are combined to be the lattice structure.

However there are infinite lattice points, any two of them are completely overlapped to each other by some symmetry operations. The possible symmetry operations are the following five: the translation operation, the rotation operation, the inversion operation, the reflection operation and the identity operation. The translation operation is described by $\boldsymbol{r} = l\boldsymbol{a} + m\boldsymbol{b} + n\boldsymbol{c}$ $(l, m, n$: integer), where $\boldsymbol{a}, \boldsymbol{b}, \boldsymbol{c}$ are the unit cell vectors.

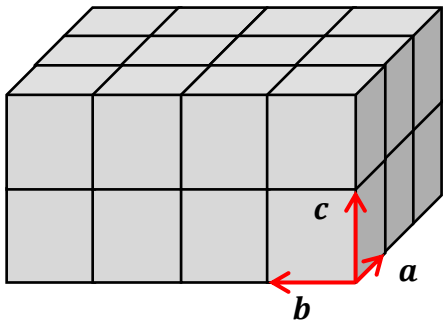

Figure 161 Unit cell vectors $\boldsymbol{a}, \boldsymbol{b}, \boldsymbol{c}$.

The rotation operation reproduces the same lattice when a lattice is rotated by $360°/n = 2\pi/n$ $(n = 1, 2, 3, 4, 6)$ around a specified axis. That axis is called as the *n*-fold rotation axis. The compatible rotation axes with a translational symmetry operation are only $n = 1, 2, 3, 4, 6$.

The inversion operation converts a coordinate (x, y, z) into $(-x, -y, -z)$ about a certain inversion center. If we choose a lattice point as the inversion center, then any other lattice point moves to another lattice point. The reflection operation converts a coordinate into the symmetric coordinate about a certain mirror surface.

There are 14 unique three-dimensional lattices called the Bravais lattices, made by the combination of the translational symmetry and the other symmetries. The Bravais lattices are classified into 7 crystal systems based on the kind of the rotation axes and its number; such as Triclinic, Monoclinic, Orthorhombic, Tetragnal, Rhombohedral, Hexagonal and Cubic lattices.

We here simply explain the point group. Among the symmetry operation, the rotation, the reflection and the inversion act around a specified point. Only that point keeps the invariant position after those operations. Therefore, those symmetries are called the point symmetry, and each operation is called the point symmetry operation. A combination of the point symmetry operations makes a various closed sets of the symmetry operations, called the point groups.

For example, think of four propellers of an electric fan, which has only one 4-fold rotation axis as the symmetry operation. Let us consider a set of the symmetry operations $\{E, C_4, C_4^2, C_4^3\}$, where a single 4-fold rotation operation is C_4, and an identity operation is E. The twice of C_4 is C_4^2, three times of C_4 is C_4^3, and four times of C_4 is $C_4^4 = E$, the identity operation. A combination of any two elements in the set becomes another element. The inverse operation of an element in the set becomes another element. That is how the set is closed. Thus the set makes up a group.

There are infinite point groups according to the combination of symmetry operations, however, only 32 point groups are compatible with the translation symmetry. Besides, combined with 7 lattices, 32 point groups and the translation symmetry, new closed systems are made up, which is called the space group. There are 230 types of the space group in total, and any lattice belongs to one of them.

A lattice structure is defined by the space group number, the lengths and the angles of the basis vectors of a unit cell, and the fractional coordinates (x_j, y_j, z_j) of several atoms in a unit cell. A fractional coordinate lies in $0 \leq x_j < 1$, and means a coordinate when the basis vectors $\boldsymbol{a}, \boldsymbol{b}, \boldsymbol{c}$ of a unit cell are chosen as the coordinate axes. The corresponding Cartesian coordinate is given by $\boldsymbol{r}_j = x_j\boldsymbol{a} + y_j\boldsymbol{b} + z_j\boldsymbol{c}$. The essential symmetry operations are defined depending on the space group. The coordinates of all atoms in the lattice structure are obtained after performing all possible symmetry operations for given fractional coordinates. Usually, a literature does not explicitly show the coordinates which can be reproduced by some symmetry operations.

The Modeling Tool recognizes the symmetry operations (identity, rotation, reflection, inversion, screw and glide) corresponding to each space group among 230 types of the space group. Once the minimum information of the fractional coordinates is given, the tool reproduces not only a unit cell structure but also any size of the crystal lattice.

We show a usage of the Modeling Tool, how to make a graphite thin film with a defect.

Launch the Modeling Tool, and look at the [New Slab] tab to input the lattice information (see below).

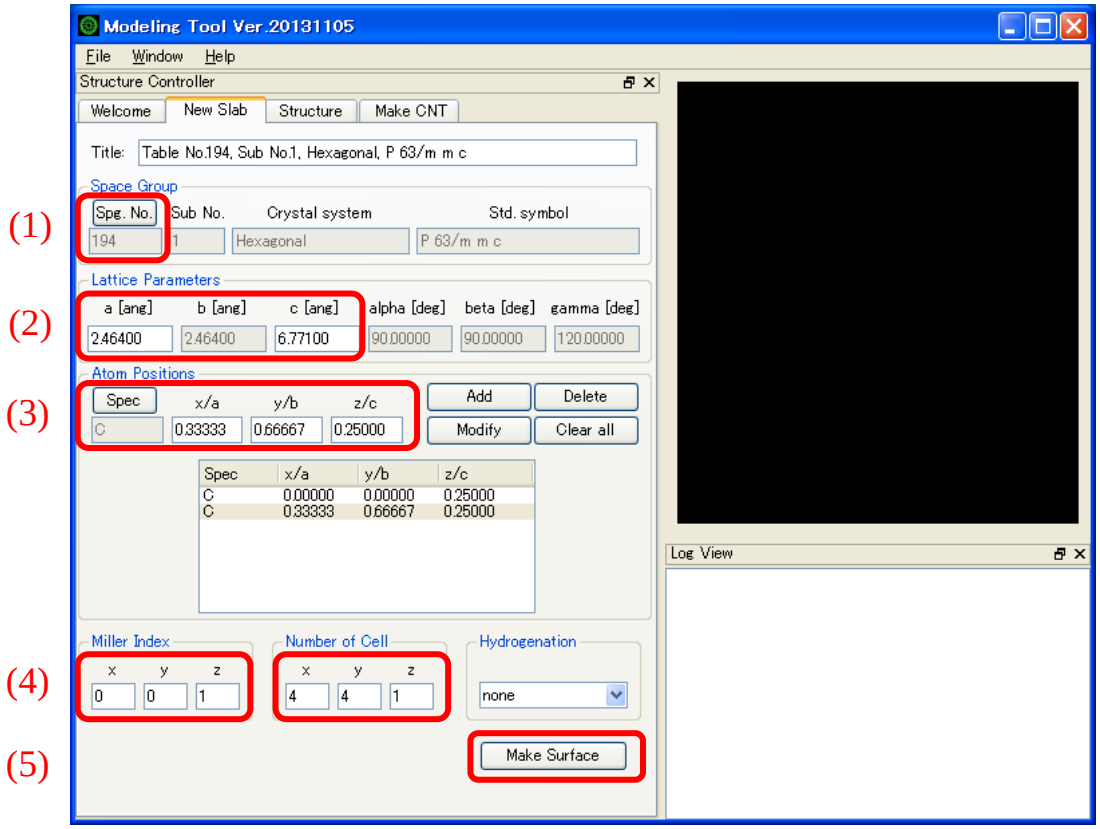

Figure 162 Start-up screen of the Modeling Tool.

(1) Select 194 $(P\ 6_3/m\ m\ c)$ as the space group number, to make a hexagonal lattice structure.

(2) Input the lattice constants; $a = 2.464$, $c = 6.711$ (Å). The other lattice constants (lengths and angles) are automatically determined according to the symmetry of the space group.

(3) Specify the leading constituent atoms in a unit cell. Graphite has two leading atoms; one is a carbon (atomic number 6) at a fractional coordinate (0.0, 0.0, 0.25), and another is a carbon at (0.33333, 0.66667, 0.25).

(4) Set the Miller index as (0 0 1) to make a (0001) surface. In case of the hexagonal lattice structure, the Miller index is usulally described by four indexes, which may be converted to a three-index description. Input (4, 4, 1) as the number of cells to extend the unit cell in three-dimension.

(5) Press [Make Surface] button to construct the crystal thin film model. After the calculation, the 3D model is shown in the main view.

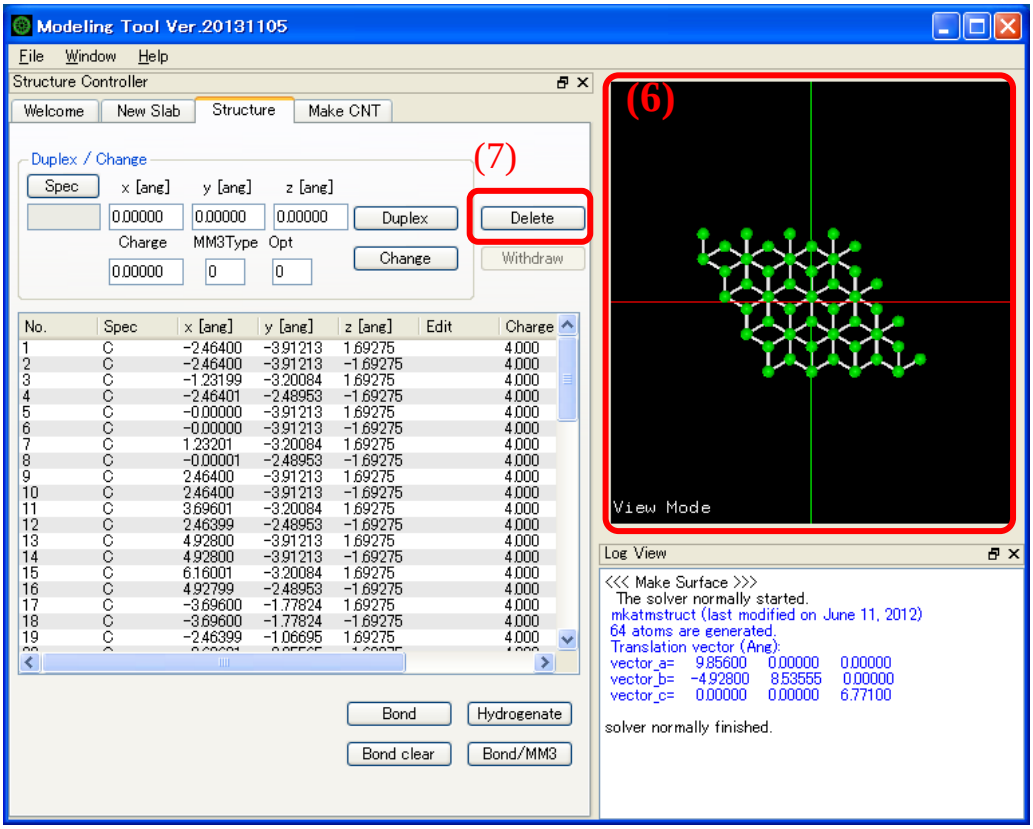

Figure 163 Overview of the Modeling Tool after constructing the crystal thin film.

(6) Drag by a mouse on the main view to change the view point as we like. Double-click the atom which will be removed to make a defect. That atom gets selected.

(7) Press [Delete] button to remove the selected atom.

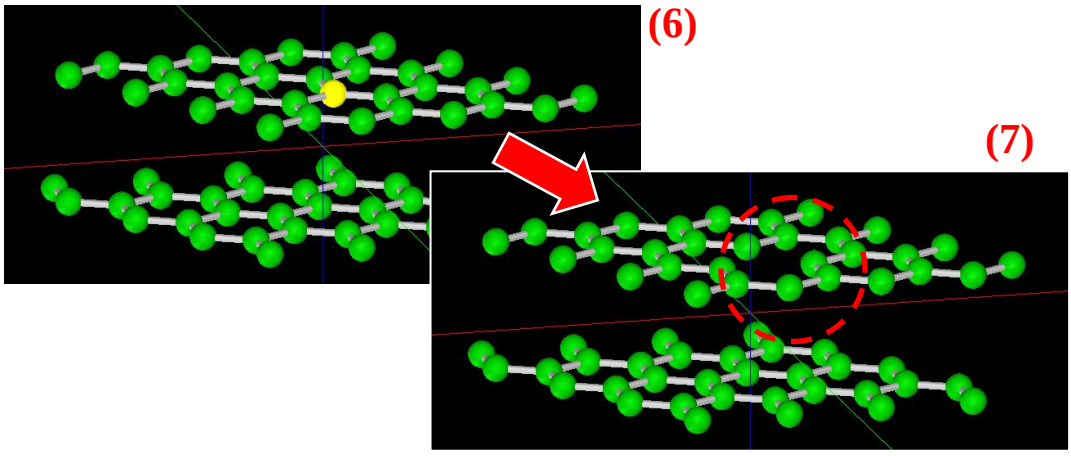

Figure 164 One atom is removed from the surface of the thin film model by the [delete] button.

[Save as] under the [File] menu saves the model as a *.txyz format or a *.xyz format. The saved data is available in the SPM Simulator.

12.3 Modeling of tips

The SPM probe tip is a very sharp needle attached to the top of a cantilever. The top point of the needle may be only one atom. We show how to make such an atomic model of the tip using the Modeling Tool.

For example, we have already made a supercell composed of several unit cells. We will see a sharp corner of the cell, which may be a candidate of a quasi-tip structure after cutting down the supercell. Figure 165(A) shows an image to cut down a triangular pyramid whose apex may become a tip, from a supercell composed of eight unit cells. Figure 165 (B) shows an image to cut down a quadrangular pyramid whose top apex may become a tip, from a supercell composed of four unit cells.

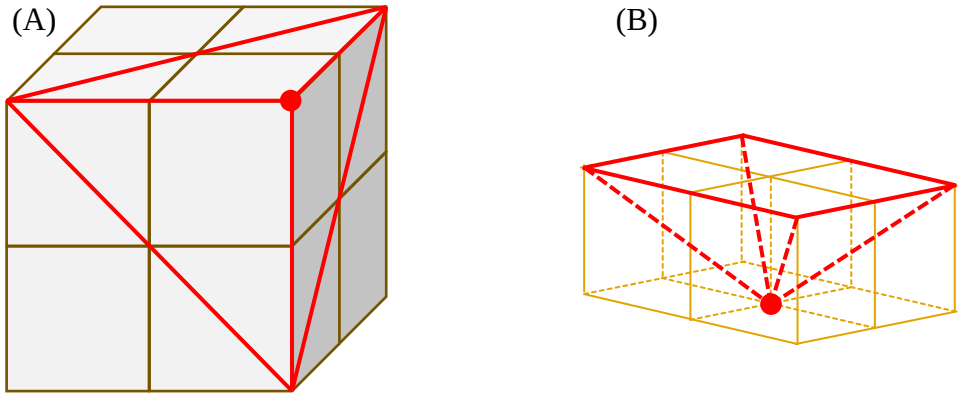

Figure 165 Images to cut down a quasi-tip structure from a supercell.

The Modeling Tool is able to make an atomic model of a tip from any lattices. We introduce how to make a silicon tip. To be brief, prepare a large crystal lattice, and then cut off the useless parts to make an apex structure with a sharp top.

Launch the Modeling Tool, and look at the [New Slab] tab to input the lattice information. Since the crystal silicon forms a diamond structure, select the space group number as 227 ($F\ d\ \bar{3}\ m$). Set 5.4 (Å) as a length of a side of the cubic unit cell. The other lattice constants (lengths and angles) are automatically determined according to the symmetry of the space group. Specify the leading constituent atoms in a unit cell. Silicon has one leading atom; a silicon (atomic number 14) at a fractional coordinate (0.0, 0.0, 0.0). Set the Miller index as (1 1 1) so that the one apex of a cubic cell is located at the bottom of a tip structure. The index makes a (1 1 1) surface of a crystal. Input (2, 2, 3) as the number of cells to extend the unit cell in three-dimension. Choose "All surfaces" to hydrogenate the dangling bonds of silicon atoms. Press [Make Surface] button to construct the crystal thin film model. After the calculation, the 3D model is shown in the main view.

Drag by a mouse on the main view to change the view point as we like, and cut off the useless parts to make an apex structure with a sharp top.

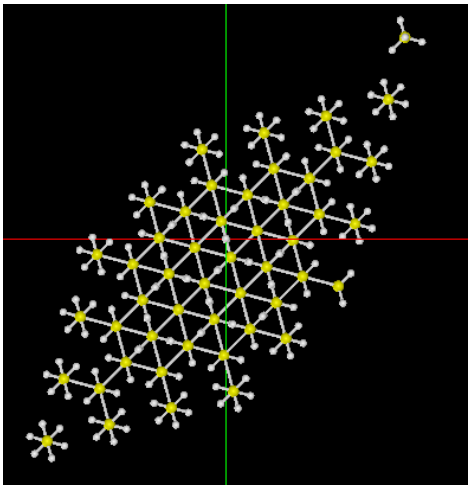

Figure 166 The top view of the model before cutting off.

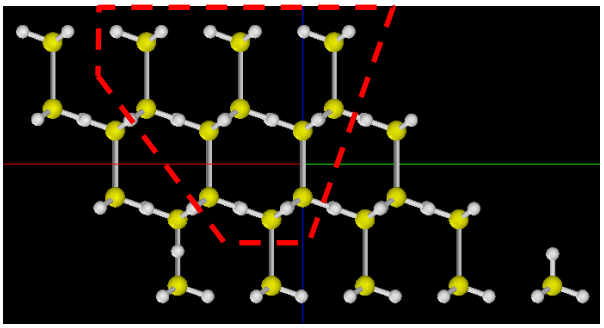

Figure 167 The side view of the model before cutting off. The atoms outside the red frame are removed.

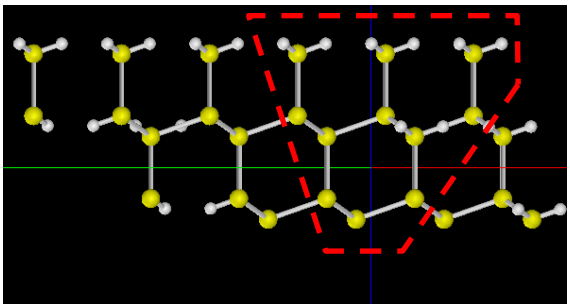

Figure 168 The side view (rotated) after the first cutting off. The atoms outside the red frame are removed.

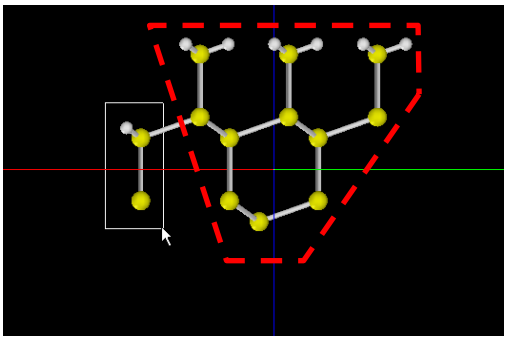

Figure 169 The side view (rotated) after the second cutting off. The atoms outside the red frame are removed.

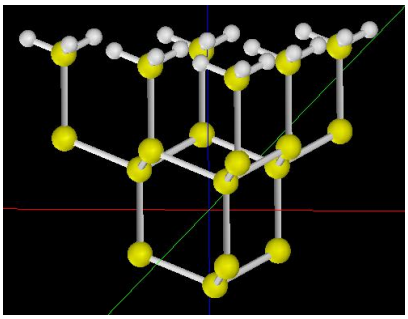

Figure 170 The accomplished quasi-tip model after cutting off.

As a result, we have a quasi-tip model shown in Figure 170. There is one silicon atom at the lowermost apex of the inverted triangular pyramid structure. After saved as a *.txyz format or a *.xyz format, the model data is available in the SPM Simulator.

The Modeling Tool equips various functions to edit the atomic model data. The tool can load the file formats of xyz, txyz and PDB (protein data bank). The prepared model files are combined into one model, which can be written down as a new xyz or txyz format. The tool can remove, modify and add any atoms in a model. It also equips the undo/redo function. Furthermore, various sizes of a carbon nanotube or a fullerene are constructed by this tool. See the tutorial of the SPM Simulator for more details.

12.4 Modeling of molecules

One may choose a molecule on a substrate as a target sample. It is hard for the modeling tool to construct an organic molecule which does not form a lattice[2]. In such a case, we recommend using other software. For example, the ACD/ChemSketch is a freeware to construct organic molecular models produced by the Advanced Chemistry Development. After the user registration, we may download the software. And we have to respond to the License Agreement before installing the software. The ACD/ChemSketch is available from the URL below:

URL: http://www.acdlabs.com/resources/freeware/chemsketch/

The ChemSketch provides a lot of templates of organic molecules, and has a variety of functions to edit the molecular models. After we save the created model as a "MDL Molfiles [V2000] (*.mol)" format, then we may convert it to *.txyz format by the use of the freeware, OpenBabel. Finally, our model is available in the SPM Simulator or the Modeling Tool. The OpenBabel is available from the URL below:

URL: http://openbabel.org/wiki/Main_Page

We show several examples of the created organic molecules by the ChemSketch, and their screen when loaded to the Modeling Tool.

[2] Strictly speaking, it is possible. But we have to put all atoms by hand. The Modeling Tool may show the power when constructing an organic molecular crystal, once the all constituents have been completed (it seems very hard).

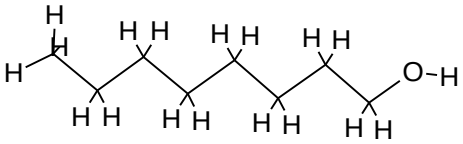

Figure 171 The structure of a 1-octanol [$CH_3(CH_2)_7OH$] created by the ChemSketch.

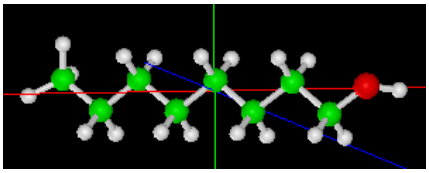

Figure 172 The screen of a 1-octanol on the Modeling Tool.

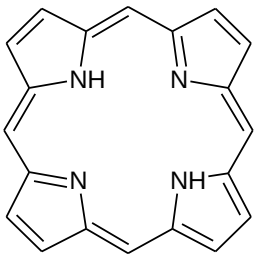

Figure 173 The structure of a porphin ring [$C_{20}H_{14}N_4$] created by the ChemSketch.

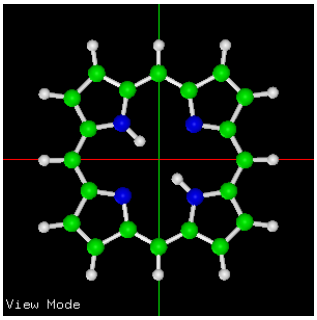

Figure 174 The screen of a porphin ring on the Modeling Tool.

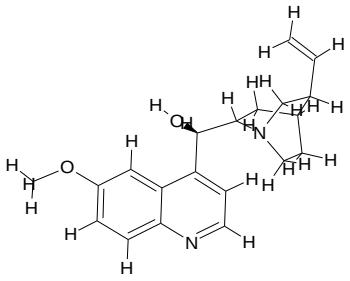

Figure 175 The structure of a (-)-quinine [$C_{20}H_{24}O_2N_2$] created by the ChemSketch.

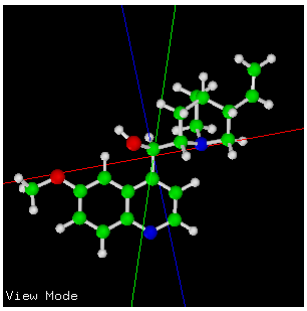

Figure 176 The screen of a (-)-quinine on the Modeling Tool.